Summer 7-5-2019

Field Monitoring of a Tieback Wall and Comparison to Common Design Methods

Matheus Barbosa Santos de Miranda

Field Monitoring of a Tieback Wall and Comparison to Common Design Methods

A Thesis

Submitted to the Faculty

of

Rose-Hulman Institute of Technology

by

Matheus Barbosa Santos de Miranda

In Partial Fulfillment of the Requirements for the Degree

of

Master of Science in Civil Engineering

July 2019

ROSE-HULMAN INSTITUTE OF TECHNOLOGY

Final Examination Report

Matheus Barbosa Santos de Miranda — Name

Civil Engineering — Graduate Major

Thesis Title: **Field Monitoring of a Tieback Wall and Comparison to Common Design Methods**

DATE OF EXAM: July 5, 2019

EXAMINATION COMMITTEE:

	Thesis Advisory Committee	Department
Thesis Advisor:	Kyle Kershaw	CE
	Matthew Lovell	CE
	Kevin Sutterer	CE
	Simon Jones	ME

PASSED X **FAILED** _____

ABSTRACT

de Miranda, Matheus Barbosa Santos

M.S.C.E.

Rose-Hulman Institute of Technology

June 2019

Field Monitoring of a Tieback Wall and Comparison to Common Design Methods

Thesis Advisor: Dr. Kyle Kershaw

This thesis presents the monitoring of a 28-foot high retaining wall located on the Rose-Hulman Institute of Technology (RHIT) campus and compares inclinometer and load cell data with common design methods. In addition, it briefly provides discussion regarding how the retaining structure is used to enhance student learning. The wall consists of soldier piles and wood lagging with tiebacks that vary from 22.5 to 40 feet. Construction was completed in 2017. Instrumentation, including load cell and inclinometers were installed to measure deflection, tieback load, and water level. This thesis describes the construction activities and the data gathered to date. It also compares the RHIT retaining wall data with other similar cases. In addition, it analyzes if deflected shape predictions from common design methods match with the field data. Finally, it presents lessons learned from developing a full-scale structure into a living laboratory that can be used directly in engineering courses.

Keywords: Civil Engineering, Retaining Wall, Tieback Wall, Student Learning.

DEDICATION

I would like to dedicate this thesis to my parents Eduardo and Jimena Miranda and my sister Manuela Miranda. I would not be able to achieve anything without their support, education, help and motivation.

ACKNOWLEDGMENTS

I am very grateful to my advisor, Dr. Kyle Kershaw. The work done for this thesis wouldn't be possible without his help, support, guidance and knowledge. He gave me an amazing opportunity to grow as an engineer and a person; it was a pleasure to be part of his research.

The help and partnership from several institutions, companies, RHIT professors and staff was also crucial for the completion of this research. I would like to acknowledge Beatty Construction Inc., subcontractor responsible for the design of the wall, for the partnership and shared data; Garmong Construction, general contractor responsible for construction of the wall, for coordinating the installation of the instrumentation and allowing site access when necessary; RHIT administration office and staff for allowing project access during construction; RHIT dean of faculty and department of Civil and Environmental Engineering for the financial and equipment support during the research and Earth Exploration Inc. for borrowing the inclinometer when necessary. Lastly, I would like to say thank you to my committee members, Dr. Kevin Sutterer, Dr. Matthew Lovell and Dr. Simon Jones for their help, advice and support during the research.

TABLE OF CONTENTS

Contents

LIST OF FIGURES ..... **v**
LIST OF TABLES ..... **vii**
LIST OF ABBREVIATIONS ..... **viii**
LIST OF SYMBOLS ..... **x**
GLOSSARY ..... **xi**
1. INTRODUCTION **1**
2. BACKGROUND **5**
2.1 Subsurface Conditions 5
2.2 Wall Construction 6
2.3 Rose-Hulman Institute of Technology 12
3. LITERATURE REVIEW **15**
3.1 Definition and types of retaining walls 15
3.2 Case Studies with Inclinometer Data 16
3.2.1 Tieback Wall in High Plasticity Expansive Soil at San Antonio, Texas 18
3.2.2 Tieback Anchored Pile Wall in Sand at Shenyang, China 20
3.2.3 Tieback Wall in Sand at Texas A&M University 23
3.2.4 Tieback Wall in Alluvial Soil in Taipei, Taiwan 28
3.2.5 Online Database of Deep Excavation Performance 30
3.3 Case Studies with Load Cell Data 33
3.3.1 Tieback Wall in Alluvial Soil in Taipei, Taiwan 34
3.3.2 Long-Term Monitoring at Harvard Square 35
3.4 Living Laboratory 37
4. PREDICTION OF WALL BEHAVIOR **41**
5. EXPERIMENTAL METHODS **55**
6. EXPERIMENTAL RESULTS **60**

6.1 Inclinometer Monitoring 60
6.2 Load Cell Monitoring 69
7. DISCUSSION 70
7.1 Mussallem Union Wall Experimental Results 70
7.1.1 Inclinometer Evaluation 70
7.1.2 Load Cell Evaluation 72
7.2 Comparison between MU Wall and Literature Review Cases 74
7.2.1 Inclinometer Cases 74
7.2.2 Load Cell Cases 77
7.3 Comparison between MU Wall and Limit Equilibrium Method – Full Depth 79
7.3.1 Deflection Comparison 79
7.3.2 Load Comparison 82
7.4 Comparison between MU Wall and Limit Equilibrium Method – Project Milestones 84
7.5 Student Learning 86
8. LIMITATIONS 89
9. CONCLUSIONS 91
10. FUTURE WORK 93
LIST OF REFERENCES 96
APPENDICES 99
APPENDIX A 100
APPENDIX B 106
APPENDIX C 147
APPENDIX D 161
APPENDIX E 181
APPENDIX F 184
APPENDIX G 197

LIST OF FIGURES

Figure Page

Figure 2.1: Aerial View of RHIT Campus (Google Maps 2019 [5]) 7
Figure 2.2: Northwest Corner of the MU Before Construction (05/25/2016) 8
Figure 2.3: Wall Construction (08/02/2016) 9
Figure 2.4: Installation of Tiebacks (08/11/2016) 9
Figure 2.5: Completed Wall before Concrete Facing (08/29/2016) 10
Figure 2.6: Wall After Construction (06/05/2018) 11
Figure 3.1: Typical Inclinometer Operation (Dunnicliff 1982 [11]). 17
Figure 3.2: Detail of Torpedo Containing Tilt Sensor (Machan and Bennett 2008 [12]) 17
Figure 3.3: Lateral Displacement of the Tieback Wall at Different Stages of Construction (Ahmed, Bin-Shafique, Huang, Papagiannakis and Rezaeimalek 2016 [13]) 19
Figure 3.4: Unbonded Length Effect on Horizontal Deflection for the wall in Texas (Ahmed, Bin-Shafique, Huang, Papagiannakis and Rezaeimalek 2016 [13]) 20
Figure 3.5: Cross Section Profile of Retaining Wall in China (Han, Zhao, Chen, Jia and Guan 2017 [14]) 21
Figure 3.6: Comparison Between Observed Data and Calculation Methods (Han, Zhao, Chen, Jia and Guan 2017 [14]) 22
Figure 3.7: Section of Retaining Wall at Texas A&M (Briaud and Lim 1999 [15]) 24
Figure 3.8: Comparison Between Deflections of Wall at Texas A&M (Briaud and Lim 1999 [15]) 25
Figure 3.9: Lateral Deflection Compared to First Tieback Location of Wall at Texas A&M (Briaud and Lim 1999 [15]) 26
Figure 3.10: Lateral Deflection Compared to Tieback's Unbonded Length - Texas A&M (Briaud and Lim 1999 [15]) 27
Figure 3.11: Cross Section of Wall located in Taipei (Liao and Hsieh 2002 [16]) 28
Figure 3.12: Lateral Wall Movement of Wall in Taipei (Liao and Hsieh 2002 [16] 29
Figure 3.13: Typical Section and Wall Deformations (mm) of Anchor Supported Keyed Wall Excavations (Konstantakos 2008 [17]) 32
Figure 3.14: Typical Section and Wall Deformations of Floating Excavations with Soil Anchors and Inclined Rakers (Konstantakos 2008 [17]) 33
Figure 3.15: Change in Tieback Load of Taipei Wall Over Time (Liao and Hsieh 2002 [16]) ... 34
Figure 3.16: Typical Tieback Installation through Slurry Wall at Harvard Square Station (Hansmire and Rawsley [18]) 36

Figure 3.17: Long-Term Measurement of Tieback Load, Harvard Square (Hansmire and Rawsley [18]) 37
Figure 3.18: The Living Lab Triangle (Veeckman, Schuurman, Leminen and Westerlund 2013 [21]) 39
Figure 4.1: Apparent Earth Pressure Diagrams for Clay - Pile P004 – Full Depth 43
Figure 4.2: Earth Pressure Diagram for pile P004 – Clay – Full Depth 44
Figure 4.3: Moment Diagram for pile P004 - Clay - Full Depth 45
Figure 4.4: Deflected shape for pile P004 – Limit Equilibrium Method – Clay – Full Depth 47
Figure 4.5: Deflected shape for pile P004 – Limit Equilibrium Method – Sand – Full Depth 48
Figure 4.6: Deflected shape for pile P005 – Limit Equilibrium Method – Clay – Full Depth 49
Figure 4.7: Deflected shape for pile P005 – Limit Equilibrium Method – Sand – Full Depth 50
Figure 4.8: Earth Pressure for piles P004 and P005 – Limit Equilibrium Method - 11 feet Excavation 51
Figure 4.9: Moment Diagram for piles P004 and P005 - Limit Equilibrium Method - 11 feet Excavation 52
Figure 4.10: Deflected shape for pile P004 – Limit Equilibrium Method 53
Figure 4.11: Deflected shape for pile P005 – Limit Equilibrium Method 54
Figure 5.1: Plan View of the Retaining Wall 55
Figure 5.2: Location of Angle Iron 56
Figure 5.3: Load Cell Installed at a Tieback 57
Figure 5.4: Load vs Deflection Curve for Pile P004 Tieback 1 Performance Test 58
Figure 5.5: Load vs Deflection Curve for Pile P005 Tieback 1 Performance Test 58
Figure 6.1: Profile Change for Pile P004 61
Figure 6.2: Profile Change for Pile P005 62
Figure 6.3: Profile Change for Pile P021 63
Figure 6.4: Profile Change for Pile P026 64
Figure 6.5: Profile Change at P4/5@5 65
Figure 6.6: Profile Change at P5/6@5 66
Figure 6.7: Profile Change at P4/5@12 67
Figure 6.8: Profile Change at P5/6@12 68
Figure 6.9: Load vs Time Plot for Tiebacks 69
Figure 7.1: Plot Comparison between the field data and the limit equilibrium method prediction – Pile P004 – Full Depth 80
Figure 7.2: Plot Comparison between the field data and the limit equilibrium prediction – Pile P005 – Full Depth 81
Figure 7.3: Plot Comparison between the field data and the limit equilibrium prediction – Pile P004 and P005 – 11 foot Depth 84
Figure 7.4: Plot Comparison between the field data and the limit equilibrium prediction – Pile P004 and P005 – 18 foot Depth 85

LIST OF TABLES

Table Page

Table 2.1: Material Description 6
Table 2.2: Tieback Bar Properties 10
Table 2.3: Construction Sequence 12
Table 3.1: Soil Parameters (Han, Zhao, Chen, Jia and Guan 2017 [14]) 22
Table 3.2: Soil Properties at Site Location in Taipei (Liao and Hsieh 2002 [16]) 28
Table 3.3: Retaining Structures Listed in the Database with Some Similarities to MU (Konstantakos 2008 [17]) 31
Table 3.4: Characteristics of Tiebacks With Long-Term Monitoring, Harvard Square Station (Hansmire and Rawsley [18]) 36
Table 4.1: Soil Parameters 42
Table 5.1: Wall Height and Number of Tiebacks 56
Table 7.1: Comparison of Tieback loads over time for MU and TCC walls 78
Table 7.2: Comparison Between UM Data and Limit Equilibrium Prediction – Pile P004 79
Table 7.3: Comparison Between UM Data and Limit Equilibrium Prediction – Pile P005 81
Table 7.4: Comparison between Field Data and Limit Equilibrium Method 83

LIST OF ABBREVIATIONS

CL	Lean Clay
CL-ML	Lean Clay - Silt
CLSM	Controlled Low Strength Material
CPT	Cone Penetration Test
FEM	Finite Element Analysis
GWL	Groundwater Level
HS	Hardening-Soil Model
MC	Mohr-Coulomb Model
P004-TB1	Pile Number 004 – Tieback Number 1
P4/5@12	Location 12 feet Behind Between Piles 004 and 005
P4/5@5	Location 5 feet Behind Between Piles 004 and 005
PVC	Polyvinyl Chloride
RHIT	Rose Hulman Institute of Technology
SM	Silty Sand

SPT	Standard Penetration Test
TP	Bearing Capacity of Anchor
USCS	Unified Soil Classification System
MU	Mussallem Union

LIST OF SYMBOLS

E	Young's Modulus
Fy	Yield Strength
I	Moment of Inertia

GLOSSARY

B7X-51 – typical steel bar for anchoring that can be used for several applications including soil nails, micro piles and prestressed tiebacks, for this particular case, the bars were used as tiebacks for a retaining wall;

HP 12x53 – typical steel section with standard dimensions and properties. Used at 22 of the 27 soldier piles;

HP 14x73– typical steel section with standard dimensions and properties. Used at 5 of the 27 soldier piles;

in^2 – inches square, area unit;

Inclinometer – typical instrument used for measuring deflection and displacement of soil and geotechnical structures, for this particular case, it was used to measure the deflection of a retaining wall;

Kips – force unit, it is equivalent to 1000 pounds-force;

Ksi – unit of stress or pressure, it represents 1000 pounds-force per square inch;

Load Cells – instrument used to create electrical signals that can be converted into force, typically used to measure loads in any type of structure, for this particular case, it was used to measure the tieback loads in a retaining wall;

Yield Strength – the yield strength represents the point where a certain material goes from the elastic behavior to the plastic behavior in the stress-strain curve.

1. INTRODUCTION

Engineers must develop new ideas, advanced technology, and creative solutions every day in order to keep up with the exponential growth of the world's population. The U.S. population increased from 272.6 million in 1997 to 325.7 million in 2017 (U.S. Census Bureau 2018 [1]), representing a growth of 20% in a 20 year interval. The need for a better use of space necessitates higher buildings, longer bridges, and better infrastructure.

Due to the increase in the number of sites with limited space, the use of retaining structures is crucial. Thus, engineers are seeking better understanding of retaining structures and the development of new techniques for building quicker, safer, and more sustainable in order to find techniques that will make construction more suitable to face the problems above. To achieve these goals, additional empirical data is needed to assess the applicability of current design methods. Further, it is critical for civil engineering students to understand the design and behavior of retaining structures. The existence of a full-scale retaining wall on campus can surely help achieving these goals and this is what this thesis is focused on.

Gathering and analyzing data from a full-scale retaining wall with a maximum exposed cut height of 28 feet was one of the main goals of this thesis. This particular structure is located on the Rose-Hulman Institute of Technology (RHIT) campus in Terre Haute, IN. The wall has 27 permanent soldier piles (22 are HP12x53 and 5 are HP14x73) varying in length from 22.5 to 40 feet with wood lagging between the soldier piles. Permanent, hollow-bar tiebacks in single or double rows were used to support the majority of the soldier piles. Construction started during

the summer of 2016 with the goal of facilitating a new loading dock adjacent to an existing building and a relatively steep existing slope, and it was completed in 2017. Currently, a road is located at the bottom of the wall, and a walkway for students, visitors, and staff at the top.

In order to gather the data, instrumentation was installed. The installation of load cells, inclinometers, survey points, and water level indicator was possible during construction due to a partnership between Rose-Hulman and the construction company. The survey points consisted of prism stickers on vertical surfaces and survey pins on horizontal surfaces in order to monitor displacement on the existing building, the new retaining wall, and the ground behind the new retaining structure. Currently, with the assistance of an inclinometer, it is possible to monitor lateral displacement for 4 soldier piles and at 4 locations within the retained soil behind the wall. This thesis shows the analysis of the inclinometer data from July 2016 to July 2018.

The monitored piles are located in two different parts of the retaining wall. Two piles are in the highest section of the wall and each one has 2 tiebacks in order to resist the load; the other two are located in a shorter section of the structure with only one tieback each.

The load cells allow the monitoring of a total of 6 tieback loads at the same 4 soldier piles used for the inclinometer analysis. It is important to compare the current loads at the structure with the design loads and check if the retaining wall is behaving accordingly with what was expected. All this data has been gathered periodically since the start of construction, the thesis presents the analysis from July 2016 to July 2018.

Common design methods were used to predict the deflected shape of the wall as well as tieback loads at three construction stages. The apparent earth pressure method was used for the

full height of the wall and limit equilibrium analysis with active and passive earth pressures for two intermediate construction steps (excavation to 11 feet and 18 feet).

In addition, this thesis discusses how to implement an active learning experience to enhance students' performance. Active learning, defined as any activity that make students participate in the process and think about what they are doing (Bonwell & Eison 1991 [2]), is crucial to improve student's understanding. Professors must help students take control of their own learning (Bransford, Brown, and Cocking 1999 [3]). The retaining wall can be very useful for several active learning exercises and helping students comprehend how to learn on their own.

Most universities and colleges apply the experimental learning technique using laboratories and field trips. Both are powerful practices that can introduce new and fundamental concepts to students, however laboratories usually do not show the full complexity and scale of real projects, while the quality of a field trip depends heavily on the tour guide and what activities are being done on the site. In addition, the students do not have a real active learning experience, but rather more a visual learning experience (Kershaw, Lovell, and Price 2017 [4]).

The retaining wall described in this thesis is a living laboratory that was incorporated into an existing facility on campus. It has been used to demonstrate engineering concepts for geotechnical and structural courses and it solves the limitations listed above for the laboratories and field trips. This thesis provides recommendations for additional activities and assessment to best utilize the retaining wall living laboratory. If properly harnessed, the structure will continue to help students to aggregate and synthesize knowledge across disciplines and it will surely

enhance student's performance in several classes. Finally, as a consequence of all improvements, it will create better engineers.

Lastly, a survey is proposed in order to have a better understanding about the background of civil engineering students at Rose-Hulman and collect information about their goals, preferences, opinions and areas of interest. This survey can be used to develop new teaching techniques, implement new concepts and give new ideas regarding how to use this retaining wall or other available structures on campus as a living laboratory.

2. BACKGROUND

This section is divided into three parts. The first one (Subsurface Conditions) describes the conditions of the soil where the retaining wall was constructed, that includes data that was not gathered by the student or any other RHIT staff for the thesis; the subsurface exploration was conducted during an earlier phase of the project to develop the design of the wall itself.

The second part describes the construction of the wall and shows the construction sequence for the retaining structure. It is crucial to be familiar with the construction sequence in order to fully comprehend the inclinometer analysis for this thesis. The installation of tiebacks interferes directly in the wall movement, so, knowing when the tiebacks were installed is important when discussing soil movement in the area.

The third part of this section gives background information about the Rose-Hulman Institute of Technology. In order to understand how this structure can be used for classes as a living laboratory and enhance student's performance, it is important to understand how the institute works, what classes are taught and the campus lifestyle. This part gives information about the campus environment that is crucial to understand some concepts discussed in further section.

2.1 Subsurface Conditions

On February 29, 2016 a soil boring was completed in the vicinity of the tallest portion of the retaining structure. Table 2.1 has the material description, the USCS classification and average standard penetration test blow counts for each soil layer at the boring location. The soil encountered during drilling for installation of the inclinometer casing behind the wall was also

logged and soil conditions were found to be consistent with the material descriptions shown below.

Table 2.1: Material Description

Depth	Material Description	USCS Classification	Average SPT
0 – 4in	Topsoil - Sandy Clay with organics	N/A	N/A
4in – 12ft	Clay – trace to some sand – trace gravel – medium to stiff – brown	CL	9
12ft – 22ft	Fine Silty Sandy – medium dense - brown	SM	20
22ft – 35ft	Silty Clay – and sand – trace gravel – hard brown	CL - ML	75

The test boring was terminated at 35 feet and no groundwater was observed during drilling or at completion; in addition, the moisture content varied from around 20 percent in the upper 7 feet to about 7 percent in the lower layer. Subsequent water level readings in the installed monitoring well indicate that the static water level is approximately 27 feet below the ground surface which is about 1 foot above the base of the wall at the maximum cut depth.

2.2 Wall Construction

The RHIT campus is basically divided into two sections. The east part has the classroom and lecture buildings, containing Professors's offices, laboratories and the library. The residence halls are located on the west part of campus. The Mussallem Union (MU) is roughly located in the center of the institute, and is one of the most important buildings on campus. Inside the MU it is possible to find, but not limited to, the cafeteria, a restaurant, common area for students, health center, student affairs, bookstore and conference rooms.

In the past, all the entrances of the MU were located on the south and east part of the building, causing traffic and conflicts betweeen the student's flow and workers in charge of delivering food and suplies for the union. As a consequence, the institute decided to develop a new MU layout in order to address some necessary changes to the campus, create a new atmosphere for students and improve campus' life.

The retaining wall described in this thesis was part of the construction for the new Hulman Mussallem Union to facilitate access through the back of the building via a new loading dock that was needed to decrease truck traffic through the main part of campus. The loading dock is located in the bottom part of the wall, while the top part is a walkway for students and staff. This walkway is used by students who live on campus to go from the resident halls to the union or to class. Figure 2.1 shows an aerial view of the institute during construction of the wall, it is possible to see the retaining wall's location, the MU and the resident halls nearby the construction site.

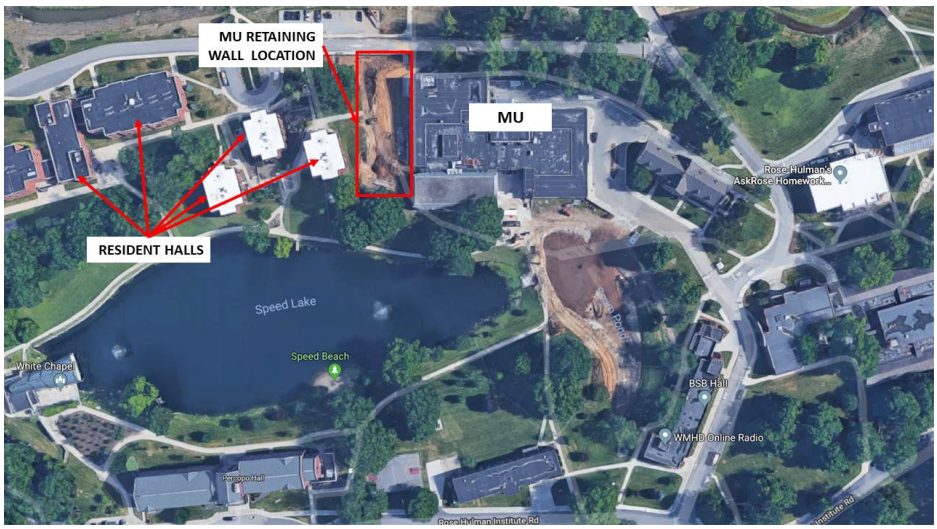

Figure 2.1: Aerial View of RHIT Campus (Google Maps 2019 [5])

Figure 2.2 shows the site for the retaining wall before construction. The stairs were removed and the area covered in grass was excavated for construction of the MU retaining wall. This is where the service entrance of the building is currently located.

Figure 2.2: Northwest Corner of the MU Before Construction (05/25/2016)

The MU retaining structure was designed to have 27 permanent soldier piles with wood lagging between the piles. The soldier piles are steel HP sections (22 HP12x53 and 5 HP14x73) grade A572-50, 24 in. diameter holes were drilled and backfilled with “Flexfill” grout (100psi after 28 days) (Beaty Construction [6]). Single or double rows of tiebacks were installed to support the majority of piles according to the height of the wall. Figure 2.3 shows construction of the wall after the soldier piles had been installed, but before the first row of tiebacks had been installed. The soldier piles were installed by pre-drilling holes with an augercast pile rig, placing the soldier piles into the pre-drilled holes, and backfilling with controlled low strength material (CLSM). This method was chosen because the contractor was concerned with pile driving vibrations adjacent to the existing structure.

Figure 2.3: Wall Construction (08/02/2016)

Figure 2.4 shows the installation of the second row of tiebacks along the tallest section of the wall. The tiebacks consisted of a 51mm B7X-51 hollow-bar with 6 inches diameter bit, all thread steel bars (Williams Form 2018 [7]). Table 2.2 contains the properties of the bars.

Figure 2.4: Installation of Tiebacks (08/11/2016)

Table 2.2: Tieback Bar Properties

Bar Diameter	Minimum Net Area Through Threads	Minimum Ultimate Strength	Minimum Yield Strength	Nominal Weight	Average Inner Diameter
2”(55mm)	1.795 in^2	188 kips	152 kips	6.26lb/ft	1.187”

Figure 2.5 shows the completed retaining wall prior to construction of the permanent wall facing. Note the stading water at the base of the wall, confirming that the groundwater level was approximately located 27 feet below the surface.

Figure 2.5: Completed Wall before Concrete Facing (08/29/2016)

Figure 2.6 shows the west part of the MU after construction with the new layout. It is possible to see the loading dock in the bottom of the wall, the union in the left and one of the residence halls on the right side of the picture.

Figure 2.6: Wall After Construction (06/05/2018)

Instrumentation was installed to monitor the behavior of the wall in four locations. Two of the locations, Piles P004 and P005, were installed at or near the maximum wall height and are therefore of the most interest for this project. A plan view of the retaining wall showing the exact location of the piles and instrumentation is shown on Figure 5.1, page 55. The construction sequence for these piles, including excavation depth and installation of tiebacks can be found on

Table 2.3. It is important to mention that the soil boring conducted was located near these two piles.

Table 2.3: Construction Sequence

Date	Activity
07/27/2016	Piles P004 and P005 Installed
07/29/2016	Excavate to 2’8” at P004 and 2’10” at P005
08/01/2016	Excavate to 5’11” at P004 and 5’7” at P005
08/02/2016	Excavate to 9’9” at P004 and 9’5” at P005
08/08/2016	Excavate to 9’10” at P004 and 9’10” at P005
08/09/2016	Installation, test and lock off tiebacks at 11’ at P004 and P005
08/12/2016	Excavate to 16’5” at P004 and 16’4” at P005
08/17/2016	Excavate to 19’0” at P004 and 18’2” at P005
08/17/2016	Installation, test and lock off tiebacks at 18’ at P004 and P005
08/29/2016	Excavate to 24’9” at P004 and 23’8” at P005

2.3 Rose-Hulman Institute of Technology

Rose-Hulman Institute of Technology (RHIT) is a small private college located in Terre Haute, IN. RHIT has currently more than 2,200 undergraduate students and more than 70 graduate students. Its average class size is 20 students and it has a 1:13 faculty-student ratio (Rose-Hulman Institute of Technology 2018 [8]).

These numbers show that RHIT has small classes when compared to other universities. For example, in the 2017-18 academic year, the average class size for the Indiana University was 42 students, for Purdue University, 42 students, and, for the University of Notre Dame, 32. (Public University Honors [9])

One of the main goals of the institute is to provide a hands-on learning experience for the students and give them as many opportunities as possible outside the classroom. The class size and faculty-student ratio help professors in providing a better learning experience to the students. It is much easier to plan and organize a laboratory or field trip with smaller classes, making it easier for the staff to use the retaining wall analyzed in this thesis as a living lab.

Understanding the classes offered by the institute is a crucial step on planning lectures, projects and homework assignments using the MU retaining wall. At RHIT, there are approximately 110 civil engineering undergraduate students in the 2018-19 academic year, including 27 seniors. The Civil and Environmental Engineering Department offers a total of 4 undergraduate structural classes (Structural Mechanics I and II, Structural Design-Concrete I, Structural Design in Steel I) and 2 undergraduate geotechnical classes (Foundation Engineering and Soil Mechanics). In addition, the structural graduate program at Rose-Hulman includes 9 classes (Matrix Methods and Structural Analysis, Structural Design in Concrete II, Structural Design in Prestressed Concrete, Structural Dynamics, Advanced Solid Mechanics, Retaining Structure Design, Bridge Design, Building Engineering and Connections and Detailing) (Rose-Hulman Institute of Technology 2018 [8]) The structure can be used for the majority of classes listed above and some that are not directly related to structural or geotechnical engineering. For example, Construction Engineering, Cost Engineering and Engineering Surveying. This could increase the non-lecture time of these classes since only a few of them already have laboratory exercises or field trips on their schedules.

Until the academic year of 2017-18 only 3 out of the 15 courses listed above presented required weekly laboratory exercises on its syllabus. A new structures laboratory is being

developed and should be available in the fall of 2019 for all 6 undergraduate structural and geotechnical required classes in order to give students another way of applying the concepts learned in class. It is believed that this new facility will impact positively students' learning experience. The MU retaining wall gives professors and staff an additional source of outside classroom learning experience for the students; it has potential to increase the value of the Civil Engineering program at RHIT and also create better engineers since it would give the students more hands-on opportunities and practical knowledge.

3. LITERATURE REVIEW

3.1 Definition and types of retaining walls

Retaining walls are well known structures in the civil engineering field designed typically to support lateral earth pressures. Their main objective is to retain the soil in a desired inclination that would not be stable without the structure. Some examples of applications of retaining structures include projects of bridges, underground parking lots, and roadways.

Engineers have developed several different types of retaining structures according to a variety of factors including availability of materials, water depth, types of soil and bedrock depth. Common types of retaining walls include gravity, cantilevered and anchored walls. Since the MU retaining wall uses a structural combination of soldier piles with tiebacks, it is considered to be an anchored wall.

Cantilevered retaining walls typically consist of sheet piles, soldier piles, or drilled shafts aligned in sequence with approximately 1/3 of the pile above the soil level and 2/3 below the base of the cut. If a cantilevered wall cannot satisfy project criteria, such as geotechnical capacity or structural capacity, lateral deflection anchors (tiebacks) can be added to the cantilevered walls in order to achieve design requirements. Adding tiebacks to embedded walls is economical for walls with height less than 20 feet and it provides some advantages regarding deflection and stresses. Adding the tiebacks to the sheet piles reduces bending moment in the piles and reduces the penetration depth, the wall also undergoes less lateral deflection when compared to other types of retaining structures (braced walls, for example) and, as a result, tiebacks provide more

control to the subsidence behind the wall. Tiebacks are prestressed and, unless creep occurs, should maintain the load during the excavation sequence. (Grand Steel Piling Co. 2018 [10]).

3.2 Case Studies with Inclinometer Data

The primary goal of this thesis is to analyze the performance of the MU retaining wall by using an inclinometer and load cells to compare the commonly used design methods.

An inclinometer is an instrument that is used to measure horizontal movement underground; it is commonly used to monitor deflection of retaining walls. Other typical utilizations of this instrument include determining alignments of piles, zoning of landslide movement, monitoring toes of embankments, and monitoring sheet piling deflection (Dunnicliff 1982 [11]). There are several different types of inclinometers; the simple shear probe is the most basic one, and others were designed in an attempt to improve its accuracy.

An inclinometer probe is typically guided by an embedded casing. Depending on the space available, type of material and structure, the casing can be installed in the ground or the structure itself. A vertical inclinometer measures relative horizontal deflection in two perpendicular planes. It is easy to compare and analyze the movement over time since readings can be constantly taken at the same depth. Sometimes, due to limited access, the casing can be installed at an angle; its inclination is commonly restricted to 30 degrees from the vertical. (Machan and Bennett 2008 [12]).

One of the most common inclinometer casings in the United States consists of a pipe with internal longitudinal guide grooves. A torpedo containing a tilt sensor is lowered down following the guide grooves in the PVC pipe. Its graduated electrical cable provides the current depth of

the inclinometer, and readings can be taken at the desired depths. Figure 3.1 shows an example of this type of inclinometer, and how the readings are calculated.

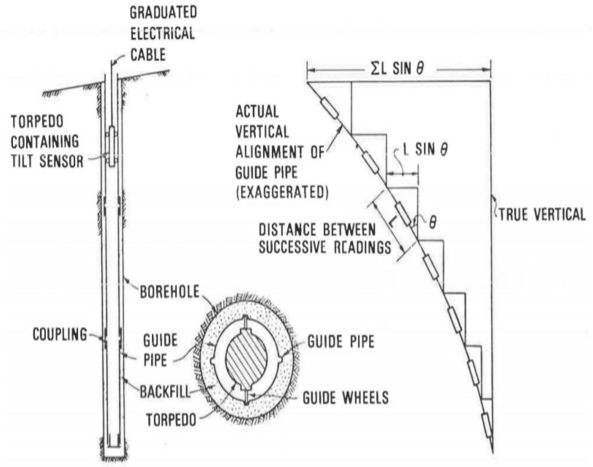

Figure 3.1: Typical Inclinometer Operation (Dunnicliff 1982 [11]).

Figure 3.2 shows the detail of the torpedo containing the tilt sensor. It shows the upper wheel and lower wheel assemblies, the control cable and the connector in the torpedo for the control cable.

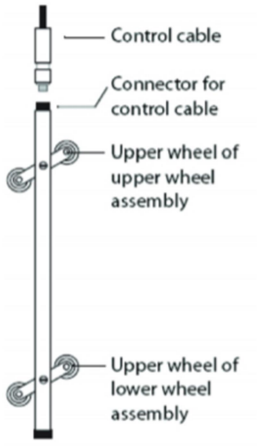

Figure 3.2: Detail of Torpedo Containing Tilt Sensor (Machan and Bennett 2008 [12])

The following subsections present summaries of published studies in which inclinometers were utilized to assess the performance of tieback walls.

3.2.1 Tieback Wall in High Plasticity Expansive Soil at San Antonio, Texas

The first case study data is from a tieback retaining wall located in San Antonio, Texas. A study of a 6-m-high wall (approximately 20 feet) in high plasticity expansive soils was conducted at a structure located at the intersection of a highway (I-35) and a street in San Antonio (Walters Street). The same soil layer exists for the whole height of the wall and it can be classified as high plasticity clay (CH) with an effective angle of friction of 27.5 degrees, a cohesion of 10 kPa, and over consolidation ratio of 2.1. (Ahmed, Bin-Shafique, Huang, Papagiannakis and Rezaeimalek 2016 [13]).

Similar to the MU wall, the retaining structure in Texas also had two rows of tiebacks, the top row with 4.5m of unbonded length (14 feet and 9 inches) and 17m of bonded length (55 feet and 9 inches) and the bottom row with 6m (19 feet and 8 inches) and 14m (45 feet and 11 inches) unbonded and bonded lengths, respectively. Figure 3.3 shows the lateral displacement gathered by the group of engineers responsible for this research. (Ahmed, Bin-Shafique, Huang, Papagiannakis and Rezaeimalek 2016 [12]).

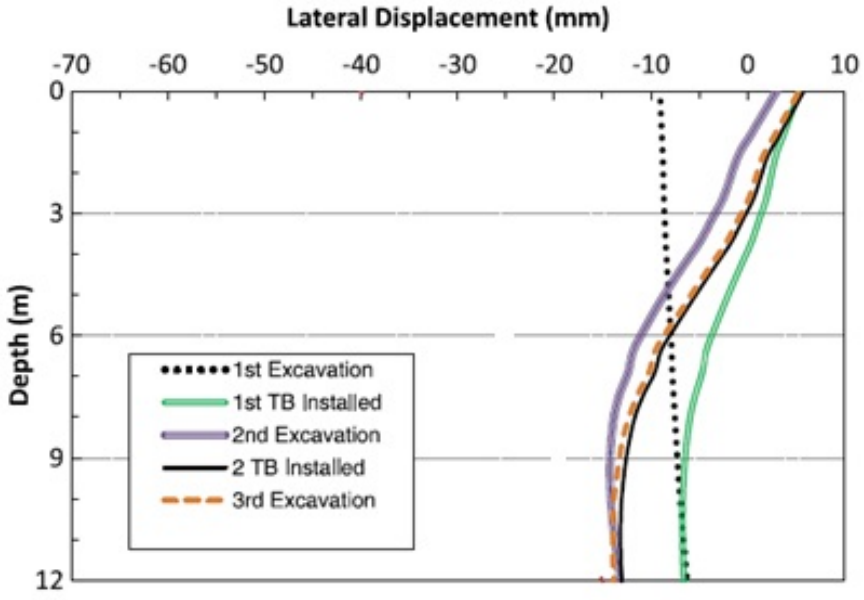

Figure 3.3: Lateral Displacement of the Tieback Wall at Different Stages of Construction (Ahmed, Bin-Shafique, Huang, Papagiannakis and Rezaeimalek 2016 [13])

The maximum outward deflection occurred during the first excavation, before the installation of any tiebacks. The figure shows a 9 mm (0.35 inches) outward deflection at the zero depth mark and a 6 mm (0.23 inches) outward deflection at the bottom of the wall. The installation of the first row of tiebacks causes an inward movement of approximately 15mm (0.59 inches) at the top of the wall and no movement was seen at the bottom. After that, the second excavation does not deflect as much as the first one, approximately 3 mm (0.12 inches) at the top of the wall and 6 mm (0.24 inches) at the bottom. Lastly, the installation of the second row of tiebacks causes an inward displacement of 3 mm (0.12 inches) at the top of the wall and no movement at the bottom.

Another important topic discussed by the group of engineers in Texas was the relationship between the unbonded length of the tieback and the deflection of the retaining structure. It can be seen in Figure 3.4 that, for this case, the deflection at the top portion of the wall decreases in a non-linear curve when the unbonded length decreases.

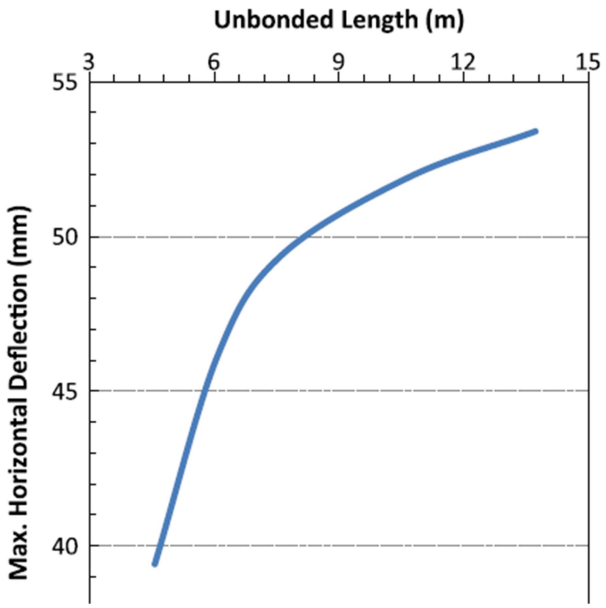

Figure 3.4: Unbonded Length Effect on Horizontal Deflection for the wall in Texas (Ahmed, Bin-Shafique, Huang, Papagiannakis and Rezaeimalek 2016 [13])

3.2.2 Tieback Anchored Pile Wall in Sand at Shenyang, China

The second retaining structure used for comparison with the MU wall is located in Shenyang, China. The structure was designed to support earth pressures for a deep excavation in an urban area with several buildings, metro tunnels and pipelines nearby. This wall is a combination of piles with mesh reinforcement, shotcrete for facing and prestressed tieback anchors to support the loads. At the tallest region, the wall section has a total of 7 tiebacks with different bonded

and unbonded lengths as shown in Figure 3.5. This figure also shows the length of the piles (approximately 90 feet), the construction sequence (a total of 8 excavations intercalated with the tieback's installation), the design capacity of the anchor (TP) and the groundwater level (GWL). (Han, Zhao, Chen, Jia and Guan 2017 [14])

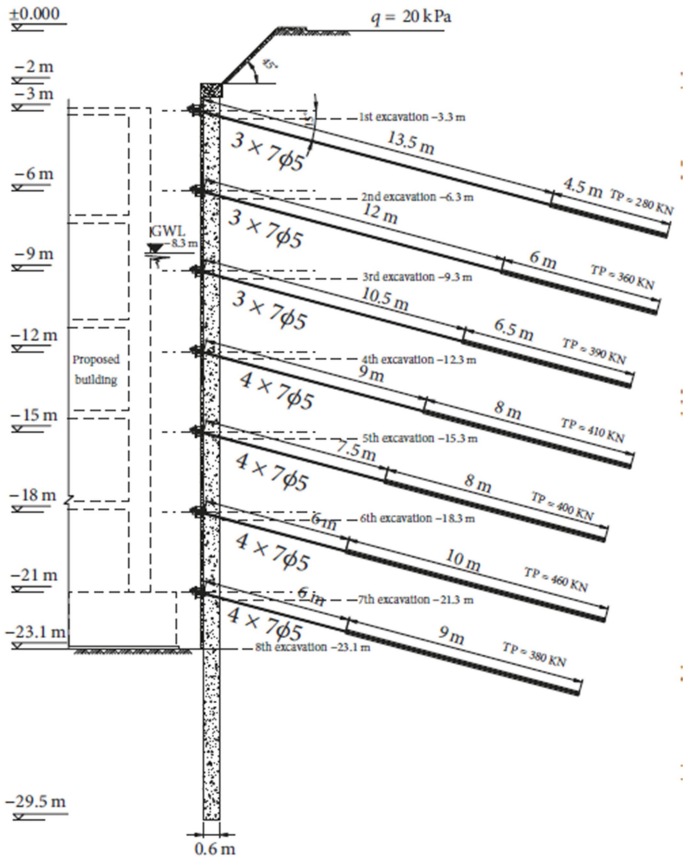

Figure 3.5: Cross Section Profile of Retaining Wall in China (Han, Zhao, Chen, Jia and Guan 2017 [14])

The soil was divided in five different layers according to its characteristics. The layer names, depths and unit weights can be found on Table 3.1. One of the main goals of this paper about the retaining wall in China was to discuss and compare different ways of predicting the deflection of

the retaining structure. The deflection observed in the field was compared to 3 common calculations methods, the linear elastic perfectly plastic Mohr-Coulomb (MC) model, the Hardening-Soil (HS) model, and the elastic method. According to Han, Zhao, Chen, Jia and Guan, the elastic method should be more reliable, but it needs accurate and precise input information, which is not always available. Figure 3.6 shows the horizontal wall deformation with the predictions from the three methods for the last stage, when excavation was completed.

Table 3.1: Soil Parameters (Han, Zhao, Chen, Jia and Guan 2017 [14])

Number	Layer	Depth		Unit Weight	
		Meter	Feet	kN/m^3	Lb/ft^3
1	Filled Soil	4.6	15.09	16.66	107.01
2	Medium-coarse sand	0.5	1.64	19.11	122.75
3	Gravelly Sand	16.9	55.45	19.60	125.89
4	Medium-coarse sand	3.1	10.17	19.11	122.75
5	Rounded Gravel	20.9	68.57	20.58	132.19

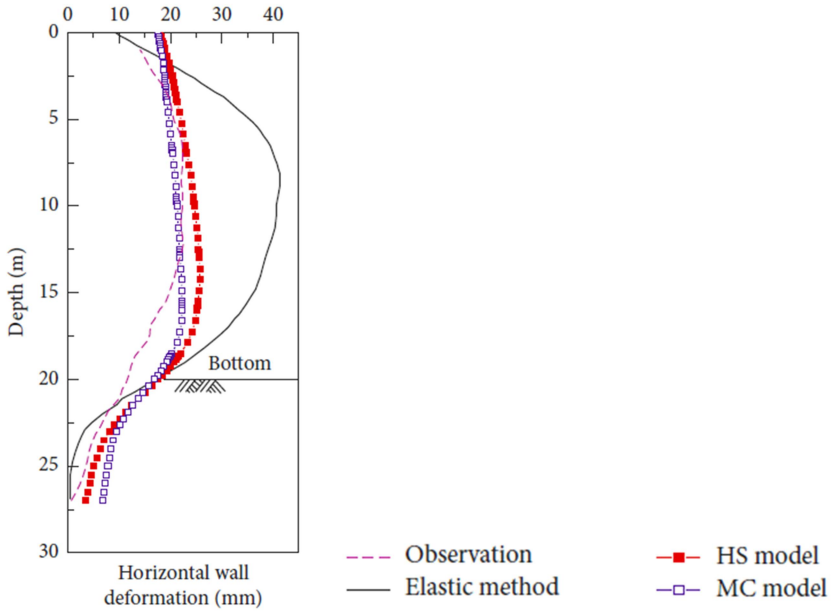

Figure 3.6: Comparison Between Observed Data and Calculation Methods (Han, Zhao, Chen, Jia and Guan 2017 [14])

This data shows that the HS model and MC model correctly predicted the deflection shape for the tieback retaining wall while the elastic method did not predict the wall deformation accurately, indicating that the input information for the elastic method was probably not precise. A deflection of 15 mm (0.59 inches) was observed at the top of the wall and a maximum deflection of 20mm (0.79 inches) in the Gravelly Sand Layer. Similar methods will be used for predicting the deflection of the MU wall and comparing with the data gathered with the inclinometer.

3.2.3 Tieback Wall in Sand at Texas A&M University

A 7.5m (24.60 feet) height tieback wall located at Texas A&M was fully instrumented for research. The wall consists of steel H piles drilled and grouted at one section and driving the same H piles in another section. The research conducted in 1999 had, as one of the goals, compared the observed deflection of the wall with FEM predictions, as well as tried to find a relationship between the unbonded length of the tiebacks and the deflection at the top of the wall (Briaud and Lim 1999 [15]).

The tieback retaining wall section analyzed by the paper had two rows of tiebacks in a 13-m-thick (42.65 feet) medium dense, fine silty soil layer with the following properties: average unit weight of 18.5 kN/m^3 (118.83 pcf), average SPT 10 at the surface and 27 at the bottom of piles, 32 degree angle of friction, and the water level was located at the 9.5 m (31.17 feet.) mark. Anchors at a 30 degree declination angle and three casings of inclinometers were installed as shown in Figure 3.7 (Briaud and Lim 1999 [15]).

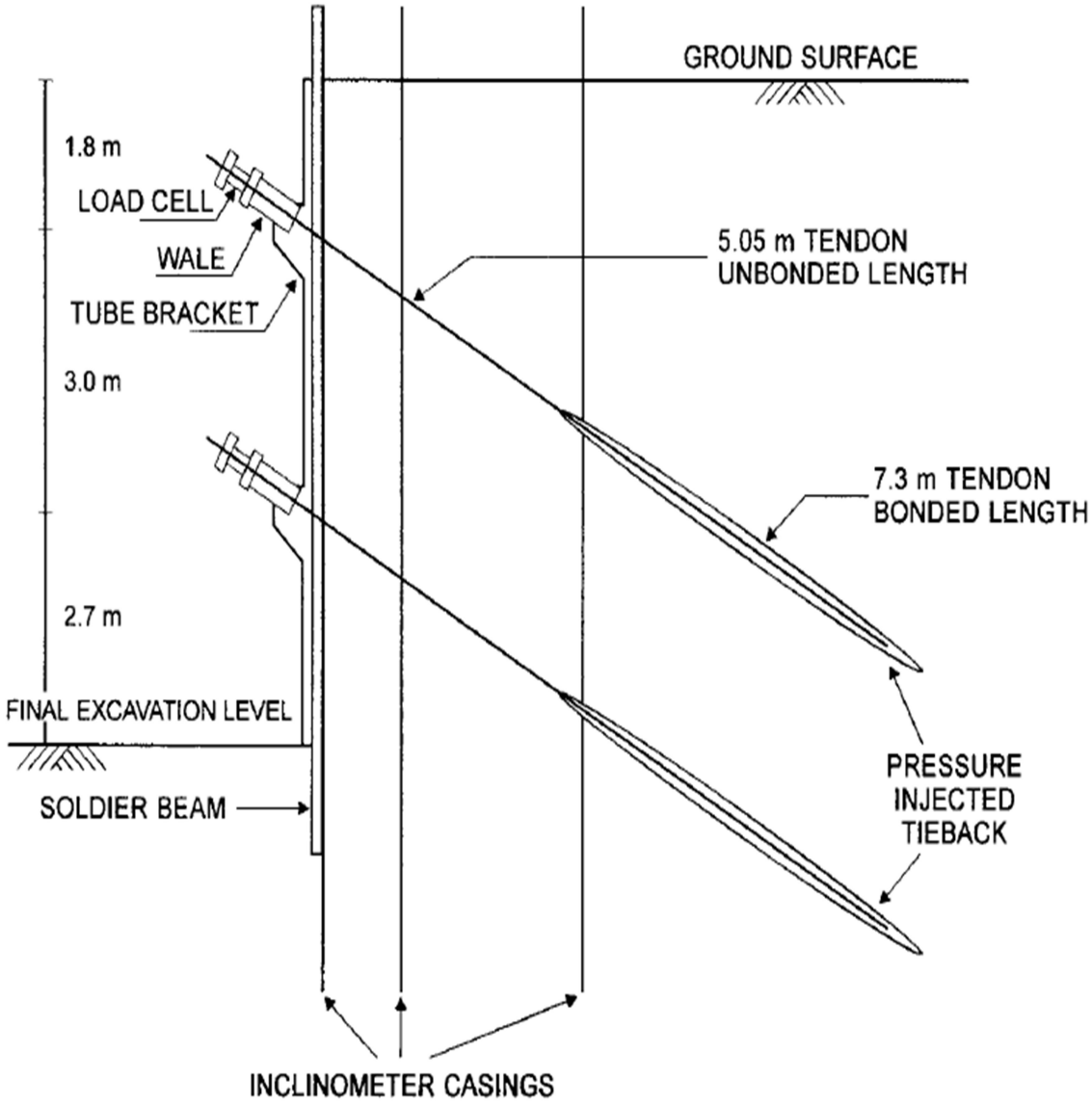

Figure 3.7: Section of Retaining Wall at Texas A&M (Briaud and Lim 1999 [15])

Figure 3.8 shows the comparison between the deflection of the wall and the FEM analysis. It is important to mention that it is not clear if the comparison is made using data from one inclinometer or an average between the three casings. The tiebacks locations are also shown in

this figure. It can be seen that the maximum measured deflection was 40mm (1.57 inches) at the surface and there is a change in slope at the tieback's locations (Briaud and Lim 1999 [15]).

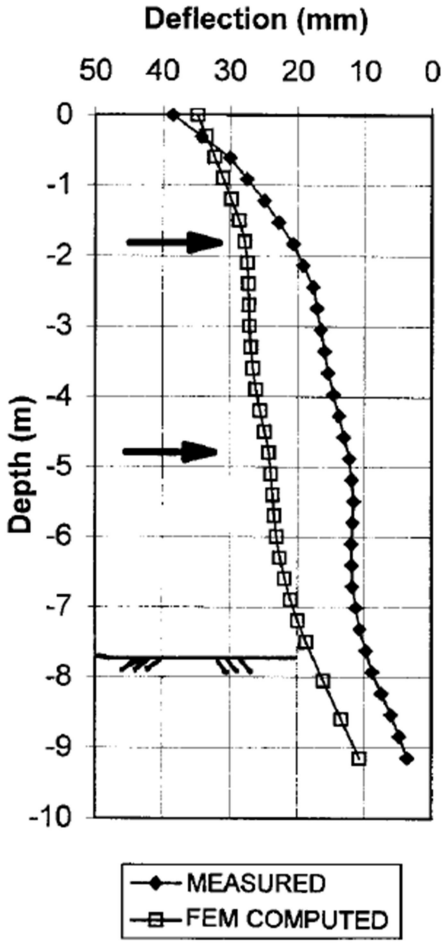

Figure 3.8: Comparison Between Deflections of Wall at Texas A&M (Briaud and Lim 1999 [15])

Another important topic discussed in the paper was the relationship between the location of the first tieback and the deflection curve. Figure 3.9 shows the relationship for the retaining wall at Texas A&M for 5 different tieback locations, 0.6 m, 0.9 m, 1.2 m, 1.5 m and 1.8 m (1.96, 2.96, 3.94, 4.92, and 5.90 feet, respectively). As expected, the results show that the first tieback

location has a significant influence on the deflection at the top 2 m (6.56 feet) of soil, but it does not strongly affect the soil displacement below that mark (Briaud and Lim 1999 [15]).

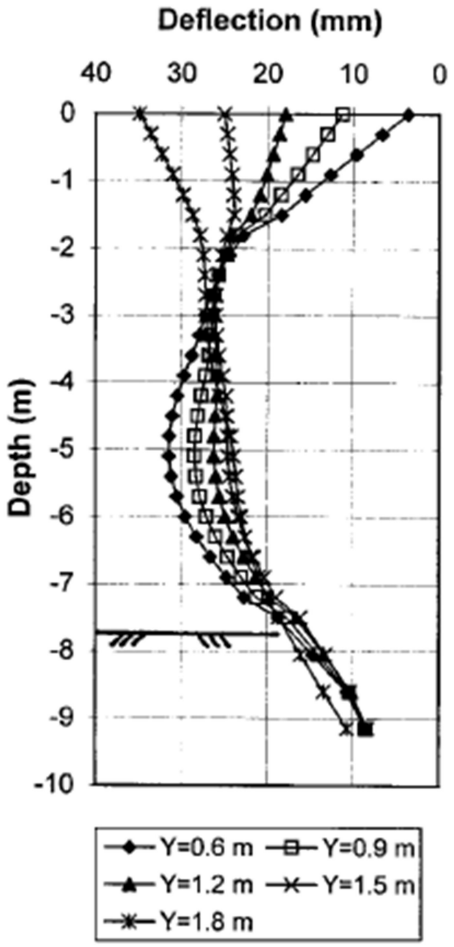

Figure 3.9: Lateral Deflection Compared to First Tieback Location of Wall at Texas A&M (Briaud and Lim 1999 [15])

The last relevant conclusion found during the research conducted in Texas was regarding the comparison between the tieback's unbonded length and the deflection at the top of the wall. Figure 3.10 shows the comparison using 7 different unbonded lengths and keeping the bonded

length and tieback loads constant. The unbonded lengths are related to the constant H (height of the wall) (Briaud and Lim 1999 [15]).

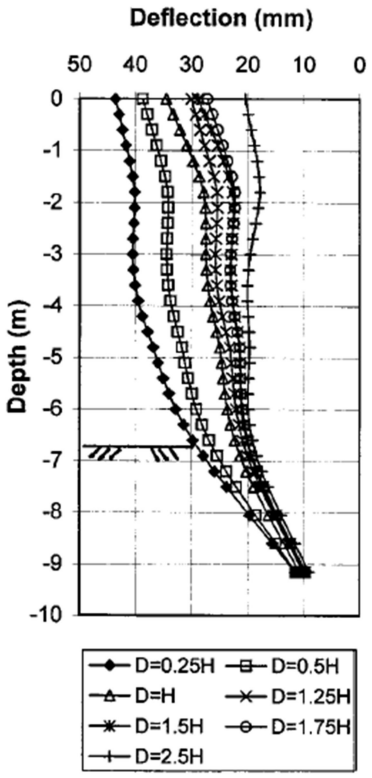

Figure 3.10: Lateral Deflection Compared to Tieback's Unbonded Length - Texas A&M (Briaud and Lim 1999 [15])

The deflection tends to decrease when the unbonded length increases. At the top of the wall, for instance, the deflection decreases from 43 mm (1.69 inches) to 20 mm (0.79 inches). This difference between the deflections decreases with the soil depth, at the 7 m (22.96 feet) mark the difference is only 8 mm (0.31 inches). At the top of the wall, a 53.5 percent decrease is seen, while at the 7 m (22.96 feet) mark, this number drops to 29.3 percent (Briaud and Lim 1999 [15]).

3.2.4 Tieback Wall in Alluvial Soil in Taipei, Taiwan

Research conducted by H. J. Liao and P.G. Hsieh with three retaining walls in Taipei Basin, a region in North Taiwan, analyzed the lateral deflection of retaining structures. The excavation depth varies between 12.5 m (41 feet) and 20 m (65.62 feet). The soil conditions are slightly different between the three walls and very typical for the area (Liao and Hsieh 2002 [16]). Since soil conditions do not change significantly between walls, only the one with height closest to 28 feet (MU wall height) will be considered for this thesis data comparison.

The second wall analyzed in Taipei was at the Taipei County Administration Center, and the bottom of excavation was located 12.5 m (41 feet) below the surface with 4 rows of tiebacks as it can be seen in Figure 3.11. The average SPT value for each soil layer is shown on Table **3.2**. (Liao and Hsieh 2002 [16]).

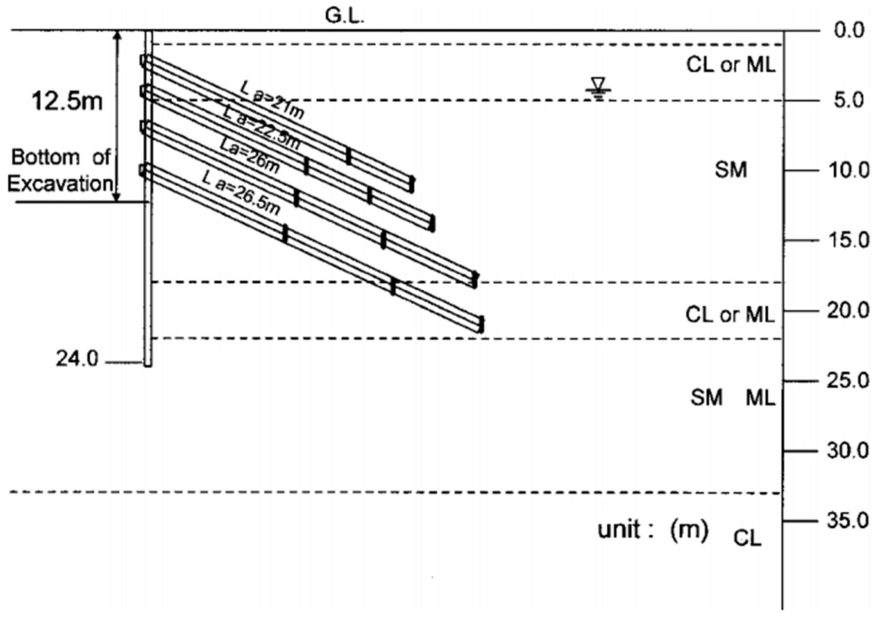

Figure 3.11: Cross Section of Wall located in Taipei (Liao and Hsieh 2002 [16])

Table 3.2: Soil Properties at Site Location in Taipei (Liao and Hsieh 2002 [16])

Number	Layer	Average SPT
1	Fill	-
2	ML	3
3	SM	10
4	ML	7
5	SM	15

Figure 3.12 shows the lateral movement of the wall with results monitored after each tieback installation. The construction was divided in five different stages; stage 1 is before excavation, and stages 2 to 5 are the measurements collected after each tieback installation. It can be seen that most lateral movement occurred during the excavation phases, and that the first tieback is the only one to cause an inward soil movement when compared to the previous profile. At the bottom of the wall, a 33mm (1.30 inch) outward soil movement is observed (Liao and Hsieh 2002 [16]).

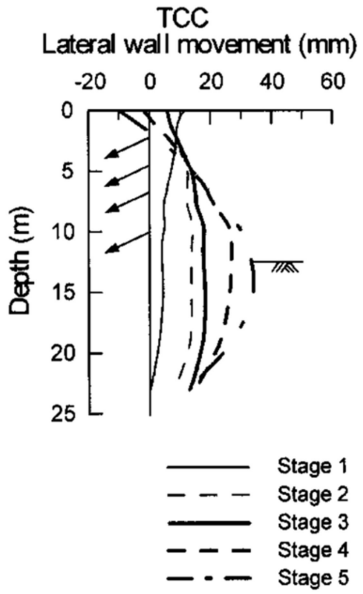

Figure 3.12: Lateral Wall Movement of Wall in Taipei (Liao and Hsieh 2002 [16]

3.2.5 Online Database of Deep Excavation Performance

A database was created by Konstantakos in 2008 [17] to gather information about deep excavations and provide easy access to wall deformation of different structures around the United States. Currently, the database's website is not available, but information can still be found in some papers.

Konstantakos wrote a paper in August 2008 summarizing the work done and data gathered until that moment. The paper contains wall deflection data for approximately forty projects in the Unites States and some in Europe and Asia. The database divides the projects into three types of wall: Diaphragm (DW), Steel Sheet Pile (SSP) and Soldier Pile and Timber Lagging (SPTL) Wall. Each type is classified according to its support and soil type (Konstantakos 2008 [17]). This thesis will focus on structures that meet at least two of the following characteristics: Wall Type: Soldier Pile and Timber Lagging Walls, Support Type: Tieback anchors (TB), and/or Soil Types: CL, ML or SM, since these are similar characteristics to the MU wall. A total of ten retaining structures fall into these requirements; Table 3.3 lists these walls.

Table 3.3: Retaining Structures Listed in the Database with Some Similarities to MU (Konstantakos 2008 [17])

ID	Year of Construction	Project Location	Soil Type	Wall Type	Bracing Method	Max Exc. Depth (ft)	Max Wall THK[4] (ft)	Max Δ (in)
B19	1986	Boston, MA	C	SPTL	TB[1]	54.8	-	0.72
W4	1990	Washington, DC	S, CL	DW	TB	30.8	2.0	0.39
W1	1991	Washington, DC	S, CL	DW	TB	60.0	2.5	0.43
W3	1999	Washington, DC	S, CL	DW	TB-R[2]	29.9	4.0	0.75
W3	2000	Washington, DC	S, CL	DW	TB	55.1	3.0	0.71
C3	1971	Chicago, IL	CL	DW	TB-SP-SB[3]	44.0	2.5	4.60
C4	1973	Chicago, IL	CL	DW	TB-R	44.0	2.0	2.52
C6	1987	Chicago, IL	CL	DW	TB-R	24.9	2.25	0.43
C9	1993	Chicago, IL	CL	DW	TB	23.0	2.0	1.53
C10	1997	Chicago, IL	CL	DW	TB	34.1	2.5	0.87

[1] TB = tieback
[2] R = rakers
[3] SB = soil berm
[4] THK = thickness

Unfortunately, the paper does not show the wall deformation and profiles for all the cases listed in Table 3.3. The first five walls (from B19 to W3) were together in a group called Anchor Supported Keyed Wall Excavation. For these walls, the toe was fixed by keying the structure into a glacial till or bedrock. Figure 3.13 shows the typical section and wall deformation for three structures (B12, W3, and W1). The first one (B12) is not considered for this thesis because it is a rock anchor example. Only the information from W1 and W3 will be discussed since its characteristics are more similar to the MU structure. (Konstantakos 2008 [17])

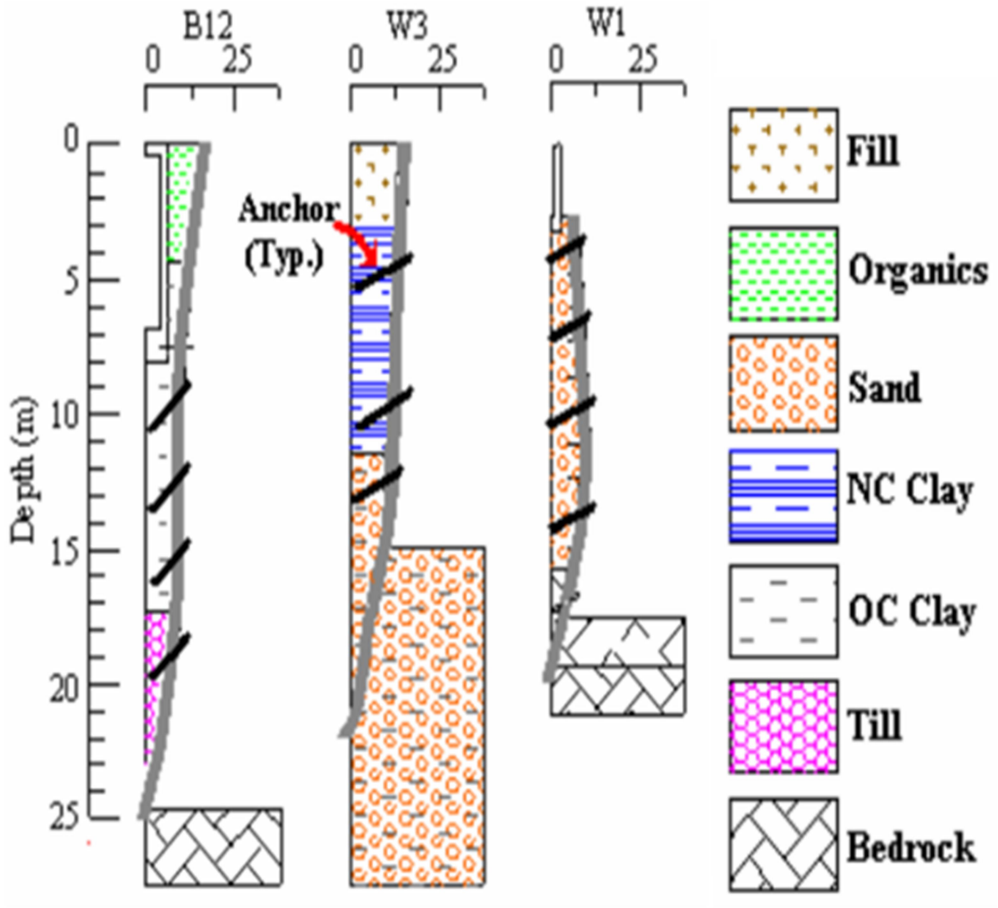

Figure 3.13: Typical Section and Wall Deformations (mm) of Anchor Supported Keyed Wall Excavations (Konstantakos 2008 [17])

Figure 3.13 shows that no soil movement was measured in the wall toe and that the maximum deflection was smaller than 25mm (1.0 in). According to Konstantakos, anchor elongation and surcharge coming from nearby structures appear to control wall deflection.

The other five walls (from C3 to C10) fall into another category: Floating Wall Excavations. For the walls discussed in this thesis, the wall was extended at least 1.5 m (5 feet) into a stiff clay stratum. For these structures, tiebacks were the first bracing option, but some of them also used

rakers. Figure 3.14 shows the wall deformation for four of the five structures discussed in this paper (C4, C6, C9 and C10). Information for the other wall could not be found in the paper by Konstantakos.

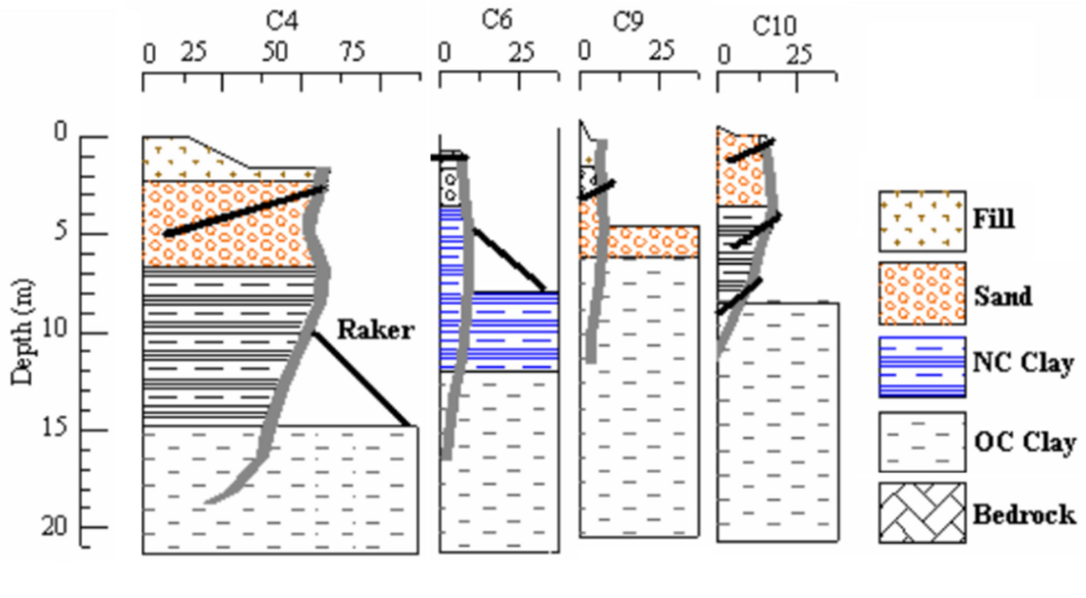

Figure 3.14: Typical Section and Wall Deformations of Floating Excavations with Soil Anchors and Inclined Rakers (Konstantakos 2008 [17])

Except for wall C4, all the other structures showed a maximum wall lateral displacement smaller than 25mm (1.0 in). As expected, the toe deflection was not zero for all the cases since these structures were not fixed at the base. According to Konstantakos, the larger deformations were mainly caused by short free or bonded tieback length, tieback creep and load loss, inadequate toe-embedment, and influence of other construction activities.

3.3 Case Studies with Load Cell Data

As previously discussed, a primary goal of this thesis is to analyze the behavior of the MU wall using load cell and inclinometers. Load cells were installed in some tiebacks in order to

monitor the tensioning load during and after construction. The objective is to compare the tieback loads with other similar published data and common calculation methods to check their accuracy on predicting tieback forces.

3.3.1 Tieback Wall in Alluvial Soil in Taipei, Taiwan

Section 3.2.4 of this thesis summarizes and briefly describes the research conducted by H. J. Liao and P.G. Hsieh (Liao and Hsieh 2002 [15]) with three retaining walls in Taipei Basin and shows the inclinometer data gathered by them. This section is focused on presenting the tieback load data gathered at the Taipei County Administration Center (one of the three walls) for a period of approximately 200 days. The wall selected was the one with height closest to the MU retaining structure (28ft), using the same criteria of the inclinometer analysis.

Figure 3.15 shows the measured tieback loads for the four levels of tiebacks in the TCC (Taipei County Administration Center) wall (Liao and Hsieh 2002 [16]).

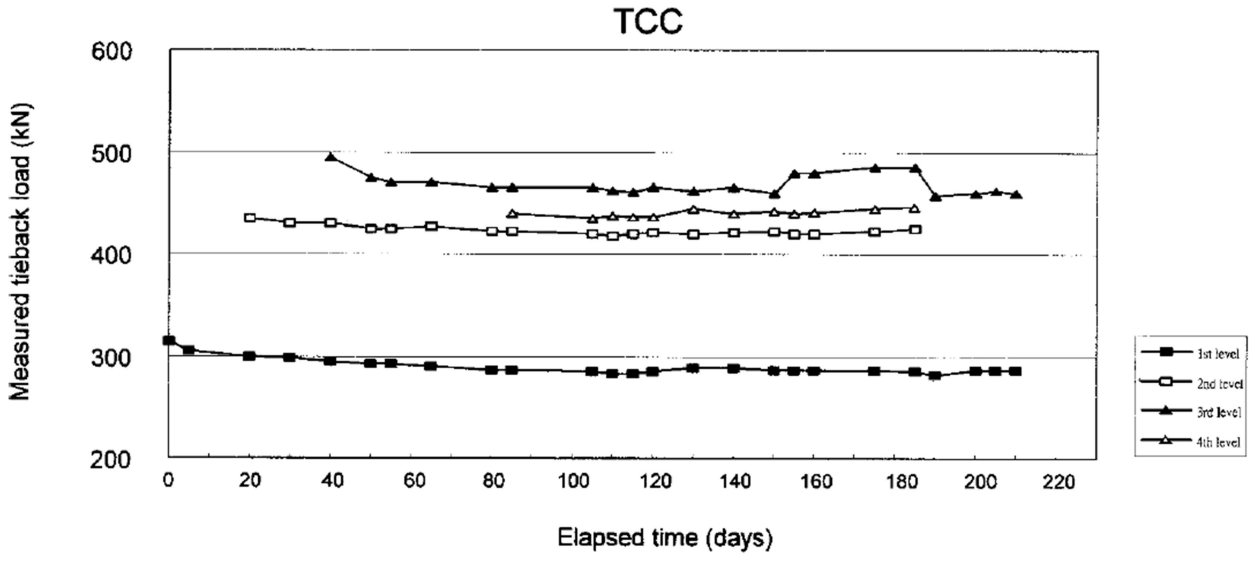

Figure 3.15: Change in Tieback Load of Taipei Wall Over Time (Liao and Hsieh 2002 [16])

It can be seen that the first level of tiebacks carries the smallest load and that its value is basically constant over time (300 KN or 67.4 kips). The other tieback levels have similar loads, all located in the zone between 400 KN (89.9 kips) and 500 KN (112.4 kips). The second level and third level are almost constant at 425 KN (95.5 kips) and 450 KN (101.2 kips), respectively. The fourth level shows a peak of almost 500 KN (112.4 kips) in the beginning, but then it drops and stays constant at 475 KN (106.8 kips) with the exception of the period between 150 days and 190 days, where it can be seen an increase of approximately 15 KN (3.4 kips).

3.3.2 Long-Term Monitoring at Harvard Square

In 1980, the reconstruction of the Harvard Square station located in Cambridge, Massachusetts started; the design included a slurry wall and tiebacks for lateral support. Load cells were installed at two locations in order to monitor the axial loads at some tiebacks during and after construction (Hansmire and Rawsley [18]).

The thickness of the slurry wall is 3 feet and 6 inches and it was built to a depth of about 42 feet (12.8 m) with approximately 14 feet of exposed height. The two rows of tiebacks were installed with a 20 degree and 30 degree angle, respectively. At this location, bedrock was encountered only by the top row of tiebacks and neither by the bottom row nor the slurry wall (Hansmire and Rawsley [18]).

For this particular case, the tiebacks had no structural importance in the final design, but they were left in place for research purposes since there was no interference to final station use. Figure 3.16 shows the typical tieback installation at Harvard Square station and the slurry wall dimensions (Hansmire and Rawsley [18]).

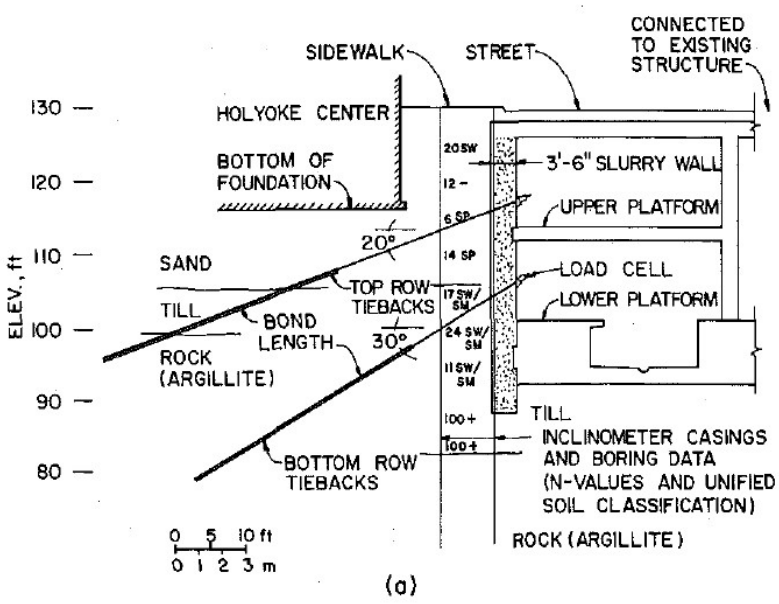

Figure 3.16: Typical Tieback Installation through Slurry Wall at Harvard Square Station (Hansmire and Rawsley [18])

All tiebacks were designed for an allowable bond stress of 35 psi, which means that the force along the length is equal to 8 kips/feet for a 6 inch diameter drill hole. Also, the design load for each tieback was 282 kips; this represents a minimum bond length of 35 feet. Six tiebacks were monitored and their information can be found on Table 3.4.

Table 3.4: Characteristics of Tiebacks With Long-Term Monitoring, Harvard Square Station (Hansmire and Rawsley [18])

Tieback Number	Free Length (ft)	Bond Length (ft)	Total Length (ft)	Remarks
1	26.5	35	61.5	Grouted with packer
2	26.5	35	61.5	Grouted with packer
3	17.5	35	52.5	No packer
4	17.5	35	52.5	No packer
5	17.5	35	52.5	No packer
6	17.5	35	52.5	No packer

The load monitoring results from 1980 to 1983 are shown in Figure 3.17. It can be seen that during the time period, all tiebacks loads were less than the design load (282 kips). Also, all loads decreased over time due to some relaxation of the soil and installation of the other tiebacks. Figure 3.17 also shows that the top row tiebacks decreased in load when the bottom row tiebacks were installed. According to Hansmire and Rawsley, once construction was completed, the tiebacks were locked off at the slurry wall as a rigid point, so, long term, all load loss is expected to be a result from anchor creep (Hansmire and Rawsley [18]).

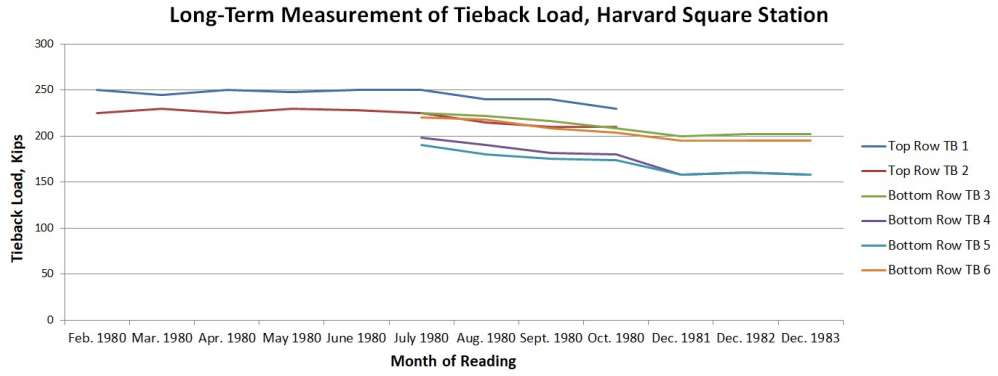

Figure 3.17: Long-Term Measurement of Tieback Load, Harvard Square (Hansmire and Rawsley [18])

3.4 Living Laboratory

A living laboratory (living lab) is a research concept that is used to eliminate the existing gaps between research and innovation/learning. A living lab can be characterized by a partnership between companies, universities, technological centers and/or government where users are focused on developing researches validated in real life environments (Almirall and Wareham 2010). [19]

A traditional lab user, most of the time, works as a spectator for testing products/services against requirements. In another words, traditional labs do not include hands-on opportunities for experimental learning where students can fully develop its learning. A living lab constitutes an experiential environment, where users are exposed to a creative social space and can design, explore and refine new policies and ideas (Schumacher 2013) [20], creating a more effective learning atmosphere for students.

According to Schumacher, a living lab works basically under four main activities: Co-creation, Exploration, Experimentation and Evaluation. Co-creation is related to the relationship between universities and real life, where research conducted at colleges can develop products and innovation to be used in real life scenarios. Exploration requires that all stakeholders are being incorporated in the research, including students, university, community, companies and the environment, for instance. Experimentation means that progress can only be made by testing and acquiring data. Finally, Evaluation includes the assessment of new ideas and concepts and its application in real life situations considering a variety of factors (Schumacher 2013) [20].

For civil engineering, living labs are crucial for developing new technologies, databases or innovative practices, but, mostly, living labs help the students acquire a better comprehension about several subjects because it provides more hands-on opportunities. Students have the opportunity to apply the concepts learned in class and are constantly challenged to come up with new ideas and solutions for real life problems.

In December 2013, a group of researchers created a conceptual framework to analyze four living labs in Europe, including three in Belgium and one in Finland. A living lab triangle was

developed as the basis for the analysis and evaluation of the four living labs. Figure 3.18 shows the living lab triangle (Veeckman, Schuurman, Leminen and Westerlund 2013 [21]).

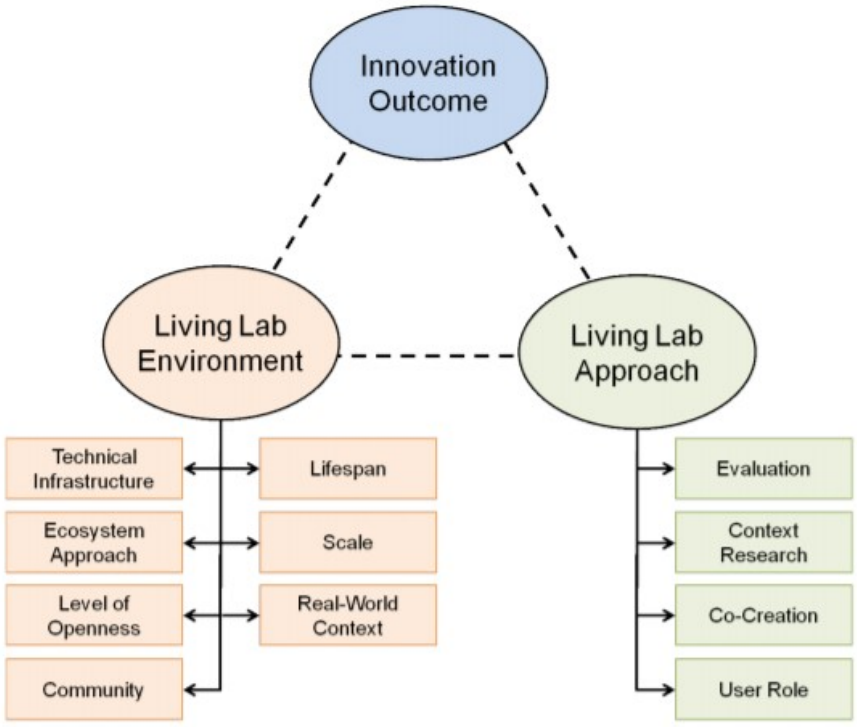

Figure 3.18: The Living Lab Triangle (Veeckman, Schuurman, Leminen and Westerlund 2013 [21])

Three pillars were used for this analysis; the first one is called the Living Lab Environment and includes the technical infrastructure, ecosystem approach, level of openness, community, lifespan, scale and real-world context. This pillar considers the accuracy of the lab, if there is an added value for all the partners involved in the lab, how the living lab helps the community, what drives users to participate in the lab, for how long the lab can be useful, what size the lab is and if it can be applied in a real-world context.

The second pillar takes into consideration the living lab approach including the evaluation, context research, co-creation and user role. This pillar evaluates if the test users are given the chance to analyze the lab critically and interact with researchers and developers. It also checks what the user role is. There are several different roles for the users in a living lab. According to the researchers in Europe, the user role should depend on the company's views for integrating the living lab and real world scenarios.

The third pillar considers the innovation outcome of the lab; this pillar analyzes if the living lab brings innovation to the real world and considers that its success is directly related to the innovation outcome. Some components were used to analyze and measure the level of innovation for each lab. It considers the amount of different participants in the network, what motivates the parties (e.g., companies, university, or community) to collaborate with the lab and what is the passion that drives the lab.

The three living labs studied in Belgium were FLELLAP (The Flemish Living Lab Platform), LeYLab and Mediatiun, while the one in Finland is called Laurea Living Labs Networks. Each main factor in the Living Lab Triangle was ranked from one to four in order to be evaluated where one represents the lowest score and four represents the highest score. In the end, it was possible to compare all four living labs and find their strengths and weaknesses.

4. PREDICTION OF WALL BEHAVIOR

The behavior of the highest portions of the retaining wall was predicted using common design methods and structural analysis procedures that can be accomplished without the need for specialized software. The purpose of the prediction was to compare the observed wall behavior with accepted design practice.

The limit equilibrium method used in the calculations included the use of apparent earth pressures for the full height wall and limit equilibrium analysis using active and passive earth pressures for several intermediate construction steps. Appendix B shows the calculation process to find the deflected shape of the highest section of the wall (piles P004 and P005) after construction was completed, two cases were used for each location, one assuming the soil as clay and the other one assuming the soil as sand. Appendix C shows the calculation process to find the deflected shape for the same two locations during two project milestones (excavation to the 11 foot depth and the 18 foot depth).

The use of apparent earth pressures to design retaining structures with multiple rows of tieback has been used since Peck (1969) proposed the concept 50 years ago and is a primary method of design today. This design was utilized to compare a common simple design method to the tieback load data and inclinometer data gathered during and after construction of the MU wall. This check was done just for the two piles located in the highest section of the wall, P004 and P005. The following paragraphs describe the calculation sequence for the P004 section of the wall considering the full depth (after construction was completed).

Initially it was necessary to find the soil data for the three soil types encountered during the SPT test (Appendix A). The top layer is classified as a Clay Soil (CL) with average SPT of 9 blow counts, the middle layer is classified as a Silty Sand (SM) material with average SPT of 20 blow counts and the bottom layer is classified as Silty Clay (CL-ML), for that layer the average blow counts was assumed as 52 to be conservative since that is the minimum N value for the layer. Table 2.1 shows the soil description, average blow counts and height for each layer.

Using solely the blow counts from the SPT test shown on Appendix A, it was possible to determine values for the cohesion, friction angle and unit weight based on the default geotechnical parameters for Clay and Sand. In addition, with all the soil properties, the active and passive lateral earth pressures were calculated. Table 4.1 shows the soil parameters for the three layers.

Table 4.1: Soil Parameters

Soil	Cohesion (psf)	Friction Angle (º)	Unit Weight (pcf)
Clay (CL)	1500	0	120
Silty Sand (SM)	0	32	120
Silty Clay (CL-ML)	100	26	125

The next step was to develop the earth pressure diagrams using the model described in the Geotechnical Engineering Circular No. 4 – Ground Anchors and Anchored Systems (U.S. Department of Transportation – Federal Highway Administration (FHWA) [22]). The method considers the soil as uniform (just one layer) and, since the location for the MU wall had three different soil layers, an assumption was needed in order to consider the soil as one uniform layer. The approach considered two cases, for case 1 (described in this section), the soil was assumed to be all clay, and for case 2, described only on Appendix B, all sand.

The earth pressure diagram was developed and is shown in Figure 4.1. T1 and T2 are the tieback loads that will be compared with the data from the load cells; R1 is the reaction from the soil in front of the wall below the maximum cut depth.

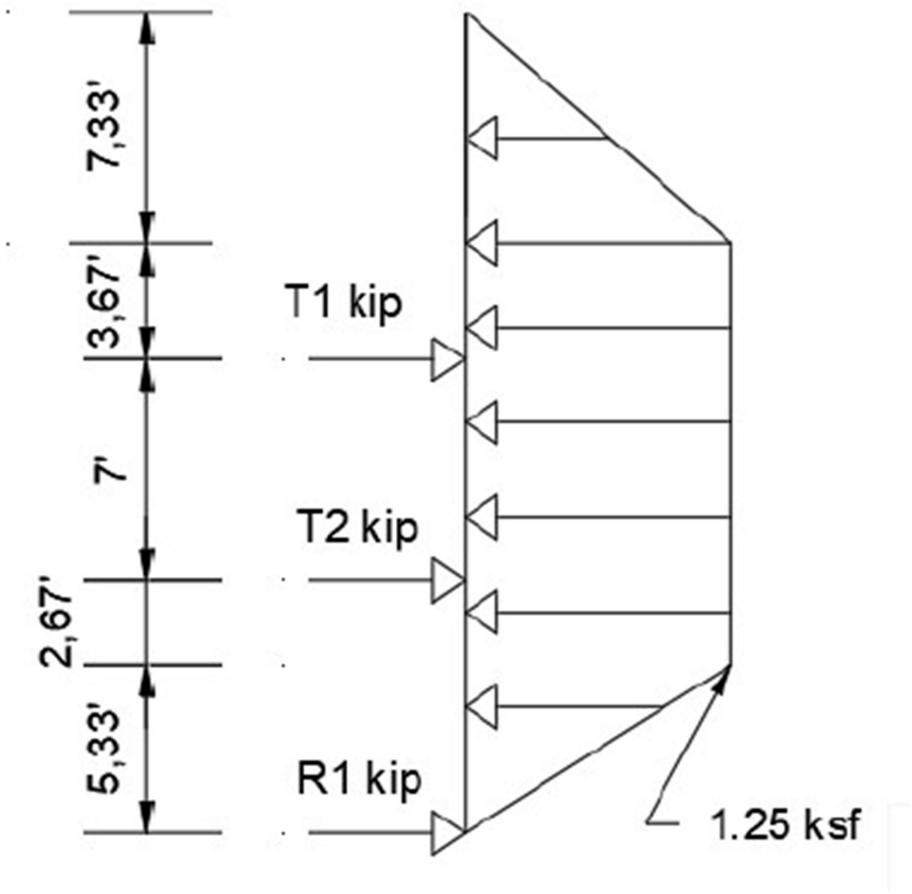

Figure 4.1: Apparent Earth Pressure Diagrams for Clay - Pile P004 – Full Depth

The next step was to calculate the applied forces, tieback loads and reactions. Using the tributary area method, the Tieback 1 load calculated was 101.4 kips and the Tieback 2 load was 68.6 kips. The reaction at the bottom of excavation was calculated and equal to 14.0 kips.

The following method was used to find the penetration depth, in general accordance with chapter 5.5.3 of the FHWA ground anchor manual [22]. The penetration depth is the length of pile below the maximum excavation depth to achieve horizontal force equilibrium with reaction 1 found in the previous step (14.0 kips). For this particular case, the penetration depth was 9.3 feet. FHWA recommended adding 20 percent to the value as a factor of safety, so the final penetration depth was equal to 11.1 feet. The final force diagram for pile P004 is shown in Figure 4.2.

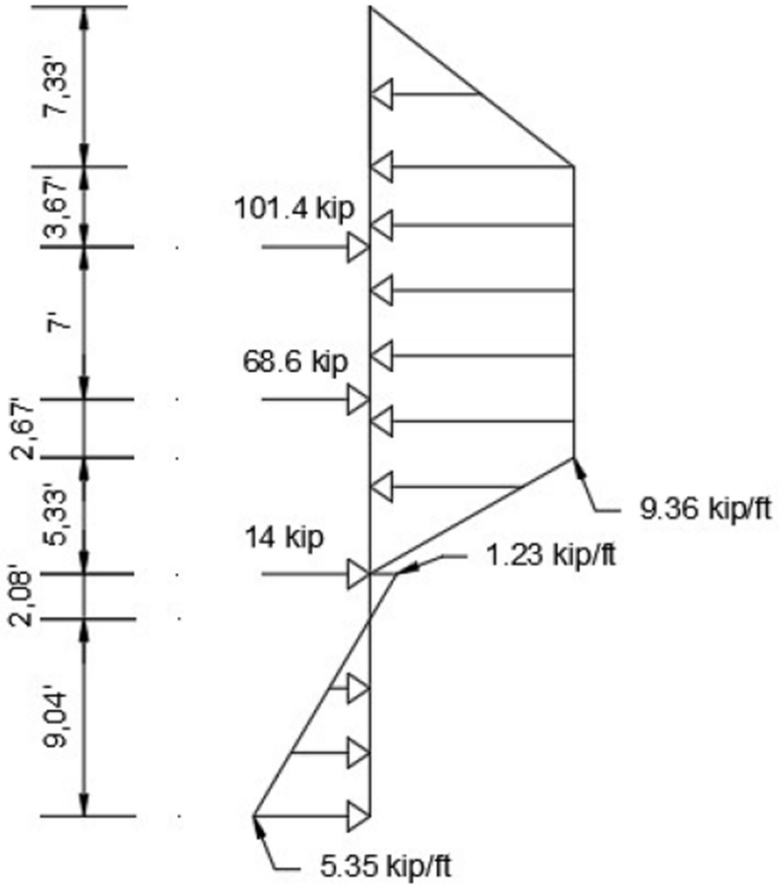

Figure 4.2: Earth Pressure Diagram for pile P004 – Clay – Full Depth

The next step was to find the moment diagram for the structure. It is possible to find the moment equations for each section of the structure using the earth pressure diagram, the moment equations were found manually from the top to the bottom of the structure at the depth Y and using the loads above this depth. The moment diagram was developed from the top to the bottom of the structure, starting at the 0 foot depth and going to the toe. An excel spreadsheet created using a 0.1 feet depth increment in order to generate the moment diagram for this scenario.

Figure 4.3 shows the moment diagram for pile P004 considering the soil as clay for the full depth of excavation.

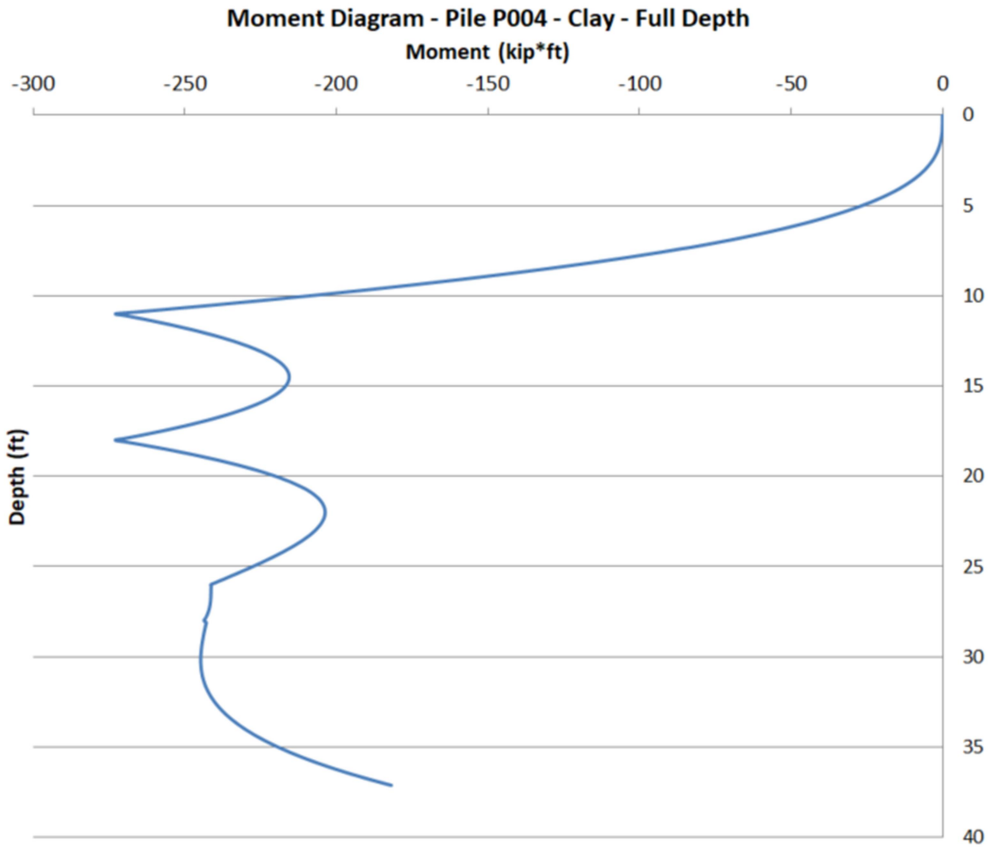

Figure 4.3: Moment Diagram for pile P004 - Clay - Full Depth

Finally, the deflected shape was calculated using the trapezoidal approximation using a three step process to go from moment to deflection. The first step is to find the curvature of the moment diagram, that value can be found simply by dividing the moment value at each depth by the Young's Modulus (E = 29000ksi) and the Moment of Inertia (I = 393 in^4). The second step is the transition from curvature to slope, for that, it is necessary to find the area of the curvature for each increment assuming the shape is trapezoidal; this process starts from the bottom of the pile assuming the slope at the toe is zero. The last step is the transition from slope to deflection, this process used the same technique as the one going from the curvature to the slope and it assumes the deflection at the toe of the wall is zero.

Three methods were used in order to validate the results from the excel spreadsheet. Initially, the moment diagram and deflected shape for two known structures were developed; the structures selected were a cantilever column with a point load and a cantilever column with a uniform load. In addition, a Mathcad spreadsheet was developed using the Mohr Theorems to find the deflected shape, for this case, the moment diagram was drawn on AutoCAD to scale since the theorems use the moment area and distance from the centroid to the desired point in order to find the deflection at that point. The Mathcad spreadsheet using the Mohr Theorems was used to find the deflected shape of the two known structures (cantilever beam with point load or uniform load) and the deflected shape for the 11 foot excavation. Lastly, the earth pressure diagrams of all the six structures (pile P004 clay and sand, pile P005 clay and sand, 11 foot excavation and 18 foot excavation) were uploaded to a structures software in order to check if the moment equations input in the excel spreadsheet were correct. The results from the validation

checks are shown on Appendix D, an example of the excel spreadsheet used for the design is shown on Appendix E and the structural check is shown on Appendix E.

Figure 4.4 shows the prediction of the deflected shape for the pile P004 after construction assuming the soil as clay.

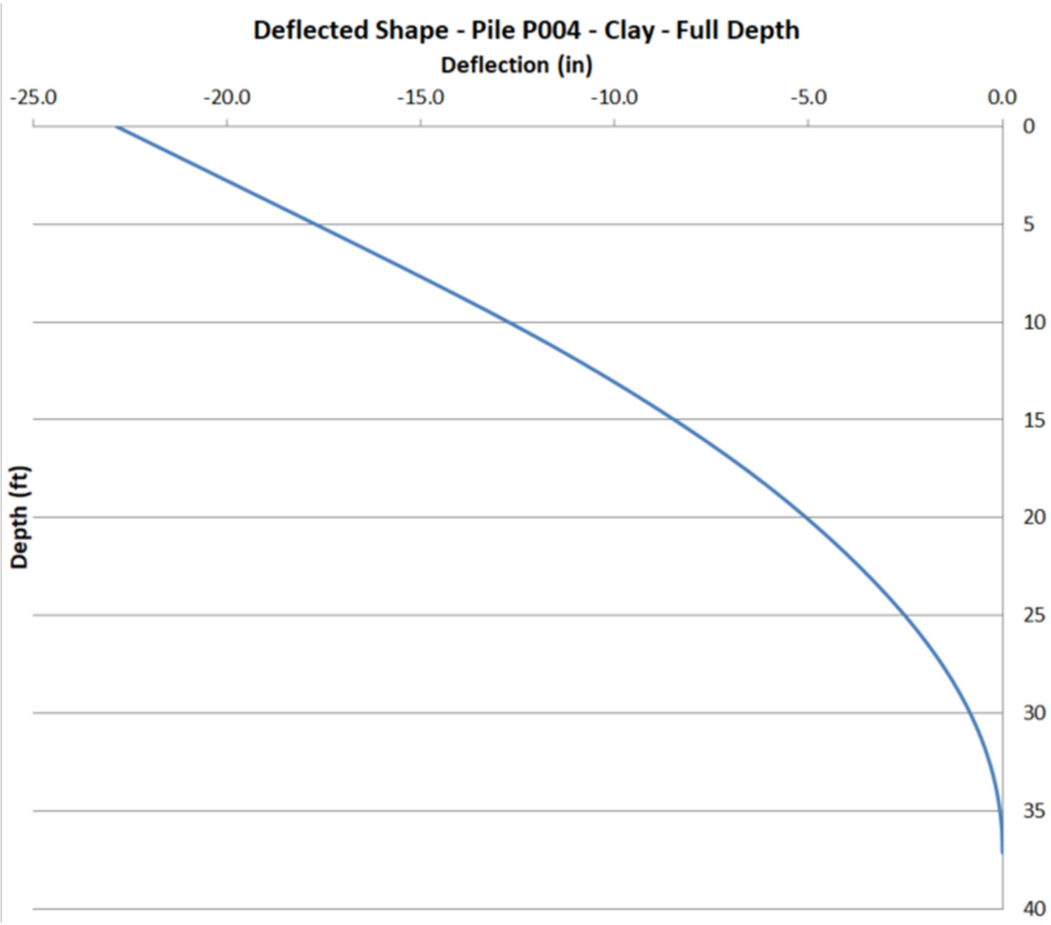

Figure 4.4: Deflected shape for pile P004 – Limit Equilibrium Method – Clay – Full Depth

The process described above was repeated for the remaining full-depth cases, as described in Appendix B. Appendix B shows the four calculation predictions for the deflected shape after

construction was completed, with two predictions for pile P004 (sand and clay) and two for pile P005 (sand and clay). The deflected shapes are also shown below for the other three cases.

Figure 4.5 shows the deflected shape for pile P004 assuming the soil as sand for the full depth stage.

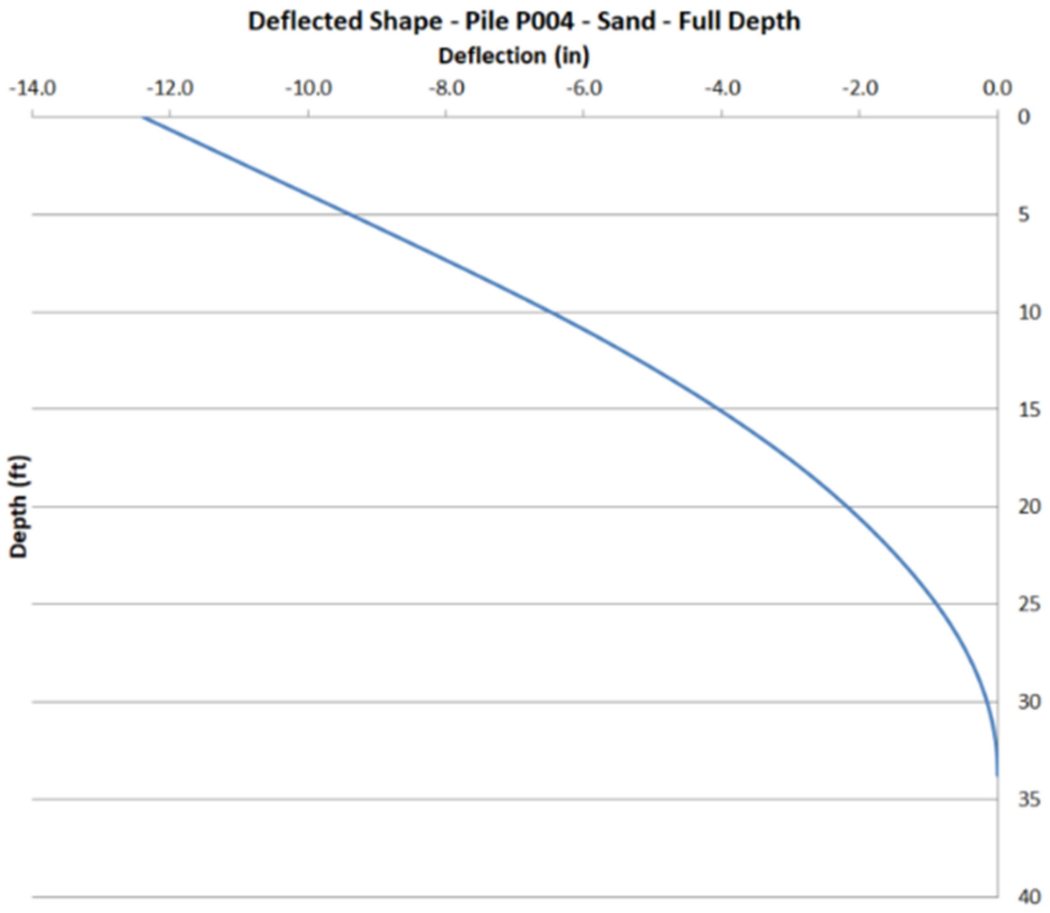

Figure 4.5: Deflected shape for pile P004 – Limit Equilibrium Method – Sand – Full Depth

Figure 4.6 shows the deflected shape for pile P005 assuming the soil as clay for the full depth stage.

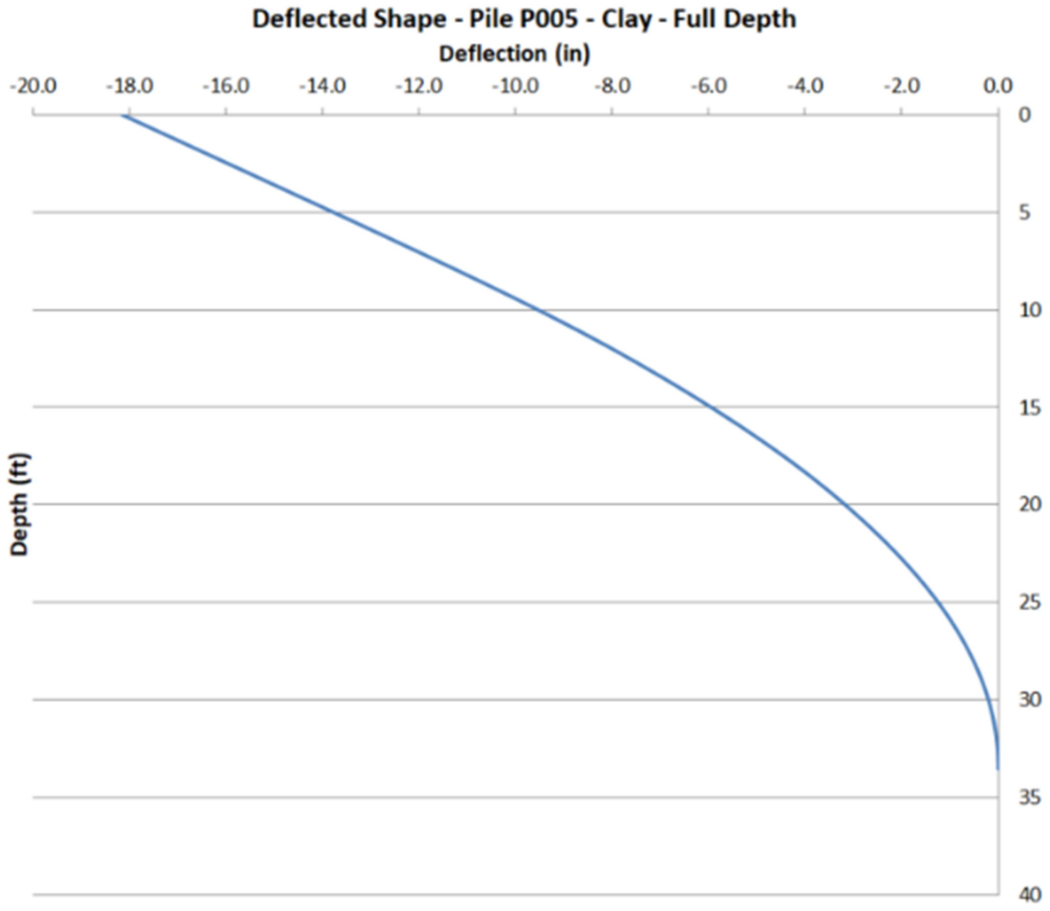

Figure 4.6: Deflected shape for pile P005 – Limit Equilibrium Method – Clay – Full Depth

Figure 4.7 shows the deflected shape for pile P005 assuming the soil as clay for the full depth stage.

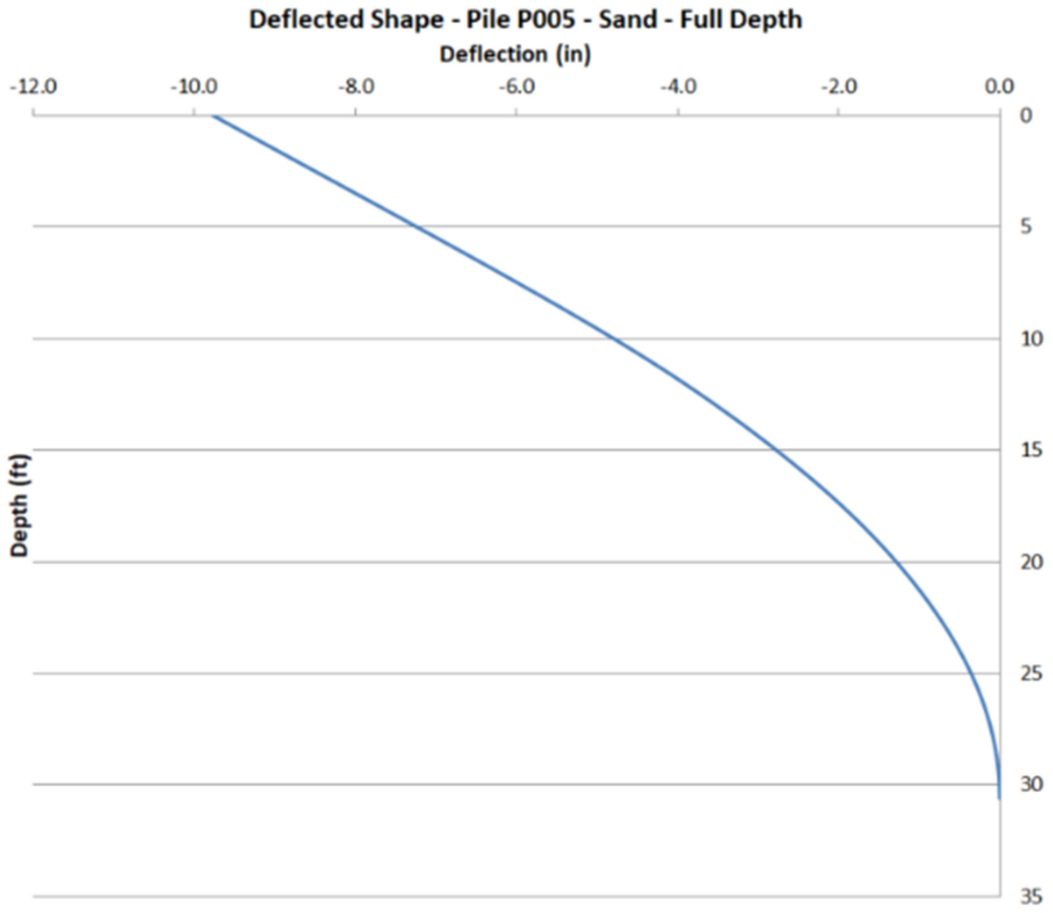

Figure 4.7: Deflected shape for pile P005 – Limit Equilibrium Method – Sand – Full Depth

The depths selected for prediction of behavior during intermediate construction scenarios were the maximum cut depths before each level of tieback was installed (11 feet and 18 feet). Therefore, the 11-foot depth was a cantilevered wall without tieback support, and the 18-foot depth included a single row of tiebacks. Because there were not multiple rows of tiebacks for either of the two intermediate scenarios, analysis using apparent earth pressures was not

appropriate. Instead, these cases were evaluated using active and passive earth pressures in a limit-equilibrium analysis, in general accordance with the method shown in sections 25.3 and 25.4 of the Foundation Design book (Coduto [23]).

The main difference between the apparent earth pressure method and the active and passive earth pressure with limit-equilibrium analysis is on the approach to find the earth pressure diagram for the structure. The second method can take into consideration multiple layers in order to find the earth pressures and it uses the moment and force equilibrium to find the embedment depth. The earth pressure and moment diagrams for the 11 foot excavation depth are shown below as an example. Figure 4.8 shows the apparent earth pressure for pile P004 and P005 for the 11 feet excavation depth.

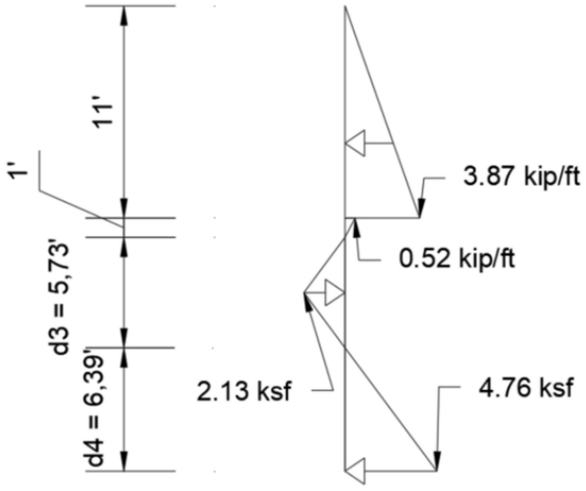

Figure 4.8: Earth Pressure for piles P004 and P005 – Limit Equilibrium Method - 11 feet Excavation

Figure 4.9 shows moment diagram for pile P004 and P005 for the 11 feet excavation depth.

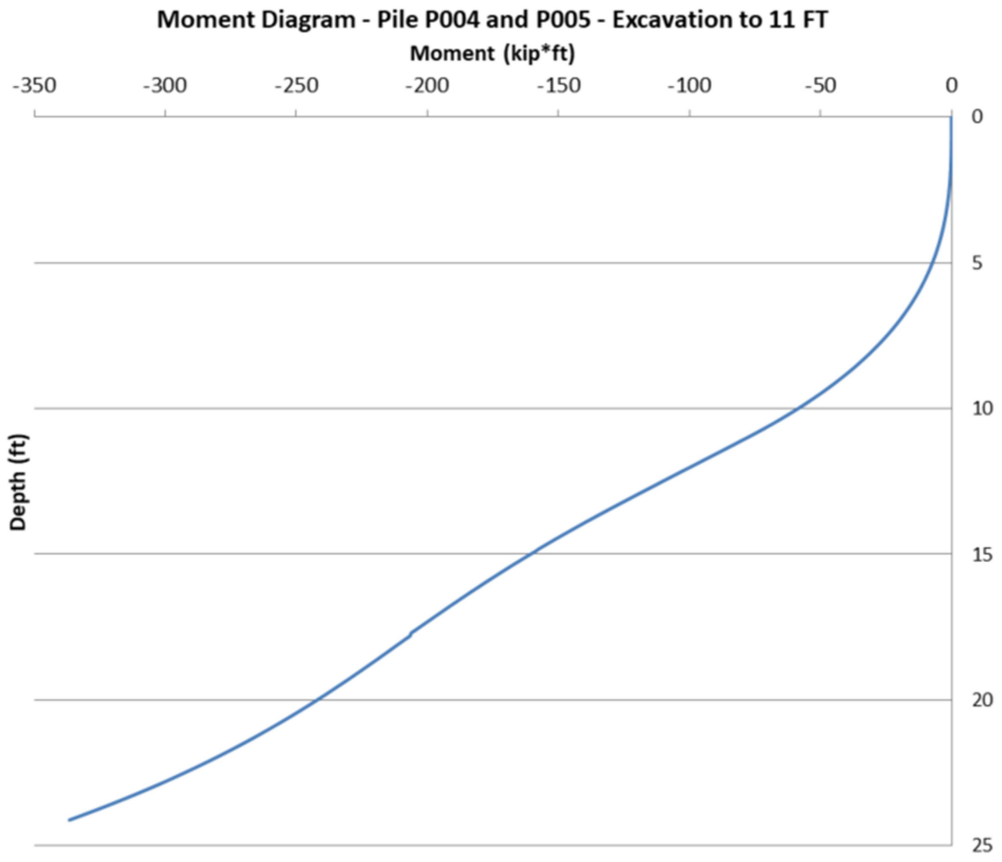

Figure 4.9: Moment Diagram for piles P004 and P005 - Limit Equilibrium Method - 11 feet Excavation

Appendix C shows the detailed calculations for two project milestones at piles P004 and P005. All the predicted deflected shapes are also shown below. Figure 4.10 shows the deflected prediction for pile P004 for all the three excavation stages considered.

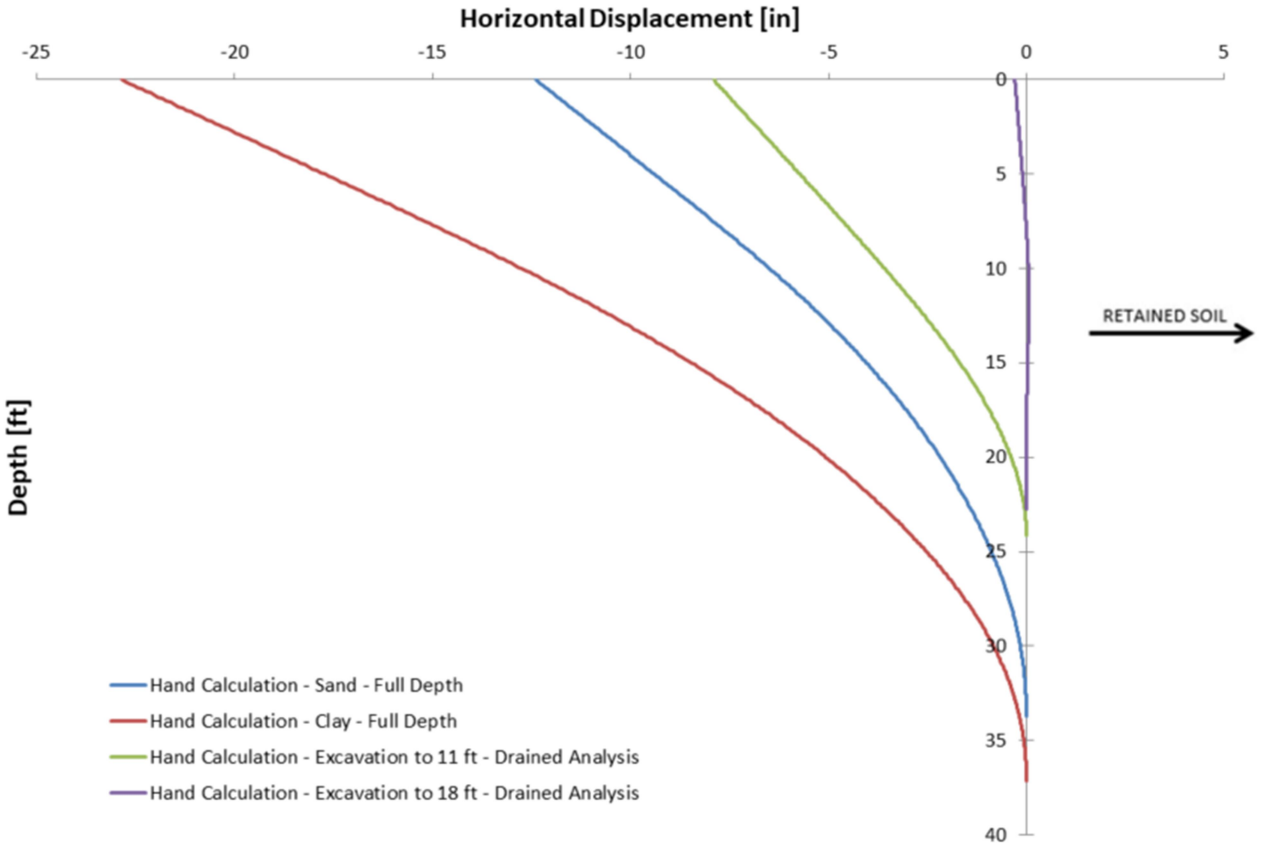

Figure 4.10: Deflected shape for pile P004 – Limit Equilibrium Method

Figure 4.10 Figure 4.11 shows the deflected prediction for pile P005 for all the three excavation stages considered.

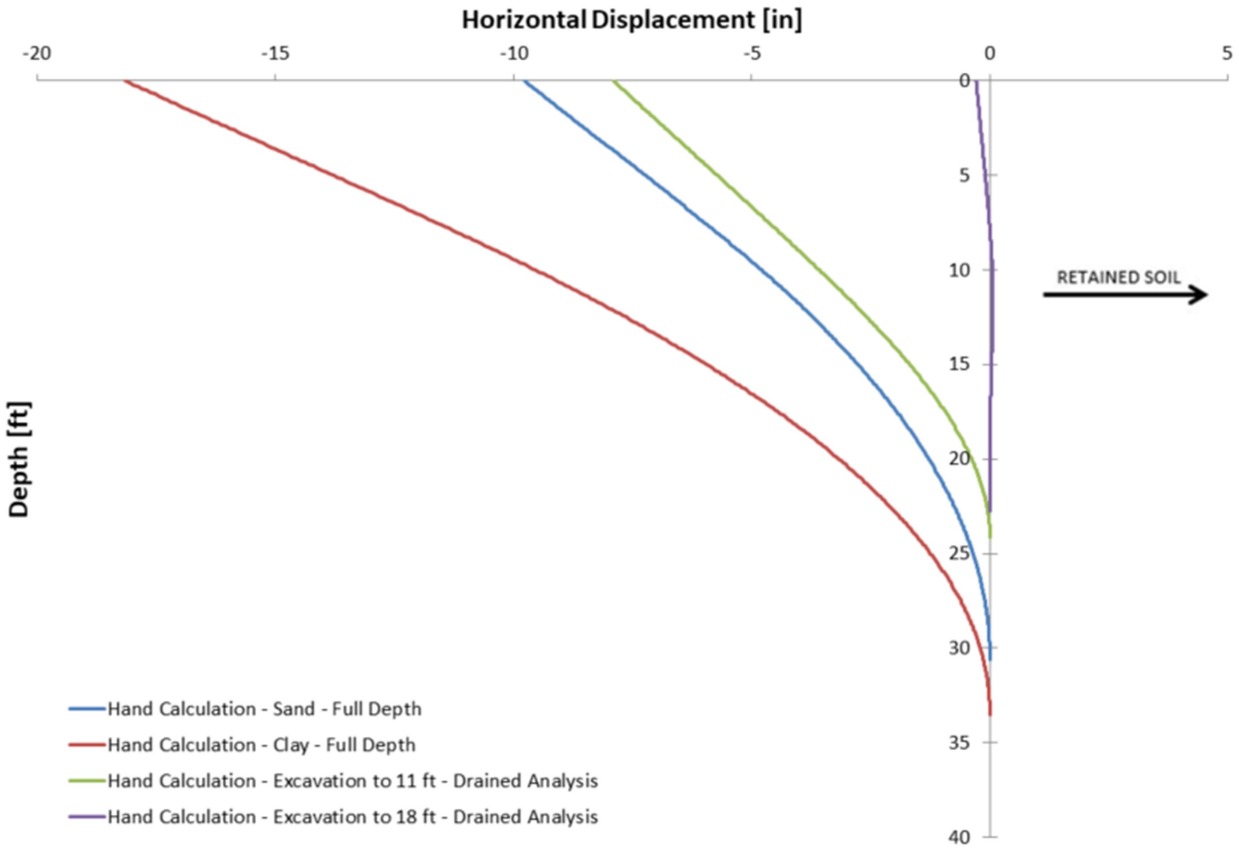

Figure 4.11: Deflected shape for pile P005 – Limit Equilibrium Method

5. EXPERIMENTAL METHODS

To monitor the retaining wall performance, four wall locations were instrumented (near of P004, P005, P021, and P026) as shown in Figure 5.1. Instrumentation included inclinometer casing installed within and behind the wall, load cells on the tiebacks, survey monitoring points, and a groundwater level monitoring well. Table 5.1 shows the pile length, the wall height and the number of tiebacks at the four locations instrumented.

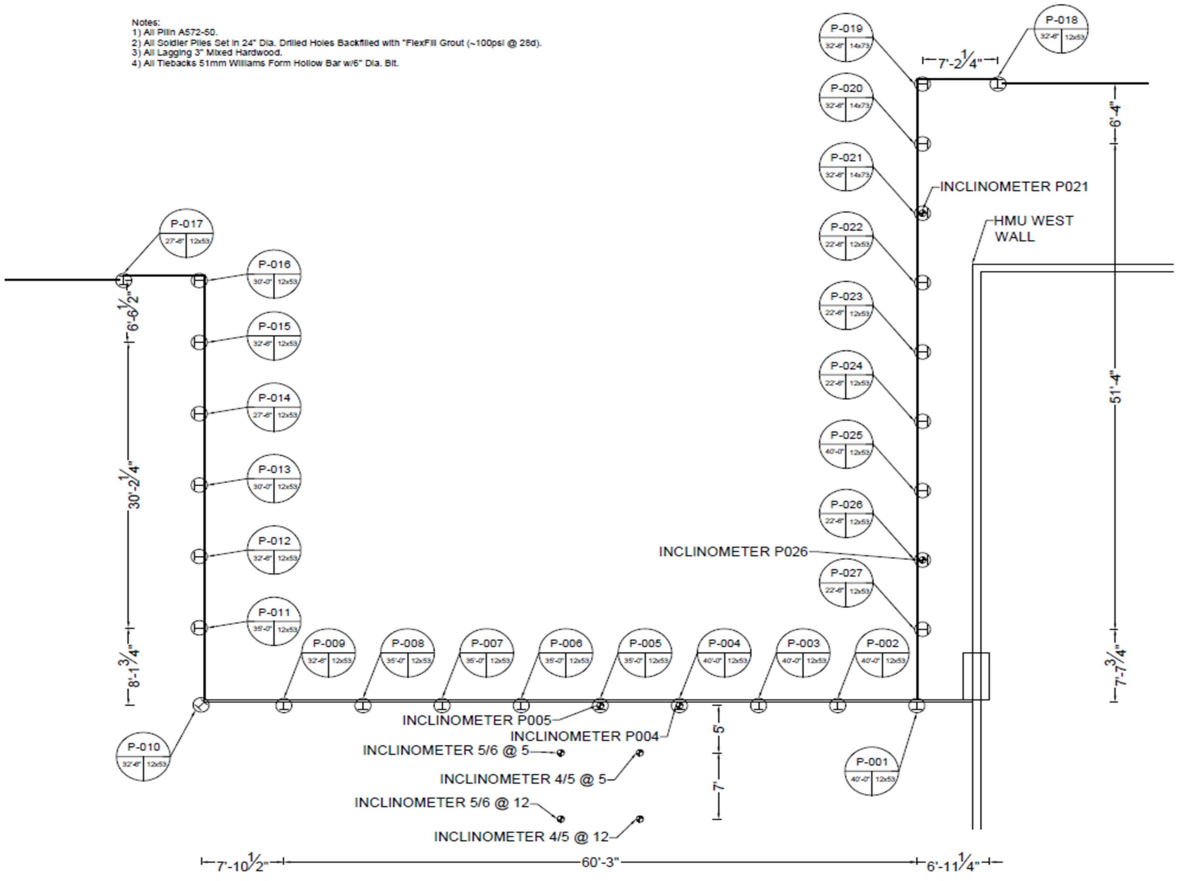

Figure 5.1: Plan View of the Retaining Wall

Table 5.1: Wall Height and Number of Tiebacks

Pile	Pile Length (ft)	Wall Height (ft)	Number of Tiebacks
P004	40	26	2
P005	35	22	2
P021	32.5	11	1
P026	22.5	11	1

PVC inclinometer casing was installed at distances of 5 feet and 12 feet behind the face of the wall at P004 and P005 prior to construction. The vertical casing was installed to depths of approximately 30 feet below the ground surface behind the highest portion of the structure to monitor the soil movement behind the wall. To monitor the lateral deflection of the soldier piles at the four instrumented cross-sections, a square channel was welded to the soldier piles to serve as inclinometer casing; Figure 5.2 shows the location of angle iron used for inclinometer casing on soldier piles.

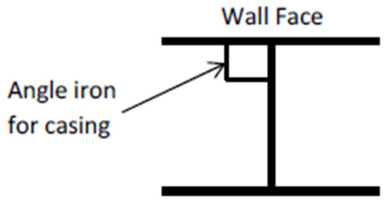

Figure 5.2: Location of Angle Iron

After the installation of all the required equipment for monitoring displacement in the pile and in the soil, an inclinometer was used to read tilt data prior to excavation and periodically during construction milestones. The data was analyzed using the DigiPro2 software (Durham Geo Enterprises 2018 [24]). Due to the construction sequence and available space at the site, the

steel channel was installed square to the face of the soldier piles (Figure 5.2), so the inclinometer readings were taken at a 45-degree angle to the predominant direction of wall movement. Therefore, post-processing of the data was necessary to determine wall deflection perpendicular to the wall face.

Load cells (Figure 5.3) were installed to obtain the loads from a total of six tiebacks in the four different instrumentation sections (2 tiebacks each at P004 and P005, and one tieback each at P021 and P026) during and after construction. The load cells were left in place and data could still be gathered.

Figure 5.3: Load Cell Installed at a Tieback

The contractor conducted tieback performance tests on two tiebacks and proof tests on the remaining tiebacks. All the tiebacks were B7X1-51 hollow bars with a yield strength of 85 ksi and 1.795in^2 cross-sectional area. The bond zone diameter was 6 inches. Figure 5.4 shows the load vs. displacement curve for the pile P004 tieback number 1. Its design load was 91.5 kips with a bond length of 55 feet and an unbonded length of 15 feet. Figure 5.5 shows the load vs. displacement curve for the pile P005 tieback number 1. Its design load was 78 kips with a bond length of 45 feet and an unbonded length of 15 feet.

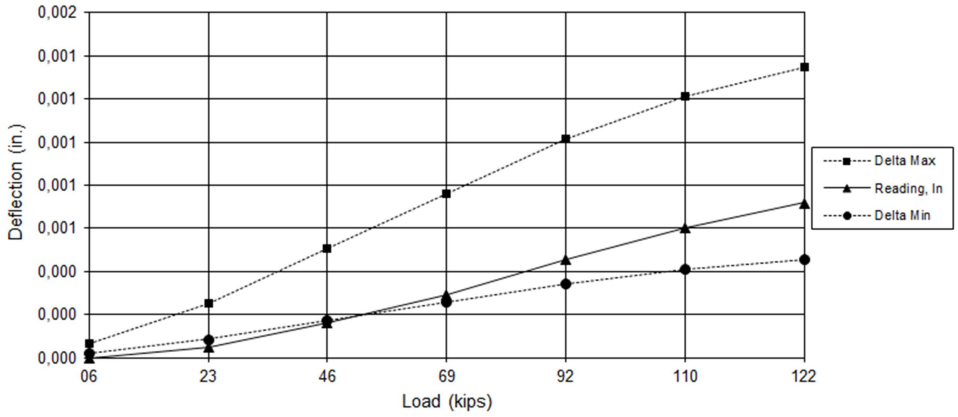

Figure 5.4: Load vs. Deflection Curve for Pile P004 Tieback 1 Performance Test

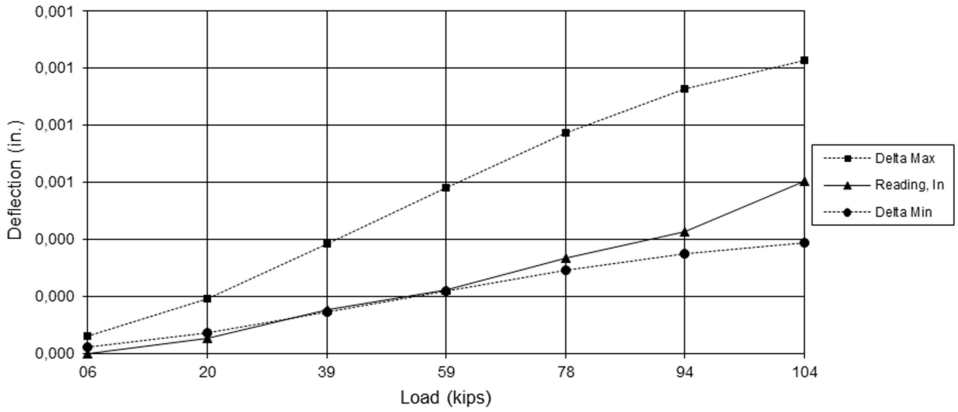

Figure 5.5: Load vs. Deflection Curve for Pile P005 Tieback 1 Performance Test

In both cases, the data shows that the tiebacks were approved during the performance tests by achieving a capacity of at least 133 percent of the design load. In addition, the load-deflection curve plots between the Delta Max and Delta Min curves; therefore, both tiebacks met the test criteria.

The instrumentation installed can also provide other information such as surface movement and water level data that will not be discussed in this thesis. Its main focus is to evaluate soil

displacement and tieback loads during and shortly after construction, as well as to explore how the project can improve student learning. The results, all data gathered, and graphics can be found in the results section of the thesis. All the discussion and analysis of the data is located in the discussion section, which also provides suggestions and debates about how to enhance student performance.

6. EXPERIMENTAL RESULTS

6.1 Inclinometer Monitoring

Lateral displacement monitoring was completed using data collected from four piles: P004, P005, P021, and P026. Lateral displacement of the retained soil was also monitored at four locations, at distances of 5 feet and 12 feet behind the wall face, between piles P004 and P005 and piles P005 and P006, as shown in Figure 5.1.

For all of the inclinometer plots (Figure 6.1 - Figure 6.8), the direction of wall excavation is to the left. The construction sequence was shown previously in Table 2.3 (page 12) helps with the comprehension of the profile change and earth movement. This data was plotted in the figures using a horizontal line in the left to show the excavation depth when the respective set of data was collected; excavation and respective set of data have the same color. The figures also show the tieback position, its color matches with the set of data collected right after its installation.

Figure 6.1 shows the profile change at pile P004. For this pile, the first set of data is the initial position of the wall, assumed to be vertical to show the relative movement with time better, and it was collected on July 29th of 2016. The last set of data was collected on October 10th of 2016, totaling 12 readings. The location of both tiebacks and the elevation at the base of the wall are also shown.

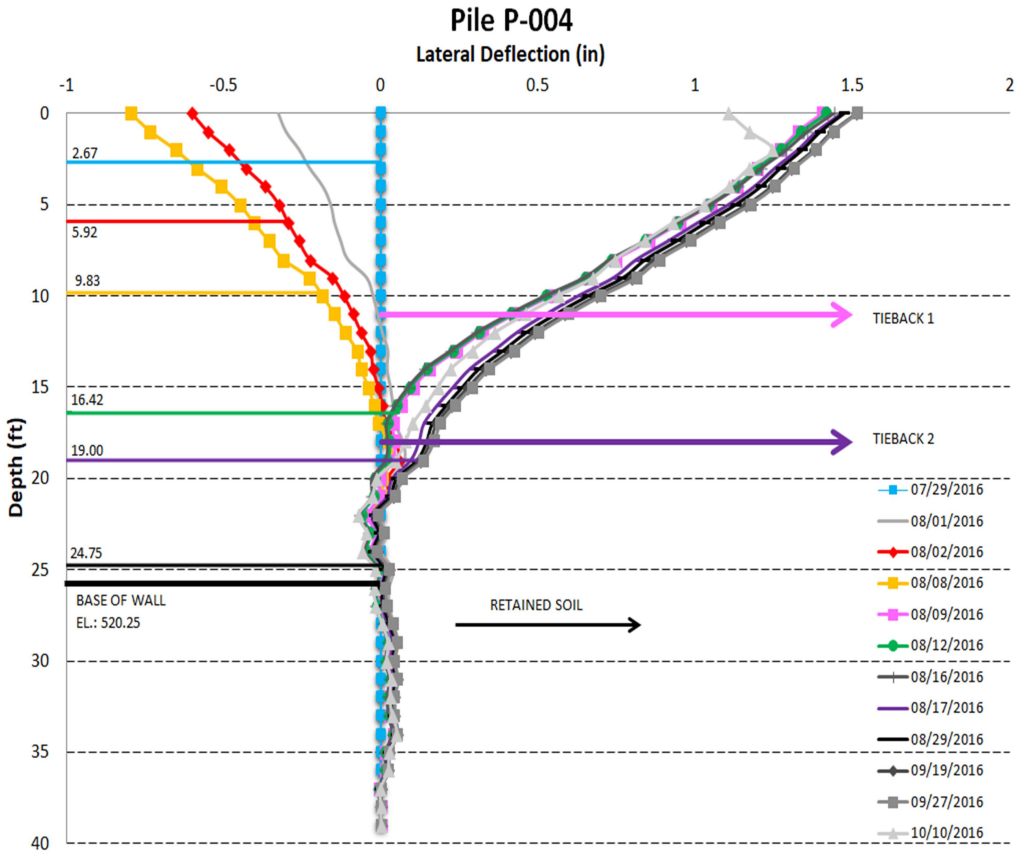

Figure 6.1: Profile Change for Pile P004

Figure 6.2 shows the profile change at pile P005, this data was also collected from July 2016 to October 2016 and it has 12 readings in total. The first reading is the initial position of the wall, assumed to be vertical to show the relative movement with time better. The locations for Tiebacks 1 and 2 can be seen in the figure and also the elevation at the base of the wall.

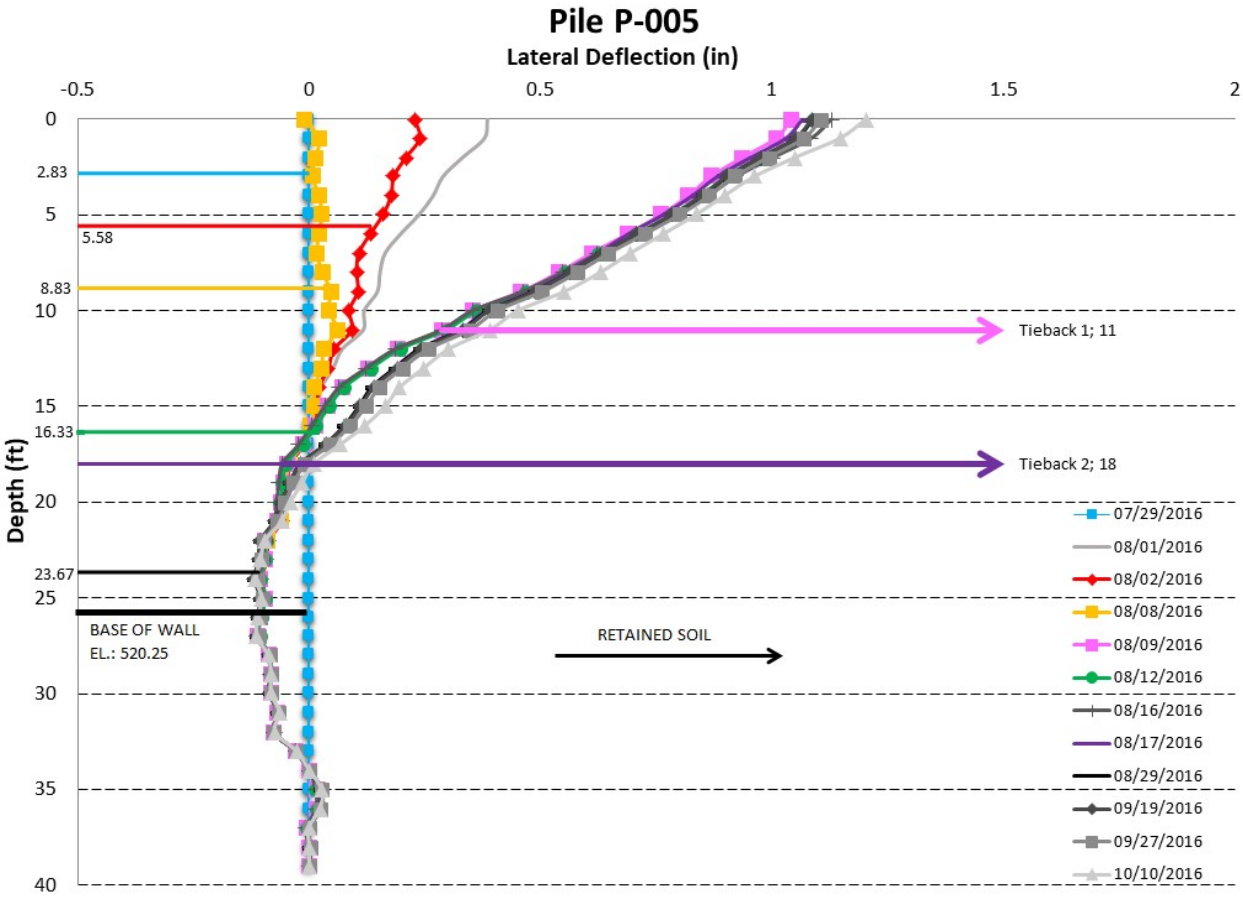

Figure 6.2: Profile Change for Pile P005

Figure 6.3 shows the profile change for pile P021. The first set of data, showing the initial position of the wall assuming to be vertical to show relative movement with time better, was collected on August 19th of 2016. The last one was on October 21st of 2016. The figure shows the date for each of the 8 readings, the position of Tieback 1 and the elevation at the base of the wall.

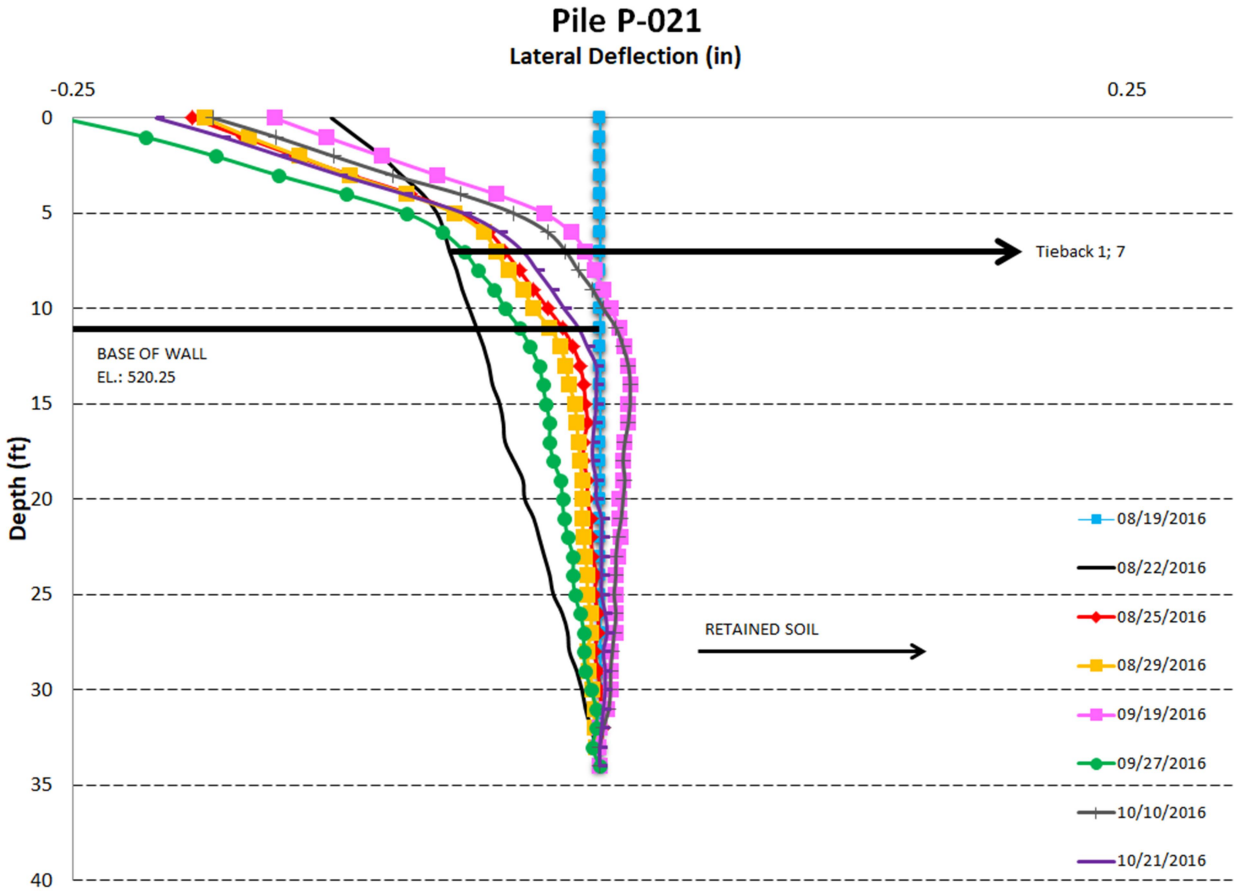

Figure 6.3: Profile Change for Pile P021

Figure 6.4 shows the profile change for pile P026, the first set of data, initial position of the wall assuming to be vertical to show the relative movement with time better, was collected on August 17th of 2016 and the last one on October 10th of 2016, totaling 8 readings. The elevation at the base of the wall and the location for Tieback 1 can be seen in the figure.

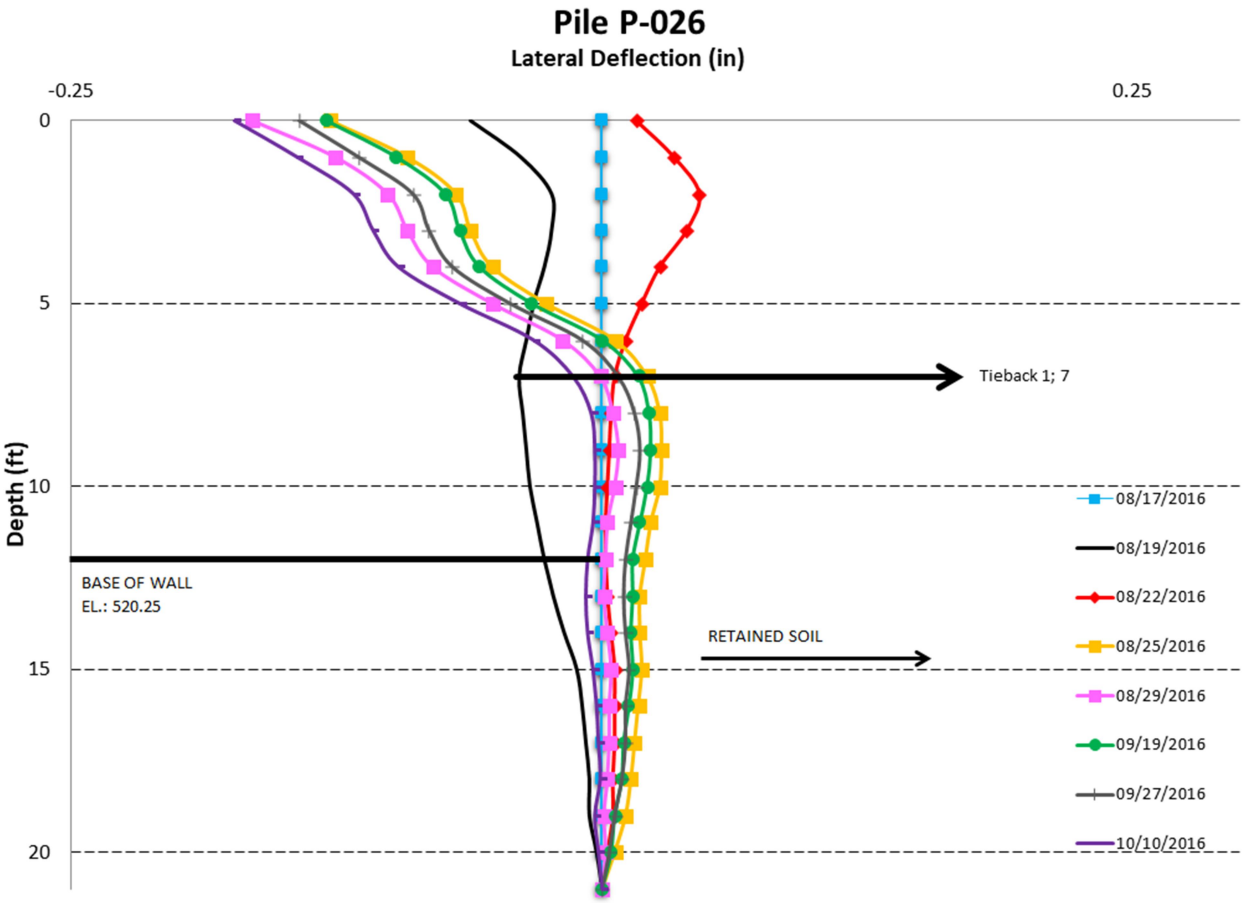

Figure 6.4: Profile Change for Pile P026

Figure 6.5 shows the profile change for the soil located 5 feet behind the wall between piles P004 and P005 (P4/5@5). It shows a total of 9 readings, the depth of the two tiebacks installed in the area and the elevation at the base of the wall. The first reading was assumed to be vertical to show the relative movement with time better. It is important to mention that landscaping activities might have bumped or knocked around the inclinometer casing, causing unexpected movement in the last two readings.

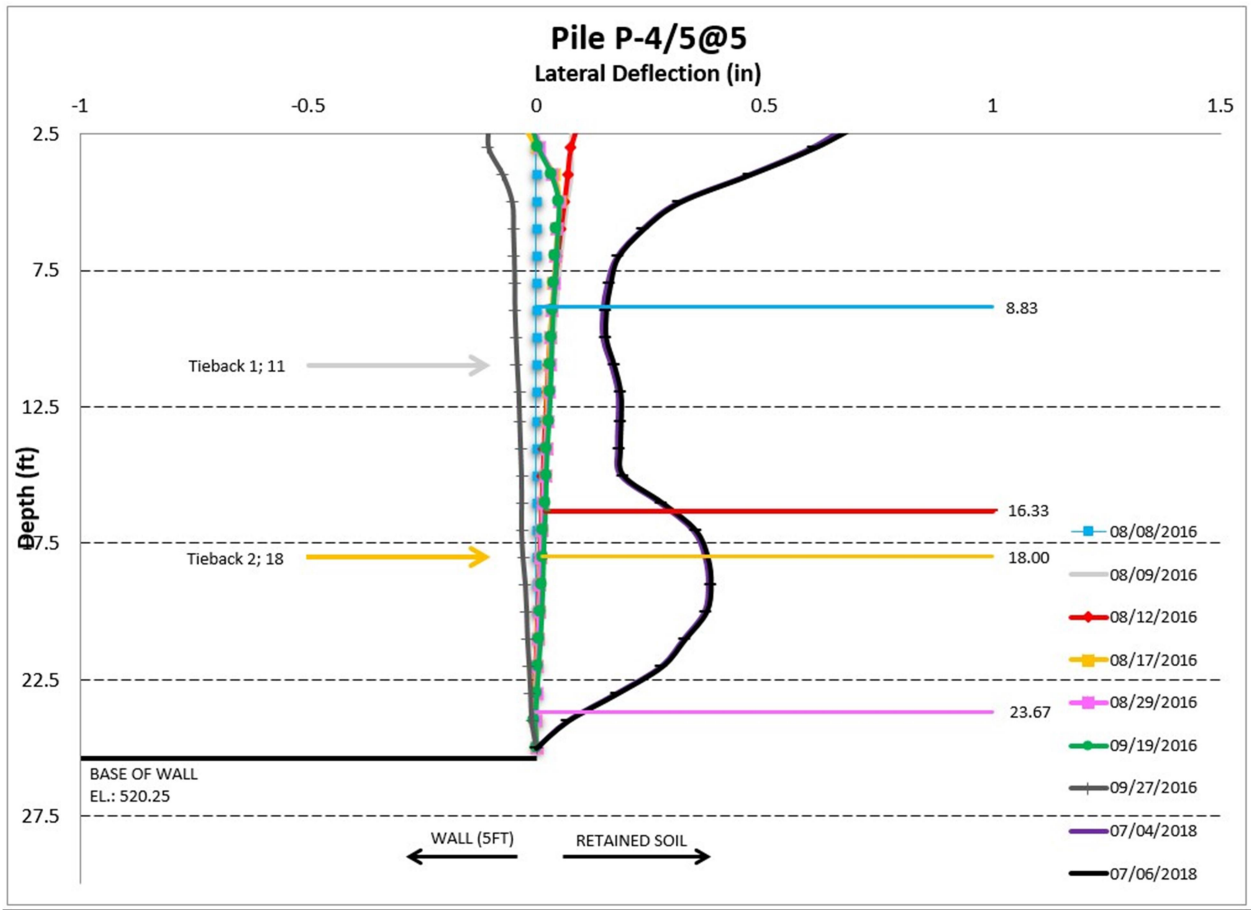

Figure 6.5: Profile Change at P4/5@5

Figure 6.6 shows the eight readings for the profile change at the soil located 5 feet behind the wall between piles P005 and P006 (P5/6@5). It also shows the depth for the two tiebacks installed in the area and the elevation at the base of the wall. The initial reading was assumed to be vertical to show the relative movement with time better. It is important to mention that landscaping activities might have bumped or knocked around the inclinometer casing, causing unexpected movement in the last two readings.

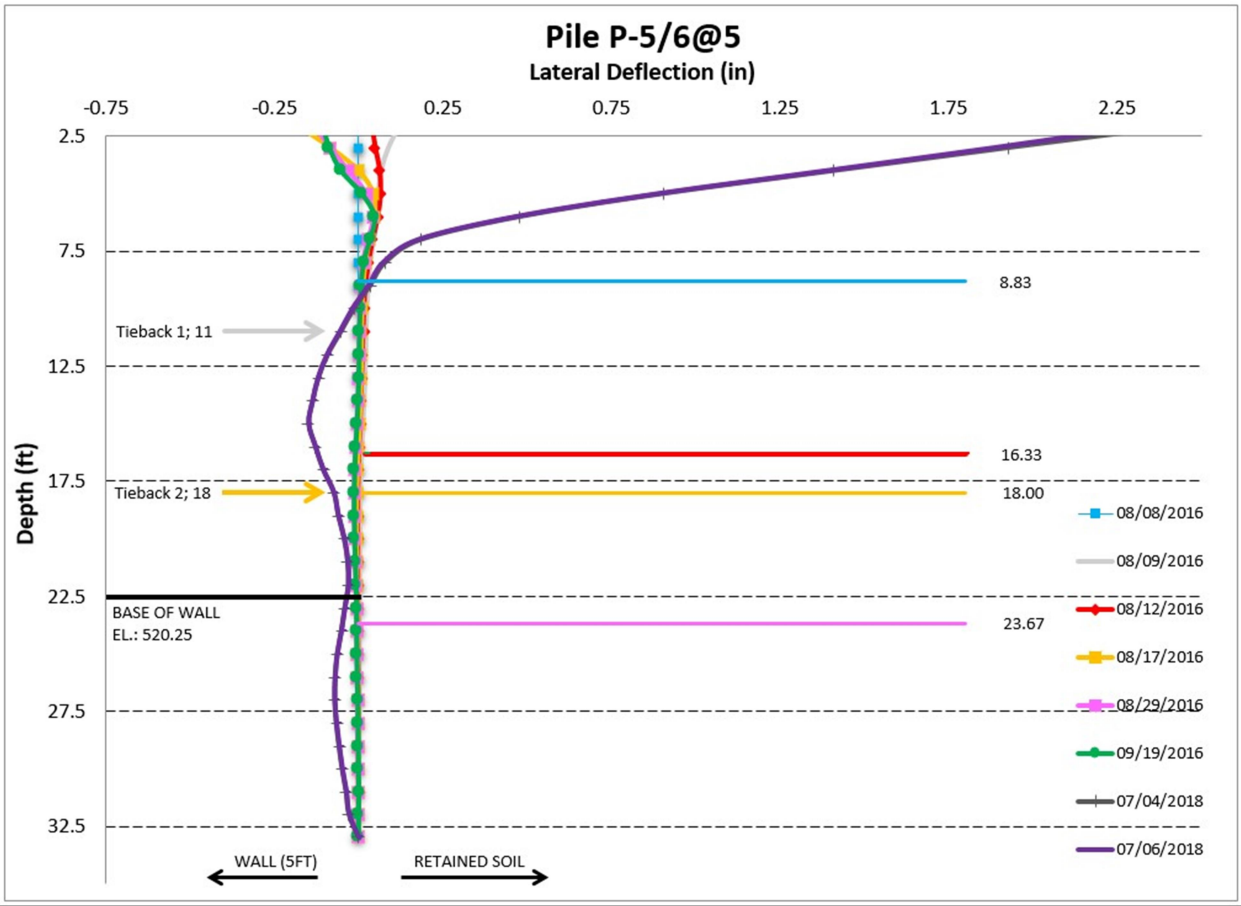

Figure 6.6: Profile Change at P5/6@5

Figure 6.7 shows the profile change for the soil located 12 feet behind the wall between piles P004 and P005 (P4/5@12). It has seven readings, shows the elevation at the base of the wall and the depth for the tiebacks located in the area. The initial reading was assumed to be vertical to show the relative movement with time better. It is important to mention that landscaping activities might have bumped or knocked around the inclinometer casing, causing unexpected movement in the last two readings.

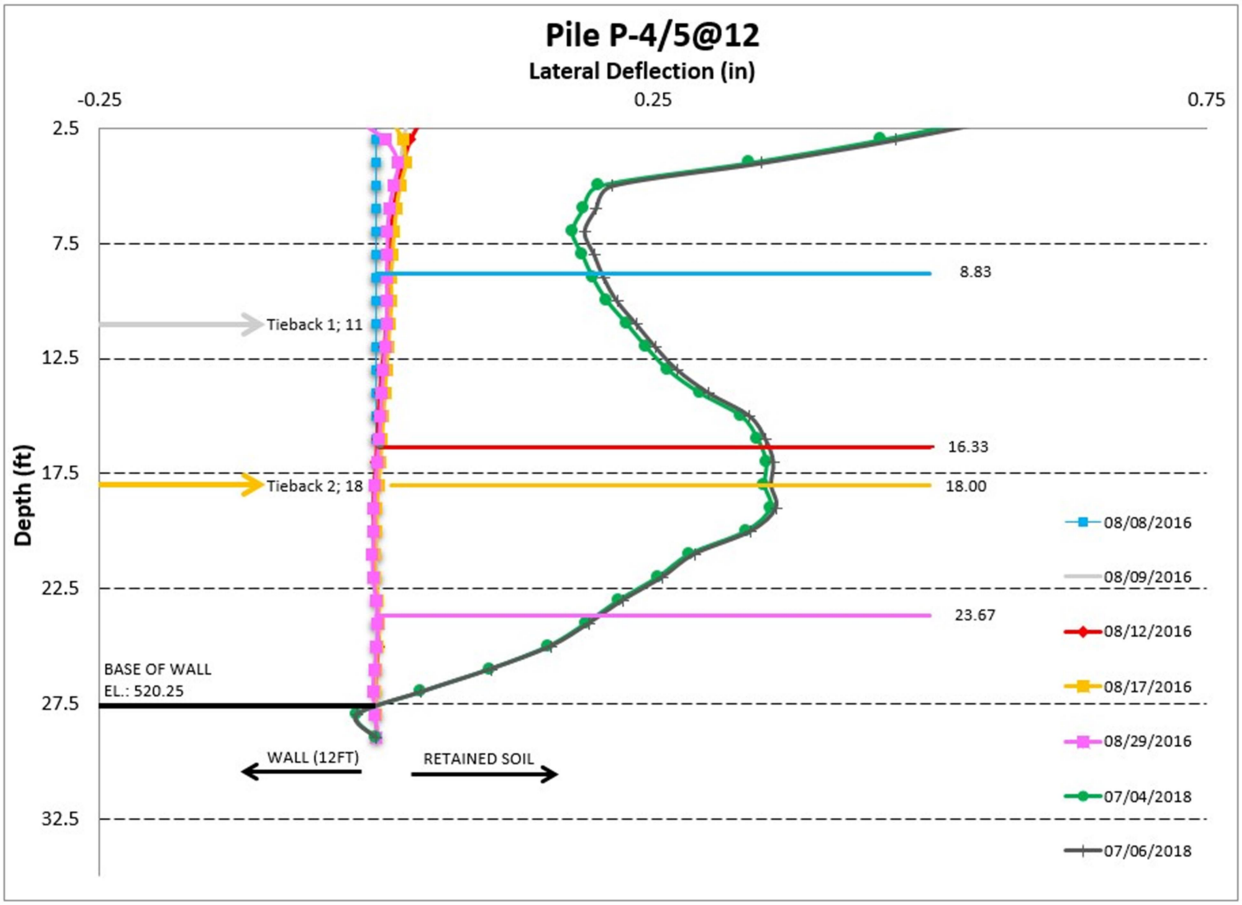

Figure 6.7: Profile Change at P4/5@12

The profile change for the soil located 12 feet behind the wall between piles P005 and P006 (P5/6@12) is shown in Figure 6.8. It can be seen in the picture the location for the two tiebacks installed in the area and the elevation at the bottom of the wall. The initial reading was assumed to be vertical to show the relative movement with time better.

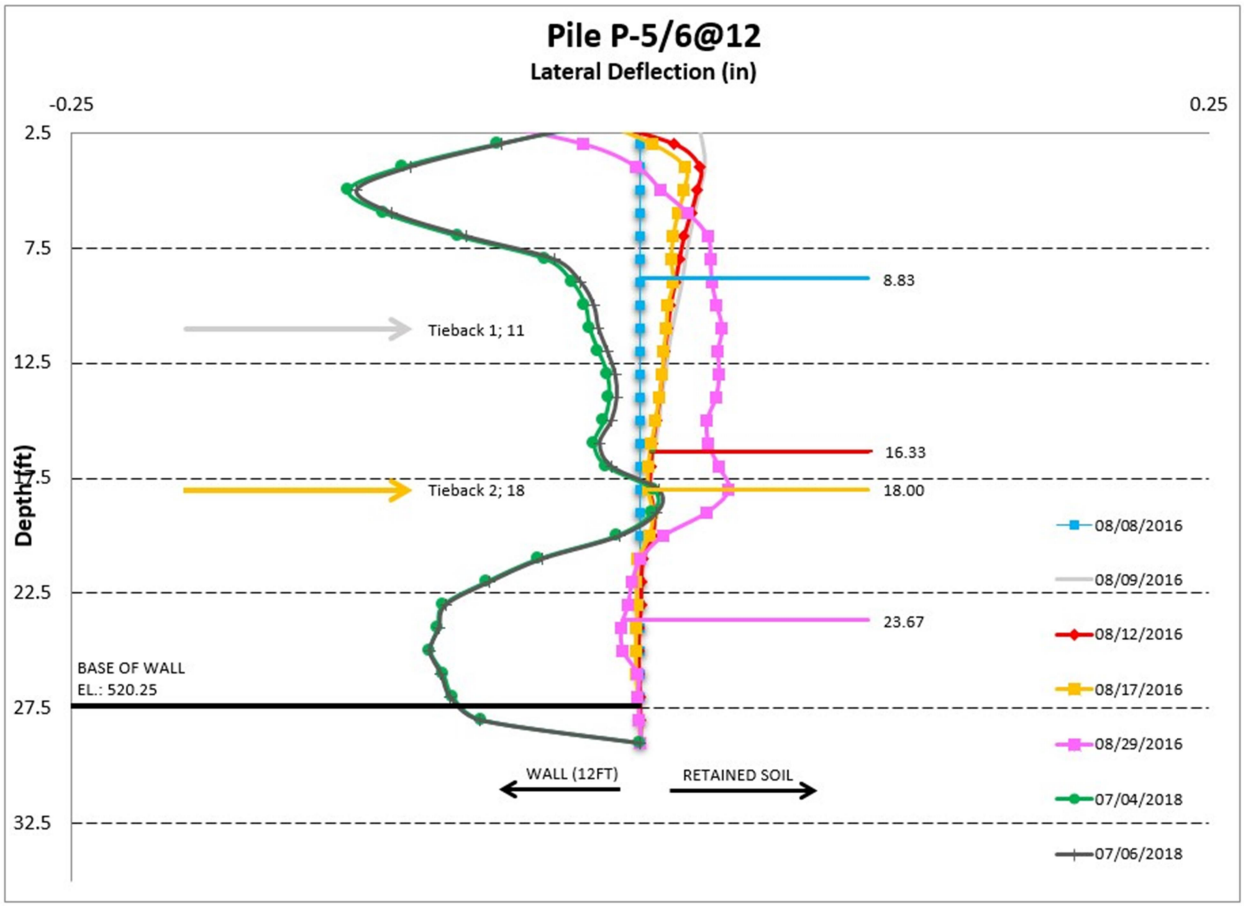

Figure 6.8: Profile Change at P5/6@12

6.2 Load Cell Monitoring

With the load cells installed at four different piles, it was possible to analyze the tieback loads over time for piles P004, P005, P021, and P026. Figure 6.9 shows the load vs. time plot. Pile P004 has two tiebacks; the design load for tieback 1 was 91.5 kips and 70 kips for tieback 2. Pile P005 also has two tiebacks; the design loads were 78 kips and 51 kips for tiebacks 1 and 2, respectively. Piles P021 and P026 have one tieback each with a design load of 57 kips.

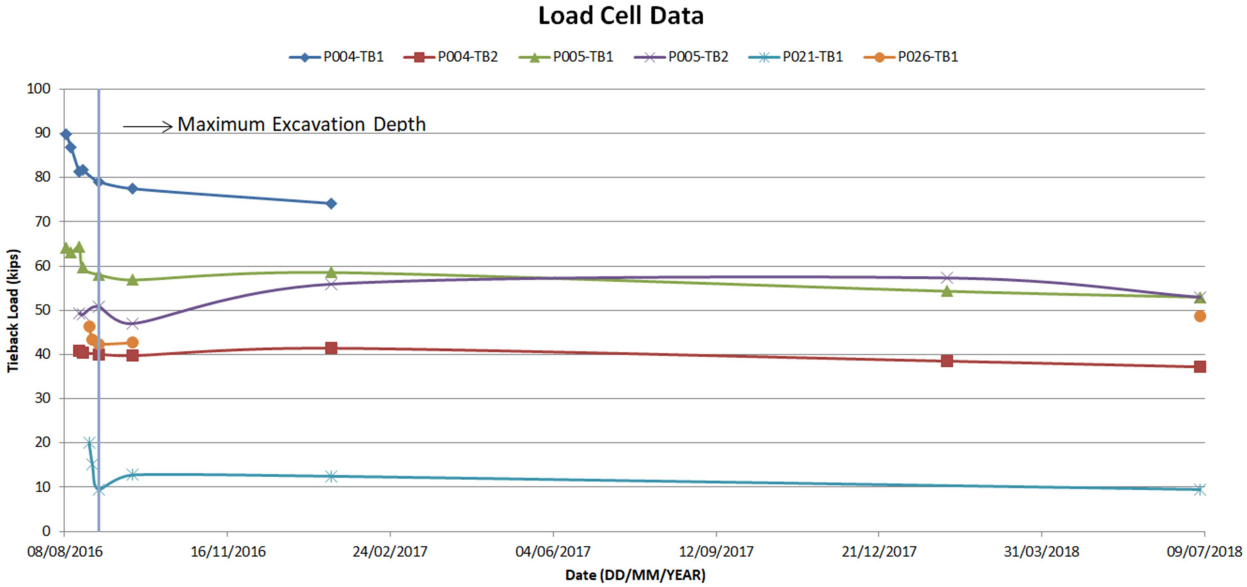

Figure 6.9: Load vs. Time Plot for Tiebacks

7. DISCUSSION

7.1 Mussallem Union Wall Experimental Results

7.1.1 Inclinometer Evaluation

The first evaluation done was with the set of data related to the piles P004 and P005 (Figure 6.1 and Figure 6.2). As excavation begins, the pile moves toward the excavation above the 17 feet depth for P004, as expected. This phenomenon can be seen through four sets of data, 07/29/2016, 08/01/2016, 08/02/2016 and 08/08/2016. After that, the pile profile shows a 2.25-inch movement (from -0.75 to 1.5 inches) between the fourth and fifth readings (08/09/2016). On this day, the first tiebacks were tensioned, so, it is expected to see pile movement toward the retained soil. After the installation of the first tieback, minimum soil movement is observed.

A similar situation occurred with the readings for pile P005 (Figure 6.2). In the first readings, until 08/08/2016, the pile shows a small movement into the excavation above the 15 feet mark. The second set of data, 08/01/2016, shows a maximum 0.4-inch movement in the surface mark. After that reading, the next two sets of data show a movement towards the wall. The fourth set (08/08/2016) shows the soil profile almost back to its initial position. The installation of the first set of tiebacks (08/09/2016) caused a 1.1-inch pile movement toward the retained soil, as expected. This difference can be seen between the readings from the fourth and fifth sets of data. After the tieback installation, minimum soil movement is observed.

The second analysis includes the data collected from piles P021 and P026 (Figure 6.3 and Figure 6.4). The data collected at pile P021 is very similar to the data for pile P026. Neither

show significant lateral movement when compared to the data from piles P004 and P005. The main reason is that the wall heights at P021 and P026 are much shorter and the tieback design loads are much smaller. The maximum lateral deflection observed between these two piles was 0.25 inches.

It is not possible to see a pattern when analyzing the data from the locations 5 feet behind the wall (Figure 6.5 and Figure 6.6). The maximum profile change seen at P4/5@5 in 2016 is approximately 0.3 inches. For the P5/6@5 data, the numbers are slightly larger with maximum deflection of 0.55 inches until September 2016. This data shows that there was minimal movement 5 feet behind the wall until that date. Two more sets of data were added to these two piles, those readings were observed in July 2018. It is possible to see that the maximum lateral deflection between piles 4 and 5 was approximately 0.7 inches at the 2.5 feet depth mark, and even smaller at deeper locations. The location between piles 5 and 6 shows a maximum deflection of 2.25 inches at the 2.5 depth mark, this movement might have been caused by human activities near the wall, and, the fact that the lateral deflection decreases to 0.1 inches at the 7.5 feet depth mark shows that the structure has been performing well.

The data collected 12 feet behind the wall (Figure 6.7 and Figure 6.8) also shows minimal movement of the soil behind the wall. Until 2016, for the P4/5@12 location, the maximum movement recorded was approximately 0.1 inches and, for the P5/6@12 location, the maximum movement was 0.12 inches. Two more sets of data were added in July 2018 for these two locations, the maximum lateral deflection was 0.5 inches at the 2.5 feet depth mark. Because the lateral soil movement was small and sporadic at both 5 feet and 12 feet behind the wall, it is

likely a result of construction activity (earthwork) behind the wall rather than from movement of the retaining structure.

7.1.2 Load Cell Evaluation

Figure 6.9 illustrates that the load in the tieback is almost constant after the maximum excavation depth is achieved. The P004-TB1 load cell shows a reduction of about 15 kips (17%) from August 9, 2016 to September 19, 2016 while the P004-TB2 cell shows a maximum difference of about 4 kips between its maximum value (January 19, 2017) and the minimum value (September 7, 2018). Unfortunately, it was not possible to gather data from the P004-TB1 after January of 2017 because the load cell is no longer functioning properly.

The analysis for the P005 pile had similar results, showing a reduction of about 10 kips (17%) for the P005-TB1 cell and a difference of about 10 kips (18%) between maximum (February 1, 2018) and minimum (September 19, 2017) values for the P005-TB2. The only difference for pile P005 is that the second tieback had an increase in its load cell readings after September of 2016, but the number decreases again in 2018. Another interesting fact is that the last reading shows the same loads for both tiebacks (TB1 and TB2). From the first reading to the last, the data shows that TB1 had a decrease from 64kips to 53 kips and TB2 increased from 50 kips to 53 kips. These results indicate that, although the tiebacks were designed with different lock-off loads, redistribution of stress is occurring.

For P021-TB1 there was a reduction of about 11 kips (52%) and for P026-TB1 a difference of about 6 kips (13%) between its maximum and minimum values. The plot for P021-TB1 does not show a point where the load was above 20 kips. These lows numbers were expected since the

pile P021 is located in a lower section of the wall. For pile P026, the last load information (48.6 kips) gathered in 2018 shows an increase when compared to the previous (42.6 kips), it is important to keep monitoring that location to see if the load will continue to increase or not.

The load cell data also shows that five out of 6 tiebacks' loads are within the expected range and below the designed capacity as determined by the original wall designer. For the P004-TB1, the maximum load read in the cells was about 90 kips while for the P004-TB2 this number was 41 kips; the design load for these tiebacks was 91 kips and 70 kips respectively. P005-TB1 also met the expectations with a maximum value of about 65 kips while the design capacity was 78 kips. P021-TB1 had a maximum value of 20 kips and P026-TB1 of 48 kips while their design capacity was 57 kips each. The only tieback that had some readings above its design capacity was P005-TB2; one reading was about 56 kips and another one approximately 57 kips, while the design capacity for this tieback was 51 kips. Since the value represents an increase of around 10%, it is important to keep track of this tieback, in particular, to check if the load will decrease over time.

The tieback proof test report mentions the lock-off loads for two out of the six tiebacks monitored in this thesis. The lock-off load for P004-TB1 was 92 kips and for P005-TB1 was 78 kips. All the load information gathered for the two years are below the lock-off loads.

Overall, the load cell analysis shows that the tiebacks loads are decreasing slightly over time which may be a result of relaxation, particularly during the first several readings after the tiebacks were tensioned.

7.2 Comparison between MU Wall and Literature Review Cases

7.2.1 Inclinometer Cases

It is possible to evaluate and compare the field data gathered from the MU Wall with the five cases discussed in the literature review of this thesis. Since the piles P004 and P005 are the ones at the highest section of the MU Wall, only the inclinometer data from these two piles will be used in this comparison.

The first case discussed was the Tieback Wall in High Plasticity Expansive Soil at San Antonio, Texas (Section 3.2.1). Figure 3.3 shows the lateral displacement of this structure before and after the installation of two rows of tiebacks, and it is possible to see a similar pattern in the deflected shape between that plot and the inclinometer data at Figure 6.1 and Figure 6.2. All three plots show a maximum lateral displacement to the left (excavation) prior to the installation of the first row of tiebacks. Also, the maximum lateral displacement to the right (retained soil) is seen when the first tieback is installed, and, after the installation, the lateral wall deflection reduces significantly.

Another finding by the researchers in Texas was the relationship between unbonded length and horizontal deflection. According to their case study, if the unbonded length decreases, the horizontal deflection also decreases. Piles P004 and P005 have the same unbonded length (15 feet) and different bonded lengths (55 feet and 45 feet respectively), but, since the two piles are under different soil and load conditions, it is not possible to discuss any information regarding the unbonded and bonded lengths at the MU wall.

The second case listed in the literature review was the Tieback Anchored Pile Wall in Sand at Shenyang, China (Section 3.2.2). Figure 3.6 shows a horizontal wall deformation comparison between three methods and the field data gathered in the retaining wall. It is possible to see that two of the methods (HS Model and MC model) could predict very well the deformed shape of the tieback wall, and that the Elastic Method was not very successful in that prediction.

The Elastic Method considers more variables and parameters for the analysis, so it needs more reliable input data in order to predict the deformed shape correctly. If the input data is not reliable, or if there is a lack of information, the Elastic Method will not predict the wall deformation correctly.

The Tieback Wall in Sand at Texas A&M University was the third case discussed in the literature review (Section 3.2.3). Figure 3.8 shows a comparison between the deflection measured in the field and predicted by the FEM analysis. It is possible to see that the two curves have similar shapes and results with a maximum discrepancy of about 10mm (0.4 inches) at a depth of approximately 5m (16.4 feet). This figure shows that the results from the FEM analysis will, most likely, not match perfectly with what is gathered in the field. As it was discussed before, it is difficult to create a model that represents the field conditions perfectly.

The last topic discussed during the research conducted at Texas A&M was the relationship between the unbonded length of the tieback and the deflection at the retaining wall. Figure 3.10 shows that, for this particular case, when the unbonded length increases, the maximum deflection of the wall decreases. The results found in Figure 3.4 and Figure 3.10 are conflicting, the first

one shows that the deflection decreases when the unbonded length decreases, while the second one shows the opposite.

As it was said before, piles P004 and P005 have the same unbonded length (15 feet), but for pile P004, this number represents 21.4% of the total length (70 feet) and for pile P005 it represents 25% of the total length (60 feet). The maximum lateral deflection for these two piles is 1.5 inches and 1.2 inches, respectively. This might be a consequence of several different causes, including different soil profiles, applied loads, wall heights, pile heights and tieback total lengths. But, pile P005 has a higher relative unbonded length (25%) and a lower maximum wall deflection, which follows the findings by the research team at Texas A&M in Figure 3.10. It is also important to mention that the three retaining walls compared are in different locations, under different load and structural conditions.

The fourth case discussed in the literature review was the Tieback Wall in Alluvial Soil in Taipei, Taiwan (Section 3.2.4). Figure 3.12 shows the deflected shape of the TCC wall in five different stages: the first one is before the installation of the tiebacks, and the other four stages are after the installation of each tieback. The results from this figure match with the plots in Figure 3.3, Figure 6.1 and Figure 6.2. All figures show a maximum deflection before the tieback installation and a small movement to the retained soil after the tiebacks are installed.

For the TCC case, the first tieback moves the wall towards the retaining soil about 0.4 inches at the tieback depth, and 0.2 inches, 0.1 inches and 0.05 inches for the second, third and fourth tiebacks, respectively. For the pile P004, the first and second tiebacks moves the soil 0.75 inches

and 0.1 inches at their locations, respectively. For pile P005 the numbers are 0.3 inches and 0.1 inches for the first and second tiebacks, respectively.

The last case mentioned in the literature review was the Online Database of Deep Excavation Performance (Section 3.2.5). Figure 3.13 shows the lateral deflection for three walls under different conditions. The W3 wall shows that clay is more susceptible to movement than the sand; this same conclusion can be confirmed looking at the W1 deflected shape. For the MU wall, the clay material appeared to deflect more than the sand material, but this is likely because the clay material is the top layer. When the excavation reaches the sand, the first tieback is already installed.

7.2.2 Load Cell Cases

It is possible to compare the load cell data of the MU wall with the two cases discussed during the literature review. The Tieback Wall in Alluvial Soil in Taipei, Taiwan (Section 3.3.1) was the first case analyzed in the literature review. Figure 3.15 shows the change in tieback load over time for a retaining structure located in the Taipei County Administration Center (TCC), this structure has four tiebacks and it is possible to find some similarities with the MU wall load vs. time plot in Figure 6.9.

The second case discussed in the literature review was the monitoring of six tiebacks at Harvard Square Station (HS), the tieback loads over time are plotted in Figure 3.17. This plot looks similar in shape to the ones for the MU and TCC wall.

Initially, it is possible to compare how the load changed over time for all the sixteen tiebacks (six at the MU wall, four at the TCC wall and six at the HS wall). Table 7.1 shows the first and last load readings for each tieback.

Table 7.1: Comparison of Tieback loads over time for MU and TCC walls

Tieback	First Load Reading	Last Load Reading	Variation (%)
MU P004-TB1	84.7 kips	74.14 kips	-12.47
MU P004-TB2	40.83 kips	37.21 kips	-8.87
MU P005-TB1	64.19 kips	52.96 kips	-17.49
MU P005-TB2	49.26 kips	52.96 kips	7.45
MU P021-TB1	20 kips	9.5 kips	-52.5
MU P026-TB1	46.31 kips	48.64 kips	5.03
TCC TB 1	70.81 kips	65.19 kips	-7.94
TCC TB 2	98.92 kips	96.67 kips	-2.27
TCC TB 3	101.16 kips	103.41 kips	2.22
TCC TB 4	111.28 kips	105.66 kips	-5.05
HS TB 1	250 kips	230 kips	-8.00
HS TB 2	225 kips	215 kips	-4.44
HS TB 3	225 kips	200 kips	-11.11
HS TB 4	200 kips	160 kips	-20.00
HS TB 5	190 kips	160 kips	-15.79
HS TB 6	220 kips	195 kips	-11.36

It is possible to see that the tieback loads for four out of the six locations at the MU wall decreased over time. For the TCC wall, the same situation happened with three out of four tiebacks, and, for the HS wall, with all the tiebacks. Two tiebacks in the MU wall and two tiebacks at the HS wall showed a very high variation (> 15%) when compared to the others. This significant decrease might have happened due to relaxation of the soil or redistribution of stresses over time such as other tiebacks are carrying this load.

It is important to mention that the time frame for the TCC wall plot was 210 days, while for the MU wall was one year and a half, and three years for the HS wall. But all plots are very

similar in shape, showing little variation over time for most tiebacks. Another factor that might influence the results is that the soil profiles and properties for the three walls are different.

7.3 Comparison between MU Wall and Limit Equilibrium Method – Full Depth

7.3.1 Deflection Comparison

It is possible to compare the deflection of the piles P004 and P005 after construction with what was predicted by the limit equilibrium method on Appendix B. Table 7.2 shows the deflection observed in the field and the limit equilibrium method predictions for some points for pile P004. A positive value represents a movement towards the retained soil.

Table 7.2: Comparison Between UM Data and Limit Equilibrium Prediction – Pile P004

Depth (ft)	Pile 004		
	MU Data	Prediction Clay	Prediction Sand
0	1.10 in	-22.85 in	-12.39 in
5	1.02 in	-17.72 in	-9.39 in
10	0.56 in	-12.74 in	-6.48 in
15	0.18 in	-8.46 in	-4.04 in
20	-0.013 in	-5.06 in	-2.17 in
25	-0.015 in	-2.52 in	-0.88 in
30	0.018 in	-0.83 in	-0.15 in
35	0.026 in	-0.066 in	0 in
37.12	-0.0017 in	0 in	0 in

The limit equilibrium method predicted that the soil would be moving to the left (not towards the retained soil), while the field data shows a movement to the right (towards the retained soil), this might be a result of other construction activities in the area after the wall was completed. In addition, there were some gaps between the wood lagging of the retaining wall and the soil. When the tiebacks were tensioned, the piles were pushed in order to close all these gaps. Since

the inclinometer casings are attached to the piles, the field data takes into consideration the pile movement to close the gaps. The predicted deflection values are also larger than what was observed in the field, showing that the approach used was conservative.

Figure 7.1 shows the deflect shapes predicted by the limit equilibrium method and the most recent field data gathered for pile P004.

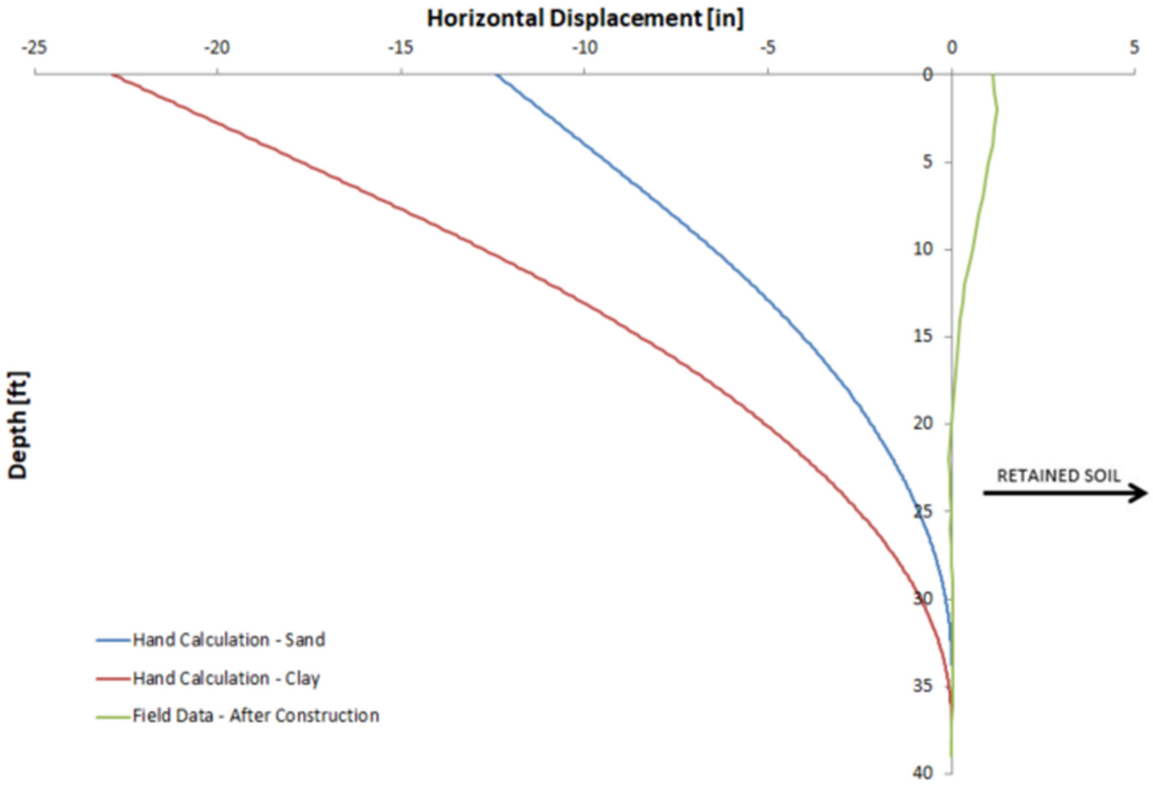

Figure 7.1: Plot Comparison between the field data and the limit equilibrium method prediction – Pile P004 – Full Depth

Table 7.3 shows the deflection observed in the field and limit equilibrium method predictions for some points for pile P005. A positive value represents a movement towards the retained soil.

Table 7.3: Comparison Between UM Data and Limit Equilibrium Prediction – Pile P005

Depth (ft)	Pile 005		
	MU Data	Prediction Clay	Prediction Sand
0	1.20 in	-18.15 in	-9.76 in
5	0.83 in	-13.77 in	-7.23 in
10	0.45 in	-9.53 in	-4.79 in
15	0.16 in	-5.94 in	-2.77 in
20	-0.04 in	-3.17 in	-1.28 in
25	-0.10 in	-1.24 in	-0.35 in
30	-0.08 in	-0.20 in	-0.0038 in
33.54	-0.01 in	0 in	0 in

The comparison for pile P005 is very similar to the one for pile P004. The predicted movement was to the left, showing negative displacements, while the field data shows positive displacements. Also, for the same reasons listed for pile P004, the predicted values were much larger than the field data. Figure 7.2 shows the deflect shapes predicted by the limit equilibrium method and the most recent field data gathered for pile P005.

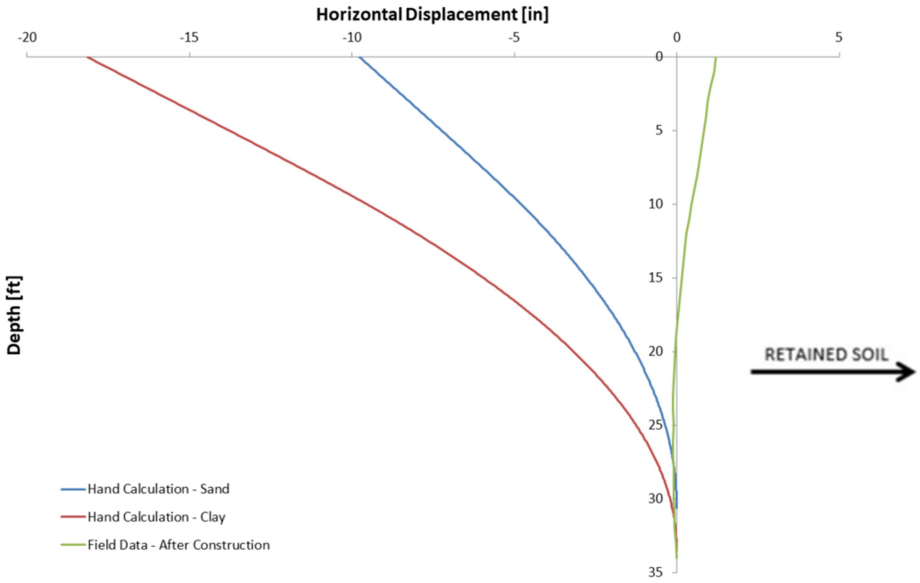

Figure 7.2: Plot Comparison between the field data and the limit equilibrium prediction – Pile P005 – Full Depth

To summarize, the limit equilibrium method did not accurately predict the wall behavior for the MU retaining wall structure, this might have happened for several reasons:

- All the design was based on only one SPT boring test that was not even located precisely at the piles P004 and P005;
- All the soil parameters and characteristics were not obtained using any lab test but based only on the average SPT provided by the boring log and default geotechnical parameters for clay and sand;
- The method also does not take construction sequence and any movement during the tieback installation into account; There were gaps between the wood lagging in the wall and the soil. The tiebacks were pushed during installation in order to close these gaps and the field data provided might be shifted to the right;

The main and most likely explanation for the discrepancy in the results is that the calculation process used is a semi-empirical method that was developed based on monitoring tieback loads, not monitoring deflections.

7.3.2 Load Comparison

The field data gathered over time can be compared with the load prediction calculated using the earth pressure diagram method. Table 7.4 shows the maximum and minimum values registered by the load cells and the tieback force calculated using the limit equilibrium method.

Table 7.4: Comparison between Field Data and Limit Equilibrium Method

	P004-TB1 (kips)	P004-TB2 (kips)	P005-TB1 (kips)	P005-TB2 (kips)
Field Data Maximum	90	40	65	55
Field Data Minimum	75	35	55	45
Limit Equilibrium Sand Prediction	65	45	60	35
Limit Equilibrium Clay Prediction	100	70	95	55

The limit equilibrium method with sand predicted the tieback load correctly for two out of the four tiebacks in piles P004 and P005. For the second tieback at pile P004 (P004-TB2), the prediction was about 5 kips over the maximum value (12%) which represents a small percentage, so, it is considered to be a correct prediction for this analysis. Another correct prediction was for the first tieback at pile P005 (P005-TB1) the value predicted was between the minimum and maximum values gathered in the field.

For the clay approach, only one tieback load was correctly predicted. For the second tieback for pile P005 (P005-TB2), the prediction was between the minimum and maximum values found in the field, for all the other tiebacks, the prediction was much higher than the maximum value gathered.

Based on these results, the method works really well for calculating the load of two tiebacks, but not for the others. This might have happened because the soil profile was not well defined, just one boring log was taken into consideration for the analysis, or because the assumptions for the limit equilibrium method do not work well for this particular case.

7.4 Comparison between MU Wall and Limit Equilibrium Method – Project Milestones

It is possible to compare the field data gathered in the MU wall before tieback installation with the limit equilibrium method predictions. Figure 7.3 shows the comparison plot for the 11-foot excavation depth for piles P004 and P005.

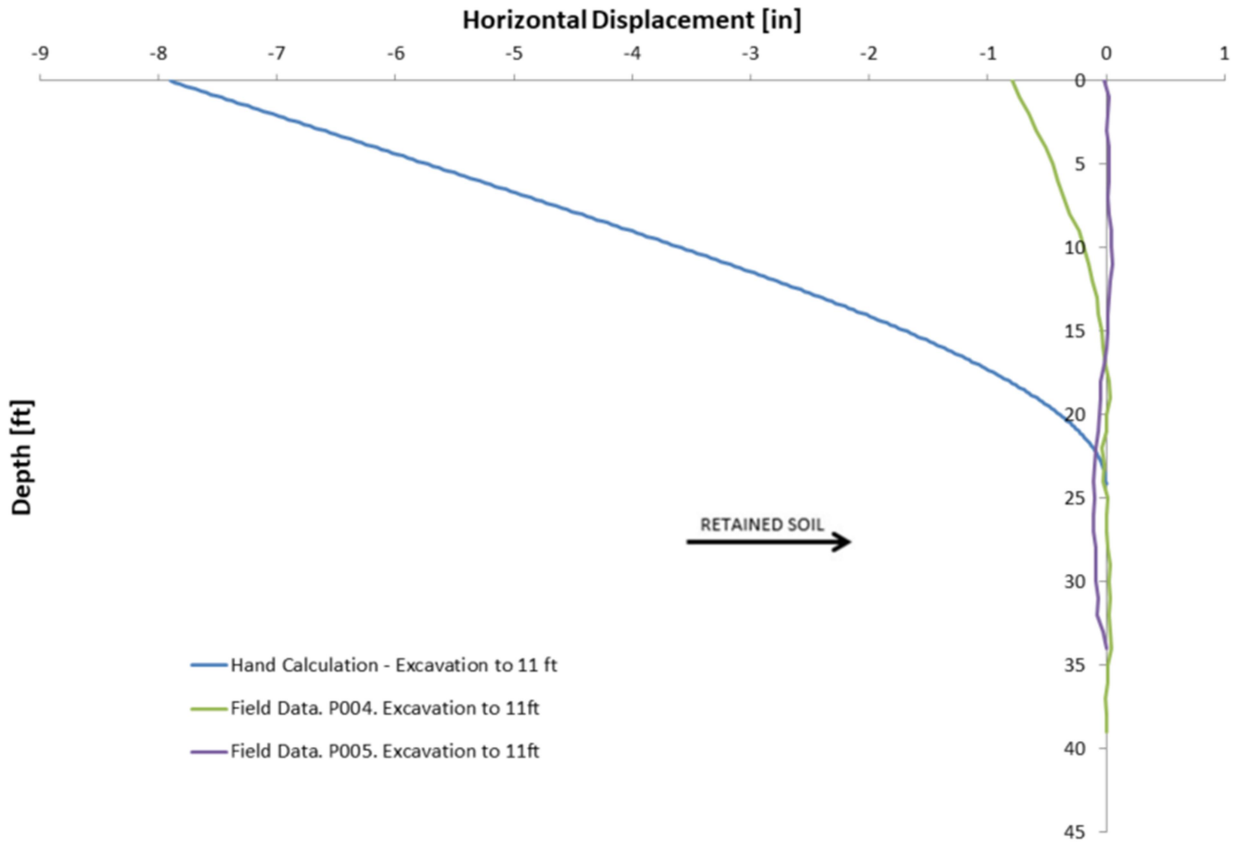

Figure 7.3: Plot Comparison between the field data and the limit equilibrium prediction – Pile P004 and P005 – 11-foot Depth

The limit equilibrium method over predicted the deflection of the wall for the 11 feet excavation mark. One of the reasons might be that the soldier pile length used during construction was longer than the suggested value found in the calculation method. This safety procedure probably reduced the deflection of the wall in the first stages of excavation. Another

reason is that, as discussed before, there were some gaps between the wood lagging of the wall and the soil. Since the soil was not touching the wood lagging, there was no earth pressure at those locations, but only on the piles themselves. So, the earth pressure is greatly reduced, resulting in greatly reduced lateral deflection. The predicted deflected shape is similar to the deflected shape observed for pile P004 at this stage of excavation.

Figure 7.4 shows the comparison plot for the 18-foot excavation depth for piles P004 and P005.

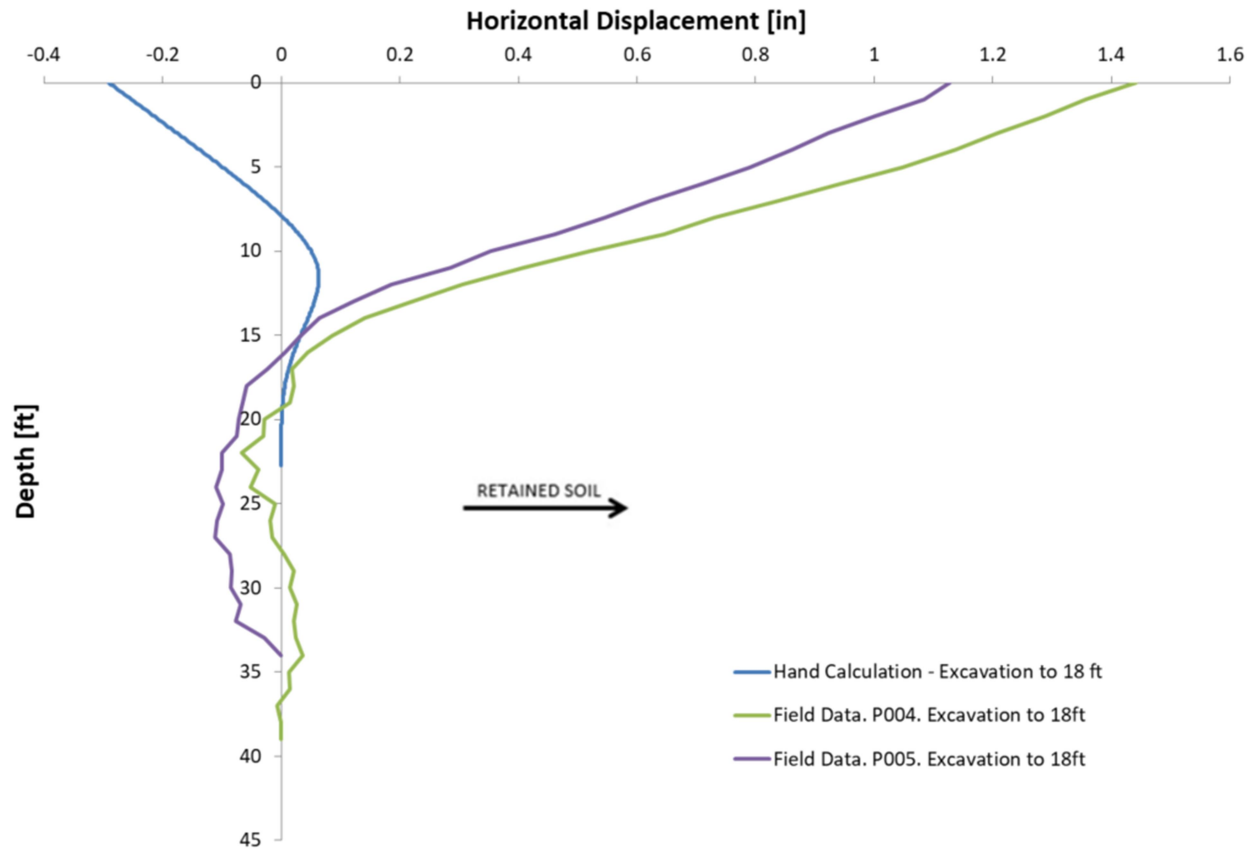

Figure 7.4: Plot Comparison between the field data and the limit equilibrium prediction – Pile P004 and P005 – 18-foot Depth

The limit equilibrium calculation method under predicted the deflection of the wall for the 18 feet excavation mark, the predicted movement is much smaller than what was observed in the field. It is imported to remember that there were gaps between the wood lagging of the wall and the soil and, because of that, the field data is shifted to the right.

7.5 Student Learning

Professors at the Rose-Hulman Institute of Technology have been using the retaining wall during class for several different examples since its construction. The main goal is to enhance student performance and raise more interest in the subject.

Providing hands-on and real-world case-based learning opportunities for students can improve their comprehension about a subject. In addition, it is crucial to give the students a chance to participate in full-scale field activities to visualize concepts learned in class. The retaining wall located on campus is very easy to access and close to the Civil Engineering Department (five-minute walk). This thesis gives suggestions about how to take full advantage of the structure.

It has been two full academic years since construction started on the wall. So far, professors have used the structure for three classes: Soil Mechanics (required undergraduate class), Foundation Engineering and Retaining Structure Design (elective undergraduate and required graduate classes). During the construction, students that were taking Soil Mechanics had the opportunity to visit the structure and obtain a general idea of the type of soil, its characteristics and properties. A similar situation happened with the Foundation Engineering class, where students were able to visit construction during the installation of the piles. The structure has been

used the most, obviously, for the Retaining Structure Design class; students were able to visit the site during construction to check the methodology and installation of tiebacks, for example. In addition, the wall is used as a design example in class and the data collected from the inclinometer and load cells is also used as a case history in class.

There are still several activities that can be done with the retaining wall in order to improve student performance even with the end of construction. For the Soil Mechanics class, videos of several construction processes were recorded and can be used. Even though videos can be recorded at any site and shown to students, it is better when it is a project they are familiar with, and they can see the final result. Usually, students show more interest and desire to learn when they have an overall idea of the project and they can picture how each process influences the final design. For this particular class, videos from the compaction process, excavation, backfill and SPT test can be useful. The SPT test data can also be used for class examples, homework or projects. The instrumentation installed in the wall can give information about water level; therefore, students can perform tests with the soil in the area, and do some examples involving soil and water pressure calculation.

For the retaining wall class, besides what is being done currently, students can use the data from the tieback performance test and plot the deflection vs. load data. Videos from the test can also be used in order to create a better understanding of how the test is run and why it is essential for tieback design. Because the inclinometer casing is still accessible, the students can also run an inclinometer test as part of an instrumentation and data acquisition module; this would provide a hands-on opportunity that could teach students important factors that need to be checked in a retaining wall.

For the Foundation Engineering class, videos and pictures from the installation of the piles can be used during the lecture. Also, the professor can create a design example based on the data used in the project. It would be good for the students to design piles for the structure and then compare it with the actual result.

The retaining wall can also be used in other classes. Structural Design in Steel can take advantage of the W-sections used for the piles. Engineering Surveying can use the survey data recorded with the equipment installed as a project or lecture example. Cost Engineering can use this project as an activity for the students to do the quantity, take off and final cost calculations. It can be a good project for Construction Engineering; students would have to come up with the schedule for the construction of the wall, listing all the activities and the relationship between them.

Finally, this structure can be presented to the freshman class as an example of a civil engineering project. It is important to show early in the curriculum all the different applications that this profession can offer, and give them an idea of the variety of opportunities and experiences that they will face during school and work.

8. LIMITATIONS

This section describes the limitations faced during the work done for this thesis, how it impacts the final analysis and how these limitations can be solved.

The first limitation involves the inclinometer data acquisition process. Rose-Hulman does not have an inclinometer, so it is necessary to borrow or rent one in order to go to the field and gather the deflection information. It makes the process slower and harder, and it would be good to have an inclinometer on campus to facilitate the process. For the last readings, for example, it was necessary to go to Indianapolis to borrow an inclinometer; if there was an inclinometer on campus, there would be definitely more deflection readings and undergrad students could also learn how to use and apply the concepts for different classes.

Two different inclinometers were used to collect data from the retaining wall. One of them was set up with imperial units while the other one used the metric system, this might cause some precision and accuracy differences between the readings. Another limitation is that some inclinometer locations and load cell reading points are covered and not currently available for reading. That is the reason why some inclinometer and load cell plots do not have recent data. It is necessary to find those locations, so data can be gathered at all the points.

The next limitation is about the soil tests conducted at the MU location and data available for the numerical analysis. There is not enough information about the soil properties in order to create a more advanced and precise limit equilibrium method prediction for the retaining wall. All the input information for the limit equilibrium method prediction came from one SPT boring

test. In order to improve the analyses, it is necessary to gather more information about the soil and conduct better tests because a lot of assumptions were used.

One solution is to perform more SPT tests in a location closer to the highest section of the wall to have a better idea of the soil in that particular area since it is the one being monitored by the inclinometers and load cells. Another idea is to perform a more sophisticated test such as a Cone Penetration Test in order to get more properties about the soil and a better idea about the exact location of each soil layer.

Lastly, the calculation used to predict the behavior of the wall is a semi-empirical method that was developed based on monitoring tieback loads and not deflections, it would be good to use another method, based on deflections, to check if the results match with the field data or not.

9. CONCLUSIONS

This thesis provides data analysis of a 28-foot high retaining wall located at Rose-Hulman Institute of Technology. The analysis includes inclinometer data showing the pile and soil profile change at six different locations and load cell data that provides plots of the deflection versus time for six tiebacks.

The profile shown by the inclinometer test met all the expectations. The majority of soil movement occurred during the early stages of construction and the maximum change in the profile was noticed exactly during the day that the tiebacks were tensioned. In addition, the load cell readings show that the load applied at five out of six tiebacks tests were under the designed loads and decreased slightly over time.

This thesis also compares the results gathered in the MU wall with other similar structures and one calculation model. The limit equilibrium method correctly predicted the load for some tiebacks, but not for others, proving to not be a reliable method for this particular case; it also overpredicted the deflection of the wall for basically all the cases, proving to be a conservative approach when this criterion is considered.

The thesis also shows that the retaining wall can be utilized as a way to improve the student learning experience. Its potential is undeniable, even though no assessment of student learning or surveying of the students' experience has been performed to date. Professors can start using the structure more often for class examples and design problems. Further assessment can be done to analyze how each suggestion described in this thesis improves student learning. It is possible to

compare student performance before and after the change, and also ask students for feedback in order to improve the teaching methodology using the retaining wall.

Overall it is seen that having a full-scale structure on campus can be very useful for multiple purposes. A living lab can arouse student interest for different subjects, help professors improve the quality of the class and increase the research that can be developed by the institute.

10. FUTURE WORK

There is still plenty of work to do at the Mussallem Union Retaining Wall. Some inclinometer pipes and load cells are available for more readings. It would be good to keep monitoring the deflection of the wall and the tieback loads over time. Since the structure has been performing well so far, it is not necessary to have weekly or monthly readings, but it would be good to have one reading per quarter, so the data can be used in the classroom as it was discussed in this thesis.

Even though most inclinometers pipes are available for reading, it was not possible to find four of them (P004, P005, P021 and P026) during the last reading in the summer of 2018, they were covered with soil and not visible even after digging a hole. It is possible that those pipes got damaged during the last phases of construction; this should be investigated because it would be important to find these four locations in order to have more data about the structure.

This thesis only presents a limit equilibrium method prediction for the tieback loads and deflected shape of the retaining structure; several computer modeling software can be also be used in order to achieve the same goal. It would be good to have a 3D software analysis in the highest section of the wall and use the whole structure (not only the tallest section) to have a better idea of how the wall should be performing and compare that data with the inclinometer and load cell data that was gathered in the field. A 3D software analysis would take longer and it would also need more detailed parameters in order to be accurate. The current data available for the soil is not enough for a model using a complex software.

Some other exercises can be done in order to evaluate and/or improve the results of this thesis. The first one is trying to find the soil properties for sand and clay that would result in a deflected shape similar to the one observed in the field. It is also possible to do the backward process and find the moment diagram based on the deflected shape observed in the field and see how that matches with the moment diagram developed using the prediction methods. One last check that is useful for the thesis is to find the deflection of the wall as soon as the first tieback is installed and ignoring the soil behind it in order to check how much movement the tieback installation caused.

This thesis discussed several ideas on how the retaining wall can be used in the classroom to enhance the student's learning experience, but nothing has been implemented so far. It would be good to work with the professors in order to use some of these ideas in the classroom and analyze the impact of it in the student's learning. It is possible to compare the homework and exam grades to evaluate if the changes were significant or not and also students can answer some surveys regarding the experience and how it could be better. Another idea on how to analyze the effect of those changes would be to ask the students to answer the same quiz before and after the exercise with the retaining wall, this way it would be possible to verify what they learned during the experiment.

It seems like most students on campus do not know how broad the civil engineering field is or the variety of areas you can work at. It would be interesting to conduct a survey to have a general idea about the profile of the Civil Engineering students at Rose-Hulman. What they think about adding a living lab to a class, what is their opinion about field trips and laboratories, their areas of interest, why they chose to be a civil engineer and when was the first time they heard

about the major, for example. With the results from this survey, it would be possible to use this structure as a way to teach students (from Rose-Hulman or High School) about the different areas of civil engineering. An example of a general survey with some questions to profile the civil engineering students on campus can be found in Appendix G.

This thesis presented a framework developed by a group of researches in Europe to analyze and evaluate the success, importance and impact of four living labs. It would be a good idea to analyze the MU wall living lab according to that framework and see how this structure would be rated

Lastly, more ideas on how to use the Mussallem Union retaining wall in class are always welcomed, as well as better soil tests in the area. If the structure starts to get more use in the classroom, it would be good to conduct more SPT tests or even a CPT test in order to have a better idea about the soil.

LIST OF REFERENCES

[1]United States Census Bureau (2018). "U.S. and World Population" <https://www.census.gov/popclock/> (2018, May 24)

[2]Bonwell, C.C., Eison, J. A. (1991). Active Learning: Creating Excitement in the Classroom. ASHE-ERIC Higher Education Reports.

[3]Bransford, J. D., Brown A.L., and R. Cocking (1999). How People Learn: Brain, Mind, Experience, and School. National Academy Press, Washington DC.

[4]Kershaw, K. A., Lovell, M. D., and Price, J.M. (2017). Creation of On-Campus Living Laboratories for Improved Student Learning. 2017 ASEE Zone II Conference.

[5]Google Maps (2019). "Rose-Hulman Campus" <https://www.google.com/maps/place/RoseHulman+Institute+of+Technology/@39.4828386,-87.326229,630m/data=!3m1!1e3!4m5!3m4!1s0x886d6e421b703737:0x96447680305ae1a4!8m2!3d39.4828386!4d-87.3240403> (2019, May 10)

[6]Beaty Construction Inc (2016). "Memorial Union Building Renovations"

[7]Williams Form Engineering Corporation (2018). "Geo-Drill Injection Anchor System" <http://www.williamsform.com/Ground_Anchors/Hollow_Bar_Ground_Anchors/hollow_bar_anchor_system.html> (2018, June 12)

[8]Rose-Hulman Institute of Technology (2018). "Get to Know Rose-Hulman" <https://www.rose-hulman.edu/about-us/get-to-know-rose-hulman/fast-facts.html?utm_source=dynamic&utm_medium=redirect&utm_campaign=301> (2018, September 17)

[9]Public University Honors (2017). "Estimated Class Sizes: More Than 90 National Universities" <http://publicuniversityhonors.com/2015 /10/20/estimated-class-sizes-more-than-90-national-universities/> (2018, September 17)

[10]Grand Steel Pile Company (2018). “Anchored Sheet Piles” <https://www.china-steelpiling.com/news /anchored-sheet-piles-185.html> (2018, October 15)

[11]Dunnicliff, J. (1982). Geotechnical Instrumentation for Monitoring Field Performance.

[12]Machan, G. and Bennet, V. (2008). Use of Inclinometers for Geotechnical Instrumentation on Transportation Projects.

[13]Ahmed M., Bin-Shafique S., Huang J., Papagiannakis A. T., and Rezaeimalek S. (2016). Tieback Retaining Wall in High Plasticity Expansive Soil. 2016 American Society of Civil Engineers.

[14]Han J., Zhao W., Chen Y., Jia P., and Guan Y. (2017). Design Analysis and Observed Performance of a Tieback Anchored Pile Wall in Sand.

[15]Briaud J. and Lim Y. (1999). Tieback Walls in Sand: Numerical Simulation and Design Implications.

[16]Liao H. J. and Hsieh P. G. (2002). Tied-Back Excavations in Alluvial Soil of Taipei.

[17]Konstantakos D. C. (2008). Online Database of Deep Excavation Performance and Prediction.

[18]Hansmire W. H. and Rawnsley R. P. (1988). Long-Term Tieback Monitoring at Harvard Square

[19]Almirall E. and Wareham J. (2010). Living Labs: Arbiters of Mid- and Ground-Level Innovation. Barcelona, Spain.

[20]Schumacher J. (2013). Alcotra Innovation Project: Living Labs. Definition, Harmonization Cube Indicators & Good Practices.

[21]Veeckman C., Schuurman D., Leminen S., and Westerlund M. (2013). Linking Living Lab Characteristics and Their Outcomes: Towards a Conceptual Framework.

[22]U.S. Department of Transportation, Federal Highway Administration (1999). Geotechnical Engineering Circular No. 4 – Ground Anchors and Anchored Systems Publication No. FHWA-IF-99-015.

[23]Coduto D. P. (2001) “Foundation Design – Principles and Practices,” second edition.

[22]Durham Geo Enterprises (2018). “DigiPro2 Software for Inclinometers” <https://www.slopeindicator.com/instruments/inclin-digipro2.php> (2018, April 25)

APPENDICES

APPENDIX A (GEOTECHNICAL DATA)

Appendix A shows the Boring Location plan and the SPT results at two locations B-01 and B-05, as well as, the Atterberg Limit results and grain size distribution for the wall location.

Figure A.1 shows the Boring Location Plan for the MU renovation construction

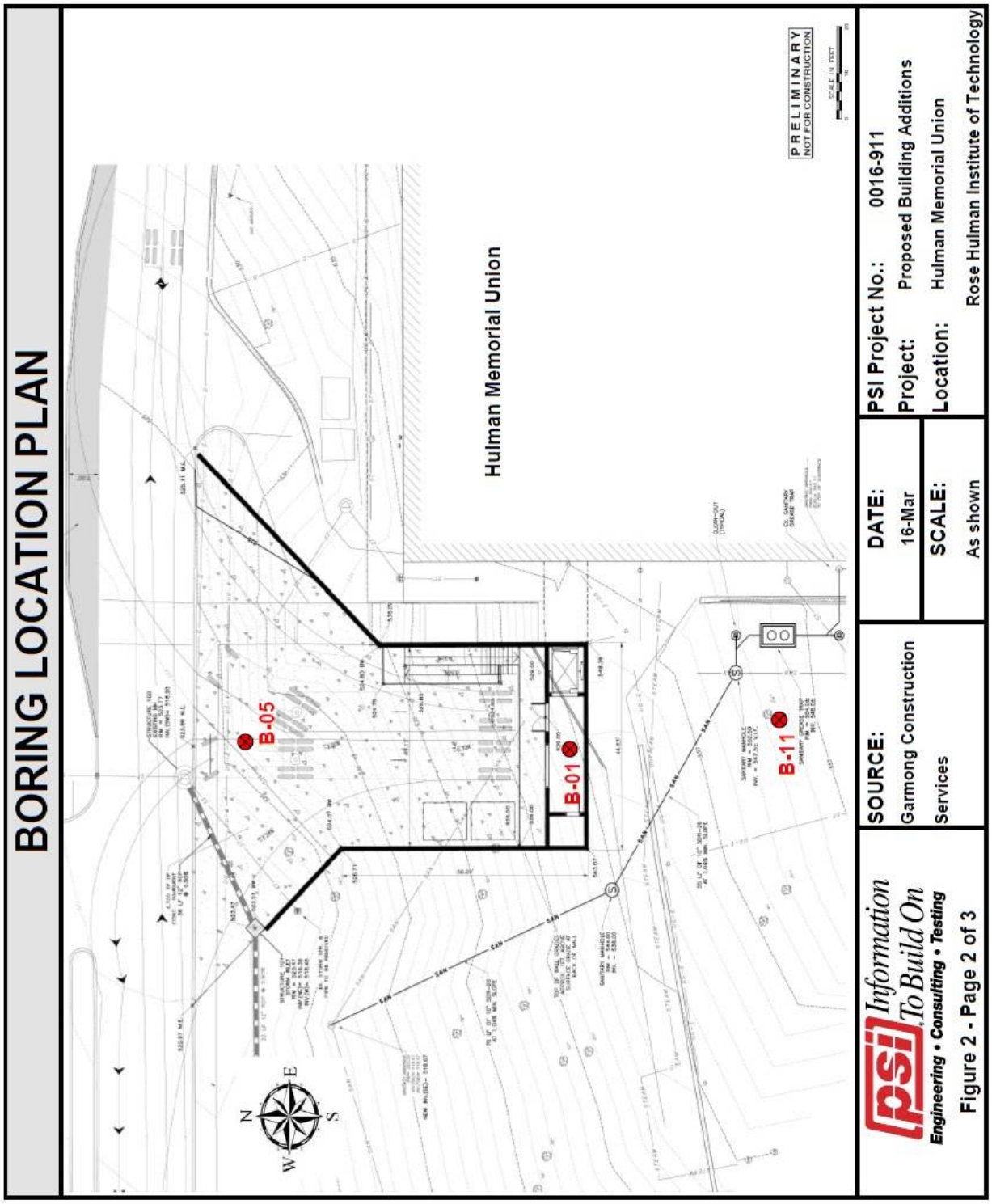

Figure A.1: Boring Location Plan for the MU renovation

Figure A.2 shows the results from the SPT test conducted in the top of the wall

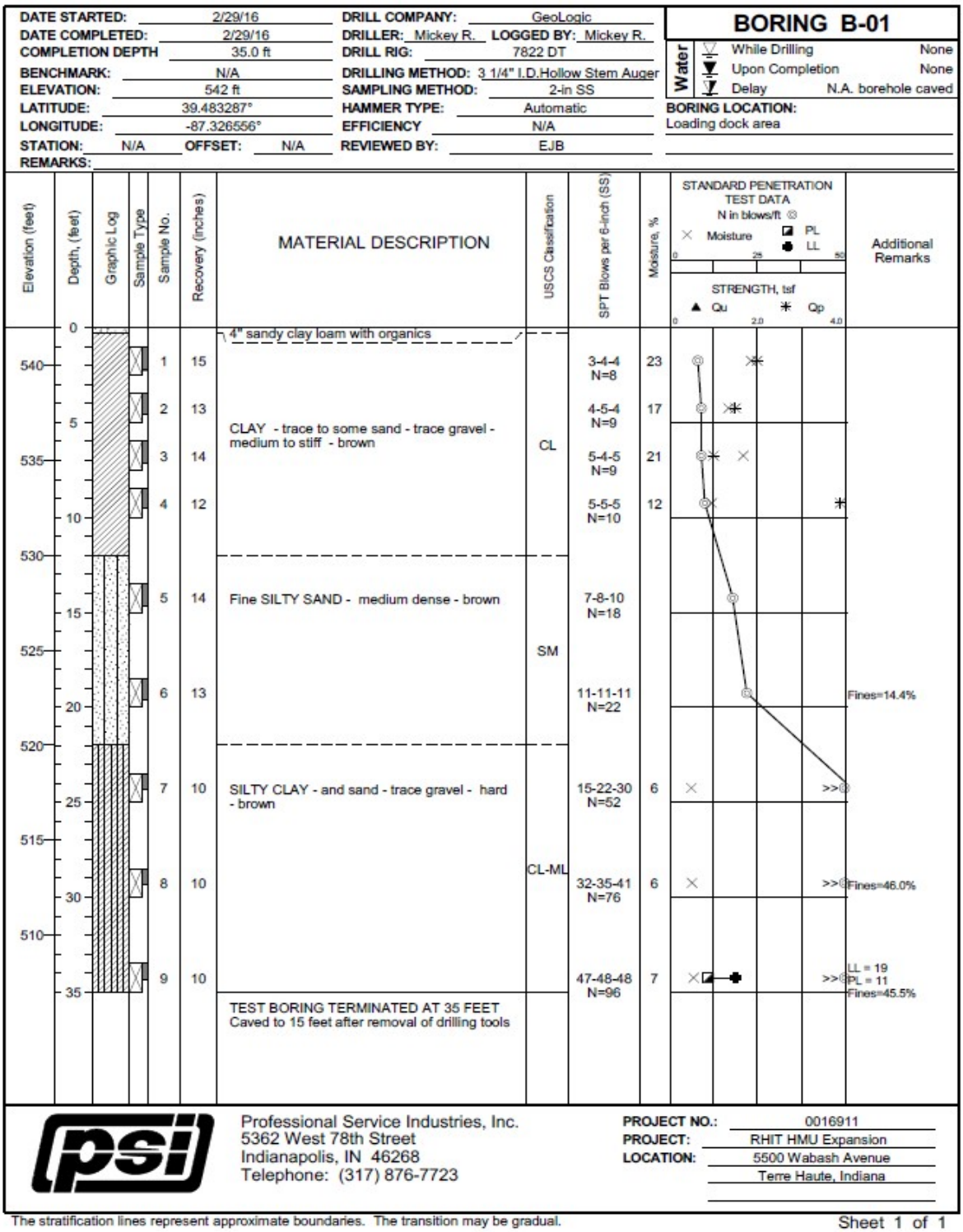

Figure A.2: SPT Results at location B-01 (Top of the Wall)

Figure A.3 shows the results from the SPT test conducted in the bottom of the wall

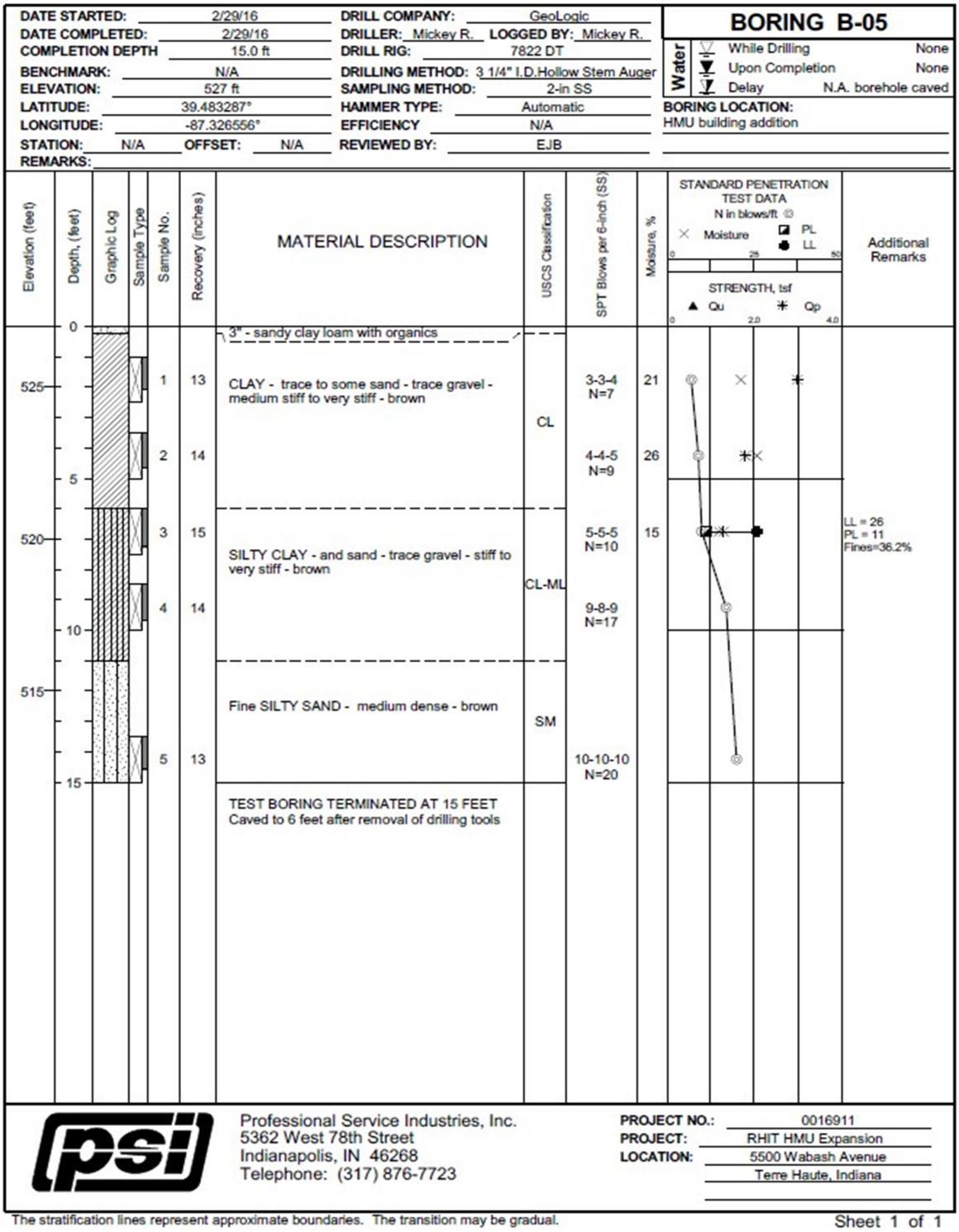

Figure A.3: SPT Results at location B-05 (Bottom of the Wall)

Figure A.4: shows the results from the Atterberg limit tests.

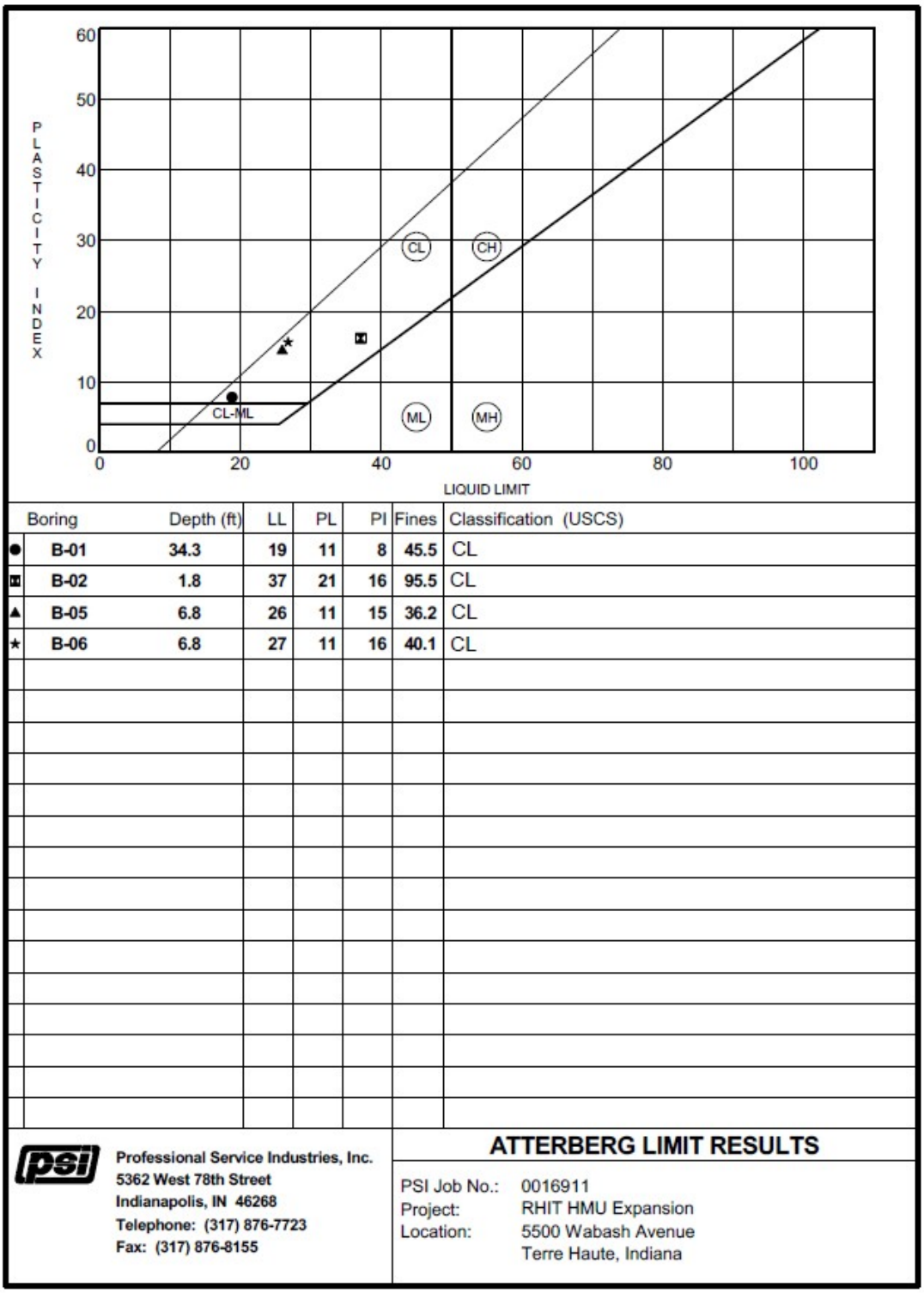

	Boring	Depth (ft)	LL	PL	PI	Fines	Classification (USCS)
●	B-01	34.3	19	11	8	45.5	CL
■	B-02	1.8	37	21	16	95.5	CL
▲	B-05	6.8	26	11	15	36.2	CL
★	B-06	6.8	27	11	16	40.1	CL

Professional Service Industries, Inc.
5362 West 78th Street
Indianapolis, IN 46268
Telephone: (317) 876-7723
Fax: (317) 876-8155

ATTERBERG LIMIT RESULTS

PSI Job No.: 0016911
Project: RHIT HMU Expansion
Location: 5500 Wabash Avenue
Terre Haute, Indiana

Figure A.4: Atterberg Limit Results

Figure A.5 shows the grain size distribution of the soil

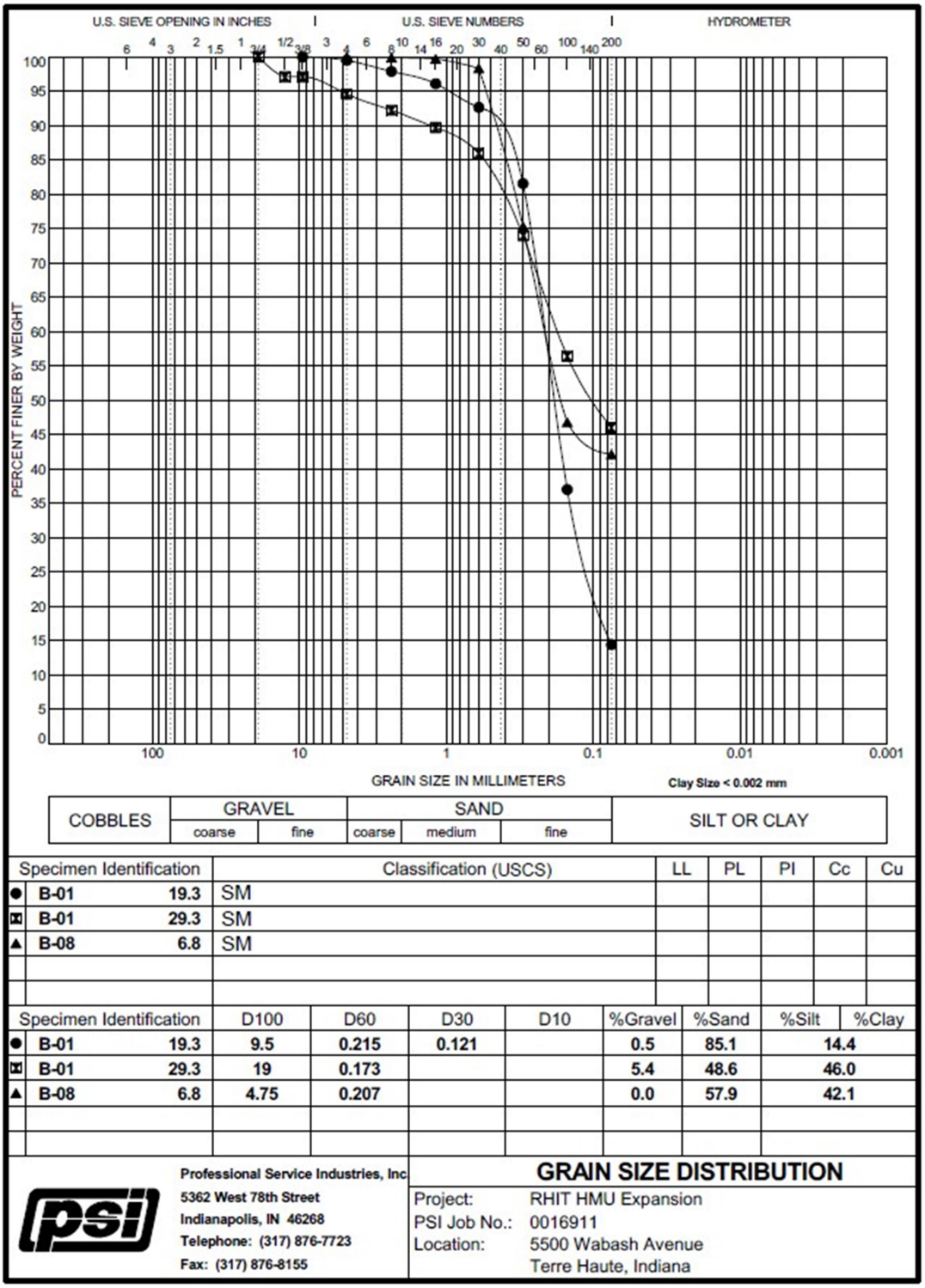

Specimen Identification		Classification (USCS)	LL	PL	PI	Cc	Cu
● B-01	19.3	SM					
⊠ B-01	29.3	SM					
▲ B-08	6.8	SM					

Specimen Identification		D100	D60	D30	D10	%Gravel	%Sand	%Silt	%Clay
● B-01	19.3	9.5	0.215	0.121		0.5	85.1	14.4	
⊠ B-01	29.3	19	0.173			5.4	48.6	46.0	
▲ B-08	6.8	4.75	0.207			0.0	57.9	42.1	

Professional Service Industries, Inc.
5362 West 78th Street
Indianapolis, IN 46268
Telephone: (317) 876-7723
Fax: (317) 876-8155

GRAIN SIZE DISTRIBUTION

Project: RHIT HMU Expansion
PSI Job No.: 0016911
Location: 5500 Wabash Avenue
Terre Haute, Indiana

Figure A.5: Grain Size Distribution

APPENDIX B (LIMIT EQUILIBRIUM METHOD – FULL DEPTH)

This appendix describes the limit equilibrium method to find the deflected shape for the high section of the wall in two locations, piles P004 and P005 after the end of construction. For each location, two approaches were used, one considering the soil as clay and the other one as sand.

The first calculation shown is the one for pile P004 assuming the soil as clay.

DESIGN OF ANCHORED SYSTEMS - PILE P004 - CLAY

The hand calculation design of the MU retaining wall will follow the procedure described in the Geotechnical Engineering Circular No. 4 - Ground Anchors and Anchored Systems by the U.S. Department of Transportation - Federal Highway Administration. Publication No. FHWA-IF-99-015.

Chapter 5 (Design of Anchored Systems) describes the design method with the recommended Apparent Earth Pressure Diagrams for various soil types. This designed will be based on this chapter.

Step 1: Define Parameters of wall and soil

$H := 26\ ft$	Height of wall	$b := 90\ in$	Spacing between piles (center to center)
$H_{pile} := 40\ ft$	Height of pile	$B := 12\ in$	Width of flange for HP12x53

$H1 := 11\ ft$ Distance from ground surface to first row of tiebacks

$H2 := 7\ ft$ Distance from first row of tiebacks to second row of tiebacks

$H3 := 8\ ft$ Distance from base of excavation to second row of tiebacks

Soil 1 - Clay (CL) - Undrained Condition
From 0 ft to 12 ft - N=9

$S_1 := 1500\ psf$ Shear Strength Soil 1 - (Terzaghi, Peck, and Mesri, 1996)

$c_1 := S_1 = 1500\ psf$ Cohesion Soil 1 - (Terzaghi, Peck, and Mesri, 1996)

$\phi_1 := 0\ °$ Fully Undrained

$\gamma_1 := 120\ pcf$ Unit Weight of Soil 1 (Terzaghi, Peck, and Mesri, 1996 and experience)

$h_1 := 12\ ft$ Height of Soil 1

Soil 2 - Silty Sand (SM) - Drained Condition
From 12 ft to 22 ft - N=20

$c_2 := 0\ psf$

$\phi_2 := 32\ °$ Friction Angle Soil 2 - (Bowles, 1998; NAVFAC, 1998; and Peck, Hanson, Thornburn, 1973)

$\gamma_2 := 120\ pcf$ Unit Weight of Soil 2 (Terzaghi, Peck, and Mesri, 1996 and experience)

$h_2 := 10\ ft$ Height of Soil 2

Soil 3 - Silty Clay (CL-ML) - Drained Condition
From 22 ft to 26 ft - N=52

$c_3 := 100\ psf$ (Local Experience)

$\phi_3 := 26\ °$ Assumed Liquid Limit (LL) of 40 (Stark, Choi and McCone, 2005)

$\gamma_3 := 125\ pcf$ Unit Weight of Soil 3 (Terzaghi, Peck, and Mesri, 1996 and experience)

$h_3 := 4\ ft$ Height of Soil 3

Surcharge

The surcharge for this retaining wall is zero.

$q := 0\ psf$

Water table

The water level is at cut level, 26 ft from the surface.

$\gamma_w := 62.4\ pcf$

Step 2: Determine values of Ka and Kp

Soil 2 - Silty Sand (SM)

$$Ka_2 := \left(\tan\left(45\,^\circ - \frac{\phi_2}{2}\right)\right)^2 = 0.31$$ Active lateral earth pressure coefficient

$$Kp_2 := \left(\tan\left(45\,^\circ + \frac{\phi_2}{2}\right)\right)^2 = 3.25$$ Passive lateral earth pressure coefficient

Soil 3 - Silty Clay (CL-ML)

$$Ka_3 := \left(\tan\left(45\,^\circ - \frac{\phi_3}{2}\right)\right)^2 = 0.39$$ Active lateral earth pressure coefficient

$$Kp_3 := \left(\tan\left(45\,^\circ + \frac{\phi_3}{2}\right)\right)^2 = 2.56$$ Passive lateral earth pressure coefficient

Step 3: Develop the active pressure diagram above the cut

The wall is basically half in the Clay (CL) layer and half in the Silty Sand (SM) layer. The apparent earth pressure for both soils will be developed in order to find the predicted deflected shape for both cases. This calculation assumes the soil as Clay.

Stiff Clay (Following Chapter 5.2.6) - Terzaghi and Peck (1967)

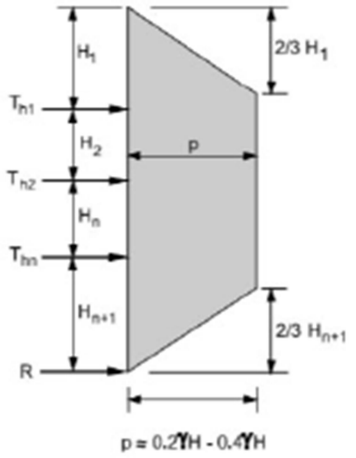

(b) Walls with multiple levels of ground anchors

$H = 26\ ft$

$N1 := \frac{\gamma_1 \cdot H}{c_1} = 2.08$ N<4.0, Stiff Clay

$p_1 := 0.4 \cdot \gamma_1 \cdot H = 1.25\ ksf$

$H1 := 11\ ft$ $H3 := 8\ ft$

$\frac{2}{3} \cdot H1 = 7.33\ ft$ $\frac{2}{3} \cdot H3 = 5.33\ ft$

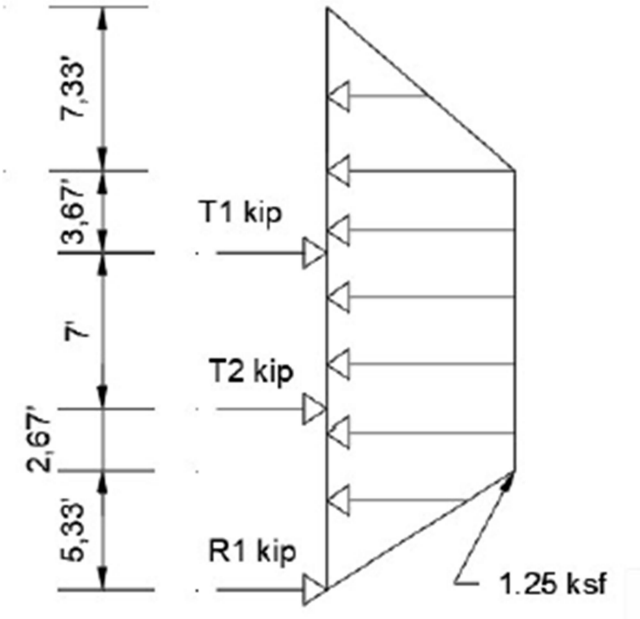

Apparent Earth Pressure Diagram - Clay

Step 4: Calculation of Tieback Loads

The calculation of tieback loads will follow the Chapter 5.3.3 and use the tributary area method.

$p_1 = 1.25\ ksf$ $\qquad P1 := p_1 \cdot b = 9.36\ \frac{kip}{ft}$

$T1 := \left(\frac{2}{3} \cdot H1 \cdot \frac{P1}{2}\right) + P1 \cdot \left(14.5\ ft - \frac{2}{3} \cdot H1\right) = 101.40\ kip$ From surface to the 14.5ft depth

$T2 := P1 \cdot 6.17\ ft + \left(\frac{3\ P1}{4} \cdot 1.33\ ft\right) + \frac{P1}{4} \cdot 1.33\ ft \cdot \frac{1}{2} = 68.64\ kip$ From the 14.5ft to 22ft depth

$R1 := 3 \cdot \frac{P1}{4} \cdot 4\ ft \cdot \frac{1}{2} = 14.04\ kip$ From the 22ft depth to the bottom

$Equi := \frac{7.33\ ft \cdot P1}{2} + 13.34\ ft \cdot P1 + \frac{5.33\ ft \cdot P1}{2} - T1 - T2 - R1 = 0.03\ kip$ OK

Step 5: Find Penetration Depth

The depth of penetration below excavation (d) will be found using the instructions on chapter 5.5.3

$\gamma_1 = 120\ pcf$ $h_1 = 12\ ft$ $Ka_1 := 1$

$\gamma_2 = 120\ pcf$ $h_2 = 10\ ft$ $Ka_2 = 0.31$

$\gamma_3 = 125\ pcf$ $h_3 = 4\ ft$ $Ka_3 = 0.39$

$B = 12\ in$ Pile width

Passive Pressure/Force:

$Kp_3 = 2.56$ $FS := 1.5$ $d := 9.27\ ft$

$Pp := \frac{Kp_3}{1.5} \cdot \gamma_3 \cdot d = 1.98\ \frac{kip}{ft^2}$ Passive Pressure

$Pf := Pp \cdot 3 \cdot B = 5.94\ \frac{kip}{ft}$ Passive Force

$PF := Pf \cdot \frac{d}{2} = 27.51\ kip$

Active Pressure/Force:

$Ka_3 = 0.39$

$Ap1 := Ka_3 \cdot (\gamma_1 \cdot h_1 + \gamma_2 \cdot h_2 + \gamma_3 \cdot h_3) = 1.23\ \frac{kip}{ft^2}$ Active Pressure bottom of excavation

$Ap2 := Ka_3 \cdot (\gamma_1 \cdot h_1 + \gamma_2 \cdot h_2 + \gamma_3 \cdot (h_3 + d)) = 1.68\ \frac{kip}{ft^2}$ Active Pressure at depth d

$Af1 := Ap1 \cdot B = 1.23\ \frac{kip}{ft}$ Active Force bottom of ecavation

$Af2 := Ap2 \cdot B = 1.68\ \frac{kip}{ft}$ Active Force at depth d

$AF := (Af2 + Af1) \cdot \frac{d}{2} = 13.46\ kip$

Check:

$PF - AF - R1 = 0.01\ kip$

$d := 1.2 \cdot d = 11.12\ ft$ Add 20% to find actual embedment depth

Step 6: Find net Pressure Diagram

$$Net(d) := \left(\left(\gamma_1 \cdot h_1 + \gamma_2 \cdot h_2 + \gamma_3 \cdot (h_3 + d)\right) \cdot Ka_3 \cdot B\right) - \left(\frac{Kp_3}{1.5} \cdot \gamma_3 \cdot d \cdot 3 \cdot B\right)$$

$d1 := 0\ ft$ $\quad P2 := Net(d1) = 1.23\ \frac{kip}{ft}$

$d1 := 11.12\ ft$ $\quad P3 := Net(d1) = -5.35\ \frac{kip}{ft}$

$d1 := 2.08\ ft$ $\quad Net(d1) = 0\ \frac{kip}{ft}$

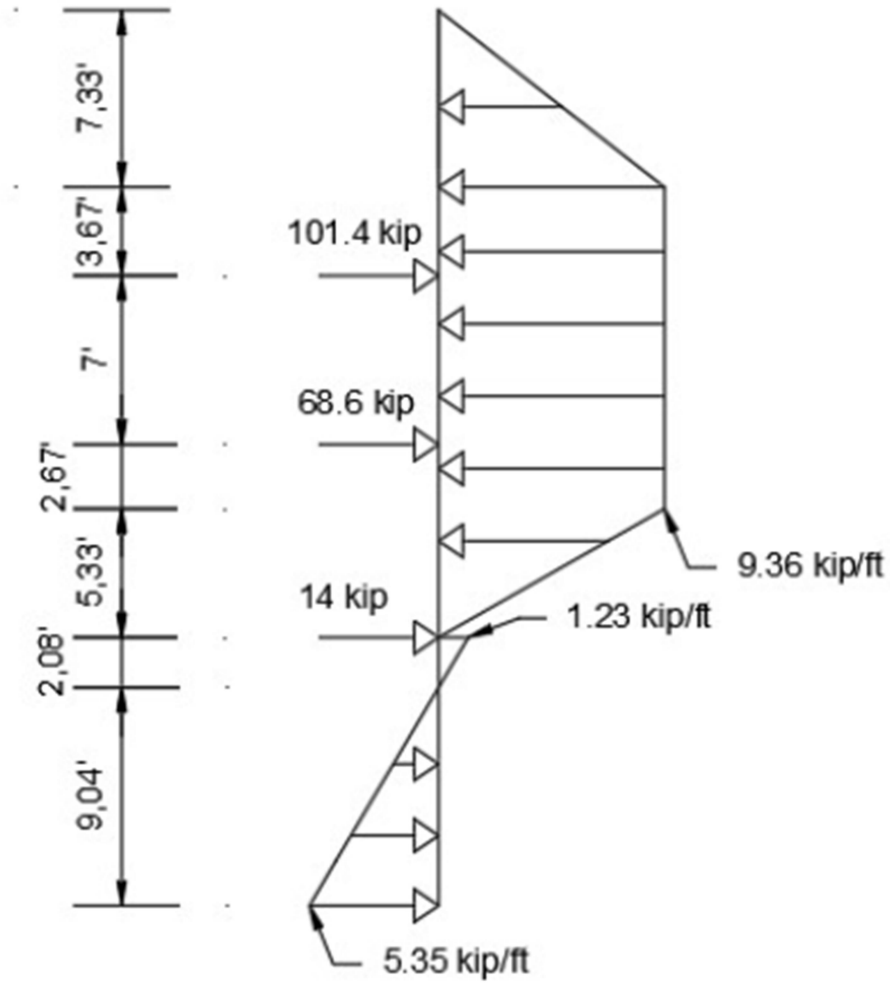

Earth Pressure Diagram - Pile P004 - Clay

Step 7: Find Moment Diagram

0 ft < y < 7.33 ft $M(y) := -0.212 \frac{kip}{ft^2} \cdot y^3$

7.33 ft < y < 11 ft $M(y) := -4.68 \frac{kip}{ft} \cdot y^2 + 34.30 \cdot kip \cdot y - 83.82\ kip \cdot ft$

11 ft < y < 18 ft $M(y) := -4.68 \frac{kip}{ft} \cdot y^2 + 135.7 \cdot kip \cdot y - 1199.2\ kip \cdot ft$

18 ft < y < 20.67 ft $M(y) := -4.68 \frac{kip}{ft} \cdot y^2 + 204.3 \cdot kip \cdot y - 2434\ kip \cdot ft$

20.67 ft < Y < 26 ft

$M(y) := 0.292667 \frac{kip}{ft^2} \cdot y^3 - 22.827173 \frac{kip}{ft}\ y^2 + 579.390811\ kip\ y - 5018.238616\ kip \cdot ft$

26 ft < Y < 28.08 ft

$M(y) := -0.493 \frac{kip}{ft^2}\ y^3 + 39.049 \frac{kip}{ft} \cdot y^2 - 1031.173\ kip \cdot y + 8837.137\ kip \cdot ft$

28.08 ft < Y < 37.12 ft

$M(y) := 0.09864 \frac{kip}{ft^2} \cdot y^3 - 8.309 \frac{kip}{ft} \cdot y^2 + 231.993\ kip \cdot y - 2389.607\ kip \cdot ft$

An excel spreadsheet was created using the equations above in order to generate the moment diagram

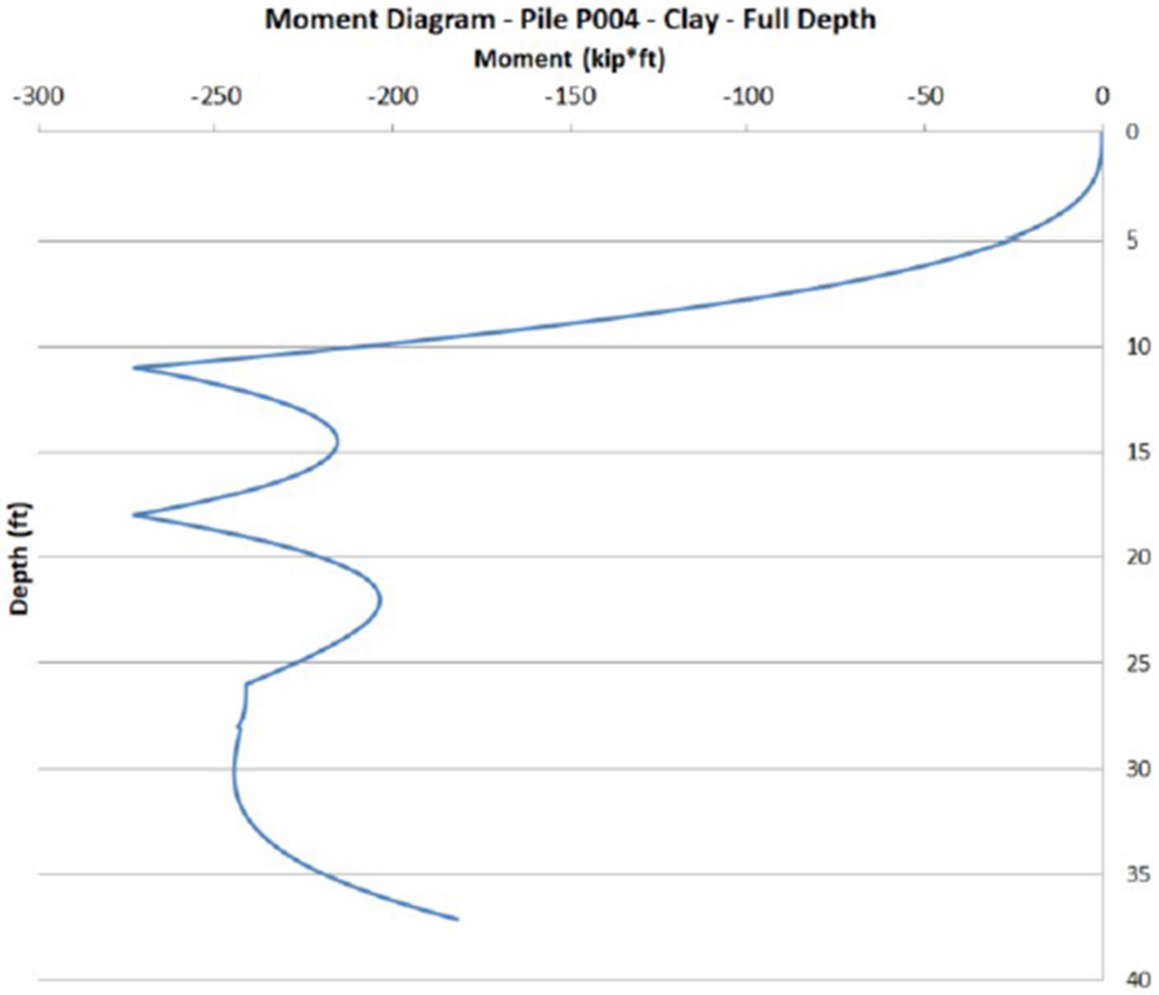

Moment Diagram - Pile P004 - Clay

Step 8: Find Deflected Shape

An excel spreadsheet was developed in order to find the deflected shape for this structure using the trapezoidal approximation.

Since the moment is known for any depth of the pile, it is possible to numerically find the curvature, slope and deflection at any depth following the steps below:

1) Find the curvature by dividing the moment by E*I. For this structure E=29000ksi and I=393 in^4.

2) The slope at the bottom is assumed to be zero. Then, adding small increments, it is possible to find the slope at any other point by using the area under the curvature curve and the distance from the centroid to the desired point. Since the increments are small, the area under the curve is a trapezoid.

3) Find the deflection at a point using the area under the slope curve and the distance from the centroid to the point, same approach used in the previous step.

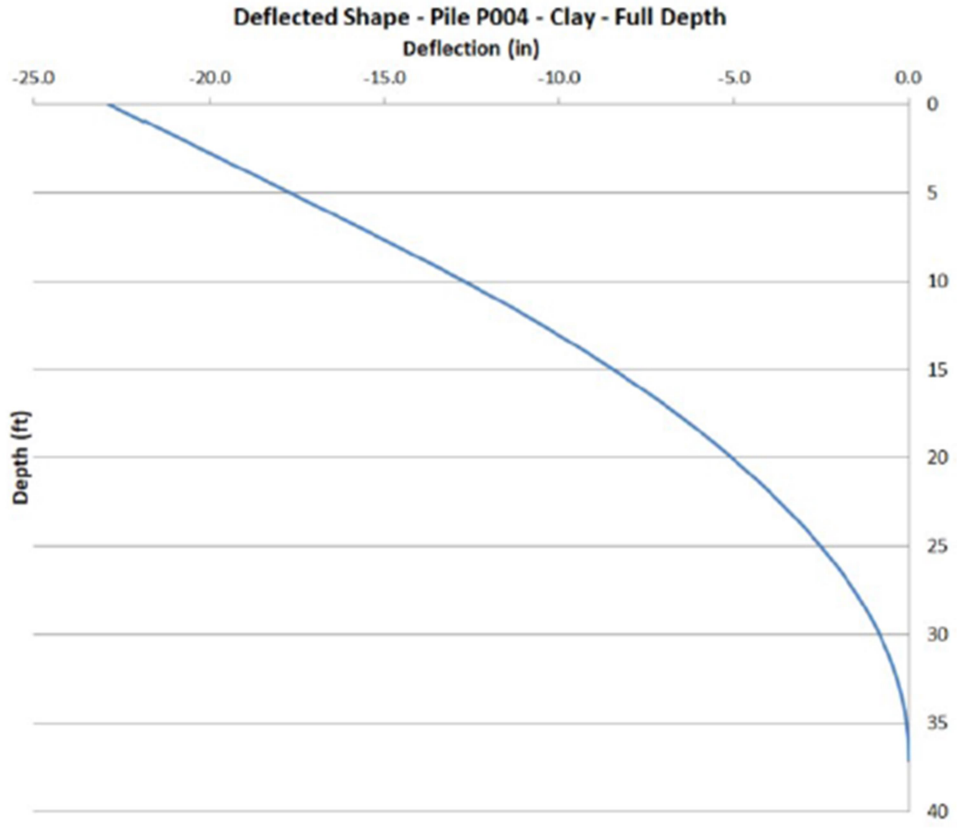

Deflected Shape - Pile P004 - Clay - Full Depth

The second calculation shown is the one for pile P004 assuming the soil as sand.

DESIGN OF ANCHORED SYSTEMS - PILE P004 - SAND

The hand calculation design of the MU retaining wall will follow the procedure described in the Geotechnical Engineering Circular No. 4 - Ground Anchors and Anchored Systems by the U.S. Department of Transportation - Federal Highway Administration. Publication No. FHWA-IF-99-015.

Chapter 5 (Design of Anchored Systems) describes the design method with the recommended Apparent Earth Pressure Diagrams for various soil types. This designed will be based on this chapter.

Step 1: Define Parameters of wall and soil

$H := 26\ ft$	Height of wall	$b := 90\ in$	Spacing between piles (center to center)
$H_{pile} := 40\ ft$	Height of pile	$B := 12\ in$	Width of flange for HP12x53

$H1 := 11\ ft$ Distance from ground surface to first row of tiebacks

$H2 := 7\ ft$ Distance from first row of tiebacks to second row of tiebacks

$H3 := 8\ ft$ Distance from base of excavation to second row of tiebacks

Soil 1 - Clay (CL) - Undrained Condition
From 0 ft to 12 ft - N=9

$S_1 := 1500\ psf$ Shear Strength Soil 1 - (Terzaghi, Peck, and Mesri, 1996)

$c_1 := S_1 = 1500\ psf$ Cohesion Soil 1 - (Terzaghi, Peck, and Mesri, 1996)

$\phi_1 := 0\ °$ Fully Undrained

$\gamma_1 := 120\ pcf$ Unit Weight of Soil 1 (Terzaghi, Peck, and Mesri, 1996 and experience)

$h_1 := 12\ ft$ Height of Soil 1

Soil 2 - Silty Sand (SM) - Drained Condition
From 12 ft to 22 ft - N=20

$c_2 := 0\ psf$

$\phi_2 := 32\ °$ Friction Angle Soil 2 - (Bowles, 1998; NAVFAC, 1998; and Peck, Hanson, Thornburn, 1973)

$\gamma_2 := 120\ pcf$ Unit Weight of Soil 2 (Terzaghi, Peck, and Mesri, 1996 and experience)

$h_2 := 10\ ft$ Height of Soil 2

Soil 3 - Silty Clay (CL-ML) - Drained Condition
From 22 ft to 26 ft - N=52

$c_3 := 100\ psf$ (Local Experience)

$\phi_3 := 26\ °$ Assumed Liquid Limit (LL) of 40 (Stark, Choi and McCone, 2005)

$\gamma_3 := 125\ pcf$ Unit Weight of Soil 3 (Terzaghi, Peck, and Mesri, 1996 and experience)

$h_3 := 4\ ft$ Height of Soil 3

Surcharge

The surcharge for this retaining wall is zero.

$q := 0\ psf$

Water table

The water level is at cut level, 26 ft from the surface.

$\gamma_w := 62.4\ pcf$

Step 2: Determine values of Ka and Kp

Soil 2 - Silty Sand (SM)

$$Ka_2 := \left(\tan\left(45\,^\circ - \frac{\phi_2}{2}\right)\right)^2 = 0.31$$ Active lateral earth pressure coefficient

$$Kp_2 := \left(\tan\left(45\,^\circ + \frac{\phi_2}{2}\right)\right)^2 = 3.25$$ Passive lateral earth pressure coefficient

Soil 3 - Silty Clay (CL-ML)

$$Ka_3 := \left(\tan\left(45\,^\circ - \frac{\phi_3}{2}\right)\right)^2 = 0.39$$ Active lateral earth pressure coefficient

$$Kp_3 := \left(\tan\left(45\,^\circ + \frac{\phi_3}{2}\right)\right)^2 = 2.56$$ Passive lateral earth pressure coefficient

Step 3: Develop the active pressure diagram above the cut

The wall is basically half in the Clay (CL) layer and half in the Silty Sand (SM) layer. The apparent earth pressure for both soils will be developed in order to find the predicted deflected shape for both cases. This calculation assumes the soil as Sand.

Sand (Following Chapter 5.2.4) - Terzaghi and Peck (1967)

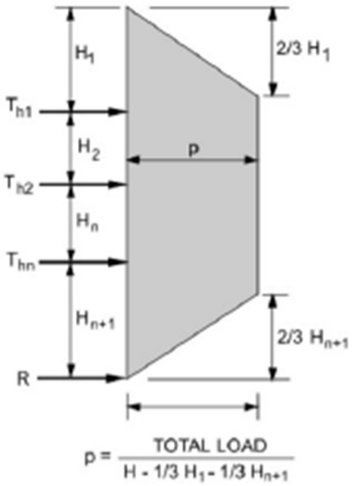

(b) Walls with multiple levels of ground anchors

$H = 26\ ft$

$H1 := 11\ ft \qquad H3 := 8\ ft$

$TotalLoad := 0.65 \cdot Ka_2 \cdot \gamma_2 \cdot H^2 = 16.2\ \frac{kip}{ft}$

$p_1 := \frac{TotalLoad}{H - \frac{H1}{3} - \frac{H3}{3}} = 0.82\ \frac{kip}{ft^2}$

$\frac{2}{3} \cdot H1 = 7.33\ ft \qquad \frac{2}{3} \cdot H3 = 5.33\ ft$

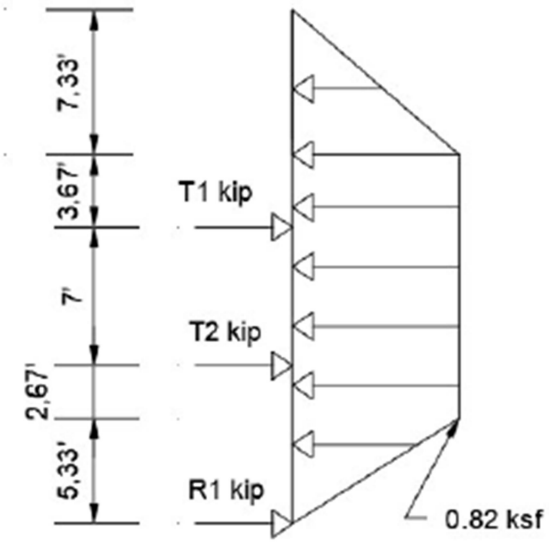

Apparent Earth Pressure Diagram - Sand

Step 4: Calculation of Tieback Loads

The calculation of tieback loads will follow the Chapter 5.3.3 and use the tributary area method.

$p_1 = 0.82\ ksf$ $\qquad P1 := p_1 \cdot b = 6.18\ \frac{kip}{ft}$

$T1 := \left(\frac{2}{3} \cdot H1 \cdot \frac{P1}{2}\right) + P1 \cdot \left(14.5\ ft - \frac{2}{3} \cdot H1\right) = 66.93\ kip$ From surface to the 14.5ft depth

$T2 := P1 \cdot 6.17\ ft + \left(\frac{3\ P1}{4} \cdot 1.33\ ft\right) + \frac{P1}{4} \cdot 1.33\ ft \cdot \frac{1}{2} = 45.31\ kip$ From the 14.5ft to 22ft depth

$R1 := 3 \cdot \frac{P1}{4} \cdot 4\ ft \cdot \frac{1}{2} = 9.27\ kip$ From the 22ft depth to the bottom

$Equi := \frac{7.33\ ft \cdot P1}{2} + 13.34\ ft \cdot P1 + \frac{5.33\ ft \cdot P1}{2} - T1 - T2 - R1 = 0.02\ kip$ OK

Step 5: Find Penetration Depth

The depth of penetration below excavation (d) will be found using the instructions on chapter 5.5.3

$\gamma_1 = 120\ pcf$ $h_1 = 12\ ft$ $Ka_1 := 1$

$\gamma_2 = 120\ pcf$ $h_2 = 10\ ft$ $Ka_2 = 0.31$

$\gamma_3 = 125\ pcf$ $h_3 = 4\ ft$ $Ka_3 = 0.39$

$B = 12\ in$ Pile width

Passive Pressure/Force:

$Kp_2 = 3.25$ $FS := 1.5$ $d := 6.46\ ft$

$Pp := \frac{Kp_2}{1.5} \cdot \gamma_2 \cdot d = 1.68\ \frac{kip}{ft^2}$ Passive Pressure

$Pf := Pp \cdot 3 \cdot B = 5.05\ \frac{kip}{ft}$ Passive Force

$PF := Pf \cdot \frac{d}{2} = 16.3\ kip$

Active Pressure/Force:

$Ka_2 = 0.31$

$Ap1 := Ka_2 \cdot (\gamma_1 \cdot h_1 + \gamma_2 \cdot h_2 + \gamma_3 \cdot h_3) = 0.96\ \frac{kip}{ft^2}$ Active Pressure bottom of excavation

$Ap2 := Ka_2 \cdot (\gamma_1 \cdot h_1 + \gamma_2 \cdot h_2 + \gamma_3 \cdot (h_3 + d)) = 1.21\ \frac{kip}{ft^2}$ Active Pressure at depth d

$Af1 := Ap1 \cdot B = 0.96\ \frac{kip}{ft}$ Active Force bottom of ecavation

$Af2 := Ap2 \cdot B = 1.21\ \frac{kip}{ft}$ Active Force at depth d

$AF := (Af2 + Af1) \cdot \frac{d}{2} = 7.03\ kip$

Check:

$PF - AF - R1 = 0\ kip$

$d := 1.2 \cdot d = 7.75\ ft$ Add 20% to find actual embedment depth

Step 6: Find net Pressure Diamagram

$$Net(d) := \left(\left(\gamma_1 \cdot h_1 + \gamma_2 \cdot h_2 + \gamma_3 \cdot \left(h_3 + d\right)\right) \cdot Ka_2 \cdot B\right) - \left(\frac{Kp_2}{1.5} \cdot \gamma_2 \cdot d \cdot 3 \cdot B\right)$$

$d1 := 0\ ft$ $\quad P2 := Net(d1) = 0.96\ \frac{kip}{ft}$

$d1 := 7.75\ ft$ $\quad P3 := Net(d1) = -4.79\ \frac{kip}{ft}$

$d1 := 1.29\ ft$ $\quad Net(d1) = 0.01\ \frac{kip}{ft}$

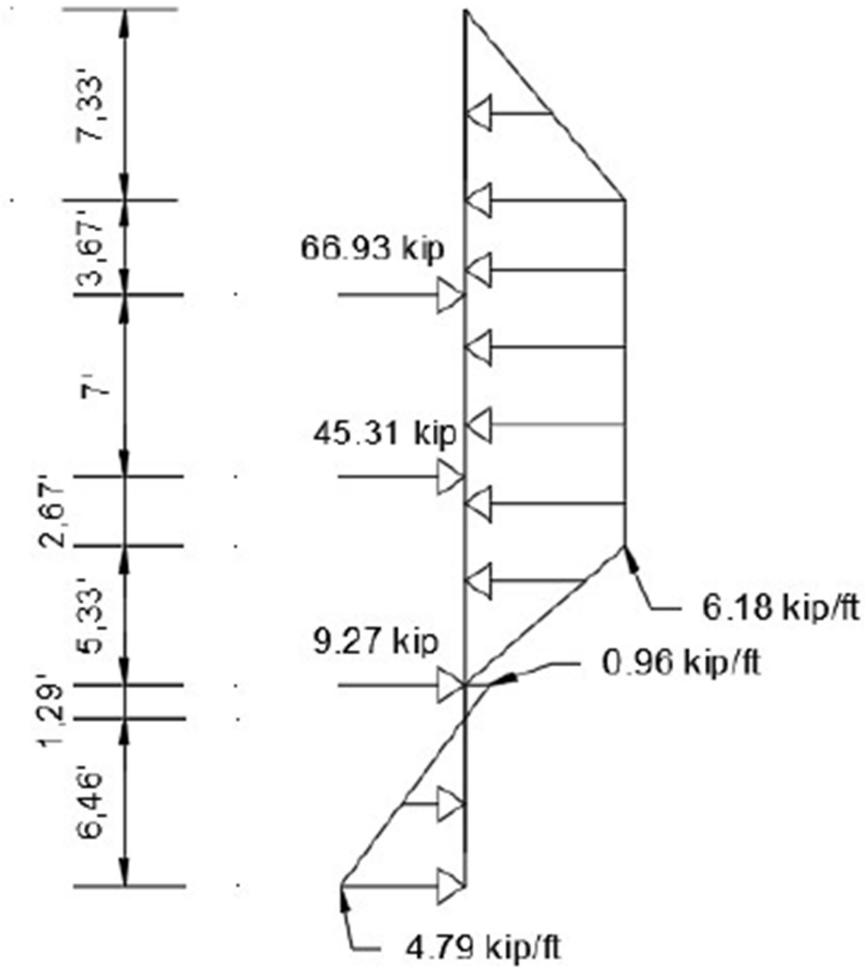

Earth Pressure Diagram - Pile P004 - Sand

Step 7: Find Moment Diagram

0 ft < y < 7.33 ft $M(y) := -0.141 \frac{kip}{ft^2} \cdot y^3$

7.33 ft < y < 11 ft $M(y) := -3.09 \frac{kip}{ft} \cdot y^2 + 22.6497 \cdot kip \cdot y - 55.3407\ kip \cdot ft$

11 ft < y < 18 ft $M(y) := -3.09 \frac{kip}{ft} \cdot y^2 + 89.5797 \cdot kip \cdot y - 791.5707\ kip \cdot ft$

18 ft < y < 20.67 ft $M(y) := -3.09 \frac{kip}{ft} \cdot y^2 + 134.8897 \cdot kip \cdot y - 1607.1507\ kip \cdot ft$

20.67 ft < Y < 26 ft

$M(y) := 0.19325 \frac{kip}{ft^2} \cdot y^3 - 15.07317 \frac{kip}{ft} y^2 + 382.58184\ kip\ y - 3313.7496\ kip \cdot ft$

26 ft < Y < 27.29 ft

$M(y) := 0.12403 \frac{kip}{ft^2} y^3 - 10.15442 \frac{kip}{ft} \cdot y^2 + 276.44428\ kip \cdot y - 2662.84059\ kip \cdot ft$

27.29 ft < Y < 33.75 ft

$M(y) := 0.12358 \frac{kip}{ft^2} \cdot y^3 - 10.11758 \frac{kip}{ft} \cdot y^2 + 275.43889\ kip \cdot y - 2653.69483\ kip \cdot ft$

An excel spreadsheet was created using the equations above in order to generate the moment diagram

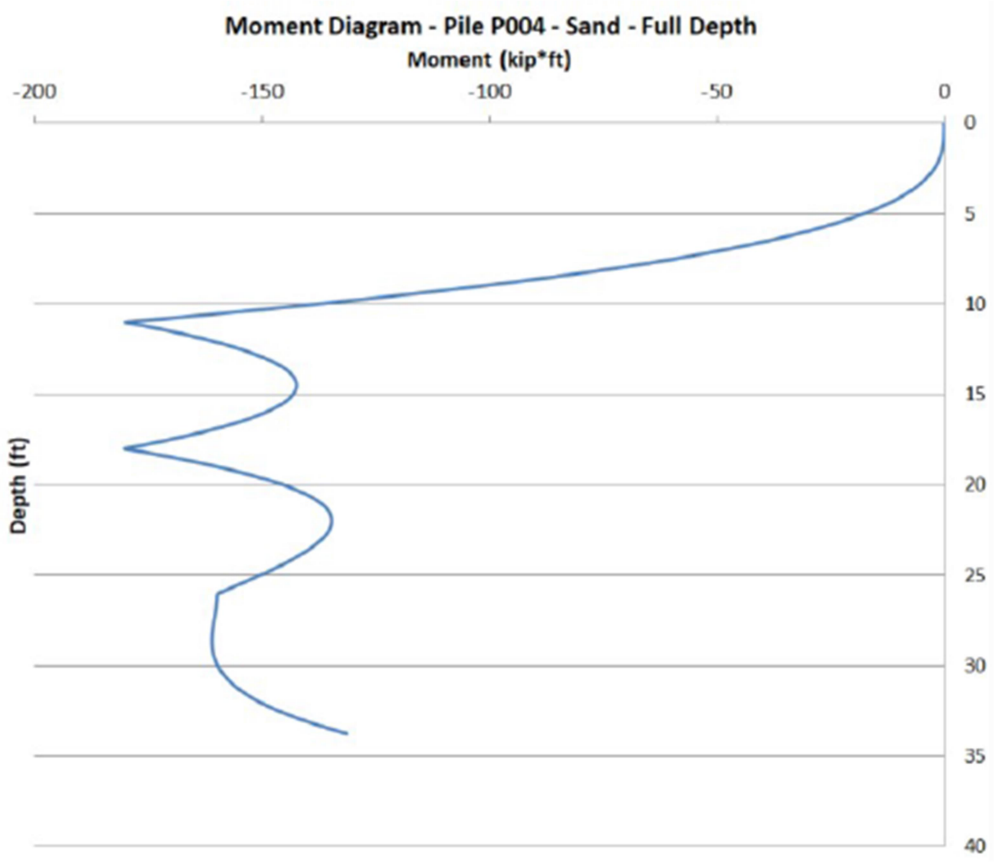

Moment Diagram - Pile P004 - Sand

Step 8: Find Deflected Shape

An excel spreadsheet was developed in order to find the deflected shape for this structure using the trapezoidal approximation.

Since the moment is known for any depth of the pile, it is possible to numerically find the curvature, slope and deflection at any depth following the steps below:

1) Find the curvature by dividing the moment by E*I. For this structure E=29000ksi and I=393 in^4.

2) The slope at the bottom is assumed to be zero. Then, adding small increments, it is possible to find the slope at any other point by using the area under the curvature curve and the distance from the centroid to the desired point. Since the increments are small, the area under the curve is a trapezoid.

3) Find the deflection at a point using the area under the slope curve and the distance from the centroid to the point, same approach used in the previous step.

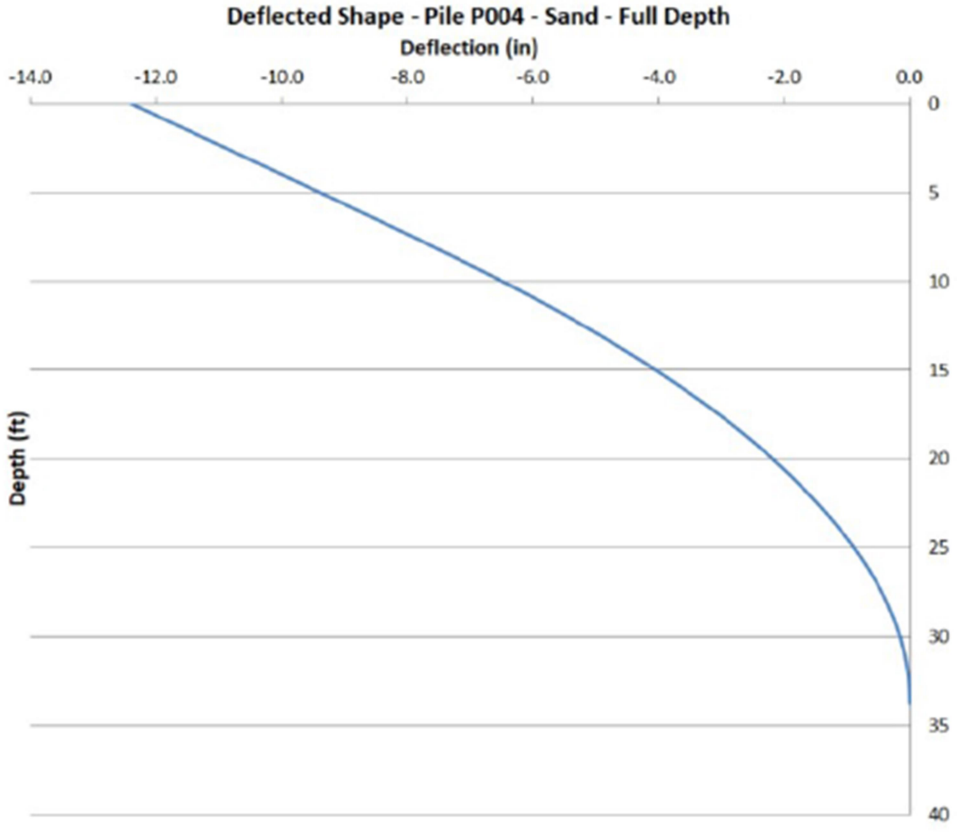

Deflected Shape - Pile P004 - Sand - Full Depth

The third calculation shown is the one for pile P005 assuming the soil as clay.

DESIGN OF ANCHORED SYSTEMS - PILE P005 - CLAY

The hand calculation design of the MU retaining wall will follow the procedure described in the Geotechnical Engineering Circular No. 4 - Ground Anchors and Anchored Systems by the U.S. Department of Transportation - Federal Highway Administration. Publication No. FHWA-IF-99-015.

Chapter 5 (Design of Anchored Systems) describes the design method with the recommended Apparent Earth Pressure Diagrams for various soil types. This designed will be based on this chapter.

Step 1: Define Parameters of wall and soil

$H := 24\ ft$	Height of wall	$B := 12\ in$	Width of flange for HP12x53
$H_{pile} := 35\ ft$	Height of pile	$b := 90\ in$	Spacing between piles (center to center)

$H1 := 11\ ft$ Distance from ground surface to first row of tiebacks

$H2 := 7\ ft$ Distance from first row of tiebacks to second row of tiebacks

$H3 := 6\ ft$ Distance from base of excavation to second row of tiebacks

Soil 1 - Clay (CL) - Undrained Condition
From 0 ft to 12 ft - N=9

$S_1 := 1500\ psf$ Shear Strength Soil 1 - (Terzaghi, Peck, and Mesri, 1996)

$c_1 := S_1 = 1500\ psf$ Cohesion Soil 1 - (Terzaghi, Peck, and Mesri, 1996)

$\phi_1 := 0\ °$ Fully Undrained

$\gamma_1 := 120\ pcf$ Unit Weight of Soil 1 (Terzaghi, Peck, and Mesri, 1996 and experience)

$h_1 := 12\ ft$ Height of Soil 1

Soil 2 - Silty Sand (SM) - Drained Condition
From 12 ft to 22 ft - N=20

$c_2 := 0\ psf$

$\phi_2 := 32\ °$ Friction Angle Soil 2 - (Bowles, 1998; NAVFAC, 1998; and Peck, Hanson, Thornburn, 1973)

$\gamma_2 := 120\ pcf$ Unit Weight of Soil 2 (Terzaghi, Peck, and Mesri, 1996 and experience)

$h_2 := 10\ ft$ Height of Soil 2

Soil 3 - Silty Clay (CL-ML) - Drained Condition
From 22 ft to 26 ft - N=52

$c_3 := 100\ psf$ (Local Experience)

$\phi_3 := 26\ °$ Assumed Liquid Limit (LL) of 40 (Stark, Choi and McCone, 2005)

$\gamma_3 := 125\ pcf$ Unit Weight of Soil 3 (Terzaghi, Peck, and Mesri, 1996 and experience)

$h_3 := 2\ ft$ Height of Soil 3

Surcharge

The surcharge for this retaining wall is zero.

$q := 0\ psf$

Water table

The water level is at cut level, 26 ft from the surface.

$\gamma_w := 62.4\ pcf$

Step 2: Determine values of Ka and Kp

Soil 2 - Silty Sand (SM)

$$Ka_2 := \left(\tan\left(45\,^\circ - \frac{\phi_2}{2}\right)\right)^2 = 0.31$$ Active lateral earth pressure coefficient

$$Kp_2 := \left(\tan\left(45\,^\circ + \frac{\phi_2}{2}\right)\right)^2 = 3.25$$ Passive lateral earth pressure coefficient

Soil 3 - Silty Clay (CL-ML)

$$Ka_3 := \left(\tan\left(45\,^\circ - \frac{\phi_3}{2}\right)\right)^2 = 0.39$$ Active lateral earth pressure coefficient

$$Kp_3 := \left(\tan\left(45\,^\circ + \frac{\phi_3}{2}\right)\right)^2 = 2.56$$ Passive lateral earth pressure coefficient

Step 3: Develop the active pressure diagram above the cut

The wall is basically half in the Clay (CL) layer and half in the Silty Sand (SM) layer. The apparent earth pressure for both soils will be developed in order to find the predicted deflected shape for both cases. This calculation assumes the soil as Clay.

Stiff Clay (Following Chapter 5.2.6) - Terzaghi and Peck (1967)

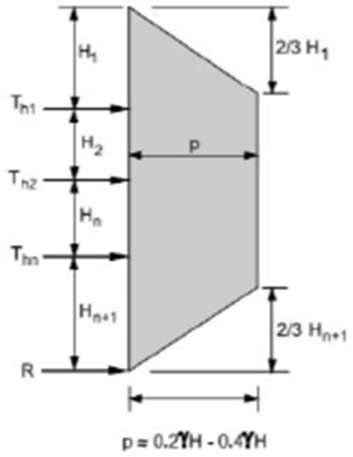

(b) Walls with multiple levels of ground anchors

$H = 24\ ft$

$N1 := \frac{\gamma_1 \cdot H}{c_1} = 1.92$ N<4.0, Stiff Clay

$p_1 := 0.4 \cdot \gamma_1 \cdot H = 1.15\ ksf$

$H1 = 11\ ft$ $H3 = 6\ ft$

$\frac{2}{3} \cdot H1 = 7.33\ ft$ $\frac{2}{3} \cdot H3 = 4\ ft$

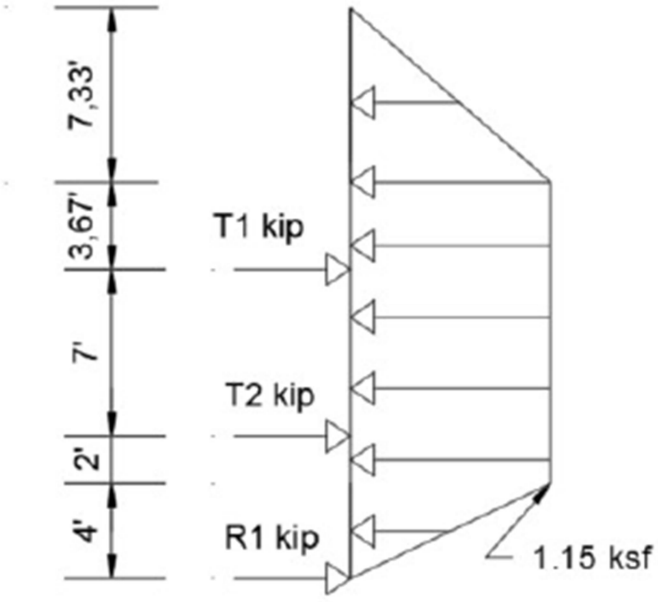

Apparent Earth Pressure Diagram - Clay

Step 4: Calculation of Tieback Loads

The calculation of tieback loads will follow the Chapter 5.3.3 and use the tributary area method.

$p_1 = 1.15\ ksf$ $\qquad P1 := p_1 \cdot b = 8.64\ \frac{kip}{ft}$

$T1 := \left(\frac{2}{3} \cdot H1 \cdot \frac{P1}{2}\right) + P1 \cdot \left(14.5\ ft - \frac{2}{3} \cdot H1\right) = 93.60\ kip$ From surface to the 14.5ft depth

$T2 := P1 \cdot 5.5\ ft + \left(\frac{3\ P1}{4} \cdot 1\ ft\right) + \frac{P1}{4} \cdot 1\ ft \cdot \frac{1}{2} = 55.08\ kip$ From the 14.5ft to 21ft depth

$R1 := 3 \cdot \frac{P1}{4} \cdot 3\ ft \cdot \frac{1}{2} = 9.72\ kip$ From the 22ft depth to the bottom

$Equi := \frac{7.33\ ft \cdot P1}{2} + 12.67\ ft \cdot P1 + \frac{4\ ft \cdot P1}{2} - T1 - T2 - R1 = 0.01\ kip$ OK

Step 5: Find Penetration Depth

The depth of penetration below excavation (d) will be found using the instructions on chapter 5.5.3

$\gamma_1 = 120\ pcf$ $h_1 = 12\ ft$ $Ka_1 := 1$

$\gamma_2 = 120\ pcf$ $h_2 = 10\ ft$ $Ka_2 = 0.31$

$\gamma_3 = 125\ pcf$ $h_3 = 2\ ft$ $Ka_3 = 0.39$

$B = 12\ in$ Pile width

Passive Pressure/Force:

$Kp_3 = 2.56$ $FS := 1.5$ $d := 7.95\ ft$

$Pp := \frac{Kp_3}{1.5} \cdot \gamma_3 \cdot d = 1.7\ \frac{kip}{ft^2}$ Passive Pressure

$Pf := Pp \cdot 3 \cdot B = 5.09\ \frac{kip}{ft}$ Passive Force

$PF := Pf \cdot \frac{d}{2} = 20.23\ kip$

Active Pressure/Force:

$Ka_3 = 0.39$

$Ap1 := Ka_3 \cdot (\gamma_1 \cdot h_1 + \gamma_2 \cdot h_2 + \gamma_3 \cdot h_3) = 1.13\ \frac{kip}{ft^2}$ Active Pressure bottom of excavation

$Ap2 := Ka_3 \cdot (\gamma_1 \cdot h_1 + \gamma_2 \cdot h_2 + \gamma_3 \cdot (h_3 + d)) = 1.52\ \frac{kip}{ft^2}$ Active Pressure at depth d

$Af1 := Ap1 \cdot B = 1.13\ \frac{kip}{ft}$ Active Force bottom of ecavation

$Af2 := Ap2 \cdot B = 1.52\ \frac{kip}{ft}$ Active Force at depth d

$AF := (Af2 + Af1) \cdot \frac{d}{2} = 10.51\ kip$

Check:

$PF - AF - R1 = 0\ kip$

$d := 1.2 \cdot d = 9.54\ ft$ Add 20% to find actual embedment depth

Step 6: Find net Pressure Diamagram

$$Net(d) := \left(\left(\gamma_1 \cdot h_1 + \gamma_2 \cdot h_2 + \gamma_3 \cdot \left(h_3 + d\right)\right) \cdot Ka_3 \cdot B\right) - \left(\frac{Kp_3}{1.5} \cdot \gamma_3 \cdot d \cdot 3 \cdot B\right)$$

$d1 := 0\ ft$ $\quad P2 := Net(d1) = 1.13\ \frac{kip}{ft}$

$d1 := 9.54\ ft$ $\quad P3 := Net(d1) = -4.51\ \frac{kip}{ft}$

$d1 := 1.91\ ft$ $\quad Net(d1) = 0\ \frac{kip}{ft}$

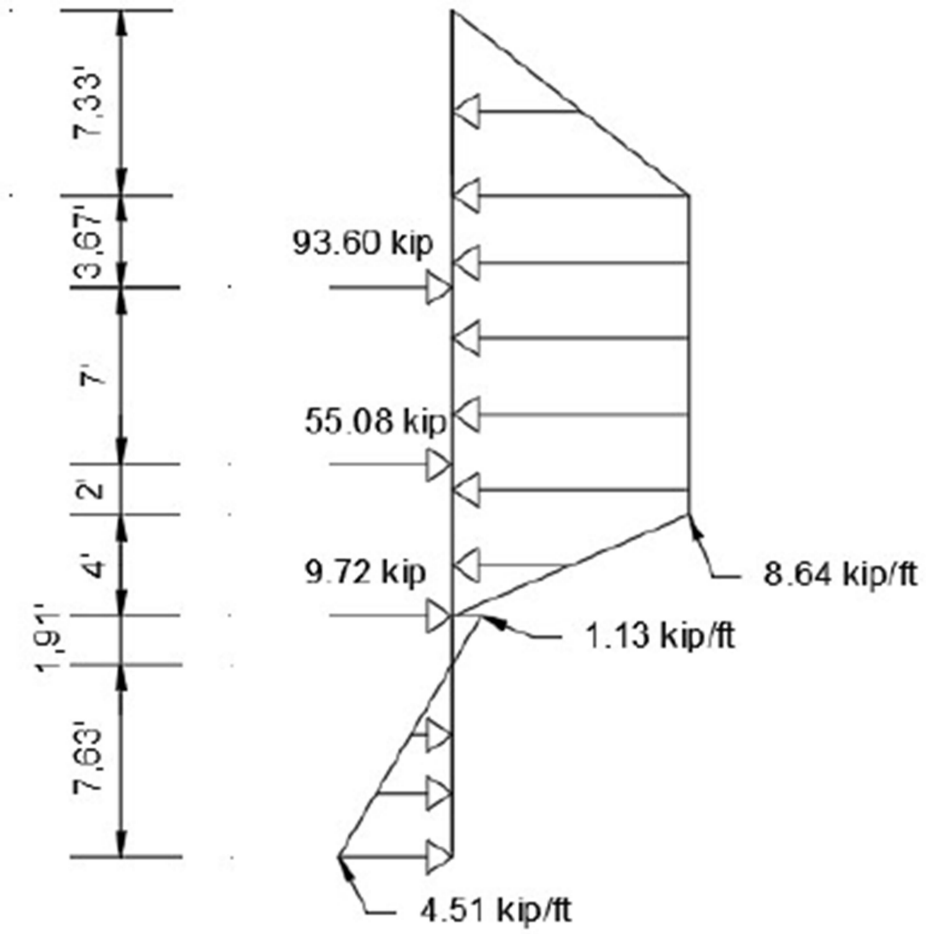

Earth Pressure Diagram- Pile P005 - Clay

Step 7: Find Moment Diagram

0 ft < y < 7.33 ft $M(y) := -0.19645 \frac{kip}{ft^2} \cdot y^3$

7.33 ft < y < 11 ft $M(y) := -4.32 \frac{kip}{ft} \cdot y^2 + 31.66 \cdot kip \cdot y - 77.3696\ kip \cdot ft$

11 ft < y < 18 ft

$$M(y) := -4.32 \frac{kip}{ft} \cdot y^2 + 125.2656 \cdot kip \cdot y - 1106.9696\ kip \cdot ft$$

18 ft < y < 20 ft

$$M(y) := -4.32 \frac{kip}{ft} \cdot y^2 + 180.3456 \cdot kip \cdot y - 2098.4096\ kip \cdot ft$$

20 ft < Y < 24 ft

$$M(y) := 0.36 \frac{kip}{ft^2} \cdot y^3 - 25.92 \frac{kip}{ft}\ y^2 + 612.34\ kip\ y - 4977.8622\ kip \cdot ft$$

24 ft < Y < 25.91 ft

$$M(y) := 0.0986 \frac{kip}{ft^2}\ y^3 - 7.66448 \frac{kip}{ft} \cdot y^2 + 197.49303\ kip \cdot y - 1923.09935\ kip \cdot ft$$

25.91 ft < Y < 33.54 ft

$$M(y) := 0.09851 \frac{kip}{ft^2} \cdot y^3 - 7.65754 \frac{kip}{ft} \cdot y^2 + 197.31338\ kip \cdot y - 1921.55491\ kip \cdot ft$$

An excel spreadsheet was created using the equations above in order to generate the moment diagram

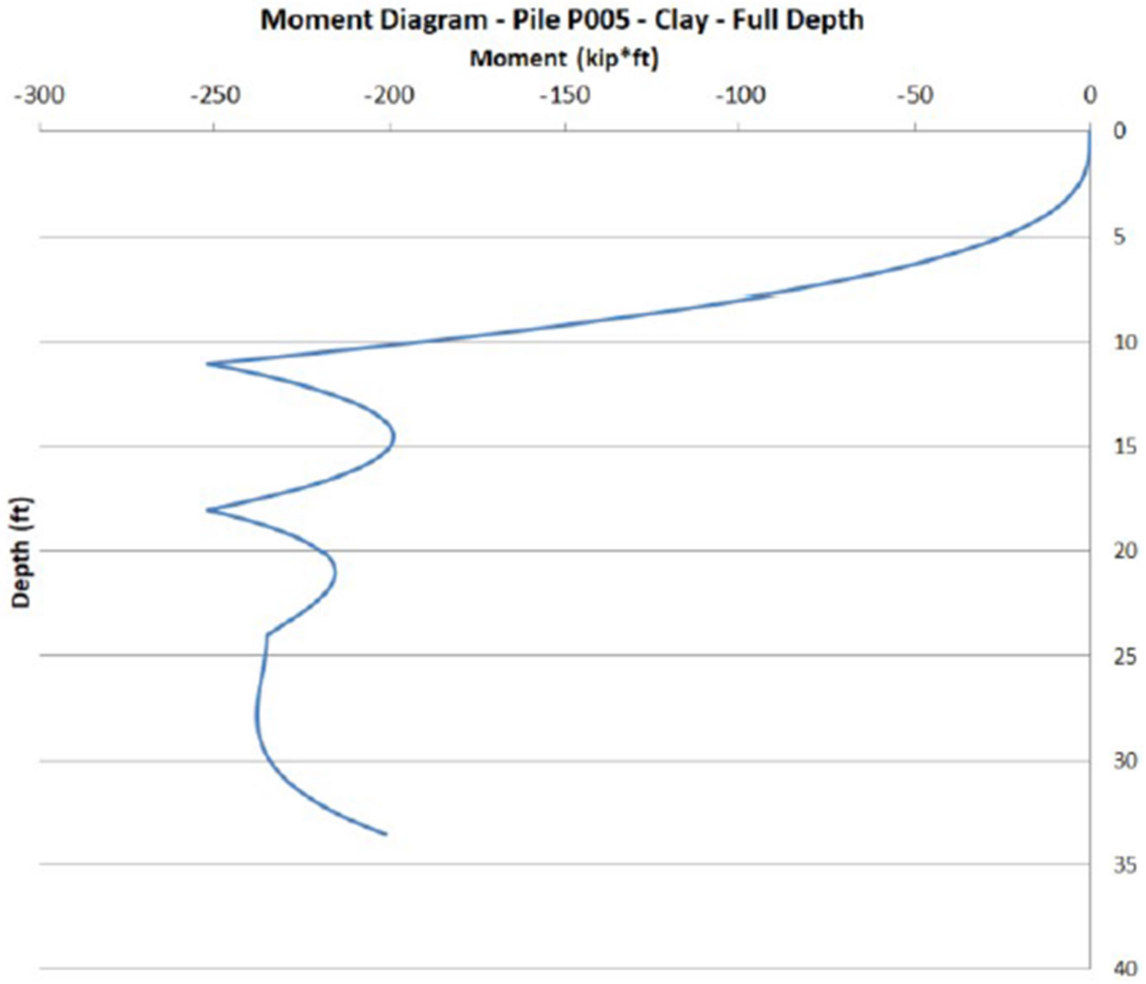

Moment Diagram - Pile P005 - Clay

Step 8: Find Deflected Shape

An excel spreadsheet was developed in order to find the deflected shape for this structure using the trapezoidal approximation.

Since the moment is known for any depth of the pile, it is possible to numerically find the curvature, slope and deflection at any depth following the steps below:

1) Find the curvature by dividing the moment by E*I. For this structure E=29000ksi and I=393 in^4.

2) The slope at the bottom is assumed to be zero. Then, adding small increments, it is possible to find the slope at any other point by using the area under the curvature curve and the distance from the centroid to the desired point. Since the increments are small, the area under the curve is a trapezoid.

3) Find the deflection at a point using the area under the slope curve and the distance from the centroid to the point, same approach used in the previous step.

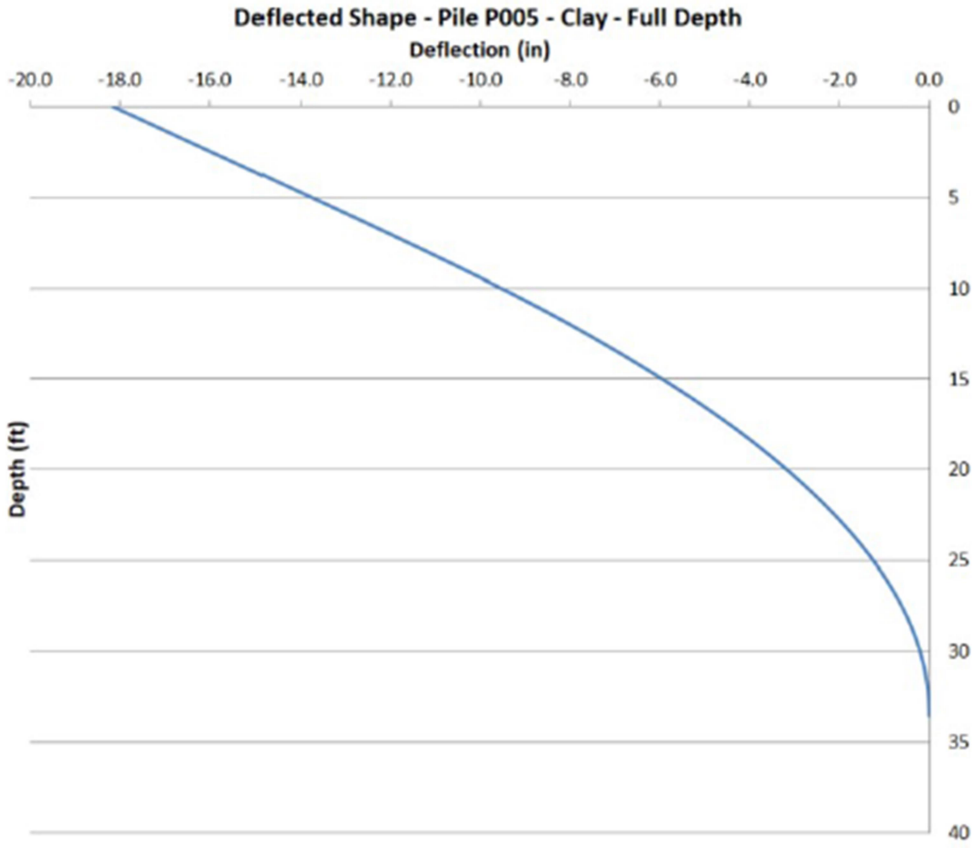

Deflected Shape - Pile P005 - Clay - Full Depth

The fourth calculation shown is the one for pile P005 assuming the soil as sand.

DESIGN OF ANCHORED SYSTEMS - PILE P005 - SAND

The hand calculation design of the MU retaining wall will follow the procedure described in the Geotechnical Engineering Circular No. 4 - Ground Anchors and Anchored Systems by the U.S. Department of Transportation - Federal Highway Administration. Publication No. FHWA-IF-99-015.

Chapter 5 (Design of Anchored Systems) describes the design method with the recommended Apparent Earth Pressure Diagrams for various soil types. This designed will be based on this chapter.

Step 1: Define Parameters of wall and soil

$H := 24\ ft$	Height of wall	$B := 12\ in$	Width of flange for HP12x53
$H_{pile} := 35\ ft$	Height of pile	$b := 90\ in$	Spacing between piles (center to center)

$H1 := 11\ ft$ Distance from ground surface to first row of tiebacks

$H2 := 7\ ft$ Distance from first row of tiebacks to second row of tiebacks

$H3 := 6\ ft$ Distance from base of excavation to second row of tiebacks

Soil 1 - Clay (CL) - Undrained Condition
From 0 ft to 12 ft - N=9

$S_1 := 1500\ psf$ Shear Strength Soil 1 - (Terzaghi, Peck, and Mesri, 1996)

$c_1 := S_1 = 1500\ psf$ Cohesion Soil 1 - (Terzaghi, Peck, and Mesri, 1996)

$\phi_1 := 0\ °$ Fully Undrained

$\gamma_1 := 120\ pcf$ Unit Weight of Soil 1 (Terzaghi, Peck, and Mesri, 1996 and experience)

$h_1 := 12\ ft$ Height of Soil 1

Soil 2 - Silty Sand (SM) - Drained Condition
From 12 ft to 22 ft - N=20

$c_2 := 0\ psf$

$\phi_2 := 32\ °$ Friction Angle Soil 2 - (Bowles, 1998; NAVFAC, 1998; and Peck, Hanson, Thornburn, 1973)

$\gamma_2 := 120\ pcf$ Unit Weight of Soil 2 (Terzaghi, Peck, and Mesri, 1996 and experience)

$h_2 := 10\ ft$ Height of Soil 2

Soil 3 - Silty Clay (CL-ML) - Drained Condition
From 22 ft to 26 ft - N=52

$c_3 := 100\ psf$ (Local Experience)

$\phi_3 := 26\ °$ Assumed Liquid Limit (LL) of 40 (Stark, Choi and McCone, 2005)

$\gamma_3 := 125\ pcf$ Unit Weight of Soil 3 (Terzaghi, Peck, and Mesri, 1996 and experience)

$h_3 := 2\ ft$ Height of Soil 3

Surcharge

The surcharge for this retaining wall is zero.

$q := 0\ psf$

Water table

The water level is at cut level, 26 ft from the surface.

$\gamma_w := 62.4\ pcf$

Step 2: Determine values of Ka and Kp

Soil 2 - Silty Sand (SM)

$$Ka_2 := \left(\tan\left(45\,^\circ - \frac{\phi_2}{2}\right)\right)^2 = 0.31$$ Active lateral earth pressure coefficient

$$Kp_2 := \left(\tan\left(45\,^\circ + \frac{\phi_2}{2}\right)\right)^2 = 3.25$$ Passive lateral earth pressure coefficient

Soil 3 - Silty Clay (CL-ML)

$$Ka_3 := \left(\tan\left(45\,^\circ - \frac{\phi_3}{2}\right)\right)^2 = 0.39$$ Active lateral earth pressure coefficient

$$Kp_3 := \left(\tan\left(45\,^\circ + \frac{\phi_3}{2}\right)\right)^2 = 2.56$$ Passive lateral earth pressure coefficient

Step 3: Develop the active pressure diagram above the cut

The wall is basically half in the Clay (CL) layer and half in the Silty Sand (SM) layer. The apparent earth pressure for both soils will be developed in order to find the predicted deflected shape for both cases. This calculation assumes the soil as Sand.

Sand (Following Chapter 5.2.4) - Terzaghi and Peck (1967)

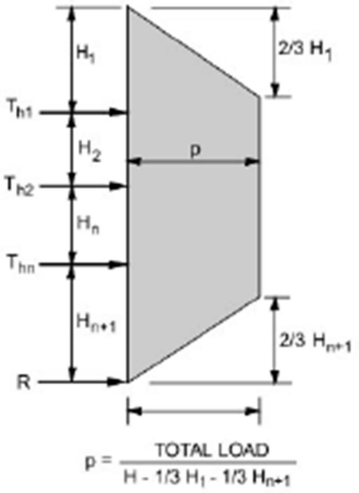

(b) Walls with multiple levels of ground anchors

$H = 24\ ft$

$TotalLoad := 0.65 \cdot Ka_2 \cdot \gamma_2 \cdot H^2 = 13.8\ \frac{kip}{ft}$

$H1 = 11\ ft \qquad H3 = 6\ ft$

$p_1 := \frac{TotalLoad}{H - \frac{H1}{3} - \frac{H3}{3}} = 0.75\ ksf$

$\frac{2}{3} \cdot H1 = 7.33\ ft \qquad \frac{2}{3} \cdot H3 = 4\ ft$

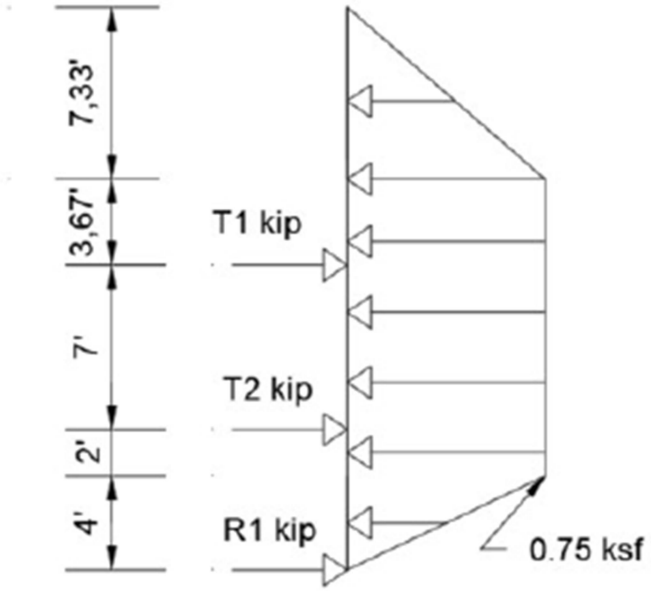

Apparent Earth Pressure Diagram - Sand

Step 4: Calculation of Tieback Loads

The calculation of tieback loads will follow the Chapter 5.3.3 and use the tributary area method.

$p_1 = 0.75\ ksf$ $\qquad P1 := p_1 \cdot b = 5.65\ \frac{kip}{ft}$

$T1 := \left(\frac{2}{3} \cdot H1 \cdot \frac{P1}{2}\right) + P1 \cdot \left(14.5\ ft - \frac{2}{3} \cdot H1\right) = 61.18\ kip$ From surface to the 14.5ft depth

$T2 := P1 \cdot 5.5\ ft + \left(\frac{3\ P1}{4} \cdot 1\ ft\right) + \frac{P1}{4} \cdot 1\ ft \cdot \frac{1}{2} = 36.00\ kip$ From the 14.5ft to 21ft depth

$R1 := 3 \cdot \frac{P1}{4} \cdot 3\ ft \cdot \frac{1}{2} = 6.35\ kip$ From the 22ft depth to the bottom

$Equi := \frac{7.33\ ft \cdot P1}{2} + 12.67\ ft \cdot P1 + \frac{4\ ft \cdot P1}{2} - T1 - T2 - R1 = 0.01\ kip$ OK

Step 5: Find Penetration Depth

The depth of penetration below excavation (d) will be found using the instructions on chapter 5.5.3

$\gamma_1 = 120\ pcf$ $h_1 = 12\ ft$ $Ka_1 := 1$

$\gamma_2 = 120\ pcf$ $h_2 = 10\ ft$ $Ka_2 = 0.31$

$\gamma_3 = 125\ pcf$ $h_3 = 2\ ft$ $Ka_3 = 0.39$

$B = 12\ in$ Pile width

Passive Pressure/Force:

$Kp_2 = 3.25$ $FS := 1.5$ $d := 5.5\ ft$

$Pp := \frac{Kp_2}{1.5} \cdot \gamma_2 \cdot d = 1.43\ \frac{kip}{ft^2}$ Passive Pressure

$Pf := Pp \cdot 3 \cdot B = 4.3\ \frac{kip}{ft}$ Passive Force

$PF := Pf \cdot \frac{d}{2} = 11.81\ kip$

Active Pressure/Force:

$Ka_2 = 0.31$

$Ap1 := Ka_2 \cdot (\gamma_1 \cdot h_1 + \gamma_2 \cdot h_2 + \gamma_3 \cdot h_3) = 0.89\ \frac{kip}{ft^2}$ Active Pressure bottom of excavation

$Ap2 := Ka_2 \cdot (\gamma_1 \cdot h_1 + \gamma_2 \cdot h_2 + \gamma_3 \cdot (h_3 + d)) = 1.1\ \frac{kip}{ft^2}$ Active Pressure at depth d

$Af1 := Ap1 \cdot B = 0.89\ \frac{kip}{ft}$ Active Force bottom of ecavation

$Af2 := Ap2 \cdot B = 1.1\ \frac{kip}{ft}$ Active Force at depth d

$AF := (Af2 + Af1) \cdot \frac{d}{2} = 5.46\ kip$

Check:

$PF - AF - R1 = 0\ kip$

$d := 1.2 \cdot d = 6.6\ ft$ Add 20% to find actual embedment depth

Step 6: Find net Pressure Diamagram

$$Net(d) := \left(\left(\gamma_1 \cdot h_1 + \gamma_2 \cdot h_2 + \gamma_3 \cdot \left(h_3 + d\right)\right) \cdot Ka_2 \cdot B\right) - \left(\frac{Kp_2}{1.5} \cdot \gamma_2 \cdot d \cdot 3 \cdot B\right)$$

$d1 := 0\ ft$ $\quad P2 := Net(d1) = 0.89\ \frac{kip}{ft}$

$d1 := 6.6\ ft$ $\quad P3 := Net(d1) = -4.01\ \frac{kip}{ft}$

$d1 := 1.2\ ft$ $\quad Net(d1) = 0\ \frac{kip}{ft}$

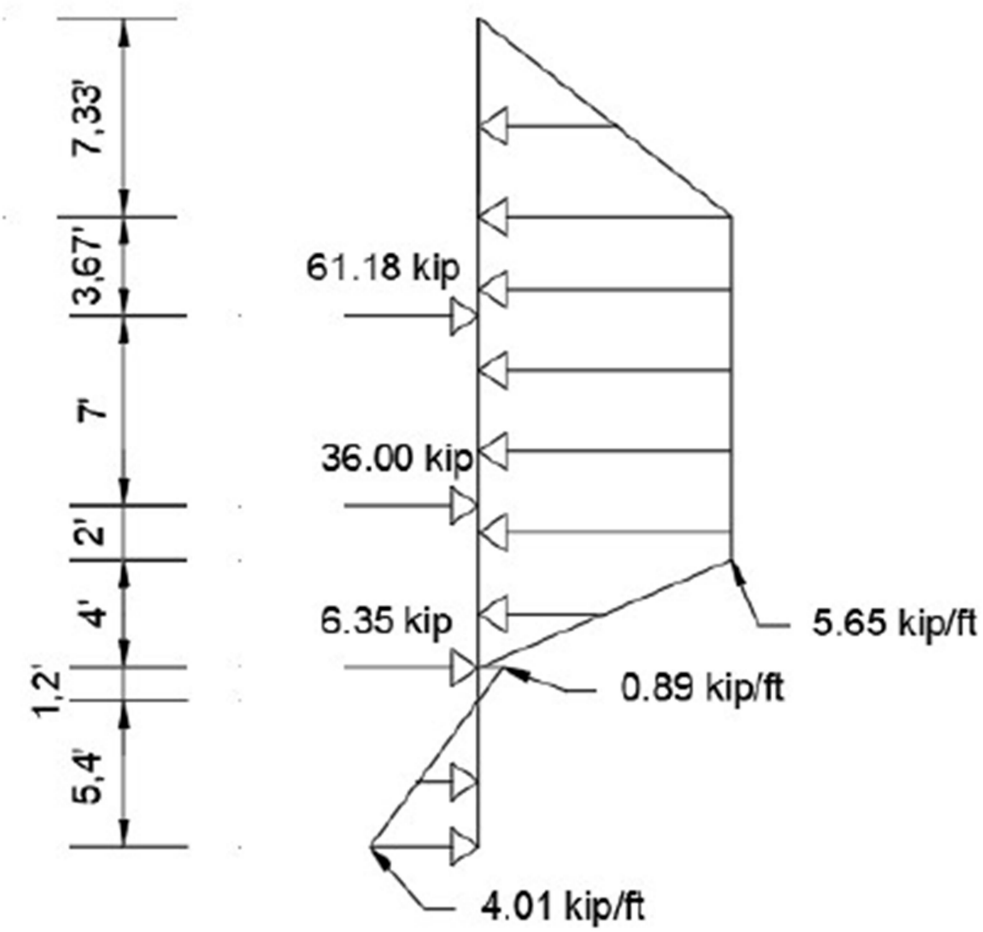

Earth Pressure Diagram - Pile P005 - Sand

Step 7: Find Moment Diagram

0 ft < y < 7.33 ft $M(y) := -0.1285 \frac{kip}{ft^2} \cdot y^3$

7.33 ft < y < 11 ft $M(y) := -2.825 \frac{kip}{ft} \cdot y^2 + 20.707\ kip \cdot y - 50.594\ kip \cdot ft$

11 ft < y < 18 ft $M(y) := -2.825 \frac{kip}{ft} \cdot y^2 + 81.887 \cdot kip \cdot y - 723.574\ kip \cdot ft$

18 ft < y < 20 ft $M(y) := -2.825 \frac{kip}{ft} \cdot y^2 + 117.887 \cdot kip \cdot y - 1371.574\ kip \cdot ft$

20 ft < Y < 24 ft

$$M(y) := 0.2354 \frac{kip}{ft^2} \cdot y^3 - 16.95 \frac{kip}{ft} y^2 + 400.3872\ kip\ y - 3254.55\ kip \cdot ft$$

24 ft < Y < 25.2 ft

$$M(y) := 0.1236 \frac{kip}{ft^2} y^3 - 9.345 \frac{kip}{ft} \cdot y^2 + 234.897\ kip \cdot y - 2117.70\ kip \cdot ft$$

25.2 ft < Y < 30.6 ft

$$M(y) := 0.12371 \frac{kip}{ft^2} \cdot y^3 - 9.356 \frac{kip}{ft} \cdot y^2 + 235.20\ kip \cdot y - 2120.17\ kip \cdot ft$$

An excel spreadsheet was created using the equations above in order to generate the moment diagram

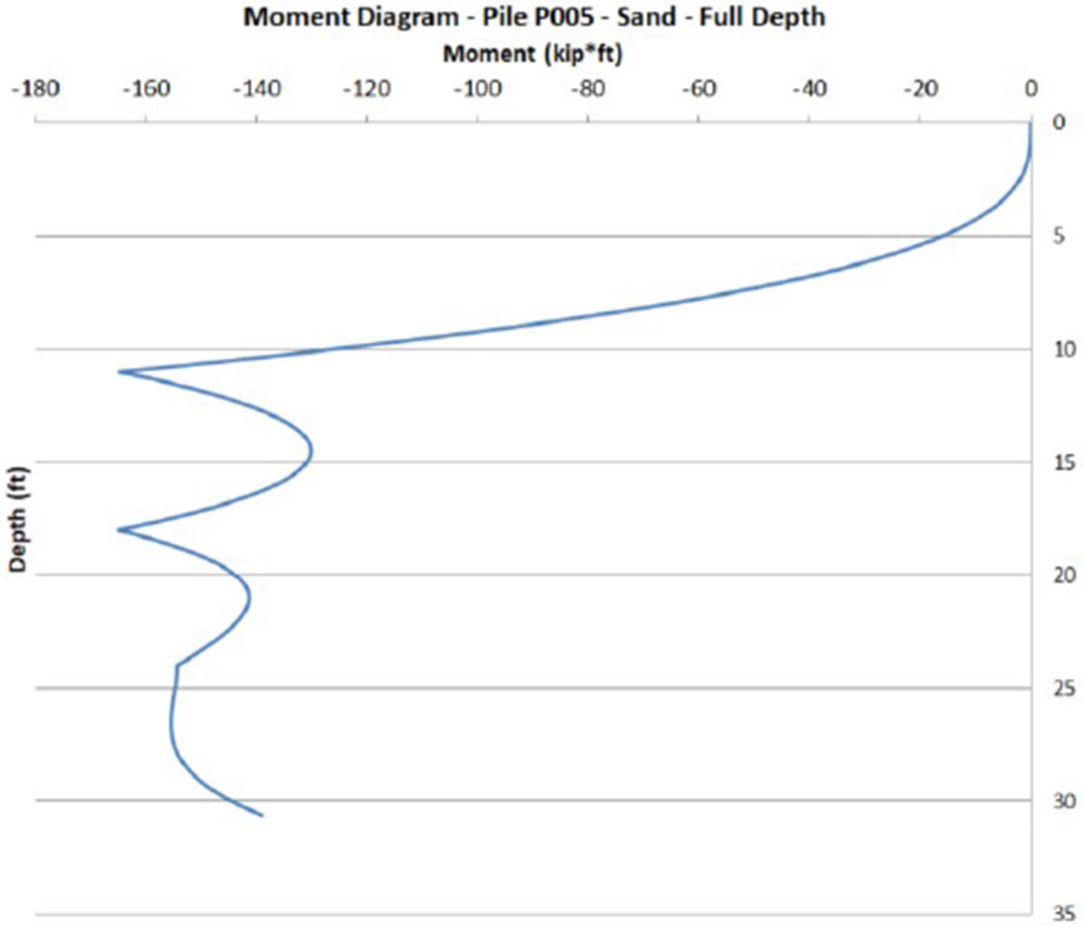

Moment Diagram - Pile P005 - Sand

Step 8: Find Deflected Shape

An excel spreadsheet was developed in order to find the deflected shape for this structure using the trapezoidal approximation.

Since the moment is known for any depth of the pile, it is possible to numerically find the curvature, slope and deflection at any depth following the steps below:

1) Find the curvature by dividing the moment by E*I. For this structure E=29000ksi and I=393 in^4.

2) The slope at the bottom is assumed to be zero. Then, adding small increments, it is possible to find the slope at any other point by using the area under the curvature curve and the distance from the centroid to the desired point. Since the increments are small, the area under the curve is a trapezoid.

3) Find the deflection at a point using the area under the slope curve and the distance from the centroid to the point, same approach used in the previous step.

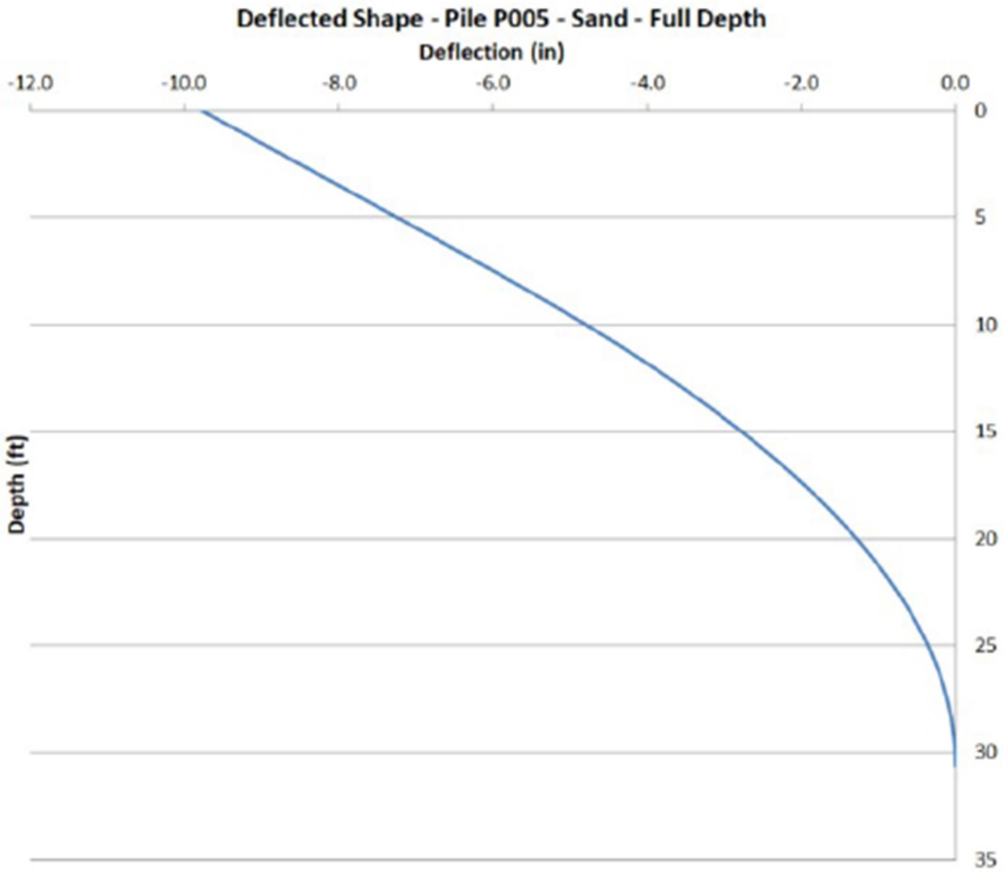

Deflected Shape - Pile P005 - Sand - Full Depth

APPENDIX C (LIMIT EQUILIBRIUM METHOD – INTERMEDIATE CONSTRUCTION MILESTONES)

This appendix describes the limit equilibrium method to find the deflected shape for the high section of the wall in two locations, piles P004 and P005 at two intermediate excavation steps, 11 foot depth and 18 foot depth, before the installation of the first and second row of tiebacks, respectively. For each location, only the drained condition was used since most part of the undrained condition would not have any loads.

The first calculation in this appendix shows the deflected shape for the 11 feet excavation.

DESIGN OF ANCHORED SYSTEMS - PILE P004 AND P005 - EXCAVATION TO 11 FT - DRAINED ANALYSIS

The hand calculation design of the MU retaining wall will follow the procedure described in the Foundation Design Principles and Practices book (Coduto, 2001). The procedure is exactly the same for piles P004 and P005

Chapter 25.3 (Cantilever Sheet Pile Walls) describes the design method with the recommended Earth Pressure Diagrams for various soil types. This designed will be based on this chapter considering drain conditions.

This goal of this calculation set is to predict the deflected shape of the wall when the excavation depth is equal to 11 ft. For this intermediate case no tieback has been installed.

Step 1: Define Parameters of wall and soil

$H := 11\ ft$ Excavation depth

$B := 12\ in$ Width of flange for HP12x53

$b := 90\ in$ Spacing between piles (center to center)

Soil 1 - Clay (CL) - Drained Condition
From 0 ft to 12 ft - N=9

$c_1 := 0\ psf$

$\phi_1 := 26\ °$ Friction Angle Soil 1 (Stark, Choi, and McCOne, 2005)

$\gamma_1 := 120\ pcf$ Unit Weight of Soil 1 (Terzaghi, Peck, and Mesri, 1996 and experience)

$h_1 := 12\ ft$ Height of Soil 1

Soil 2 - Silty Sand (SM) - Drained Condition
From 12 ft to 22 ft - N=20

$c_2 := 0\ psf$

$\phi_2 := 32\ °$ Friction Angle Soil 2 - (Bowles, 1998; NAVFAC, 1998; and Peck, Hanson, Thornburn, 1973)

$\gamma_2 := 120\ pcf$ Unit Weight of Soil 2 (Terzaghi, Peck, and Mesri, 1996 and experience)

$h_2 := 10\ ft$ Height of Soil 2

Step 2: Determine values of Ka and Kp

Soil 1 - Silty Clay (CL)

$$Ka_1 := \left(\tan\left(45\,^\circ - \frac{\phi_1}{2}\right)\right)^2 = 0.39$$

Active lateral earth pressure coefficient

$$Kp_1 := \frac{\left(\tan\left(45\,^\circ + \frac{\phi_1}{2}\right)\right)^2}{1.5} = 1.71$$

Passive lateral earth pressure coefficient with a 1.5 factor of safety

Soil 2 - Silty Sand (SM)

$$Ka_2 := \left(\tan\left(45\,^\circ - \frac{\phi_2}{2}\right)\right)^2 = 0.31$$

Active lateral earth pressure coefficient

$$Kp_2 := \frac{\left(\tan\left(45\,^\circ + \frac{\phi_2}{2}\right)\right)^2}{1.5} = 2.17$$

Passive lateral earth pressure coefficient with a 1.5 factor of safety

Step 3: Find Earth Pressure Diagram

This calculation uses the drained conditions since it is a long term analysis.

Cantilever Sheet Pile Wall (Following Chapter 25.3) - Coduto (2001)

Find active pressure at 11ft:

$Ap_1 := \gamma_1 \cdot H \cdot Ka_1 \cdot b = 3.87 \ \frac{kip}{ft}$ Above the cut

$Ap_2 := \gamma_1 \cdot H \cdot Ka_1 \cdot B = 0.52 \ \frac{kip}{ft}$ Below the cut

Find depth where net pressure is zero:

$d_1 := 1 \ ft$

$Net1 := Kp_1 \cdot \gamma_1 \cdot d_1 \cdot 3 \cdot B - Ka_1 \cdot \gamma_1 \cdot (H + d_1) \cdot B = 0 \ \frac{kip}{ft}$

$d := H + d_1 = 12 \ ft$ Depth where net pressure is zero

Find force above d and moment about point d:

$Pa1 := \frac{Ap_1 \cdot H}{2} = 21.26 \ kip$ Force above 11ft

$Pa2 := \frac{Ap_2 \cdot d_1}{2} = 0.26 \ kip$ Force between 11ft and 11.9ft

$Force1 := Pa1 + Pa2 = 21.5183 \ kip$

$Moment := Pa1 \cdot \left(d - H \cdot \frac{2}{3}\right) + Pa2 \cdot d_1 \cdot \frac{2}{3} = 99.39 \ kip \cdot ft$

Find total embedment depth:

$d_3 := 5.73 \ ft$ Distance CE in the book

$d_4 := 6.39 \ ft$ Distance EG in the book

$Slope := \gamma_2 \cdot (3 \cdot Kp_2 - Ka_2) = 0.74423 \ \frac{kip}{ft^2 \cdot ft}$ Slope at Layer 2

$TotalForce := Force1 - \frac{Slope \cdot {d_3}^2 \cdot 3 \cdot B}{2} + \frac{Slope \cdot {d_4}^2 \cdot B}{2} = 0.06 \ kip$

$TotalMoment := -Slope \cdot \frac{{d_3}^3}{8} \cdot 3 \cdot B + Slope \cdot \frac{{d_4}^2}{2} \cdot \left(d_3 + d_4 \cdot \frac{2}{3}\right) \cdot B - Moment = -0.1 \ kip \cdot ft$

$$Slope \cdot \frac{d_3}{2} \cdot B = 2.13 \ \frac{kip}{ft} \qquad Slope \cdot d_4 \cdot B = 4.76 \ \frac{kip}{ft}$$

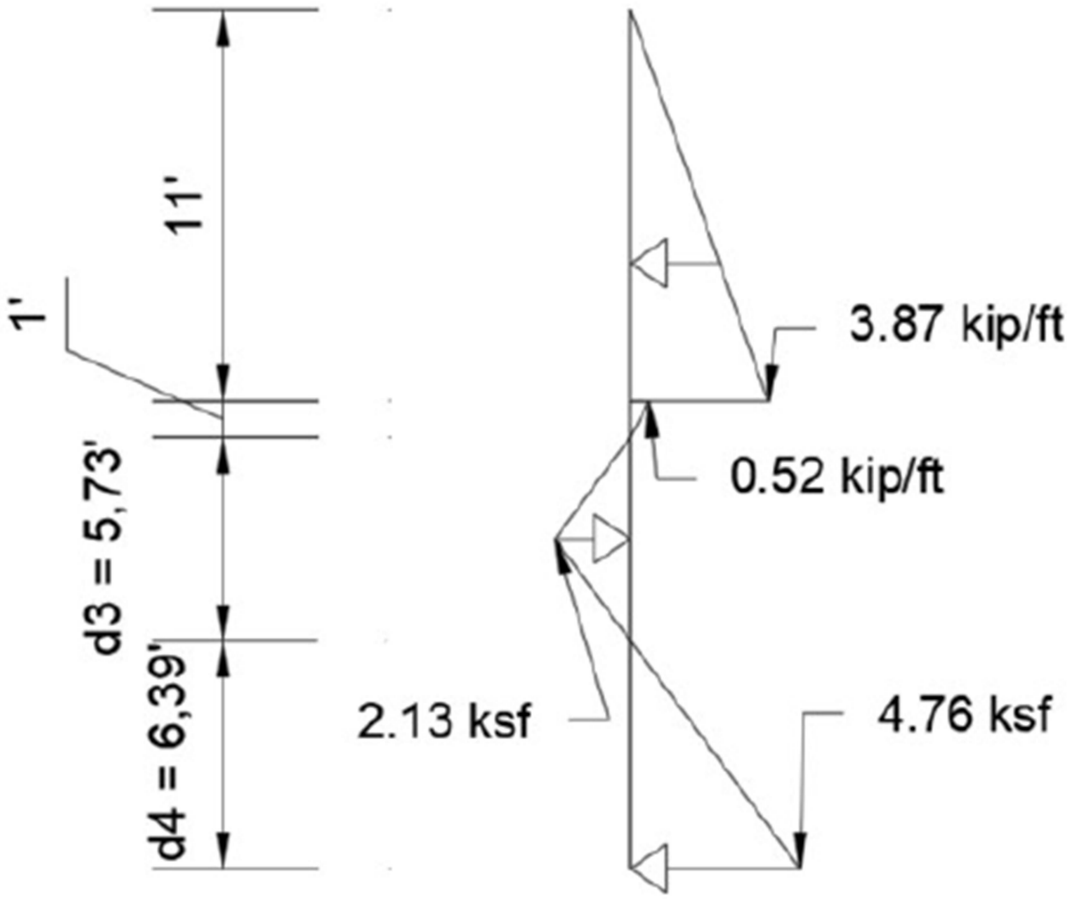

Earth Pressure Diagram - Excavation to 11ft

Step 4: Find Moment Diagram

0 ft < y < 11 ft $M(y) := -0.0586 \frac{kip}{ft^2} \cdot y^3$

11 ft < y < 12 ft $M(y) := 0.08667 \frac{kip}{ft^2} \cdot y^3 - 3.12 \frac{kip}{ft} \cdot y^2 + 15.895 \cdot kip \cdot y + 9.276\ kip \cdot ft$

12 ft < y < 14.86 ft $M(y) := 0.1241 \frac{kip}{ft^2} \cdot y^3 - 4.4685 \frac{kip}{ft} \cdot y^2 + 32.077 \cdot kip \cdot y - 55.4528\ kip \cdot ft$

14.86 ft < y < 17.73 ft $M(y) := -0.1243 \frac{kip}{ft^2} \cdot y^3 + 6.59 \frac{kip}{ft} \cdot y^2 - 132.416 \cdot kip \cdot y + 762.33\ kip \cdot ft$

17.73 ft < y < 24.12 ft $M(y) := -0.12415 \frac{kip}{ft^2} \cdot y^3 + 6.603 \frac{kip}{ft} \cdot y^2 - 132.525 \cdot kip \cdot y + 760.212\ kip \cdot ft$

An excel spreadsheet was created using the equations above in order to generate the moment diagram

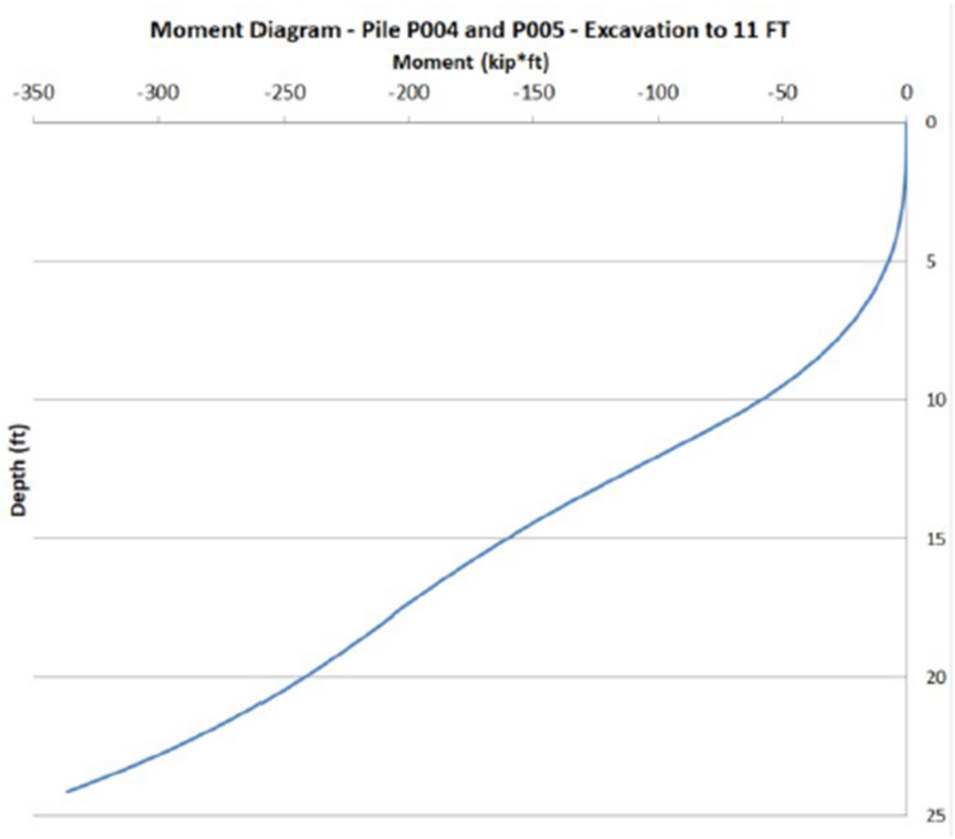

Moment Diagram - Drained Analysis - Excavation to 11ft

Step 5: Find Deflected Shape

An excel spreadsheet was developed in order to find the deflected shape for this structure using the trapezoidal approximation.

Since the moment is known for any depth of the pile, it is possible to numerically find the curvature, slope and deflection at any depth following the steps below:

1) Find the curvature by dividing the moment by E*I. For this structure E=29000ksi and I=393 in^4.

2) The slope at the bottom is assumed to be zero. Then, adding small increments, it is possible to find the slope at any other point by using the area under the curvature curve and the distance from the centroid to the desired point. Since the increments are small, the area under the curve is a trapezoid.

3) Find the deflection at a point using the area under the slope curve and the distance from the centroid to the point, same approach used in the previous step.

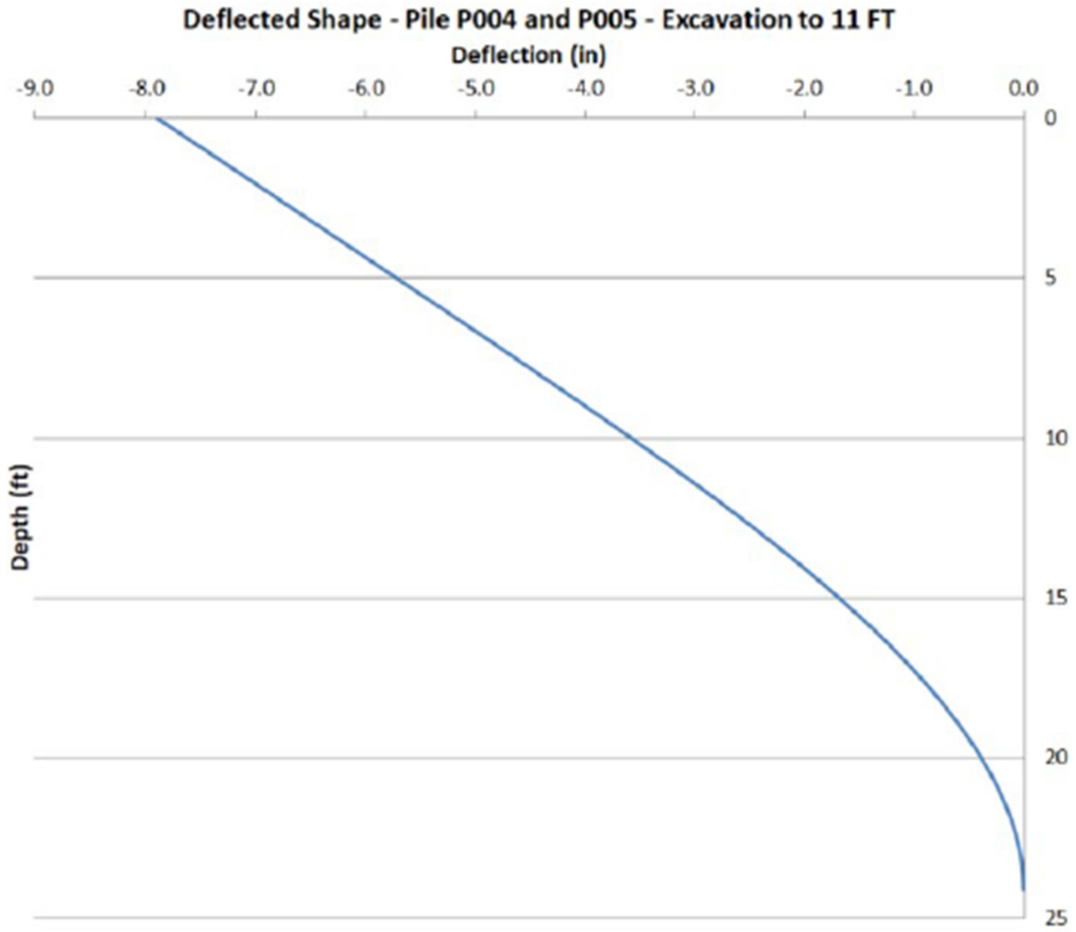

Deflected Shape - Drained Analysis - Excavation to 11ft

The second calculation in this appendix shows the deflected shape for the 18 feet excavation.

DESIGN OF ANCHORED SYSTEMS - PILE P004 AND P005 - EXCAVATION TO 18 FT - DRAINED ANALYSIS

The hand calculation design of the MU retaining wall will follow the procedure described in the Foundation Design Principles and Practices book (Coduto, 2001). The procedure is exactly the same for piles P004 and P005

Chapter 25.4 (Braced or Anchored Sheet Pile Walls) describes the design method with the recommended Earth Pressure Diagrams for various soil types. This designed will be based on this chapter.

This goal of this calculation set is to predict the deflected shape of the wall when the excavation depth is equal to 18 ft. For this intermediate case only 1 row of tieback was installed.

Step 1: Define Parameters of wall and soil

$H := 18\ ft$ Excavation depth

$B := 12\ in$ Width of flange for HP12x53

$b := 90\ in$ Spacing between piles (center to center)

$H1 := 11\ ft$ Distance from ground surface to row of tiebacks

$H3 := 7\ ft$ Distance from base of excavation to row of tiebacks

Soil 1 - Clay (CL) - Drained Condition
From 0 ft to 12 ft - N=9

$c_1 := 0\ psf$

$\phi_1 := 26\ °$ Friction Angle Soil 1 (Stark, Choi, and McCOne, 2005)

$\gamma_1 := 120\ pcf$ Unit Weight of Soil 1 (Terzaghi, Peck, and Mesri, 1996 and experience)

$h_1 := 12\ ft$ Height of Soil 1

Soil 2 - Silty Sand (SM) - Drained Condition
From 12 ft to 22 ft - N=20

$c_2 := 0\ psf$

$\phi_2 := 32\ °$ Friction Angle Soil 2 - (Bowles, 1998; NAVFAC, 1998; and Peck, Hanson, Thornburn, 1973)

$\gamma_2 := 120\ pcf$ Unit Weight of Soil 2 (Terzaghi, Peck, and Mesri, 1996 and experience)

$h_2 := 10\ ft$ Height of Soil 2

Surcharge

The surcharge for this retaining wall is zero.

$q := 0\ psf$

Water table

The water level is at cut level, 26 ft from the surface.

$\gamma_w := 62.4\ pcf$

Step 2: Determine values of Ka and Kp

Soil 1 - Clay (CL)

$$Ka_1 := \left(\tan\left(45° - \frac{\phi_1}{2}\right)\right)^2 = 0.39$$ Active lateral earth pressure coefficient

$$Kp_1 := \frac{\left(\tan\left(45° + \frac{\phi_1}{2}\right)\right)^2}{1.5} = 1.71$$ Passive lateral earth pressure coefficient

Soil 2 - Silty Sand (SM)

$$Ka_2 := \left(\tan\left(45° - \frac{\phi_2}{2}\right)\right)^2 = 0.31$$ Active lateral earth pressure coefficient

$$Kp_2 := \frac{\left(\tan\left(45° + \frac{\phi_2}{2}\right)\right)^2}{1.5} = 2.17$$ Passive lateral earth pressure coefficient

Step 3: Develop the Pressure Diagram

This calculation uses the drained conditions since it is a long term analysis.

Braced or Anchored Sheet Pile Walls (Following Chapter 25.4) - Coduto (2001)

Find active pressure and force until Excavation Depth (18ft):

$Ap_1 := Ka_1 \cdot \gamma_1 \cdot h_1 = 0.56\ ksf$ Active pressure at 12ft

$Af1 := Ap_1 \cdot b = 4.22\ \frac{kip}{ft}$ Active force at 12ft

$AF1 := \frac{Af1 \cdot h_1}{2} = 25.3\ kip$ Triangular force

$Ap_2 := Ka_2 \cdot \gamma_2 \cdot (H - h_1) + Ap_1 = 0.78\ ksf$ Active pressure at 18ft

$Af2 := Ap_2 \cdot b = 5.88\ \frac{kip}{ft}$ Active force at 18ft

$AF2 := Af1 \cdot (H - h_1) = 25.3\ kip$ Rectangular force

$AF3 := \frac{(Af2 - Af1) \cdot (H - h_1)}{2} = 4.98\ kip$ Triangular force

Find the depth d where the moment at the tieback is zero: $d := 4.74\ ft$

$Pp_1 := Kp_2 \cdot \gamma_2 \cdot d = 1.23\ ksf$ Passive pressure at d

$Pf1 := Pp_1 \cdot 3 \cdot B = 3.7\ \frac{kip}{ft}$ Passive force at d

$PF1 := \frac{Pf1 \cdot d}{2} = 8.77\ kip$

$Ap_4 := Ap_2 = 0.78\ ksf$ Active pressure at 18ft

$Af4 := Ap_2 \cdot B = 0.78\ \frac{kip}{ft}$ Active force at 18ft, below the cut

$AF4 := Af4 \cdot d = 3.71\ kip$ Rectangular force

$Ap_5 := Ka_2 \cdot \gamma_2 \cdot (H + d - h_1) + Ap_1 = 0.96\ ksf$ Active pressure at d

$Af5 := Ap_5 \cdot B = 0.96\ \frac{kip}{ft}$ Active force at d

$AF5 := (Af5 - Af4) \cdot \frac{d}{2} = 0.41\ kip$ Triangular force

$Sum := AF1 \cdot 3\ ft - AF2 \cdot 4\ ft - AF3 \cdot 5\ ft - AF4 \cdot \left(7\ ft + \frac{d}{2}\right) - AF5 \cdot \left(7\ ft + d \cdot \frac{2}{3}\right) + PF1 \cdot \left(7\ ft + d \cdot \frac{2}{3}\right) = 0\ kip \cdot ft$

Find tieback load:

$$T1 := AF1 + AF2 + AF3 + AF4 + AF5 - PF1 = 50.93\ kip$$

$$Net(d) := Kp_2 \cdot \gamma_2 \cdot d \cdot 3 \cdot B - \left(Ka_2 \cdot \gamma_2 \cdot \left(H + d - h_1\right) + Ka_1 \cdot \gamma_1 \cdot h_1\right) \cdot B$$

$d1 := 0\ ft$ $\quad Net(d1) = -0.78\ \frac{kip}{ft}$

$d1 := 4.74\ ft$ $\quad Net(d1) = 2.74\ \frac{kip}{ft}$

$d1 := 1.05\ ft$ $\quad Net(d1) = 0\ \frac{kip}{ft}$

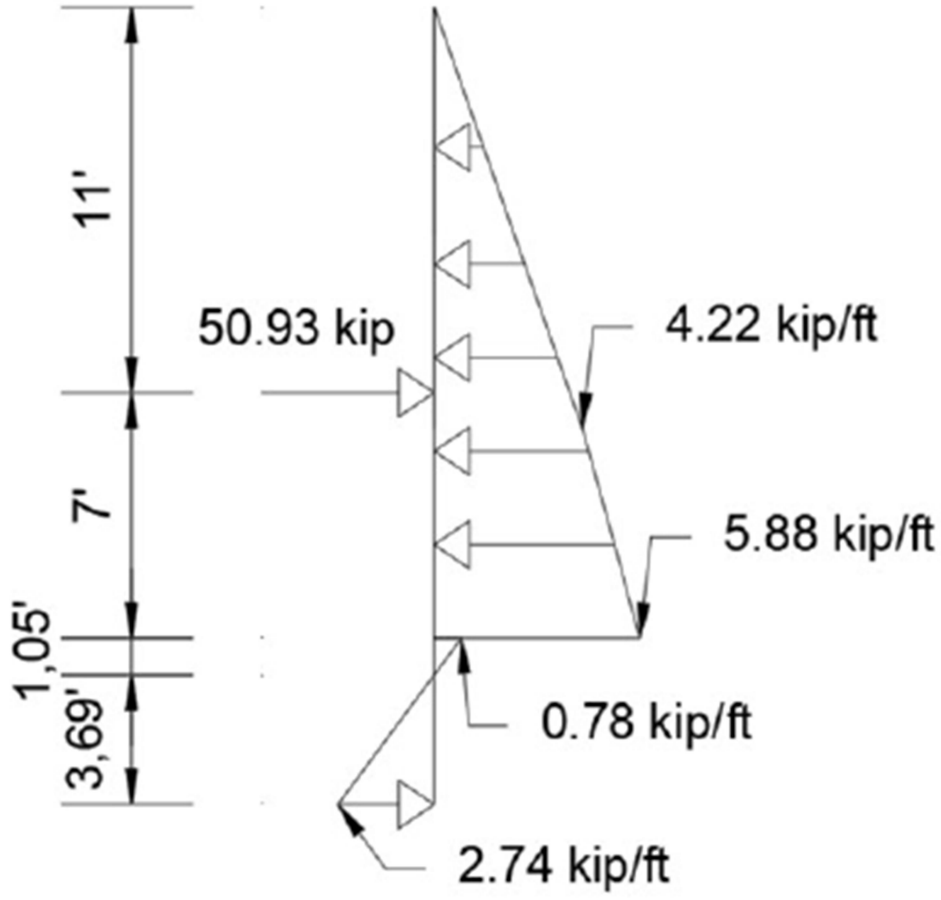

Earth Pressure Diagram - Excavation to 18ft

Step 4: Find Moment Diagram

0 ft < y < 11 ft $M(y) := -0.0586 \frac{kip}{ft^2} \cdot y^3$

11 ft < y < 12 ft $M(y) := -0.0586 \frac{kip}{ft^2} \cdot y^3 + 50.93 \cdot kip \cdot y - 560.23\ kip \cdot ft$

12 ft < y < 18 ft $M(y) := -0.0461 \cdot \frac{kip}{ft^2} \cdot y^3 - 0.45 \frac{kip}{ft} \cdot y^2 + 56.33 \cdot kip \cdot y - 581.83\ kip \cdot ft$

18 ft < y < 19.05 ft $M(y) := 0.1238 \cdot \frac{kip}{ft^2} \cdot y^3 - 7.075 \frac{kip}{ft} \cdot y^2 + 129.69 \cdot kip \cdot y - 746.60\ kip \cdot ft$

19.05 ft < y < 22.74 ft

$$M(y) := 0.1237 \cdot \frac{kip}{ft^2} \cdot y^3 - 7.072 \frac{kip}{ft} \cdot y^2 + 129.636 \cdot kip \cdot y - 746.238\ kip \cdot ft$$

An excel spreadsheet was created using the equations above in order to generate the moment diagram

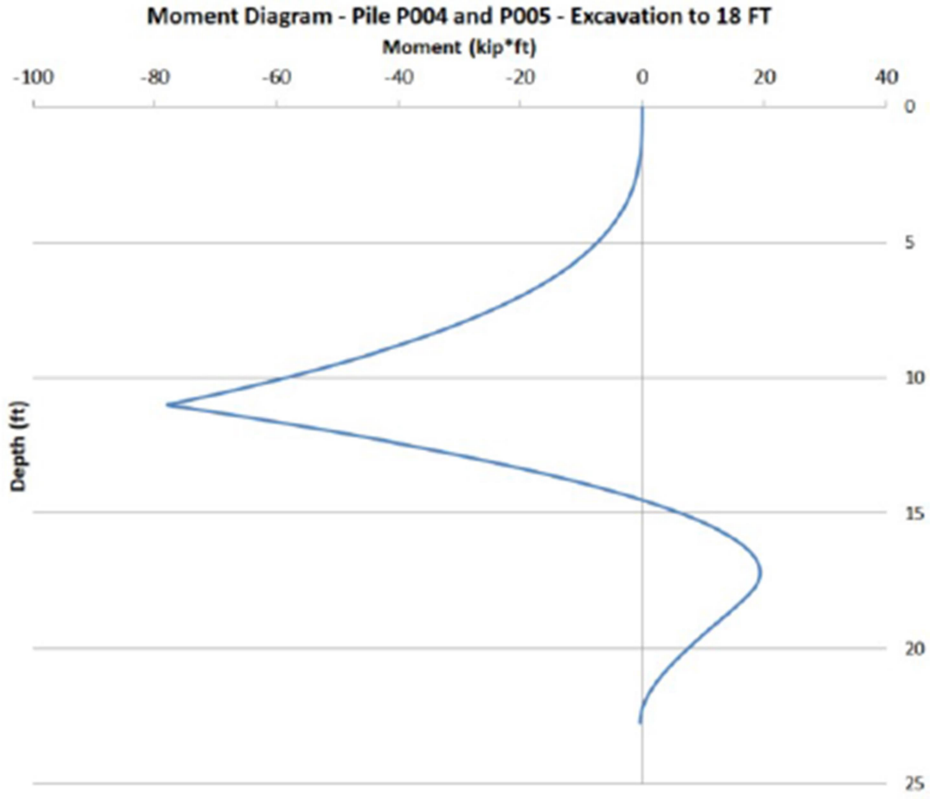

Moment Diagram - Drained Analysis - Excavation to 18ft

Step 5: Find Deflected Shape

An excel spreadsheet was developed in order to find the deflected shape for this structure using the trapezoidal approximation.

Since the moment is known for any depth of the pile, it is possible to numerically find the curvature, slope and deflection at any depth following the steps below:

1) Find the curvature by dividing the moment by E*I. For this structure E=29000ksi and I=393 in^4.

2) The slope at the bottom is assumed to be zero. Then, adding small increments, it is possible to find the slope at any other point by using the area under the curvature curve and the distance from the centroid to the desired point. Since the increments are small, the area under the curve is a trapezoid.

3) Find the deflection at a point using the area under the slope curve and the distance from the centroid to the point, same approach used in the previous step.

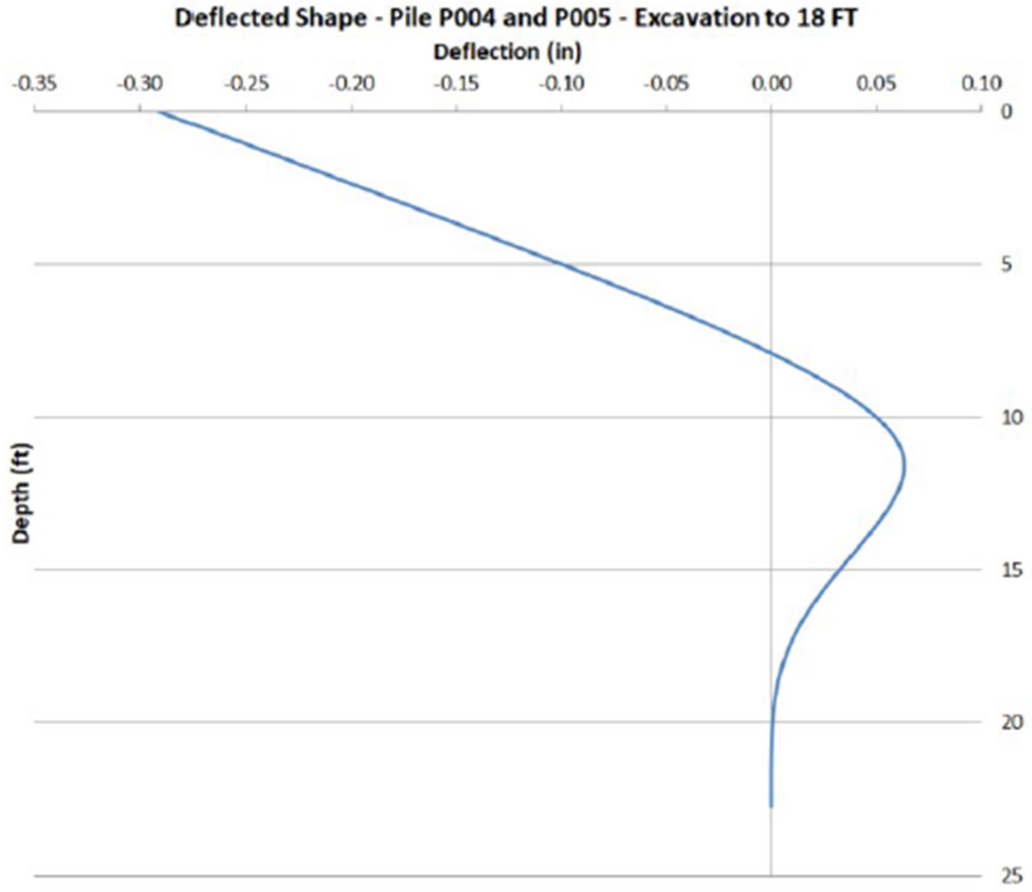

Deflected Shape - Drained Analysis - Excavation to 18ft

APPENDIX D (LIMIT EQUILIBRIUM VALIDATION CHECK)

This appendix shows the application of the limit equilibrium design method used on this thesis on two known structures, a cantilever column with a point load and a cantilever column with a uniform load. In addition, it shows the development of the deflected shape using another method (Moment Area Method) in order to check if the results using the Trapezoidal Area Approximation are reasonable.

The first calculation shows the limit equilibrium design check for the two known structures (cantilever column with a point load and cantilever column with uniform load). For this case, both deflected shape prediction methods were used, the Trapezoidal Area Approximation and the Moment Area Method.

POINT AND UNIFORM LOAD EXAMPLES

Two known examples will be used in order to check the accuracy of the two hand calculation models used in this thesis. The trapezoidal approximation and the moment area method.

Example 1: Cantilivered Beam with Point Load

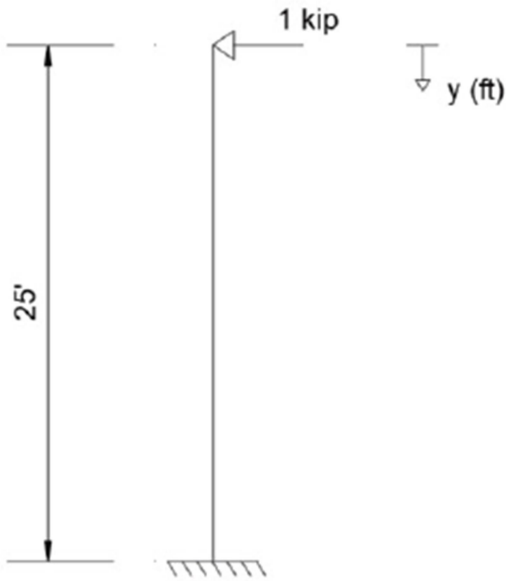

For this particular structure, the maximum deflection is known:

$P := 1\ kip$ $L := 25\ ft$ $E := 29000\ ksi$ $I := 393\ in^4$

$$\Delta := \frac{-P \cdot L^3}{3 \cdot E \cdot I} = -0.7897\ in$$

The moment at any point of the structure in function of y is:

$$M(y) := -1\ kip \cdot y$$

a) Trapezoidal Approximation

The moment equation was input in the excel spreadsheet in order to generate the moment diagram and deflected shape below.

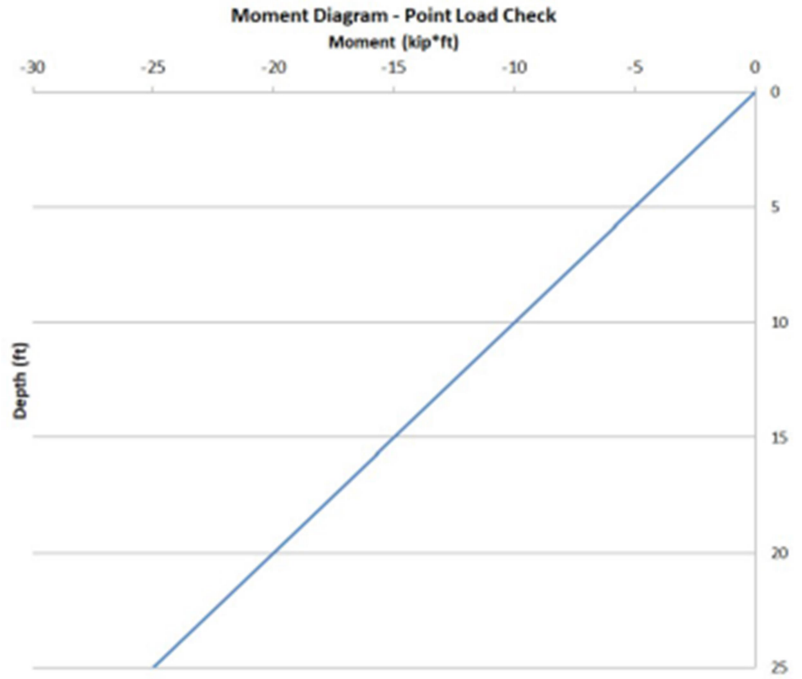

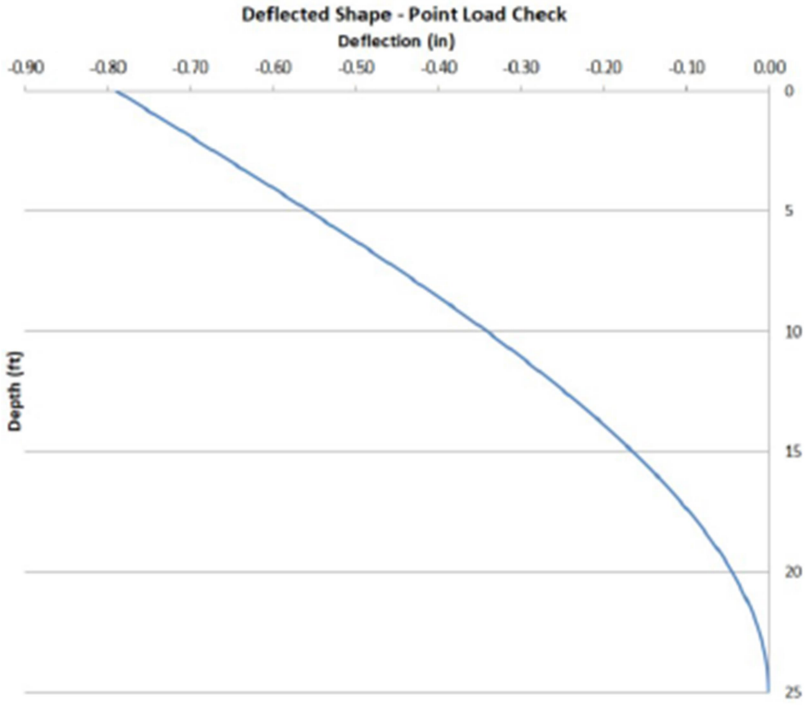

$\Delta max_{excel} := -0.7897\ in$

$\Delta = -0.7897\ in$

OK!

For this particular case, the trapezoidal method found the correct maximum displacement.

b) Moment Area Method

The moment diagram was drawn to scale on AutoCAD. And divided into 5 sections in order to predict the deflected shape.

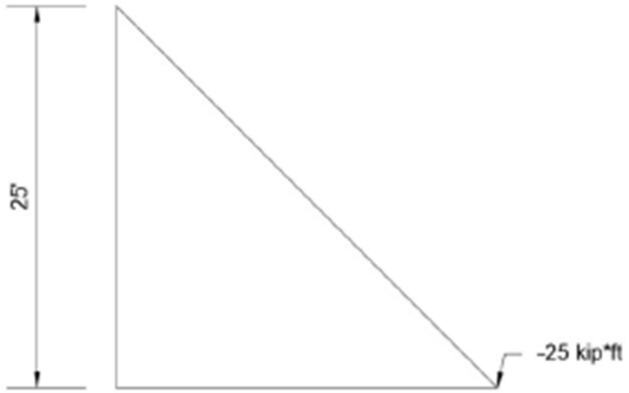

$Y_A := 25\ ft$ $\Theta_A := 0$ $V_A := 0\ in$

20 ft < y < 25 ft

$Y_B := 20\ ft$

$AreaMoment := -112.5\ kip \cdot ft^2$ $Ybar := 2.5926\ ft$ Distance from the centroid to B

$\Theta_B := \frac{AreaMoment}{E \cdot I} + \Theta_A = -0.0014$ $V_B := \frac{AreaMoment \cdot Ybar}{E \cdot I} + V_A = -0.0442\ in$

15 ft < y < 25 ft

$Y_B := 15\ ft$

$AreaMoment := -200\ kip \cdot ft^2$ $Ybar := 5.4167\ ft$ Distance from the centroid to B

$\Theta_B := \frac{AreaMoment}{E \cdot I} + \Theta_A = -0.0025$ $V_B := \frac{AreaMoment \cdot Ybar}{E \cdot I} + V_A = -0.1643\ in$

10 ft < y < 25 ft

$Y_B := 10\ ft$

$AreaMoment := -262.5\ kip \cdot ft^2$ $\quad Ybar := 8.5714\ ft$ Distance from the centroid to B

$\Theta_B := \frac{AreaMoment}{E \cdot I} + \Theta_A = -0.0033$ $\quad V_B := \frac{AreaMoment \cdot Ybar}{E \cdot I} + V_A = -0.3411\ in$

5 ft < y < 25 ft

$Y_B := 5\ ft$

$AreaMoment := -300\ kip \cdot ft^2$ $\quad Ybar := 12.2222\ ft$ Distance from the centroid to B

$\Theta_B := \frac{AreaMoment}{E \cdot I} + \Theta_A = -0.0038$ $\quad V_B := \frac{AreaMoment \cdot Ybar}{E \cdot I} + V_A = -0.5559\ in$

0 ft < y < 25 ft

$Y_B := 0\ ft$

$AreaMoment := -312.5\ kip \cdot ft^2$ $\quad Ybar := 16.6667\ ft$ Distance from the centroid to B

$\Theta_B := \frac{AreaMoment}{E \cdot I} + \Theta_A = -0.0039$ $\quad V_B := \frac{AreaMoment \cdot Ybar}{E \cdot I} + V_A = -0.7897\ in$

OK!

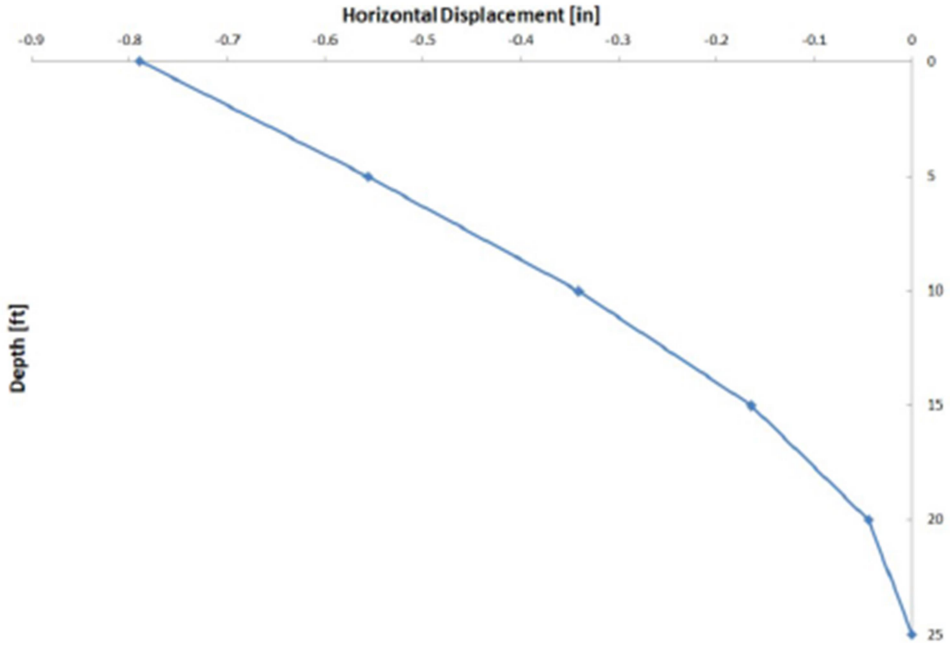

For this particular case, the moment area method found the correct maximum displacement.

Example 2: Cantilivered Beam with Uniform Load

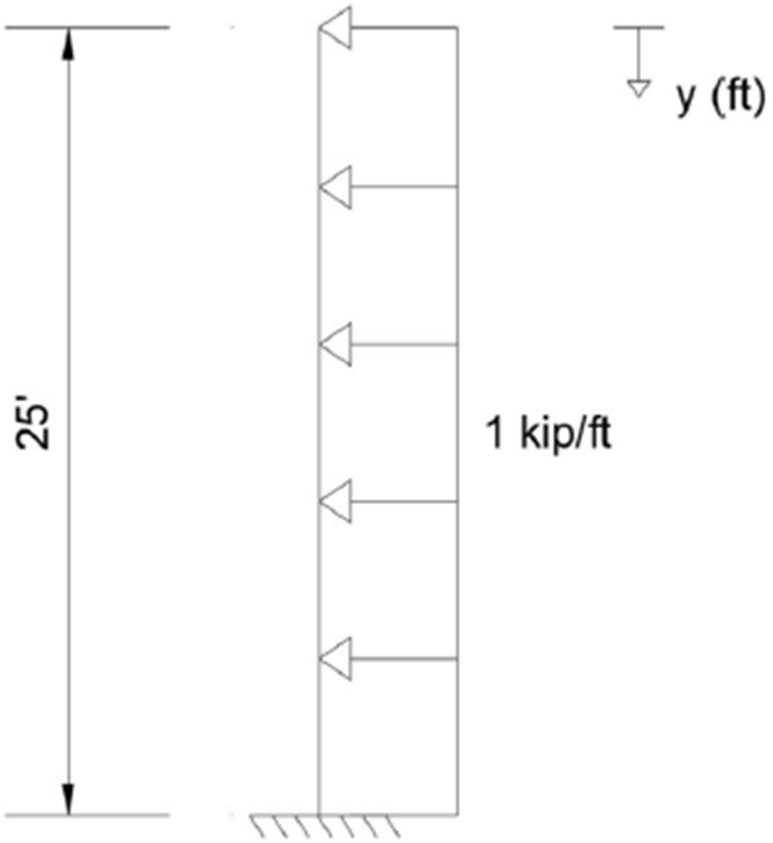

For this particular structure, the maximum deflection is known:

$q := 1\ \frac{kip}{ft}$ $L := 25\ ft$ $E := 29000\ ksi$ $I := 393\ in^4$

$$\Delta := \frac{-q \cdot L^4}{8 \cdot E \cdot I} = -7.4033\ in$$

The moment at any point of the structure in function of y is:

$$M(y) := -1\ \frac{kip}{ft} \cdot \frac{y^2}{2}$$

a) Trapezoidal Approximation

The moment equation was input in the excel spreadsheet in order to generate the moment diagram and deflected shape below.

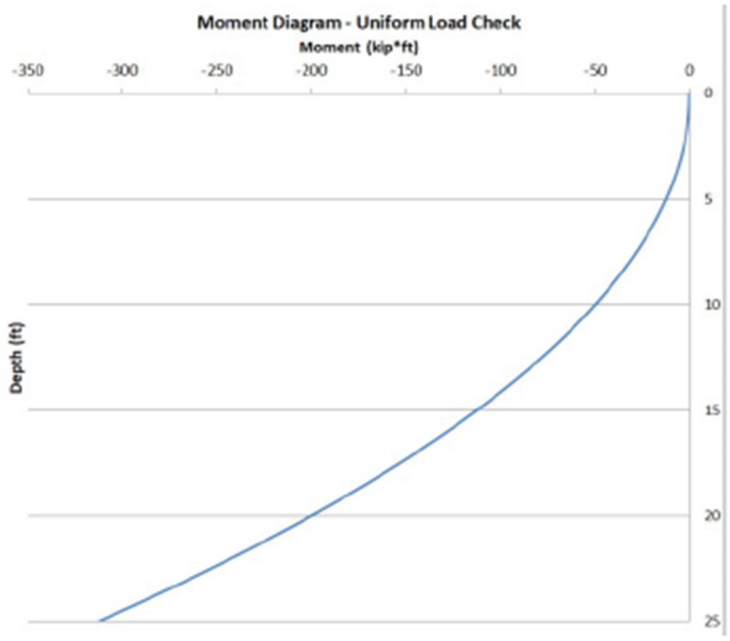

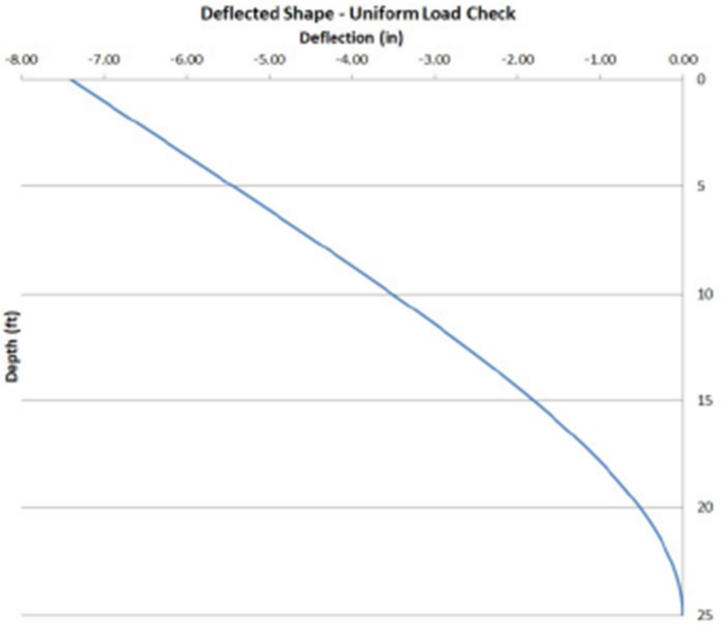

$\Delta max_{excel} := -7.4033\ in$

$\Delta = -7.4033\ in$

OK!

For this particular case, the trapezoidal method found the correct maximum displacement.

b) Moment Area Method

The moment diagram was drawn to scale on AutoCAD. And divided into 5 sections in order to predict the deflected shape.

$Y1 := 0\ ft$ $M(Y1) = 0\ kip \cdot ft$
$Y1 := 1\ ft$ $M(Y1) = -0.5\ kip \cdot ft$
$Y1 := 2\ ft$ $M(Y1) = -2\ kip \cdot ft$
$Y1 := 3\ ft$ $M(Y1) = -4.5\ kip \cdot ft$
$Y1 := 4\ ft$ $M(Y1) = -8\ kip \cdot ft$
$Y1 := 5\ ft$ $M(Y1) = -12.5\ kip \cdot ft$
$Y1 := 6\ ft$ $M(Y1) = -18\ kip \cdot ft$
$Y1 := 7\ ft$ $M(Y1) = -24.5\ kip \cdot ft$
$Y1 := 8\ ft$ $M(Y1) = -32\ kip \cdot ft$
$Y1 := 9\ ft$ $M(Y1) = -40.5\ kip \cdot ft$
$Y1 := 10\ ft$ $M(Y1) = -50\ kip \cdot ft$
$Y1 := 11\ ft$ $M(Y1) = -60.5\ kip \cdot ft$
$Y1 := 12\ ft$ $M(Y1) = -72\ kip \cdot ft$
$Y1 := 13\ ft$ $M(Y1) = -84.5\ kip \cdot ft$
$Y1 := 14\ ft$ $M(Y1) = -98\ kip \cdot ft$
$Y1 := 15\ ft$ $M(Y1) = -112.5\ kip \cdot ft$
$Y1 := 16\ ft$ $M(Y1) = -128\ kip \cdot ft$
$Y1 := 17\ ft$ $M(Y1) = -144.5\ kip \cdot ft$
$Y1 := 18\ ft$ $M(Y1) = -162\ kip \cdot ft$
$Y1 := 19\ ft$ $M(Y1) = -180.5\ kip \cdot ft$
$Y1 := 20\ ft$ $M(Y1) = -200\ kip \cdot ft$
$Y1 := 21\ ft$ $M(Y1) = -220.5\ kip \cdot ft$
$Y1 := 22\ ft$ $M(Y1) = -242\ kip \cdot ft$
$Y1 := 23\ ft$ $M(Y1) = -264.5\ kip \cdot ft$
$Y1 := 24\ ft$ $M(Y1) = -288\ kip \cdot ft$
$Y1 := 25\ ft$ $M(Y1) = -312.5\ kip \cdot ft$

$Y_A := 25\ ft \qquad \Theta_A := 0 \qquad V_A := 0\ in$

20 ft < y < 25 ft

$Y_B := 20\ ft$

$AreaMoment := -1270.8560\ kip \cdot ft^2 \qquad Ybar := 2.6845\ ft$ Distance from the centroid to B

$$\Theta_B := \frac{AreaMoment}{E \cdot I} + \Theta_A = -0.0161 \qquad V_B := \frac{AreaMoment \cdot Ybar}{E \cdot I} + V_A = -0.5173\ in$$

15 ft < y < 25 ft

$Y_B := 15\ ft$

$AreaMoment := -2041.6885\ kip \cdot ft^2 \qquad Ybar := 5.8164\ ft$ Distance from the centroid to B

$$\Theta_B := \frac{AreaMoment}{E \cdot I} + \Theta_A = -0.0258 \qquad V_B := \frac{AreaMoment \cdot Ybar}{E \cdot I} + V_A = -1.8005\ in$$

10 ft < y < 25 ft

$Y_B := 10\ ft$

$AreaMoment := -2435.1255\ kip \cdot ft^2 \qquad Ybar := 9.5277\ ft$ Distance from the centroid to B

$$\Theta_B := \frac{AreaMoment}{E \cdot I} + \Theta_A = -0.0308 \qquad V_B := \frac{AreaMoment \cdot Ybar}{E \cdot I} + V_A = -3.5177\ in$$

5 ft < y < 25 ft

$Y_B := 5\ ft$

$AreaMoment := -2583.3462\ kip \cdot ft^2 \qquad Ybar := 13.8711\ ft$ Distance from the centroid to B

$$\Theta_B := \frac{AreaMoment}{E \cdot I} + \Theta_A = -0.0326 \qquad V_B := \frac{AreaMoment \cdot Ybar}{E \cdot I} + V_A = -5.4331\ in$$

0 ft < y < 25 ft

$Y_B := 0\ ft$

$AreaMoment := -2604.2168\ kip \cdot ft^2$ $Ybar := 18.7499\ ft$ Distance from the centroid to B

$\Theta_B := \frac{AreaMoment}{E \cdot I} + \Theta_A = -0.0329$ $V_B := \frac{AreaMoment \cdot Ybar}{E \cdot I} + V_A = -7.4034\ in$

OK!

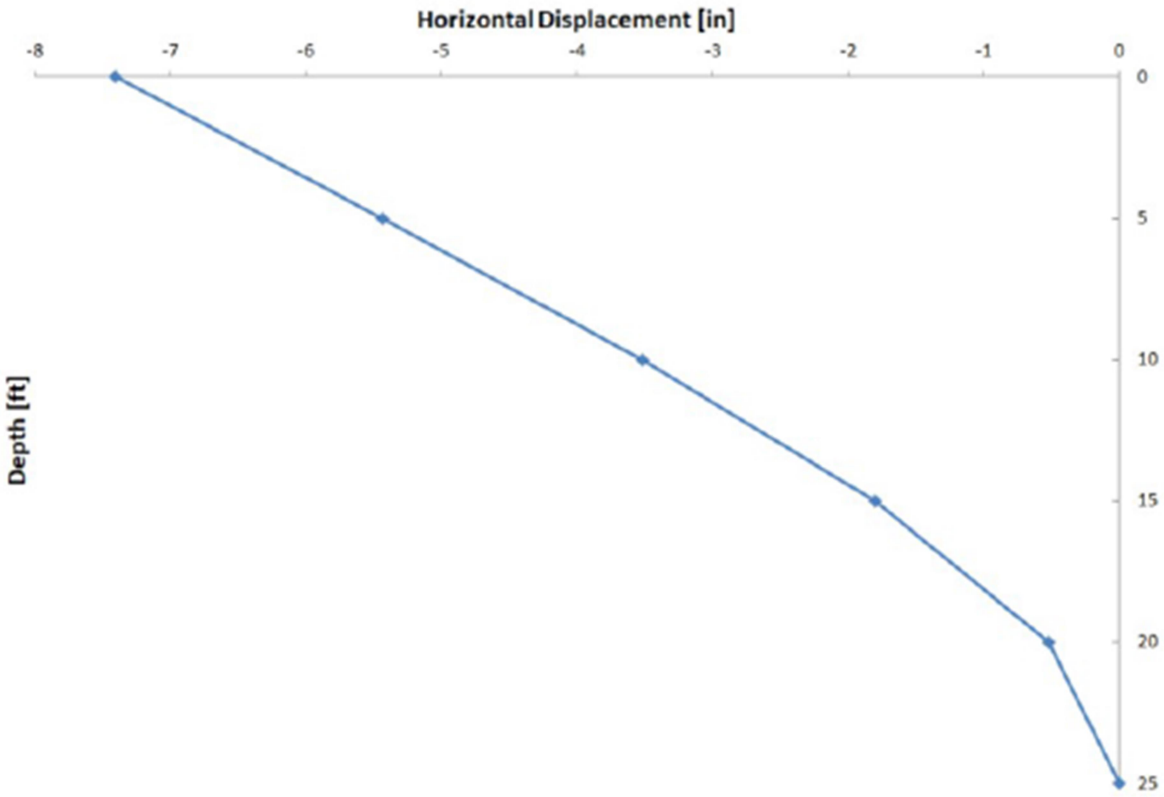

For this particular case, the moment area method found the correct maximum displacement.

This calculation shows that both models (Trapezoidal Approximation and Moment Area) can correctly predict the deflected shape and find the maximum deflection of a structure.

The second calculation check uses the Moment Area method to find the deflected shape for pile P004 and P005 for the 11 feet excavation in order to check if both methods (Moment Area and Trapezoidal Approximation) show the same deflected shape.

DESIGN OF ANCHORED SYSTEMS - PILE P004 AND P005 - EXCAVATION TO 11 FT - DRAINED ANALYSIS

The hand calculation design of the MU retaining wall will follow the procedure described in the Foundation Design Principles and Practices book (Coduto, 2001). The procedure is exactly the same for piles P004 and P005

Chapter 25.3 (Cantilever Sheet Pile Walls) describes the design method with the recommended Earth Pressure Diagrams for various soil types. This designed will be based on this chapter considering drain conditions.

This goal of this calculation set is to predict the deflected shape of the wall when the excavation depth is equal to 11 ft. For this intermediate case no tieback has been installed.

Step 1: Define Parameters of wall and soil

$H := 11\ ft$ Excavation depth

$B := 12\ in$ Width of flange for HP12x53

$b := 90\ in$ Spacing between piles (center to center)

Soil 1 - Clay (CL) - Drained Condition
From 0 ft to 12 ft - N=9

$c_1 := 0\ psf$

$\phi_1 := 26\ °$ Friction Angle Soil 1 (Stark, Choi, and McCOne, 2005)

$\gamma_1 := 120\ pcf$ Unit Weight of Soil 1 (Terzaghi, Peck, and Mesri, 1996 and experience)

$h_1 := 12\ ft$ Height of Soil 1

Soil 2 - Silty Sand (SM) - Drained Condition
From 12 ft to 22 ft - N=20

$c_2 := 0\ psf$

$\phi_2 := 32\ °$ Friction Angle Soil 2 - (Bowles, 1998; NAVFAC, 1998; and Peck, Hanson, Thornburn, 1973)

$\gamma_2 := 120\ pcf$ Unit Weight of Soil 2 (Terzaghi, Peck, and Mesri, 1996 and experience)

$h_2 := 10\ ft$ Height of Soil 2

Step 2: Determine values of Ka and Kp

Soil 1 - Silty Clay (CL)

$$Ka_1 := \left(\tan\left(45\,^\circ - \frac{\phi_1}{2}\right)\right)^2 = 0.39$$

Active lateral earth pressure coefficient

$$Kp_1 := \frac{\left(\tan\left(45\,^\circ + \frac{\phi_1}{2}\right)\right)^2}{1.5} = 1.71$$

Passive lateral earth pressure coefficient with a 1.5 factor of safety

Soil 2 - Silty Sand (SM)

$$Ka_2 := \left(\tan\left(45\,^\circ - \frac{\phi_2}{2}\right)\right)^2 = 0.31$$

Active lateral earth pressure coefficient

$$Kp_2 := \frac{\left(\tan\left(45\,^\circ + \frac{\phi_2}{2}\right)\right)^2}{1.5} = 2.17$$

Passive lateral earth pressure coefficient with a 1.5 factor of safety

Step 3: Find Earth Pressure Diagram

This calculation uses the drained conditions since it is a long term analysis.

Cantilever Sheet Pile Wall (Following Chapter 25.3) - Coduto (2001)

Find active pressure at 11ft:

$Ap_1 := \gamma_1 \cdot H \cdot Ka_1 \cdot b = 3.87 \ \frac{kip}{ft}$ Above the cut

$Ap_2 := \gamma_1 \cdot H \cdot Ka_1 \cdot B = 0.52 \ \frac{kip}{ft}$ Below the cut

Find depth where net pressure is zero:

$d_1 := 1 \ ft$

$Net1 := Kp_1 \cdot \gamma_1 \cdot d_1 \cdot 3 \cdot B - Ka_1 \cdot \gamma_1 \cdot (H + d_1) \cdot B = 0 \ \frac{kip}{ft}$

$d := H + d_1 = 12 \ ft$ Depth where net pressure is zero

Find force above d and moment about point d:

$Pa1 := \frac{Ap_1 \cdot H}{2} = 21.26 \ kip$ Force above 11ft

$Pa2 := \frac{Ap_2 \cdot d_1}{2} = 0.26 \ kip$ Force between 11ft and 11.9ft

$Force1 := Pa1 + Pa2 = 21.5183 \ kip$

$Moment := Pa1 \cdot \left(d - H \cdot \frac{2}{3}\right) + Pa2 \cdot d_1 \cdot \frac{2}{3} = 99.39 \ kip \cdot ft$

Find total embedment depth:

$d_3 := 5.73 \ ft$ Distance CE in the book

$d_4 := 6.39 \ ft$ Distance EG in the book

$Slope := \gamma_2 \cdot (3 \cdot Kp_2 - Ka_2) = 0.74423 \ \frac{kip}{ft^2 \cdot ft}$ Slope at Layer 2

$TotalForce := Force1 - \frac{Slope \cdot {d_3}^2 \cdot 3 \cdot B}{2} + \frac{Slope \cdot {d_4}^2 \cdot B}{2} = 0.06 \ kip$

$TotalMoment := -Slope \cdot \frac{{d_3}^3}{8} \cdot 3 \cdot B + Slope \cdot \frac{{d_4}^2}{2} \cdot \left(d_3 + d_4 \cdot \frac{2}{3}\right) \cdot B - Moment = -0.1 \ kip \cdot ft$

$$Slope \cdot \frac{d_3}{2} \cdot B = 2.13 \ \frac{kip}{ft} \qquad Slope \cdot d_4 \cdot B = 4.76 \ \frac{kip}{ft}$$

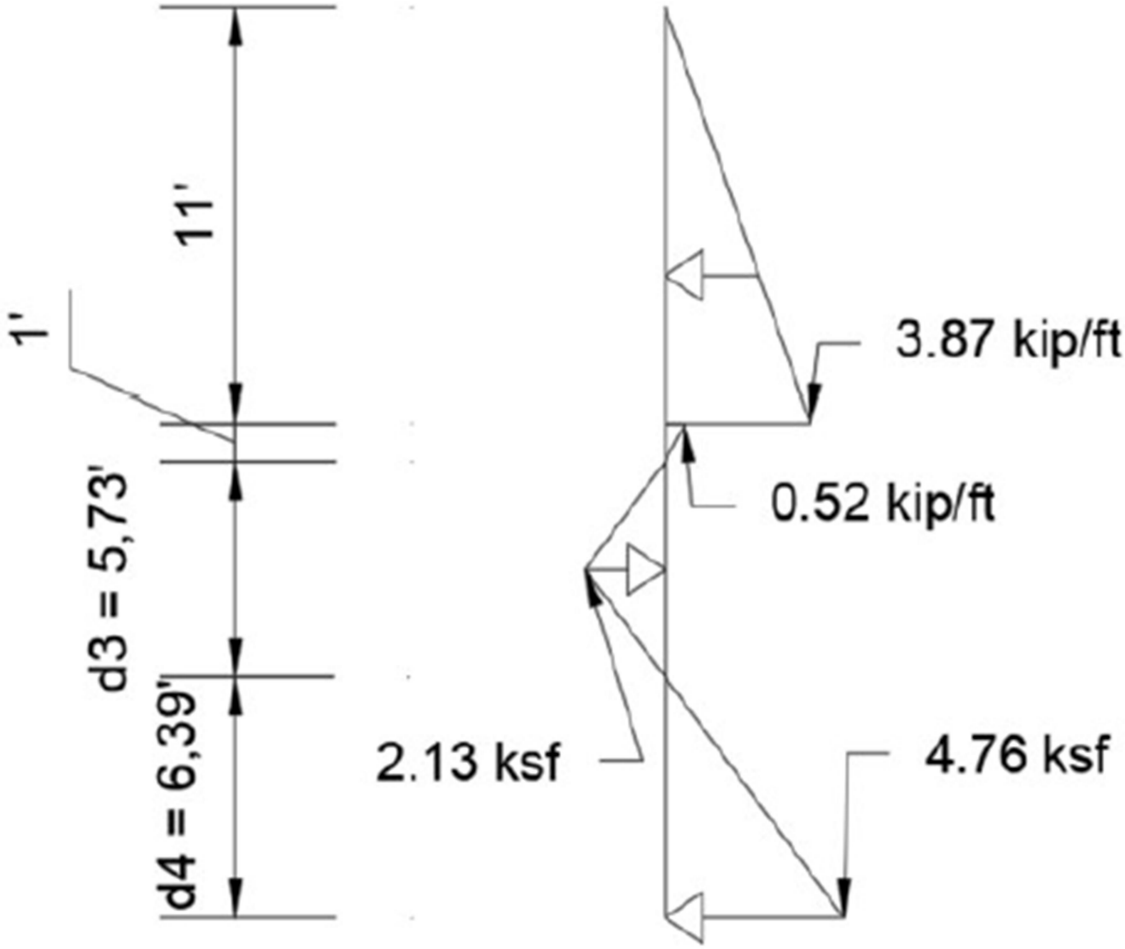

Earth Pressure Diagram - Excavation to 11ft

Step 4: Find Moment Diagram

0 ft < y < 11 ft $M(y) := -0.0586 \frac{kip}{ft^2} \cdot y^3$

$Y1 := 0\ ft$	$M(Y1) = 0\ kip \cdot ft$
$Y1 := 1\ ft$	$M(Y1) = -0.06\ kip \cdot ft$
$Y1 := 2\ ft$	$M(Y1) = -0.47\ kip \cdot ft$
$Y1 := 3\ ft$	$M(Y1) = -1.58\ kip \cdot ft$
$Y1 := 4\ ft$	$M(Y1) = -3.75\ kip \cdot ft$
$Y1 := 5\ ft$	$M(Y1) = -7.33\ kip \cdot ft$
$Y1 := 6\ ft$	$M(Y1) = -12.66\ kip \cdot ft$
$Y1 := 7\ ft$	$M(Y1) = -20.1\ kip \cdot ft$
$Y1 := 8\ ft$	$M(Y1) = -30\ kip \cdot ft$
$Y1 := 9\ ft$	$M(Y1) = -42.72\ kip \cdot ft$
$Y1 := 10\ ft$	$M(Y1) = -58.6\ kip \cdot ft$
$Y1 := 11\ ft$	$M(Y1) = -78\ kip \cdot ft$

11 ft < y < 12 ft $M(y) := 0.08667 \frac{kip}{ft^2} \cdot y^3 - 3.12 \frac{kip}{ft} \cdot y^2 + 15.895 \cdot kip \cdot y + 9.276\ kip \cdot ft$

$Y1 := 11\ ft$	$M(Y1) = -78.04\ kip \cdot ft$
$Y1 := 12\ ft$	$M(Y1) = -99.5\ kip \cdot ft$

12 ft < y < 14.86 ft $M(y) := 0.1241 \frac{kip}{ft^2} \cdot y^3 - 4.4685 \frac{kip}{ft} \cdot y^2 + 32.077 \cdot kip \cdot y - 55.4528\ kip \cdot ft$

$Y1 := 12\ ft$	$M(Y1) = -99.55\ kip \cdot ft$
$Y1 := 13\ ft$	$M(Y1) = -120.98\ kip \cdot ft$
$Y1 := 14\ ft$	$M(Y1) = -141.67\ kip \cdot ft$
$Y1 := 14.86\ ft$	$M(Y1) = -158.3\ kip \cdot ft$

14.86 ft < y < 17.73 ft $M(y) := -0.1243 \frac{kip}{ft^2} \cdot y^3 + 6.59 \frac{kip}{ft} \cdot y^2 - 132.416 \cdot kip \cdot y + 762.33\ kip \cdot ft$

$Y1 := 14.86\ ft$	$M(Y1) = -158.05\ kip \cdot ft$
$Y1 := 15\ ft$	$M(Y1) = -160.67\ kip \cdot ft$
$Y1 := 16\ ft$	$M(Y1) = -178.42\ kip \cdot ft$
$Y1 := 17\ ft$	$M(Y1) = -194.92\ kip \cdot ft$
$Y1 := 17.73\ ft$	$M(Y1) = -206.6\ kip \cdot ft$

17.73 ft < y < 24.12 ft $M(y) := -0.12415 \frac{kip}{ft^2} \cdot y^3 + 8.190 \frac{kip}{ft} \cdot y^2 - 193.858 \cdot kip \cdot y + 1348.96\ kip \cdot ft$

$Y1 := 17.73\ ft$	$M(Y1) = -205.54\ kip \cdot ft$
$Y1 := 18\ ft$	$M(Y1) = -210.97\ kip \cdot ft$
$Y1 := 19\ ft$	$M(Y1) = -229.3\ kip \cdot ft$
$Y1 := 20\ ft$	$M(Y1) = -245.4\ kip \cdot ft$
$Y1 := 21\ ft$	$M(Y1) = -260.02\ kip \cdot ft$
$Y1 := 22\ ft$	$M(Y1) = -273.91\ kip \cdot ft$
$Y1 := 23\ ft$	$M(Y1) = -287.8\ kip \cdot ft$
$Y1 := 24\ ft$	$M(Y1) = -302.44\ kip \cdot ft$
$Y1 := 24.12\ ft$	$M(Y1) = -304.28\ kip \cdot ft$

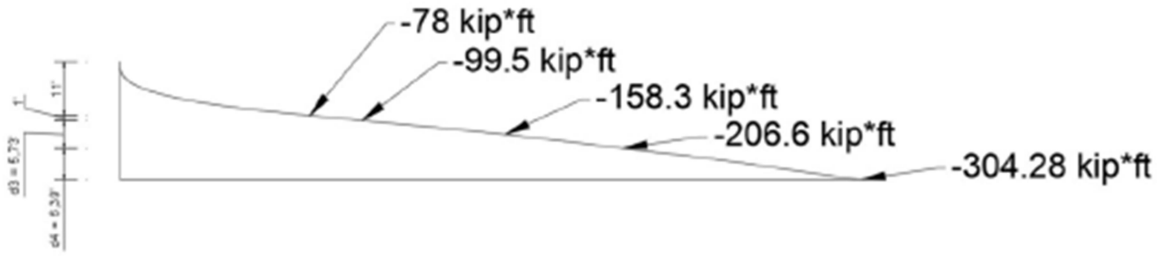

Moment Diagram - Drained Analysis - Excavation to 11ft

Step 5: Find Deflected Shape

The Mohr Theorems will be used in order to find the deflected shape. The moment diagram was drawn to scale on autocad in order to find the area and centroid for each section.

Slope and deflection at the toe of the pile are zero.

$$[\text{Change in slope}]_{AB} = \left[\text{Area of } \frac{M}{EI} \text{ diagram}\right]_{AB}$$ Mohr I

$$\begin{bmatrix}\text{Vertical}\\ \text{Intercept}\end{bmatrix}_{BA} = \left[\text{Area of } \frac{M}{EI} \text{ diagram}\right]_{BA} \times \begin{bmatrix}\text{Distance from } B \text{ to centroid}\\ \text{of } \left(\frac{M}{EI}\right)_{BA} \text{ diagram}\end{bmatrix}$$ Mohr II

$E := 29000\ ksi$ $I := 393\ in^4$ $E \cdot I = 79145.83\ kip \cdot ft^2$

$Y_A := 24.12\ ft$ $\Theta_A := 0$ $V_A := 0\ in$

20 ft < y < 24.12 ft

$Y_B := 20\ ft$

$AreaMoment := -1132.0395\ kip \cdot ft^2$ $Ybar := 2.1325\ ft$ Distance from the centroid to point B

$\Theta_B := \frac{AreaMoment}{E \cdot I} + \Theta_A = -0.01$ $V_B := \frac{AreaMoment \cdot Ybar}{E \cdot I} + V_A = -0.37\ in$

15 ft < y < 24.12 ft

$Y_B := 15\ ft$

$AreaMoment := -2148.8602\ kip \cdot ft^2$ $Ybar := 5.0226\ ft$ Distance from the centroid to point B

$\Theta_B := \frac{AreaMoment}{E \cdot I} + \Theta_A = -0.03$ $V_B := \frac{AreaMoment \cdot Ybar}{E \cdot I} + V_A = -1.64\ in$

10 ft < y < 24.12 ft

$Y_B := 12\ ft$

$AreaMoment := -2698.7561\ kip \cdot ft^2$ $Ybar := 8.5705\ ft$ Distance from the centroid to point B

$\Theta_B := \frac{AreaMoment}{E \cdot I} + \Theta_A = -0.03$ $V_B := \frac{AreaMoment \cdot Ybar}{E \cdot I} + V_A = -3.51\ in$

5 ft < y < 24.12 ft

$Y_B := 11\ ft$

$AreaMoment := -2836.0805\ kip \cdot ft^2$ $Ybar := 13.0715\ ft$ Distance from the centroid to point B

$\Theta_B := \frac{AreaMoment}{E \cdot I} + \Theta_A = -0.04$ $V_B := \frac{AreaMoment \cdot Ybar}{E \cdot I} + V_A = -5.62\ in$

0 ft < y < 24.12 ft

$Y_B := 0\ ft$

$AreaMoment := -2845.2405\ kip \cdot ft^2$ $Ybar := 18.0262\ ft$ Distance from the centroid to point B

$\Theta_B := \frac{AreaMoment}{E \cdot I} + \Theta_A = -0.04$ $V_B := \frac{AreaMoment \cdot Ybar}{E \cdot I} + V_A = -7.78\ in$

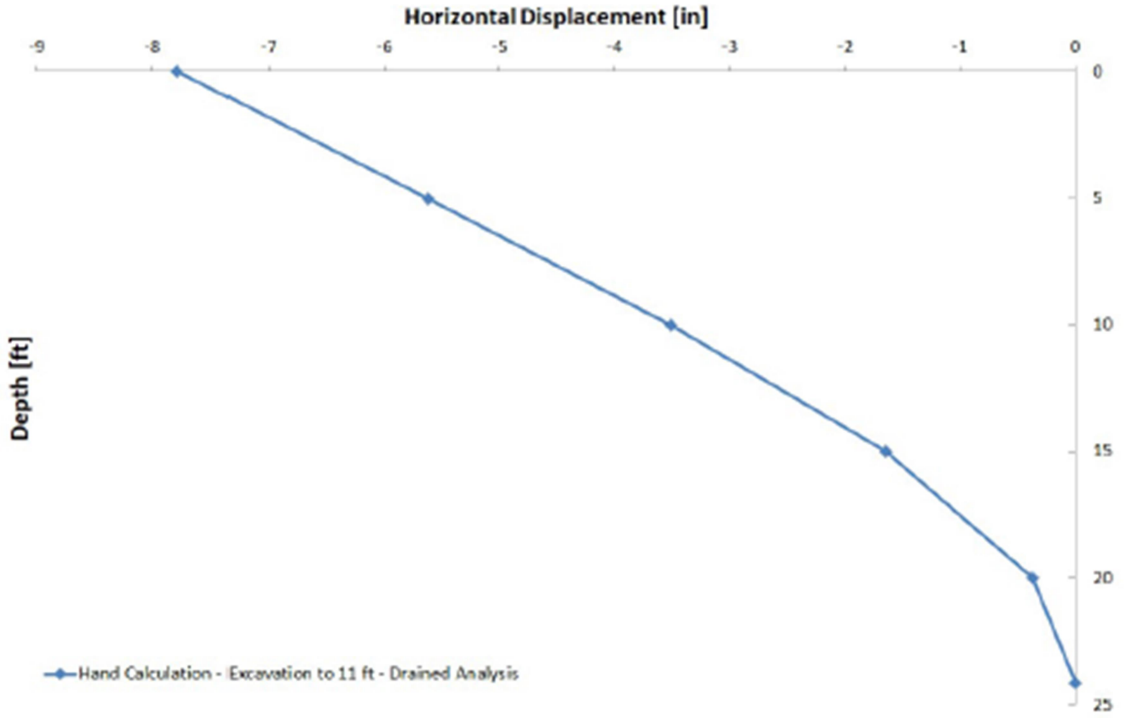

Deflected Shape - Drained Analysis - Excavation to 11ft

The deflected shape found using the moment area method is the same as the one found using the trapezoidal area approximation.

APPENDIX E (TRAPEZOIDAL AREA APPROXIMATION METHOD – EXCEL SPREADSHEET EXAMPLE)

This appendix shows the excel spreadsheet used for the trapezoidal area approximation method for the 11 feet excavation depth. Each cell is described below:

Step – increment step for each depth used in the calculation;

Pile Length – length of pile found using the appropriate method describes on Appendix C;

E – Young's Modulus;

I – Moment of Inertia;

E*I – $$EI := \frac{E \cdot I}{144}$$

Depth – pile depth

Moment (kip*ft) – moment at the respective depth using the equation described on Appendix C, the moment equation changes according to the depth;

Curvature – $$Curvature_j := \frac{Moment_j}{E \cdot I}$$

Slope – (for this case j = i +1)

$$Slope_j := \frac{(Moment_j + Moment_i) \cdot (Depth_j - Depth_i)}{2} + Slope_i$$

Deflection (ft) – (for this case j = i +1)

$$Deflection_j := \frac{(Slope_j + Slope_i) \cdot (Depth_j - Depth_i)}{2} + Deflection_i$$

Deflection (in) –

$$Deflection(in) := Deflection(ft) \cdot 12$$

Deflected Shape - Pile 004 and P005 - Excavation to 11 FT

Step	0.1	feet
Pile Length	24.12	feet

E	29000	ksi
I	393	inches^4
E*I	79145.83	kip*ft^2

Depth	Moment (kip*ft)	Curvature (1/ft)	Slope	Deflection (ft)	Deflection (in)
24.12	-304.28	-0.00384461	0	0	0.0000000
24.10	-303.98	-0.00384071	-0.00008	0.00000	-0.0000092
24.00	-302.44	-0.00382132	-0.00046	-0.00003	-0.0003313
23.90	-300.92	-0.00380212	-0.00084	-0.00009	-0.0011120
23.80	-299.42	-0.00378310	-0.00122	-0.00020	-0.0023489
23.70	-297.92	-0.00376425	-0.00160	-0.00034	-0.0040398
23.60	-296.45	-0.00374556	-0.00197	-0.00052	-0.0061824
23.50	-294.98	-0.00372703	-0.00235	-0.00073	-0.0087744
23.40	-293.52	-0.00370863	-0.00272	-0.00098	-0.0118137
23.30	-292.08	-0.00369037	-0.00309	-0.00127	-0.0152981
23.20	-290.64	-0.00367223	-0.00346	-0.00160	-0.0192253
23.10	-289.22	-0.00365421	-0.00382	-0.00197	-0.0235932
23.00	-287.80	-0.00363629	-0.00419	-0.00237	-0.0283996
22.90	-286.39	-0.00361846	-0.00455	-0.00280	-0.0336423
22.80	-284.98	-0.00360072	-0.00491	-0.00328	-0.0393193
22.70	-283.58	-0.00358306	-0.00527	-0.00379	-0.0454283
22.60	-282.19	-0.00356547	-0.00563	-0.00433	-0.0519674
22.50	-280.80	-0.00354793	-0.00598	-0.00491	-0.0589343
22.40	-279.42	-0.00353044	-0.00634	-0.00553	-0.0663269
22.30	-278.04	-0.00351298	-0.00669	-0.00618	-0.0741432
22.20	-276.66	-0.00349556	-0.00704	-0.00687	-0.0823810
22.10	-275.28	-0.00347816	-0.00739	-0.00759	-0.0910383
22.00	-273.91	-0.00346077	-0.00774	-0.00834	-0.1001130
21.90	-272.53	-0.00344337	-0.00808	-0.00913	-0.1096030
21.80	-271.15	-0.00342597	-0.00842	-0.00996	-0.1195062
21.70	-269.77	-0.00340856	-0.00877	-0.01082	-0.1298205
21.60	-268.39	-0.00339111	-0.00911	-0.01171	-0.1405438
21.50	-267.01	-0.00337363	-0.00944	-0.01264	-0.1516741
21.40	-265.62	-0.00335610	-0.00978	-0.01360	-0.1632092
21.30	-264.23	-0.00333852	-0.01012	-0.01460	-0.1751470
21.20	-262.83	-0.00332087	-0.01045	-0.01562	-0.1874855
21.10	-261.43	-0.00330315	-0.01078	-0.01669	-0.2002224
21.00	-260.02	-0.00328534	-0.01111	-0.01778	-0.2133557
20.90	-258.60	-0.00326744	-0.01144	-0.01891	-0.2268833
20.80	-257.18	-0.00324944	-0.01176	-0.02007	-0.2408030
20.70	-255.75	-0.00323133	-0.01209	-0.02126	-0.2551126
20.60	-254.30	-0.00321309	-0.01241	-0.02248	-0.2698099
20.50	-252.85	-0.00319473	-0.01273	-0.02374	-0.2848928
20.40	-251.38	-0.00317622	-0.01305	-0.02503	-0.3003591

APPENDIX F (MOMENT DIAGRAM CHECK)

The excel spreadsheet developed to find the deflected shape for the MU retaining wall has only one input, the moment equation for the structure. If the user input the right moment equations, the spreadsheet will output the correct deflected shape. So, it is important to double check the moment equations used in this thesis.

All the six earth pressure diagrams described on Appendix C and Appendix D were copied to a structural software in order to double check if the moment diagram developed by the excel spreadsheet matches with the one developed by the structural software. This appendix shows this check.

Figure F.1 shows the earth pressure diagram for the first check, pile P004, assuming the soil as Clay.

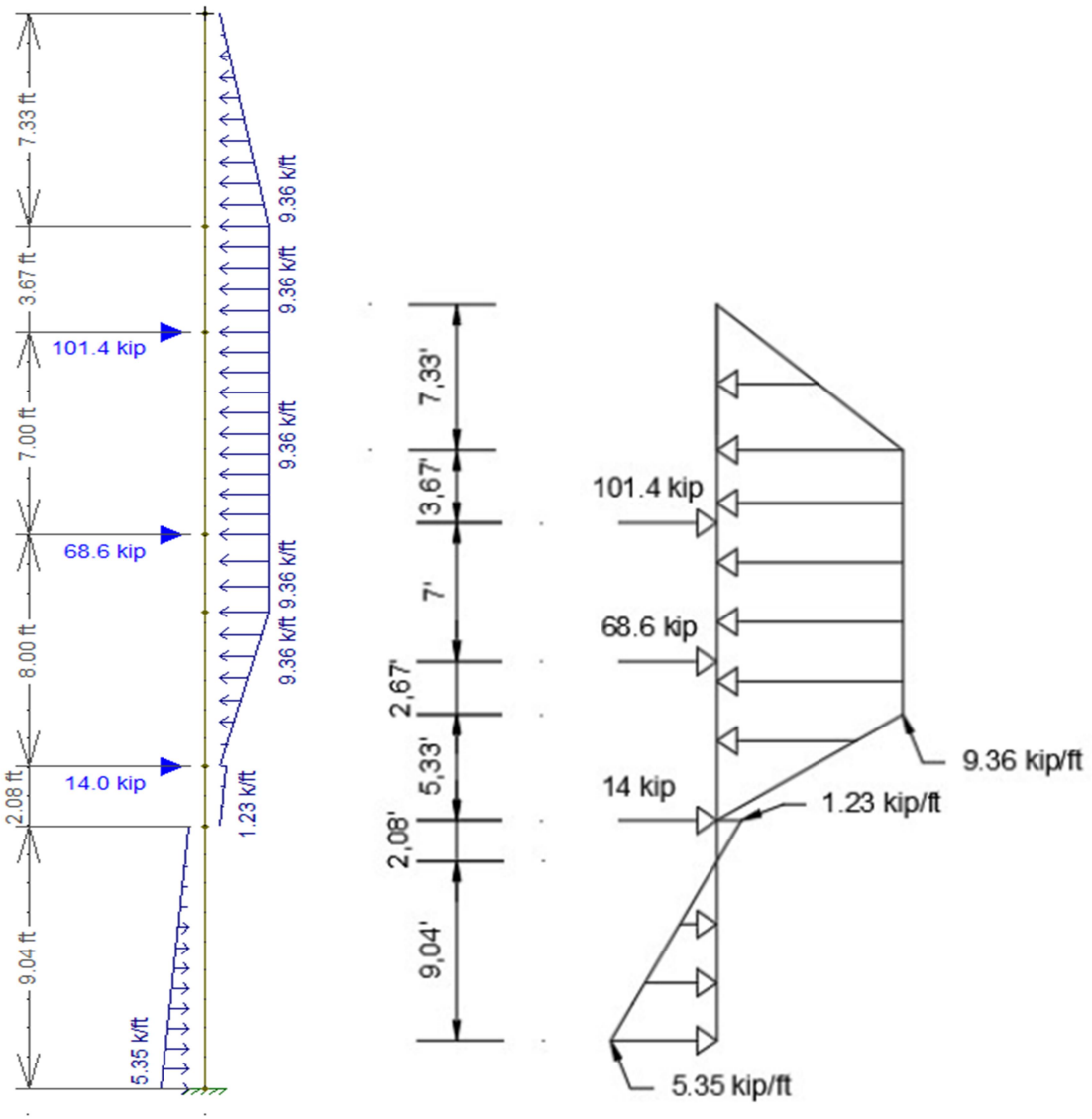

Figure F.1: Earth Pressure Diagram for pile P004 – Clay. Structural Software (left) and Limit Equilibrium (right)

Earth Pressure Diagram in the structural software matches with the limit equilibrium method.

Figure F.2 shows the moment diagram for the first check, pile P004, assuming the soil as Clay.

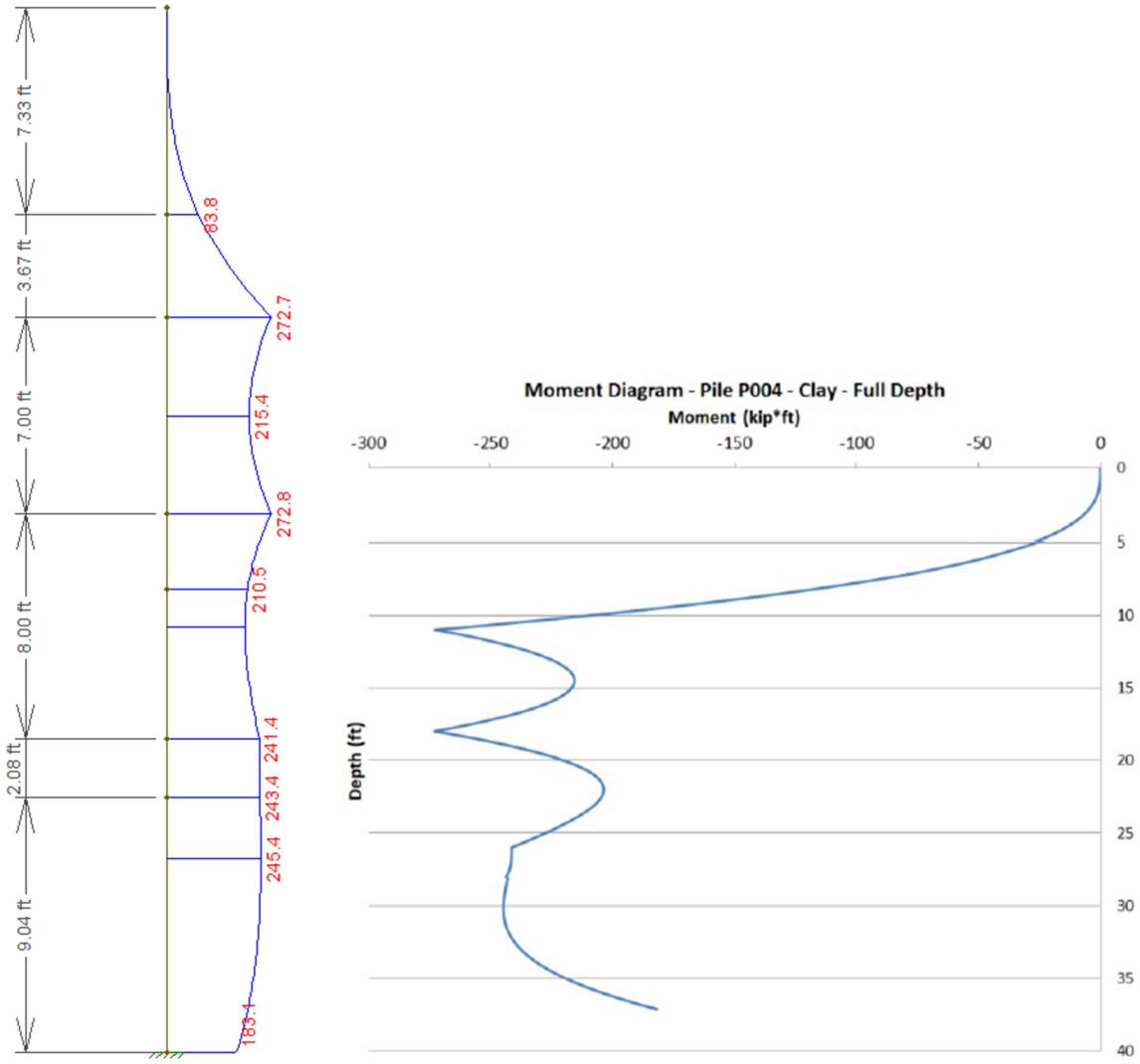

Figure F.2: Moment Diagram for pile P004 – Clay. Structural Software (left) and Limit Equilibrium (right)

Moment Diagram in the structural software matches with the limit equilibrium method.

Figure F.3 shows the earth pressure diagram for the second check, pile P004, assuming the soil as Sand.

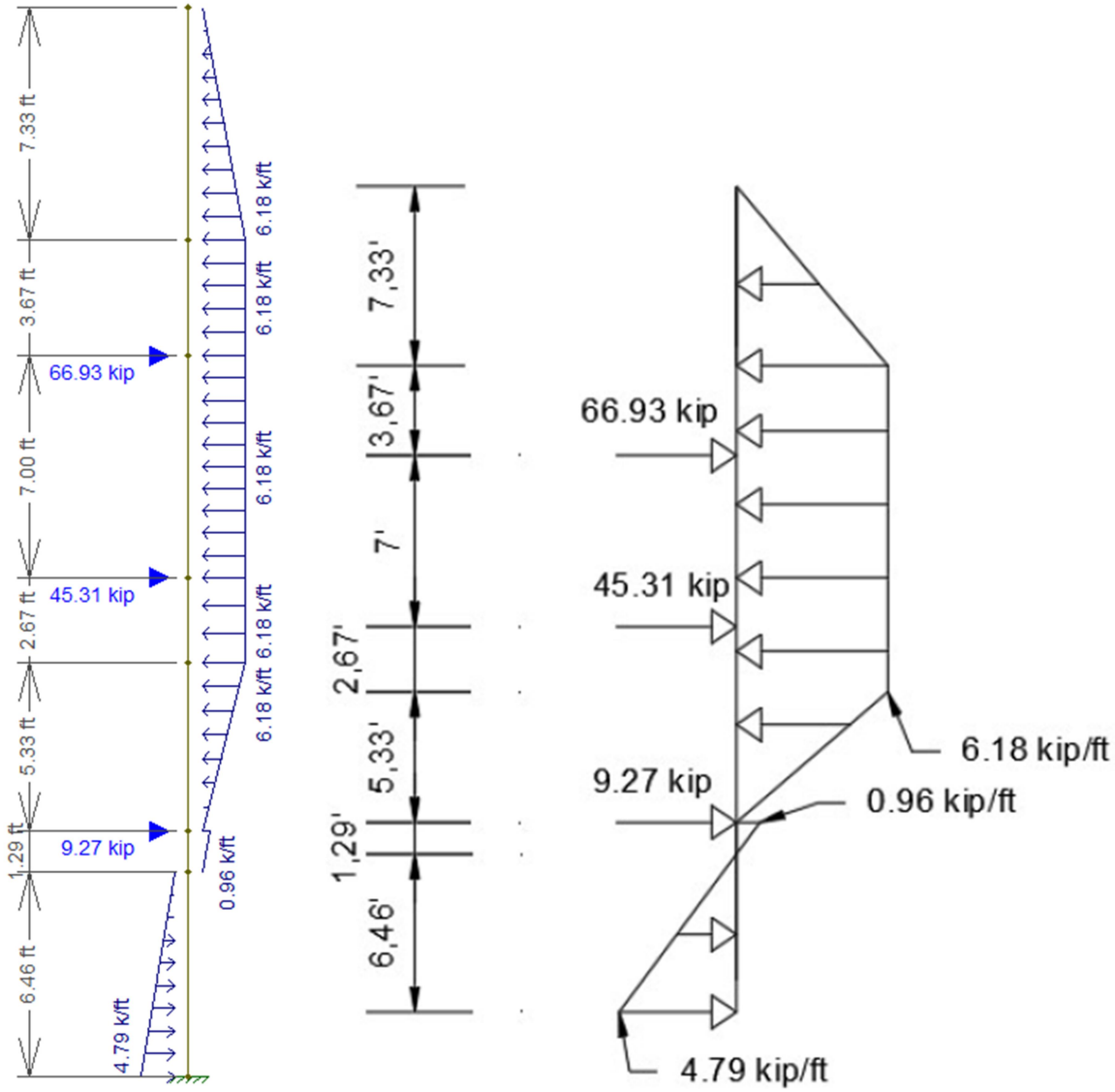

Figure F.3: Earth Pressure Diagram for pile P004 – Sand. Structural Software (left) and Limit Equilibrium (right)

Earth Pressure Diagram in the structural software matches with the limit equilibrium method.

Figure F.4 shows the moment diagram for the second check, pile P004, assuming the soil as Sand.

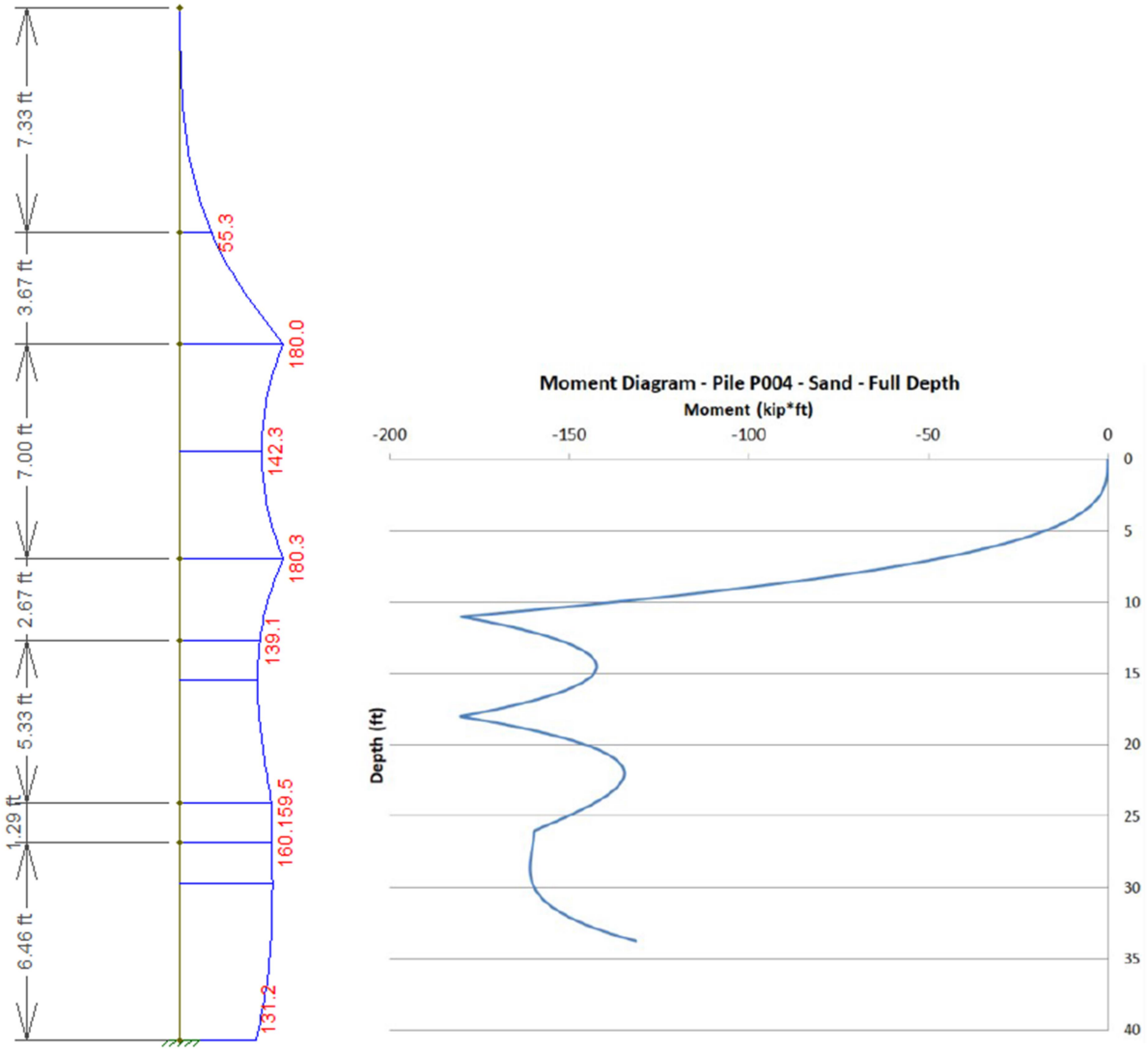

Figure F.4: Moment Diagram for pile P004 – Sand. Structural Software (left) and Limit Equilibrium (right)

Moment Diagram in the structural software matches with the limit equilibrium method.

Figure F.5 shows the earth pressure diagram for the third check, pile P005, assuming the soil as Clay.

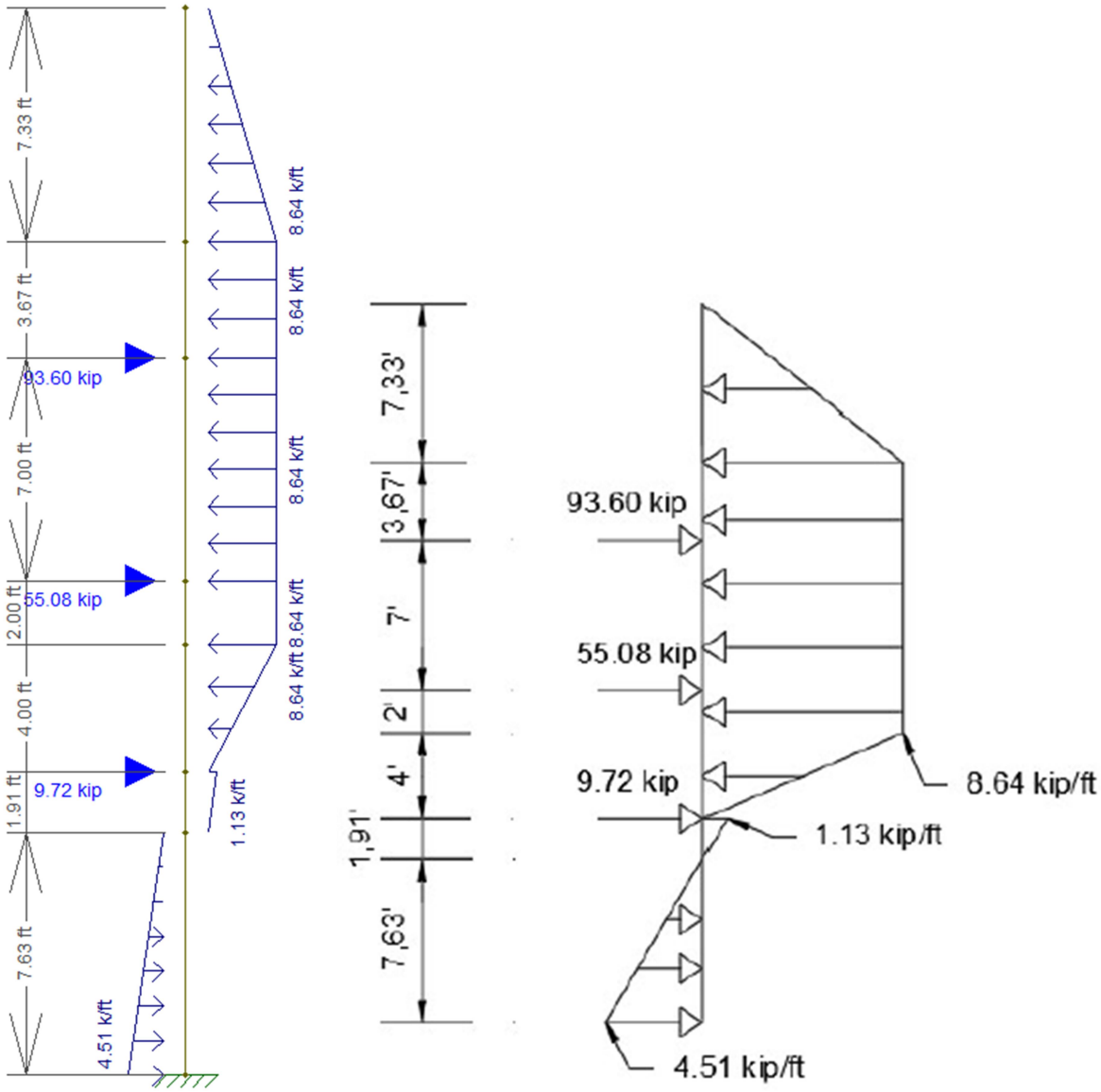

Figure F.5: Earth Pressure Diagram for pile P005 – Clay. Structural Software (left) and Limit Equilibrium (right)

Earth Pressure Diagram in the structural software matches with the limit equilibrium method.

Figure F.6 shows the moment diagram for the third check, pile P005, assuming the soil as Clay.

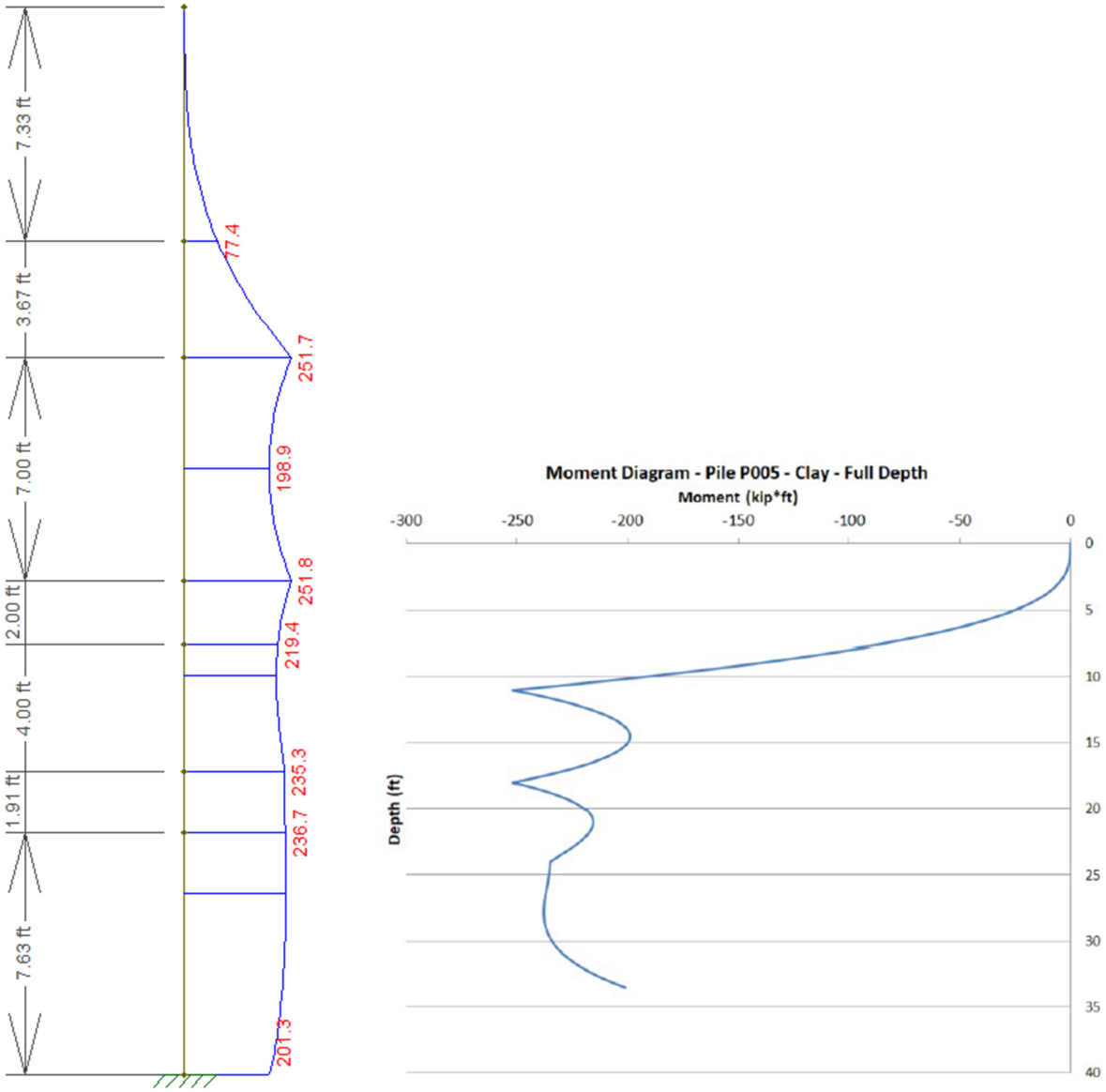

Figure F.6: Moment Diagram for pile P005 – Clay. Structural Software (left) and Limit Equilibrium (right)

Moment Diagram in the structural software matches with the limit equilibrium method.

Figure F.7 shows the earth pressure diagram for the fourth check, pile P005, assuming the soil as Sand.

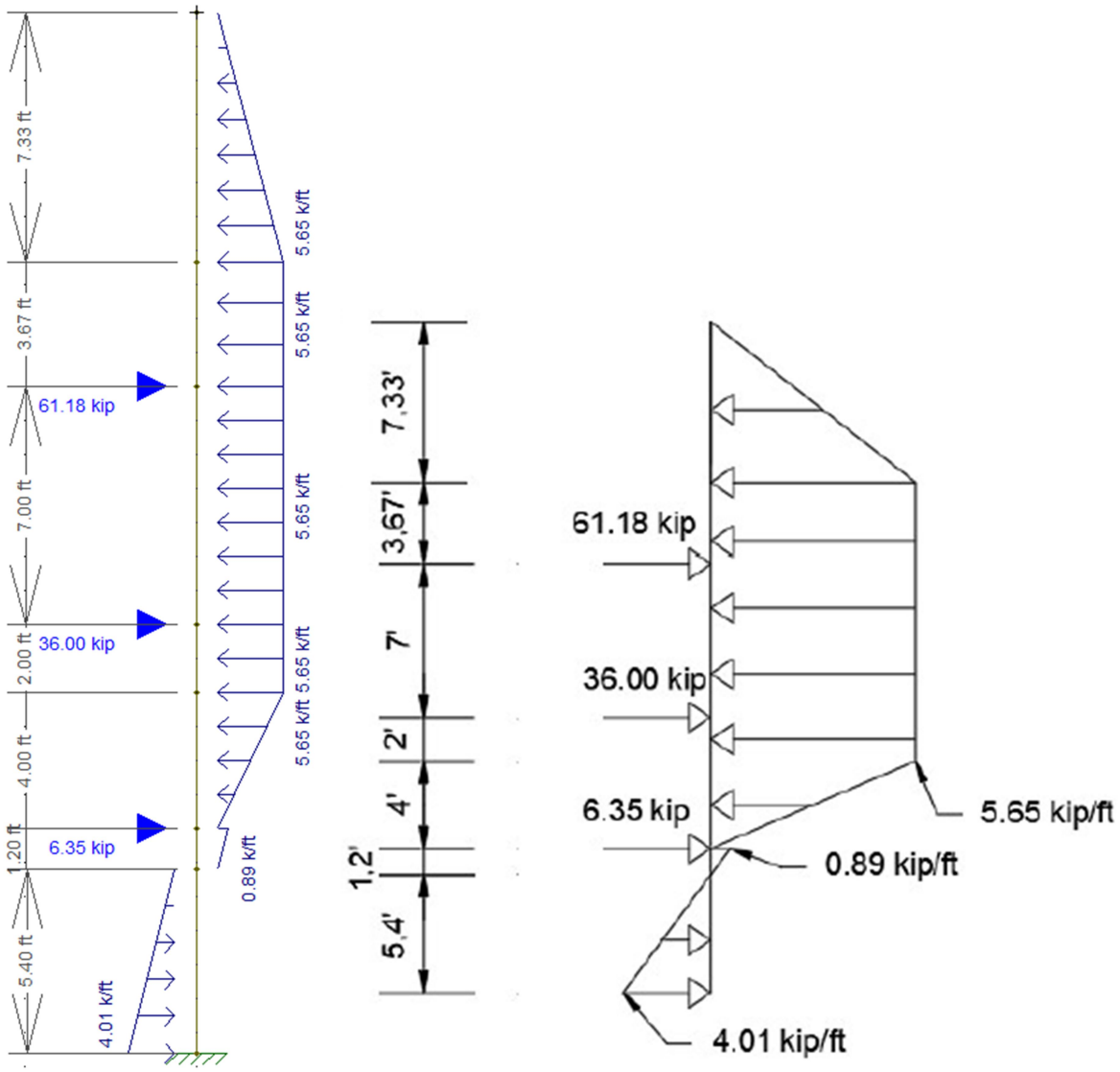

Figure F.7: Earth Pressure Diagram for pile P005 – Sand. Structural Software (left) and Limit Equilibrium (right)

Earth Pressure Diagram in the structural software matches with the limit equilibrium method.

Figure F.8 shows the moment diagram for the fourth check, pile P005, assuming the soil as Sand.

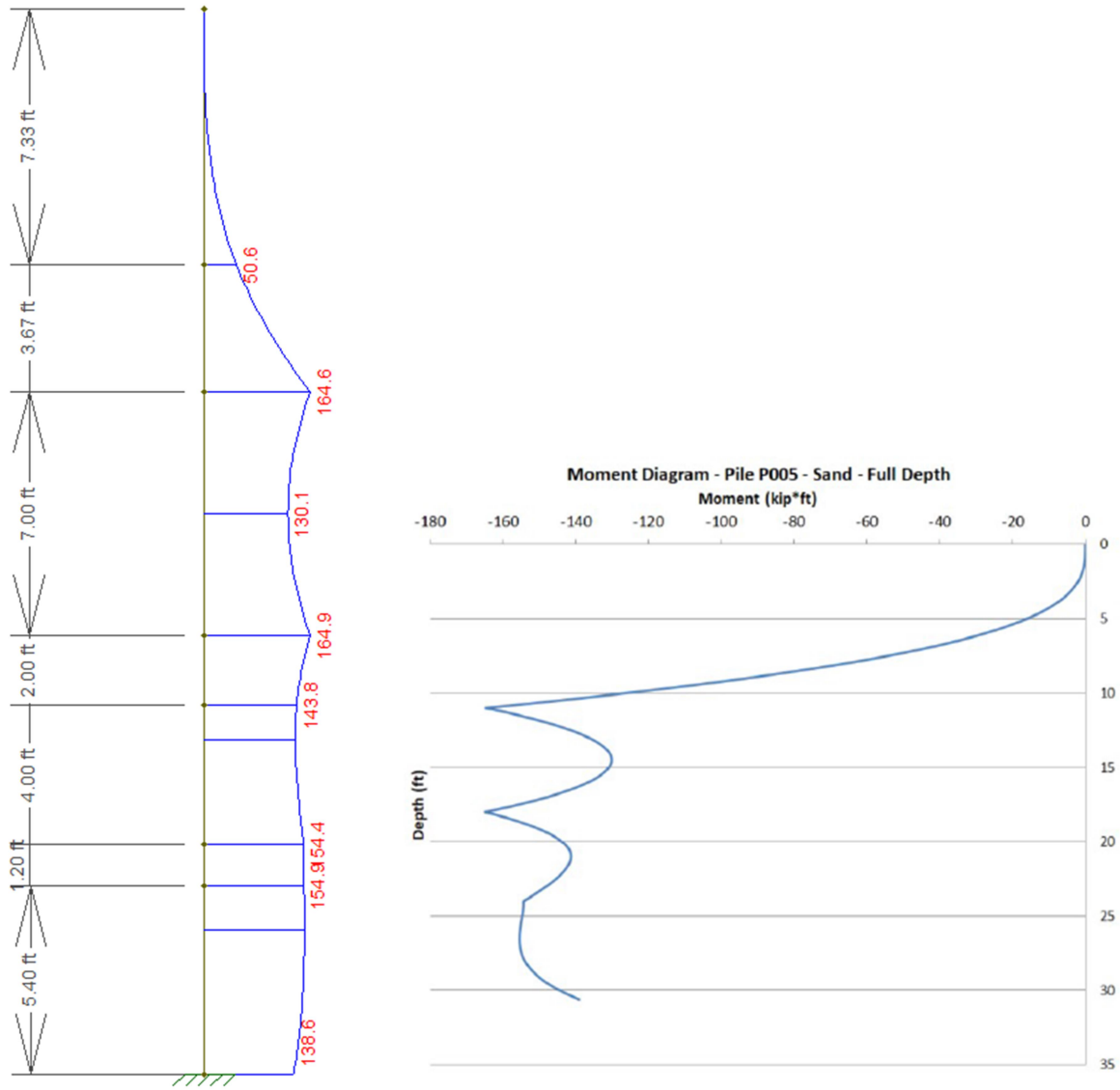

Figure F.8: Moment Diagram for pile P005 – Sand. Structural Software (left) and Limit Equilibrium (right)

Moment Diagram in the structural software matches with the limit equilibrium method.

Figure F.9 shows the earth pressure diagram for the fifth check, excavation to the 11 foot depth.

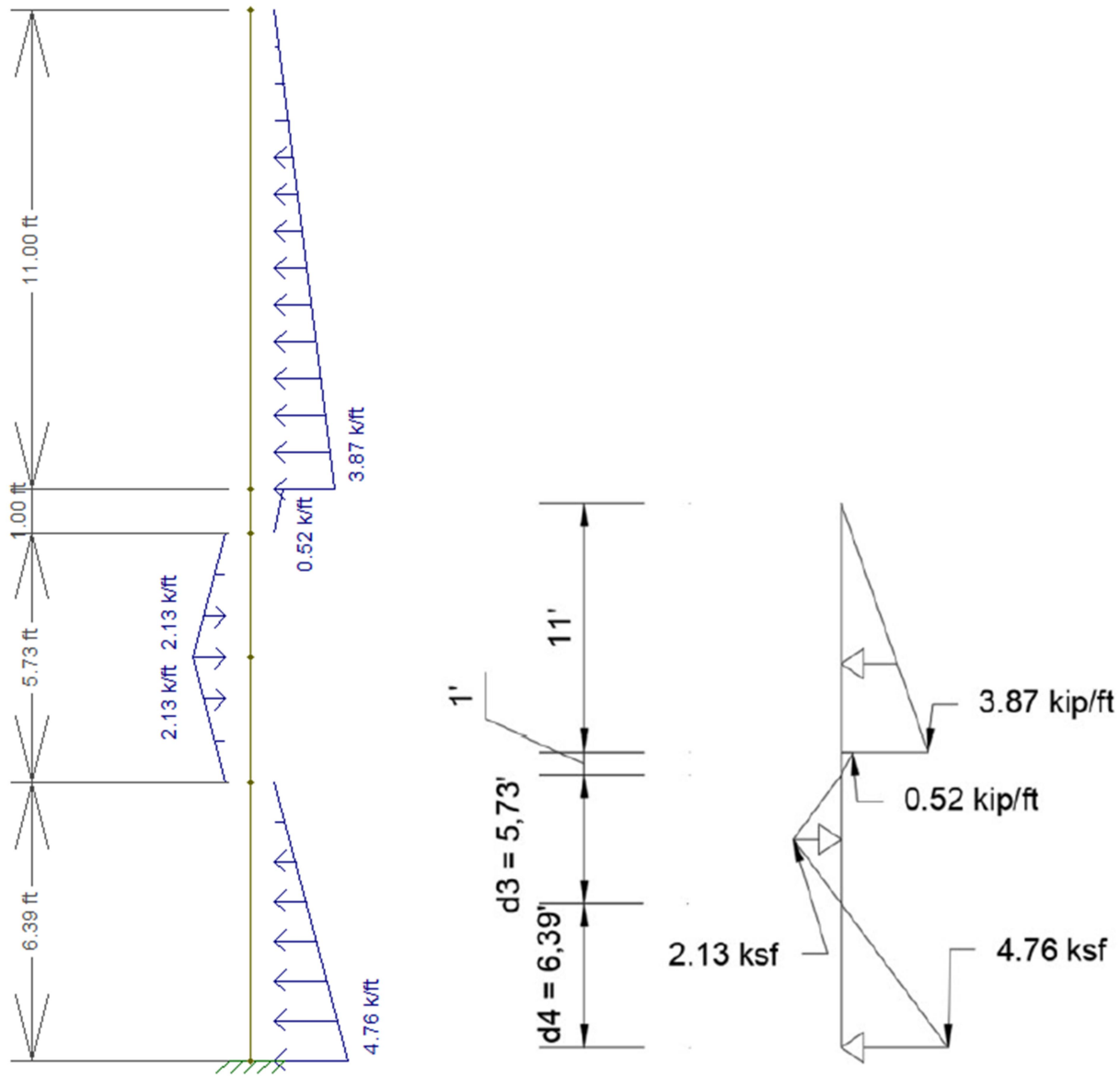

Figure F.9: Earth Pressure Diagram for 11 foot depth excavation. Structural Software (left) and Limit Equilibrium (right)

Earth Pressure Diagram in the structural software matches with the limit equilibrium method.

Figure F.10 shows the moment diagram for the fifth check, excavation to the 11 foot depth.

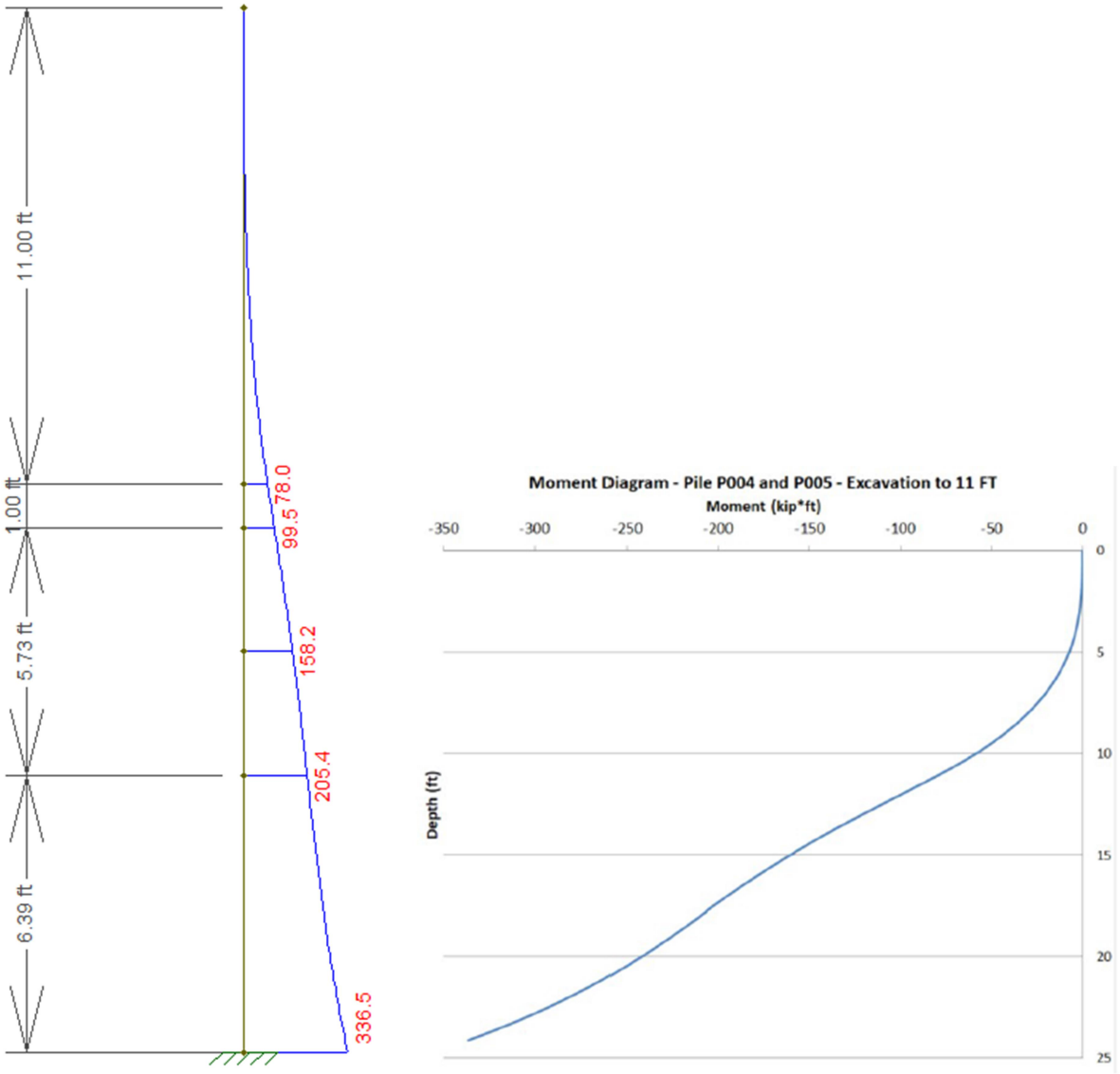

Figure F.10: Moment Diagram for 11 foot depth excavation. Structural Software (left) and Limit Equilibrium (right)

Moment Diagram in the structural software matches with the limit equilibrium method.

Figure F.11 shows the earth pressure diagram for the sixth check, excavation to the 18 foot depth.

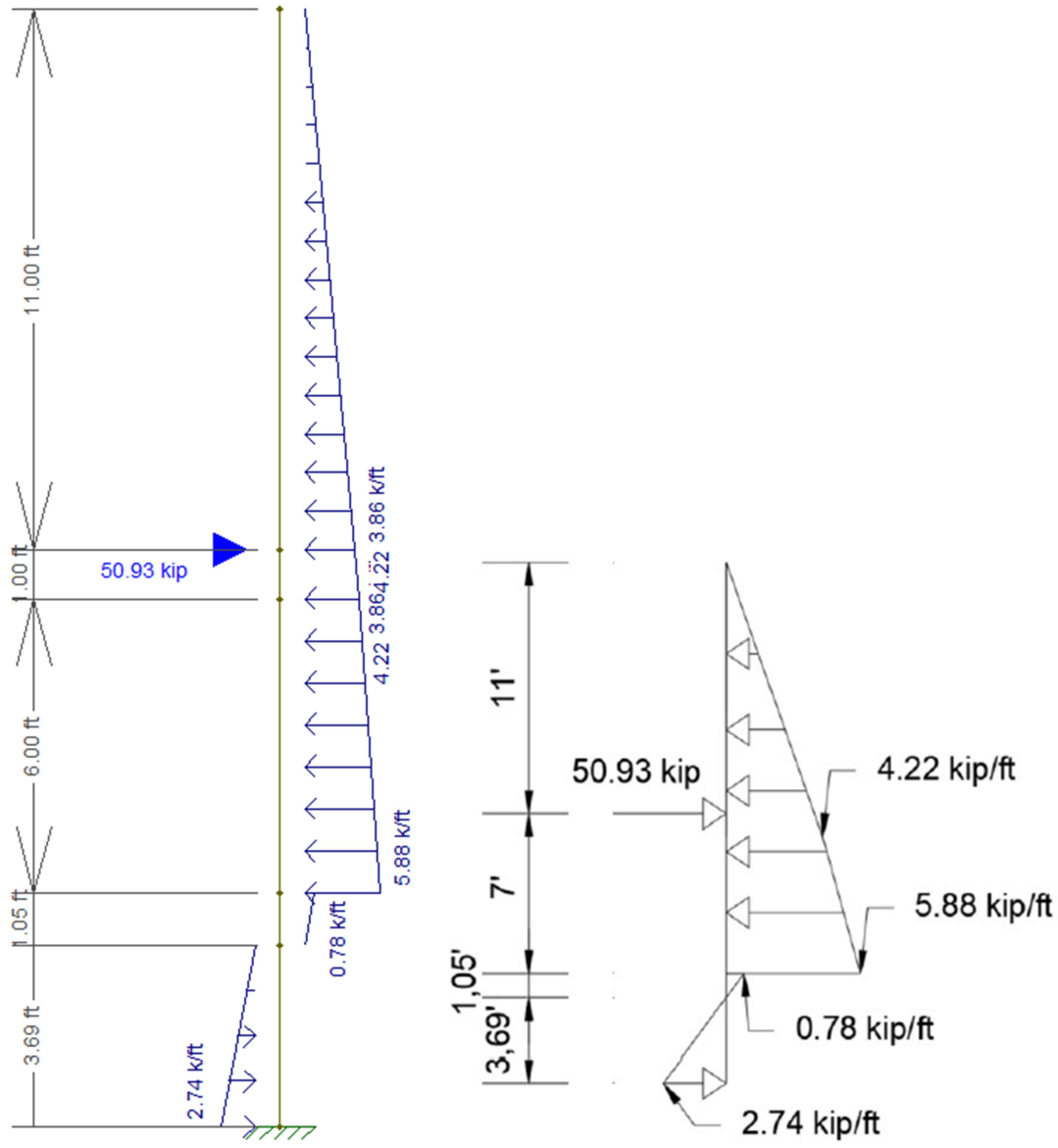

Figure F.11: Earth Pressure Diagram for 18 foot depth excavation. Structural Software (left) and Limit Equilibrium (right).

Earth Pressure Diagram in the structural software matches with the limit equilibrium method.

Figure F.12 shows the moment diagram for the sixth check, excavation to the 18 foot depth.

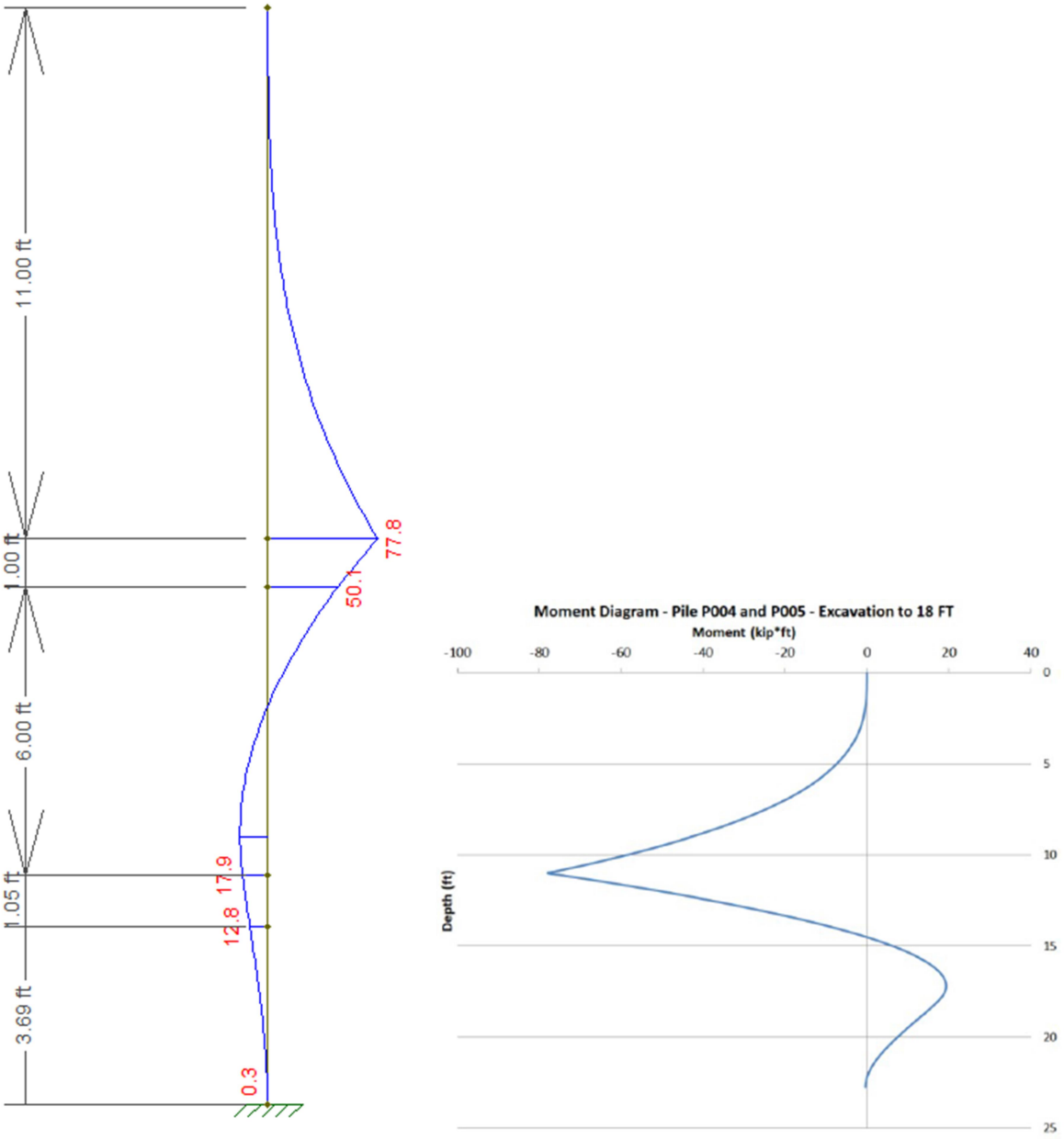

Figure F.12: Moment Diagram for 18 foot depth excavation. Structural Software (left) and Limit Equilibrium (right).

Moment Diagram in the structural software matches with the limit equilibrium method.

APPENDIX G (STUDENT SURVEY)

This appendix shows an example of a survey that can be answered by students at RHIT in order to have a better idea about their interest in civil engineering, laboratory and living labs. It can be a powerful resource in order to use the MU retaining wall to enhance the students learning experience in the institute.

General Questions

* Required

1. **Are you a Civil Engineering Student at Rose-Hulman Institute of Technology?** *
   If you are not, this form is not intended to you.
   Mark only one oval.

   - ◯ Yes

2. **Pick one of the options** *
   Mark only one oval.

   - ◯ I started college as a Civil Engineering Student
   - ◯ I switched majors during my Freshman Year
   - ◯ I switched majors after my Freshman Year

3. **What year are you in?** *
   Mark only one oval.

   - ◯ Year 1
   - ◯ Year 2
   - ◯ Year 3
   - ◯ Year 4
   - ◯ Year 5
   - ◯ Completed my undergrad at RHIT in the past 5 years
   - ◯ Prefer not to answer

4. **When was the first time you heard about civil engineering?** *
   Mark only one oval.

   - ◯ Before High School
   - ◯ Year 1 of High School
   - ◯ Year 2 of High School
   - ◯ Year 3 of High School
   - ◯ Year 4 of High School
   - ◯ Other

5. **What areas are you interested in?** *
   Check all that apply.

   - ☐ Environmental
   - ☐ Geotechnical
   - ☐ Structural
   - ☐ Transportation
   - ☐ Not Sure

6. **Pick one** *
Mark only one oval.

- ◯ I prefer classes with labs
- ◯ I prefer classes without labs
- ◯ I believe some classes are better with labs and other without labs

7. **On a scale from 1 to 5. How adding a living lab to a class would impact your learning experience? Where 1 represents Very Badly and 5 Very Well** *
Definition of Living Lab in the top of this section
Mark only one oval.

- ◯ 1
- ◯ 2
- ◯ 3
- ◯ 4
- ◯ 5

8. **On a scale from 1 to 5. Please rate your interest on having more opportunities to design and work with structures located on campus? Where 1 represents no interest and 5 very interested.** *
Mark only one oval.

- ◯ 1
- ◯ 2
- ◯ 3
- ◯ 4
- ◯ 5

9. **How many Civil Engineering Classes are you currently taking?** *
Mark only one oval.

- ◯ 0
- ◯ 1
- ◯ 2
- ◯ 3
- ◯ 4
- ◯ 5
- ◯ 6

10. **How many Civil Engineering Classes that has a field trip or laboratory are you currently taking?** *
Mark only one oval.

- ◯ 0
- ◯ 1
- ◯ 2
- ◯ 3
- ◯ 4
- ◯ 5
- ◯ 6

11. **List the classes from the last question.**

12. **Have you ever worked on a project or assignment using structures located on campus?** *
    Please: answer YES or NO. And then list the classes

13. **Have you ever been in a class at RHIT where the professor uses an example from campus to enhance the learning experience?** *
    Please: answer YES or NO. And then list the classes